The role of posttranslational hypusination of the eukaryotic translation initiation factor 5A in *Zea mays* and *Fusarium graminearum*

Dissertation

A thesis submitted for the degree of Dr. rer. nat. (*rerum naturalium*)
to the Biology Department,
the Faculty of Mathematics, Informatics and Natural Sciences,
University of Hamburg

by

Chien Xuan Hoang

Lam Dong, Vietnam

Hamburg, Germany - 2017

1. Referee: Prof. Dr. Wilhelm Schäfer;

Molecular Phytopathology and Genetics, Biocenter Klein Flottbek and Botanical Garden

2. Referee: Prof. Dr. Joachim Hauber

Research Group Antiviral Strategies, Heinrich Pette Institute, Leibniz Institute for Experimental Virology

Date of disputation: **06 March 2017**

Declaration of Oath

I hereby declare, on oath, that the data in this study have been conducted by me and have not used anything other than the ackowledged resources and aids. This work has not been submitted for any other degree.

Hamburg, 08 January 2017 **Chien Xuan Hoang**

January 09, 2017

To Whom it May Concern

This letter is to certify that the English in the thesis titled "The role of posttranslational hypusination of the eukaryotic translation initiation factor 5A in *Zea mays* and *Fusarium graminearum*" submitted to the Biology Department, the Faculty of Mathematics, Informatics and Natural Sciences, University of Hamburg for the degree of Dr. rer. nat. (rerum naturalium) by Chien Xuan Hoang fulfills the language requirements of the University of Hamburg.

Sincerely

Ellis B. Monaghan

Signature:  **Date Signed:** 09/01/2017

Contact Information:

Ellis B. Monaghan

PhD Student

E-mail: e.monaghan.1@warwick.ac.uk

Address:

Room: C146.1

Life Sciences

University of Warwick

Gibbet Hill Campus

Coventry

CV4 7AL

Contents

Abbreviations

35s promoter	Cauliflower mosaic virus 35s promoter
aa	Amino acid
AC	Adenylate cyclase
ADON	Acetyldeoxynivalenol
ATP	Adenosintriphosphate
AUR	Aurofusarin
bar	Phosphinothricin acetyl transferase
BLAST	Basic Local Alignment Search Tool
bp	Base pairs
CamV	Cauliflower mosaic virus
cDNA	Coding deoxyribonucleic acid
CM	Complete medium
CMA	Corn meal agar
Cre	Cre-recombinase
CTAB	Cetyl trimethyl ammonium bromide
cv	Cultivar
DEPC water	Diethylpyrocarbonate water
DHS	Deoxyhypusine synthase
DHSoex-GFP	Deoxy hypusine synthase gene overexpressed under the gpdA promoter
DNA	Deoxyribonucleic acid
dNTP	Deoxynucleotide triphosphate
DOHH	Deoxyhypusine hydroxylase
DOHHoex-GFP	Deoxy hypusine hydroxylase under the gpd1 promoter
DON	Deoxynivalenol
dpi	Days post inoculation
DsRed	Red fluorescent protein
dsRNA	Double stranded RNA
dUTP	Desoxyuracil triphosphate
E. coli	*Escherichia coli*
EDTA	Ethylenediaminetetraacetic acid
EFP	Elongation factor P
eGFP	Enhanced Green fluorescent protein
eIF5A	Eukaryotic initiation factor 5A
FCWRE	Fungal cell wall remodeling enzymes
FGDB	*Fusarium graminearum* Genome Database
FHB	Fusarium head blight
gDNA	Genomic deoxyribonucleic acid
GFP	Green fluorescent protein

GH	Glycoside hydrolase
GLS	Gray leaf spot
gpdA	Glycerol-3-phosphate dehydrogenase promotor
GUS	Glucuronidase
HIGS	Host Induced Gene Silencing
hph/hyg	hygromycin B phosphotransferase
hpi	Hours post inoculation
HR	Hypersensitivity response
HSP	Heat shock promoter
IC	Infection cushion
IH	Infection hypha
IR	Infrared
ISR	Induced systemic resistance
JA	Jasmonic acid
kb	Kilo bases
kDa	kilo Dalton
LB	Luria-Bertani medium
LD-PCR	Long distance polymerase chain reaction
LM	Light microscopy
LMD	Laser microdissection
lncRNA	Long noncoding RNAs
LOX	Lipoxygenase genes
LRR	Leucine-rich repeat
LSM	Laser scanning microscopy
M	Molar (mol/L)
MAPK	Mitogen activated protein kinase
MCS	Multiple cloning site
MDR	Multiple disease resistance
MDR	Multiple disease resistance
min	Minute
miRNA	microRNA
MM	Minimal medium
mRNA	Messenger RNA
mRNA	Messenger RNA
MS	Methyl salicylate
NBS	Nucleotide binding site
NCBI	National Center for Biotechnology Information
NIV	Nivalenol
NPS	Nonribosomal peptide synthetase
nptII	Neomycin phosphotransferase
ORF	Open reading frame
PAL	Phenylpropanoid

PALM	Name of a subdivision of the company Carl Zeiss
PCR	Polymerase chain reaction
PD	Peptidoglycan deacetylase
PEG	polyethylene glycol
PK	Protein kinase
PCWDE	Plant cell wall degrading enzymes
PR	Pathogenesis-related proteins
PS	Papillae silica cell
q-PCR	Quantitative polymerase chain reaction
QTL	Quantitative trait loci
RGAs	Resistance gene analogues
RH	Runner hyphae
RISC	RNA-induced silencing complex
RNA	Ribonucleic acid
RNAi	RNA interference
ROS	Reactive oxygen species
rpm	Rounds per minute
rRNA	Ribosomal ribonucleic acid
RT	Room temperature
RT-PCR	Reverse transcription polymerase chain reaction
SA	Salicylic acid
SAR	Systemic acquired resistance
SCL	Selenocysteine lyase
sec	Second
SEM	Scanning electron microscopy
siRNA	Small interfering RNAs
SLB	Southern leaf blight
SM	Secondary metabolism
SMART-PCR	Switching mechanism of 5'end of RNA template
SMB	Secondary metabolite biosynthetic
SNA	Saltwater nutrient agar
ss cDNA	Single stranded cDNA
ss RNA	Single stranded ribosomal ribonucleic acid
T0, T1, T2	Original regenerated plant, first and second daughter generation
T35s terminator	Cauliflower mosaic virus 35s terminator
TEM	Transmission electron microscopy
TF	Transcription factor
TP	Transporter
Tri	Trichothecene synthase gene
Tris	Tris-(hydroxymethyl) aminomethane
tRNA	Transfer RNA
ubi promoter	Plant specific ubiquitin promoter

UTR	Untranslated region
UV	Ultra violet
v	Volume
v/v	Volume per volume
w/v	Weight per volume
WT	Wild type
YPG	Yeast extract peptone glucose
ZEA	Zeralenon

List of Figures and Tables

Figures

Tables

1. Introduction

1.1. The essential role of the eukaryotic translation initiation factor 5A.

The eukaryotic translation initiation factor eIF5A is the only cellular protein that contains the unique polyamine-derived amino acid, hypusine [N^{ε}-(4-amino-2-hydroxybutyl) lysine]. The name hypusine is derived from two of the amino acid's structural components: hydroxyputrescine and lysine (Shiba *et al.*, 1971). Hypusine is an unusual amino acid that exists as a free amino acid and as a protein component in all eukaryotes and in some archaea, but not in eubacteria (Figure 1). However, eubacteria have an orthologue of eIF5A, the elongation factor P (EF-P). EF-P, archaeal IF5A (aIF5A), and eIF5A share a significant similarity in amino acid sequence and only have small structural differences (Hanawa- Suetsugu *et al.,* 2004).

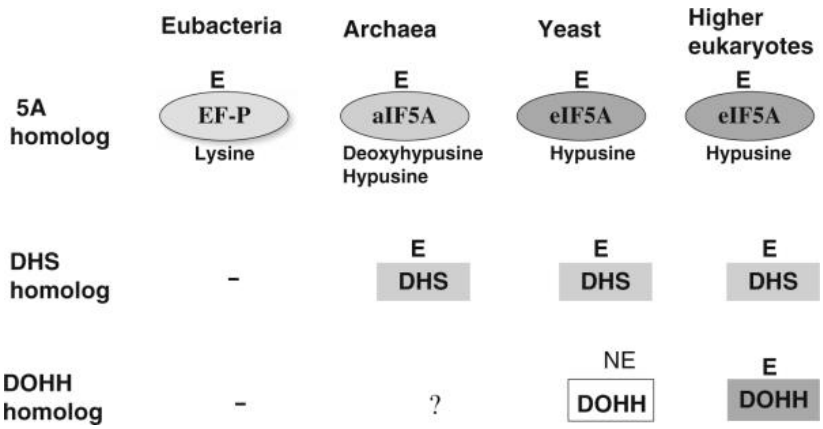

Figure 1. Evolution of eIF5A and its hypusine modification pathway. eIF5A orthologs are found in eubacteria and archaea and are essential genes in each organism. The DHS gene exists in archaea, and in all eukaryotes, but not in eubacteria. DOHH gene is found only in eukaryotes. E indicates essential gene, and NE indicates non-essential gene (Park and Nishimura, 2009).

Alignment of the predicted amino acid sequences of eIF5A from several species shows that sequence conservation is extremely high around the hypusine residue, denoting the importance of this unusual amino acid throughout eukaryotic evolution (Figure 2). At least two eIF5A genes were identified in many eukaryotic organisms, including fungi, plants, vertebrates, and mammals (Chen and Liu, 1997).

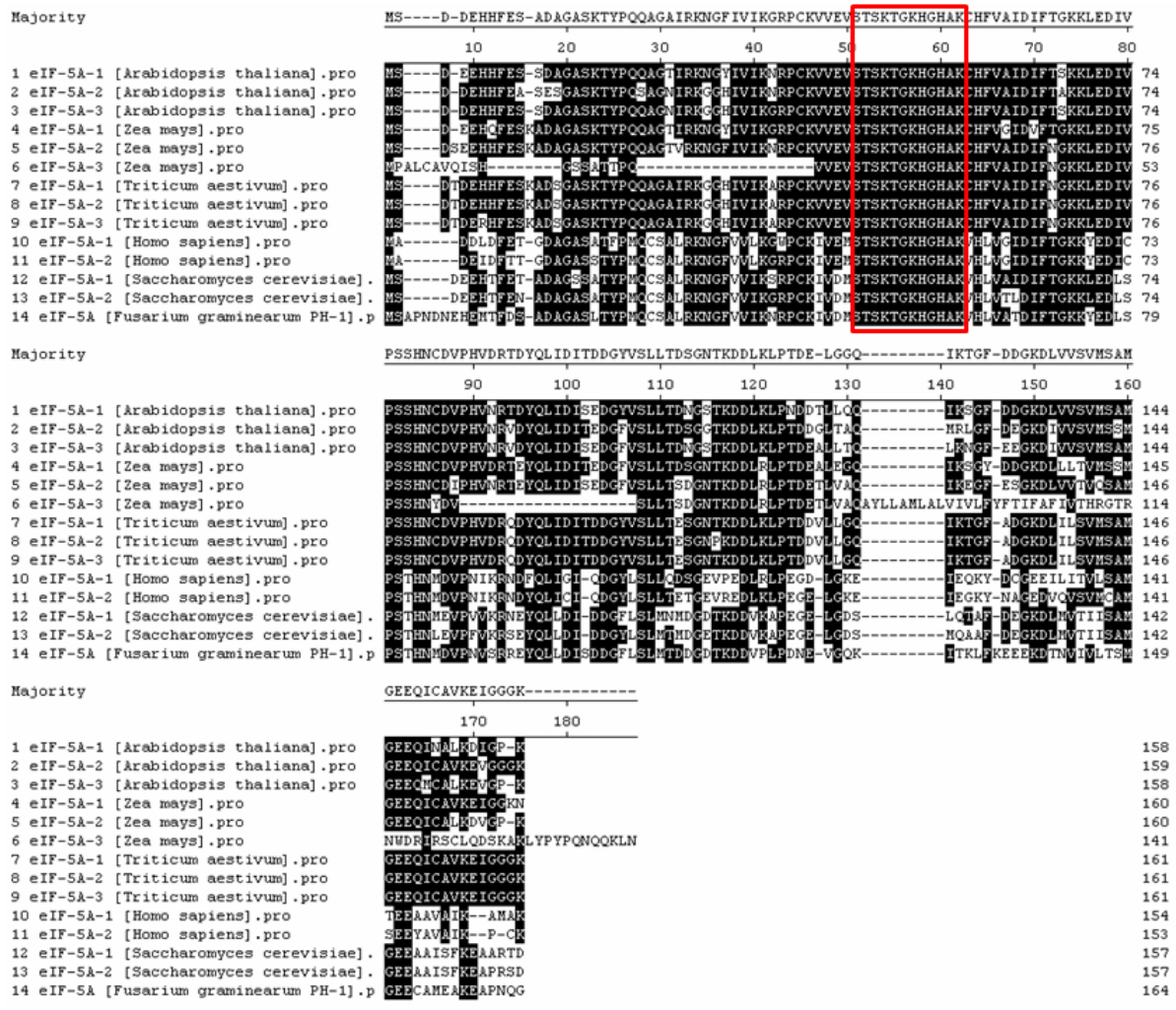

Figure 2. Multiple sequence alignment of eIF5A. The eIF5A amino acid sequence from three *Arabidopsis* genes, three *Zea mays* genes, three *Triticum aestivums* genes, two *Homo sapiens* genes, two *Saccharomyces cerevisiae* genes were compared using the clustalw alignment tool. Conserved domain indicated with a red box. The 2nd lysine inside the conserved domain is the residue modified into hypusine in active eIF5A.

In *S. cerevisiae* two eIF5A genes, *TIF51A* (aerobic gene) and *TIF51B* (anaerobic gene) are regulated through the presence of oxygen. These genes have 92% identity in their encoding sequence (Schnier *et al.*, 1991). The two genes of *S. cerevisiae* can be inactivated and alternated for each other. During cell growth their function is indistinguishable (Magdolen *et al.*, 1994; Clement *et al.*, 2003). In *C. elegans*, there are two genes IFF-1 and IFF-2, where germ cell proliferation is dependent on IFF-1, whereas IFF-2 is required for growth of somatic cells (Hanazawa *et al.,* 2004). In humans, eIF5A-1 and eIF5A-2 have an 84% similarity in their amino acid sequences (Paul *et al.*, 2006).

Co-expression of two eIF5A genes has been recorded in certain vertebrates, including amphibians, chicken and fish. On the contrary, in humans and most other mammals, there is some differentiation in expression. The eIF5A-1 gene is mostly expressed in the majority of mammalian cells and tissues. It is essential for embryonic growth, cell growth and proliferation

in mammals (Park *et al.*, 2010). A low expression of eIF5A-2 gene has been shown in normal mammalian tissues. Yet a high expression of the eIF5A-2 gene was reported in human cancer tissues and cells, such as ovarian and colorectal cancer. Due to these results the second gene of eIF5A was suggested as a candidate oncogene in mammals (Guan *et al.,* 2001; Clement *et al.*, 2003; Guan *et al.*, 2004).

Eukaryotic eIF5A has similar functions as EF-P from bacteria; it promotes methionyl-puromycin synthesis *in vitro*, it is involved in translation elongation and stimulates the peptidyl transferase activity of the ribosome (Glick and Ganoza, 1975; Benne and Hershey, 1978; Kang and Hershey, 1994). Depletion of eIF5A in *S. cerevisiae* and mammalian cells results in a decrease of total protein synthesis, accumulation of polysomes and prolonged ribosome transit times (Kang and Hershey 1994; Li *et al.*, 2010; Saini *et al.*, 2009). These results led to a proposal that eIF5A is an initiation factor specific for a subset of mRNA's (Kang and Hershey, 1994; Xu *et al.*, 2004). eIF5A is also suggested as a bimodular protein interacting with both RNA and proteins, and acts like an important factor in the translation machinery (Park, 2008). Other studies show that eIF5A acts as a cellular cofactor for HIV Rev, binding and transporting the HIV Rev protein from the nucleus to the cytoplasm (Rosorius *et al.*, 1999). Nevertheless, there are no obvious evidences to prove that the various observed phenotypes are direct or indirect consequence of eIF5A depletion or dysfunction and how the various effects are interrelated. It is possible that eIF5A is a multifunctional protein involved in several critical cellular processes (Park, 2006).

Recent studies revealed the pivotal function of bacterial EF-P and eukaryotic eIF5A within the ribosome. eIF5A stimulates the peptidyl transferase activity of the ribosome and facilitates the reactivity of poor substrates like proline. eIF5A is essential for the synthesis of a subset of proteins containing proline stretches in all cells, enhancing translation of polyproline-containing proteins and it is critical for copy-number adjustment of multiple pathways across all kingdoms of life (Doerfel *et al.*, Ude *et al.*, Gutierrez, *et al.,* 2013). Li *et al.* (2014) show that the activity of eIF5A during translation of polyprolines regulates yeast mating through formin translation. Moreover, eIF5A-dependent translation of formins could regulate polarized growth in such processes as fertility and cancer in higher eukaryotes. There are a number of eIF5A/EF-P dependent genes encoding polyproline-containing proteins. An analysis on genome and functional classification of proline repeat-rich proteins elucidates the essential role of eIF5A and its hypusine modification pathway in the course of eukaryotic evolution (Mandal *et al.*, 2014).

Recently, eIF5A genes have been cloned from several plant species such as *Arabidopsis thaliana*,

Tamarix androssowii, *Zea mays, Triticum aestivum*, *Nicotiana tabacum*, *Medicago sativa*, *Brassica napus*, *Cucurbita pepo* and *Solanum lycopersicum*. Like in mammalian cells, plants have different genes coding for eIF5A proteins, which display a high level of amino acid identity. eIF5A proteins from plants share 50 - 60% homology with eIF5A proteins found in the animal kingdom and have 80 - 97% identify across plant species. The sequence of amino acids surrounding the hypusine residue is also strictly conserved (Figure 2). There are three known eIF5A genes in *A. thaliana*, *Z. mays, T. aestivum* and four in *Lactuca sativa* (Wang *et al.,* 2003; Gatsukovich, 2004; Thompson *et al.,* 2004; Lebska *et al.,* 2009). The three eIF5A genes in *A. thaliana* share 82-84% sequence identity at the nucleotide level and 82 - 87% identity at the amino acid level (Thompson, 2004). In *A. thaliana*, eIF5A-1 is essential and plays an important role in cell proliferation and senescence (Wang *et al.,* 2003; Thompson *et al.,* 2004; Duguay *et al.,* 2007). In addition, other results indicate that modulation of eIF5A-1 expression alters xylem abundance (Liu *et al.,* 2008). eIF5A-2 appears to be implicated in programmed cell death associated with pathogen ingression (Feng *et al.,* 2007; Hopkins *et al.,* 2008). eIF5A-3 is involved in supporting growth and plays a regulatory role in the response of plants to sub-lethal osmotic and nutrient stress (Ma *et al.*, 2010). eIF5A proteins in tomato plants are involved in senescence- induced programmed cell death, as well as early development of seedlings (Wang *et al.*, 2001; Moll, 2002).

eIF5A genes are also involved in biotic and abiotic stress responses (Hopkins *et al.,* 2008). For example, eIF5A is involved in the development of disease symptoms and in pathogen-induced cell death during infection of *Arabidopsis* with *Pseudomonas syringae*. On the other hand, overexpressing RceIF5A from *Rosa chinensis* in *Arabidopsis* improved tolerance to heat, oxidative and osmotic stresses (Xu *et al.*, 2011). The importance of eIF5A activation by hypusination for plant growth and development was reported recently. It involves the control of flowering time, the aerial and root architecture, and root hair growth. Additionally, this crucial pathway is necessary for adaption to challenging growth conditions such as high salt or high glucose medium, and to increase concentrations of the plant hormone ABA (Belda-Palazón *et al.*, 2016).

However, to date the full function of eIF5A and their genes in plants is still elusive. A high number of studies about the eIF5A hypusination pathway in plants are based on overexpression or antisense approaches mostly performed in *Arabidopsis*. Therefore the information about this pathway in plants is deficient and limited (Feng *et al.*, 2007; Duguay *et al.*, 2007; Liu *et al.*, 2008; Ma *et al.*, 2010; Ren *et al.*, 2013; Belda-Palazón *et al.*, 2016).

1.2. Hypusine biosynthesis pathway

Currently there is only one cellular pathway involved in the formation of hypusine, and nothing is known about a possible role as a free amino acid (Park *et al.*, 1997). The mature form of eIF5A has to undergo two posttranslational modifications, first, phosphorylation of the N-terminal acetylated serine residue and second the hypusination of the second lysine in the C-terminal conserved domain (Kang *et al.*, 1993). The phosphorylation is mapped to the Ser2 residue of the protein; this mutation of this residue does not affect yeast cell growth, indicating that phosphorylation is not necessary for eIF5A function. However, the second post-translational modification of the eIF5A precursor, hypusination, is essential to its function (Klier *et al.*, 1993).

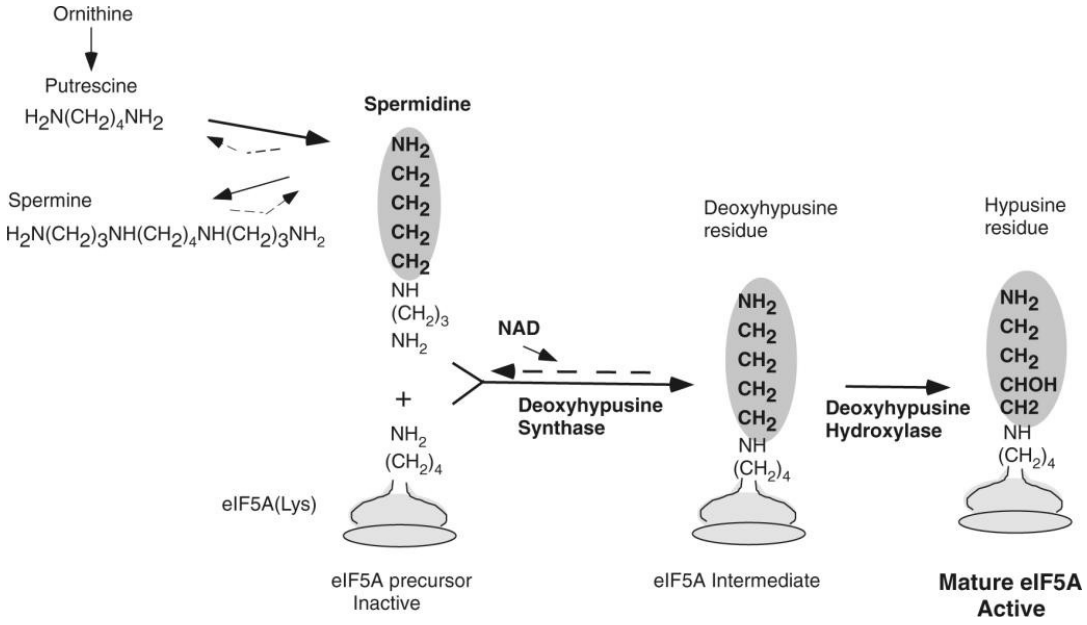

Figure 3. **Hypusine biosynthesis in eIF5A.** The polyamine spermidine is synthesized from putrescine and becomes the source of the aminobutyl moiety of hypusine, as marked by shading. Two enzymatic steps catalized by deoxyhypusine synthase (DHS) and deoxyhypusine hydroxylase (DOHH) are involved in hypusine synthesis. Firstly DHS catalyzes the cleavage and transfer of the aminobutyl moiety of spermidine to the lysine residue of the eIF5A precursor protein to form the eIF5A intermediate, deoxyhypusine. The intermediate is then hydroxylated by DOHH to form hypusine. This is the mature, active form of the eIF5A protein. This process occurs at one specific lysine residue of the eIF5A precursor protein, eIF5A (Lys) (Park *et al.,* 2010).

Two enzymatic steps participate in the biosynthesis of the hypusine residue. Deoxyhypusine synthase (DHS) starts the process when a NAD-dependent tetrameric enzyme, catalyzes the cleavage of the aminobutyl moiety of the polyamine spermidine (Joe *et al.*, 1995; Wolff *et al.*, 1995). Afterwards the ε-amino group is transferred to a specific lysine residue (Lys 50) of the eIF5A precursor forming the intermediate deoxyhypusine [N^{ε}-(4-aminobutyl)-lysine] (Wolff *et al.*, 1997; Wolff *et al.*, 2000). Deoxyhypusine hydroxylase (DOHH), the second enzyme, then hydroxylates the deoxyhypusine intermediate to complete the synthesis of the unique amino

acid hypusine, and the activation of eIF5A (Figure 3) (Park, 2006). There is no report that DHS and DOHH are present or used in any other biosynthetic pathway. They do not modify any free amino acids within the cell or short peptides that are similar to the sequence of eIF5A, assuming that they evolve solely for the modification of eIF5A (Wolff *et al.*, 2007).

Spermidine, a polyamine involved in multiple cellular eprocesses, is the source of the aminobutyl moiety that is cleaved and transferred by DHS (Chattopadhyay *et al.*, 2003). Many studies about gene disruption and knock down in *S. cerevisiae* and other eukaryotes show the importance of both modification enzymes in cellular proliferation. Either modification step of eIF5A is essential to the viability of yeast cells and the cell cycle at the G_1/S boundary (Kang and Hershey, 1994; Park *et al.*, 1997). DHS also has homologs in all eukaryotes and archaea while DOHH is conserved in all eukaryotes (Figure 1) (Park *et al.,* 2010).

1.3. Gene studies of deoxyhypusine synthase (DHS) in plants

Deoxyhypusine synthase, the first enzyme in hypusination, catalyzes a complex sequence of processes to convert one specific lysine residue of the eIF5A precursor to a deoxyhypusine residue. This step involves two substrates, spermidine and eIF5A (Lys), and a cofactor, NAD (Park, 2006). DHS cDNAs have been cloned from several plant species including *S. lycopersicum*, *A. thaliana*, *T. aestivum* , *Z. mays*, *Brassica* ssp. and *N. tabacum*, and are shown to have high sequence similarity (Chamot and Kuhlemeier, 1992; Ober and Hartmann, 1999a, b; Wang *et al.*, 2001, 2003, 2005a, b; Woriedh and Schaefer, 2010). Additionally, Wolff and Park (1999) compared amino acid sequences between several species including yeast (*S. cerevisiae*), human (*Homo sapiens*), roundworm (*Caenorhabditis elegans*), mouse (*Mus musculus*) and the filamentous fungus (*Neurospora crassa*); the results show considerable conservation of sequence identity, particularly in the C-terminal active site of the enzyme (Wolff and Park, 1999).

There is only one DHS gene in *Arabidopsis*, but there are 3 genes of the eIF5A. Hence, it has been suggested that all of the eIF5A genes are activated by the single DHS enzyme, and that DHS function is strongly associated with the cellular requirement for activated eIF5A (Thompson *et al.*, 2004). DHS expression has a multi-element promoter that possibly facilitates its up-regulation during the activation of one or all of the eIF5A genes (Duguay *et al.,* 2007). Previous studies revealed that levels of DHS protein and eIF5A-1 increase early during leaf senescence. These proteins are also increased during abiotic stress conditions of plants such as chilling and osmotic stress (Wang *et al.,* 2001; 2003; 2005; Thompson *et al.,* 2004).

Antisense suppression of DHS in *A. thaliana* causes delayed senescence and resistance to drought stress (Wang *et al.*, 2003). Similarly, the delay in fruit softening and leaf senescence is observed when overexpression of an antisense DHS is performed in tomato (Wang *et al.*, 2005). It has been proposed that different levels of suppression could lead to diverse pleiotropic effects. These effects include enhanced growth, increased tolerance to abiotic stress and, in the case of strong suppression, stunted reproductive growth, reduced seed yield and male sterility (Duguay *et al.,* 2007).

In recent research, Belda-Palazón *et al.,* (2016) demonstrated that by knocking-down DHS in *Arabidopsis* the hypusine biosynthesis was modified and resulted in a wide variety of aspects affecting many biological processes related with development such as control of flowering time, the aerial and root architecture and root hair phenotypes. Additionally this pathway is needed for adaptation to challenging growth conditions (presence of salt, glucose in medium) and increases concentrations of the plant hormone ABA (Belda-Palazón *et al.,* 2016).

To date many studies have revealed the importance of DHS in various biological processes. Yet the involvement of the hypusine pathway of eIF5A in pathogen resistance is still unknown.

1.4. Pathogen resistance in maize

Maize (*Zea mays* ssp. *mays*) is one of the most important cereal crops worldwide and represents an essential source of food, biofuel, feed and industrial products (990.64 million tons per year according to USDA WASDE report, May 2015). Losses in maize production due to fungal diseases are a major threat and lead to a critical condition for commercial agriculture. The constitutive and inducible defenses against pathogens and insects have been reported in several studies (Welz and Geiger, 2000; Parlevliet, 2002; Wisser *et al.*, 2005; Wisser *et al.*, 2006, Nurmberg *et al.*, 2007).

In plants, genetic resistance is often divided into two major classes: qualitative and quantitative disease resistance. A single major-effect resistance gene (R gene) generally provides race-specific, high-level resistance; this type of gene is called a qualitative gene. Qualitative resistance is commonly efficient against biotrophic pathogens (pathogens that derive their nutrition from living host cells). Breeders have chosen some major resistance genes, such as the *Ht* genes (qualitative resistance genes) for resistance to northern leaf blight and the *Rp* genes (quantitative trait loci genes) for resistance to common rust in maize breeding (Welz, 2000; Ramakrishna *et al.*, 2002).

Quantitative resistance has a multi-genic basis and generally provides non-race-specific intermediate levels of resistance. Quantitative traits can interact with the environment and each other (epistasis); they are controlled by few to many genes. Quantitative trait loci (QTL) are known as genomic regions (or loci) responsible for quantitative effects. Quantitative resistance tends to be more permanent in the plant defense system and it is more often associated with resistance to necrotrophic pathogens (pathogens that derive nutrition from dead cells) (Parlevliet, 2002). In contrast to quantitative resistance, qualitative resistance is generally quickly overcome when deployed in the field, though there are exceptions (Steffenson, 1992). This style of resistance often correlated with a rapid cell death called the hypersensitive response (HR) to prevent the spread of infection around the point of pathogen contamination.

The vast majority of genetic resistance used by maize breeders is quantitative resistance (Balint *et al.*, 2009). The main factor might be that maize is substantially more genetically diverse than wheat or rice and it is an outcrossing species. Another potential factor might be that there are less commercially important biotrophic pathogens in maize (Buckler *et al.*, 2001).

Another form of resistance that is still in dispute is called multiple disease resistance (MDR), in which the same locus is responsible for resistance to several pathogens (Zwonitzer *et al.*, 2010). The detection of QTL clusters conferring resistance to multiple diseases and the observation of pleiotropic effects on multiple diseases with induced gene mutations have provided more evidences for MDR in plants (Wisser *et al.*, 2005; Wisser *et al.*, 2006, Nurmberg *et al.*, 2007). Highly significant correlations between resistances to southern leaf blight, gray leaf spot, and northern leaf blight in the maize intermated B73 × Mo17 (IBM) population were observed by Balint-Kurti *et al.,* (2010), even though they did not spot any disease resistance QTL associated with resistance to all three diseases.

While MDR needs to be confirmed the different types of resistance are well understood and summarized in Figure 4 (Ali and Yan, 2012).

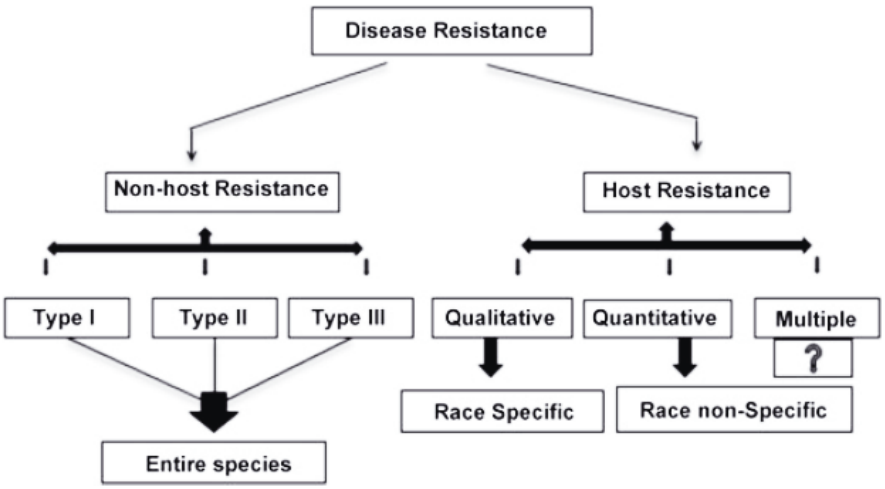

Figure 4. Basic concept of disease resistance. Qualitative: Qualitative disease resistance (mostly controlled by single major gene); Quantitative: Quantitative disease resistance (several to many minor genes); Multiple: Multiple disease resistance (defense of plants against several diseases). Nonhost resistance exhibited against bacteria, fungi and oomycetes can be of two or three types (Taken from Ali and Yan, 2012).

1.5. Systemic acquired resistance (SAR) and induced systemic resistance (ISR) in maize

In the presence of pathogens plants have a variety of inducible defenses. The timing of these defense responses is critical and can be the difference between being able to resist or surrender to the challenge of a pathogen. Systemic responses in plant defenses are preconditioned by prior infections that result in resistance (or tolerance) against subsequent challenges by a pathogen (Vallad and Robert, 2004).

In dicotyledons the systemic acquired resistance (SAR) and induced systemic resistance (ISR) pathways have been considerably characterized. However in monocotyledons such as maize, the existence of analogous pathway systems has not been convincingly demonstrated. Studies involving SAR- or ISR-like phenomena in monocotyledons are still scarce and deficient (Kogel and Langen, 2005). In cereals the conserved essential component of the SAR pathway – *NPR1* is present (Chern *et al.*, 2005; Shimono *et al.*, 2007; Yuan *et al.*, 2007). *NPR1* gene is a key regulator of the SAR pathway associated with induction of a number of pathogenesis-related (PR) genes (Grant and Lamb, 2006). *NPR1* seems to function similarly in rice and Arabidopsis (Chern *et al.*, 2001, 2005; Dong, 2004). Moreover it can induce SAR function in several monocotyledon species including maize (Gorlach *et al.*, 1996; Kogel and Huckelhoven, 1999; Morris *et al.*, 1998). A high number of beneficial microorganisms are known to induce ISR in monocots and dicots through ethylene and jasmonic acid (JA)-dependent signaling pathways (Van der Ent *et al.*, 2009). Colonization of maize roots by *Trichoderma virens* can

induce an ISR-like response against a foliar pathogen (Djonovic *et al.*, 2007). A similar situation is also observed in maize root inoculation with *Pseudomonas putida* (Planchamp *et al.*, 2014). There are no changes in disease resistance when the maize orthologue of *NPR1* is disrupted or overexpressed (Balint *et al.*, 2009). Similarly, in *Arabidopsis* the plant hormone, salicylic acid (SA) is a critical signal for expression of multiple modes of resistance, but in maize its effect on the interaction with pathogens seems to be negligible, based on the analysis of both SA-deficient and SA over-accumulating transgenic maize (Balint *et al.*, 2009). Recently, studies reported that lipoxygenase genes (LOX gene) are also involved in the activation of ISR signaling in maize (Gao *et al.*, 2007; Constantino *et al.*, 2013). In consequence the induced resistance responses are conserved between dicotyledonous and monocotyledonous systems. In maize, systemic responses and their mechanism have been surveyed widely but are still not fully understood.

1.6. The plant pathogen *Fusarium graminearum*

The fungal pathogen *Fusarium graminearum* is a broad host pathogen threatening cereal crops, causing Gibberella ear rot (GER) and stalk rot of maize and Fusarium head blight (FHB) in small grain cereals such as wheat, barely and rice. *F. graminearum* also infects other plant species without causing disease symptoms. It infects other host genera including *Agropyron*, *Agrostis*, *Bromus*, *Calamagrostis*, *Cenchrus*, *Cortaderia*, *Cucumis*, *Echinochloa*, *Glycine*, *Hierochloe*, *Lolium*, *Lycopersicon*, *Medicago*, *Phleum*, *Poa*, *Schizachyrium*, *Secale*, *Setaria*, *Sorghum*, *Spartina,* and *Trifolium* (Farr, 1989; Goswami and Kistler, 2004). The key factors influencing the distribution and severity of FHB caused by *F. graminearum* are environmental conditions, especially temperature and moisture (Shaner, 2003).

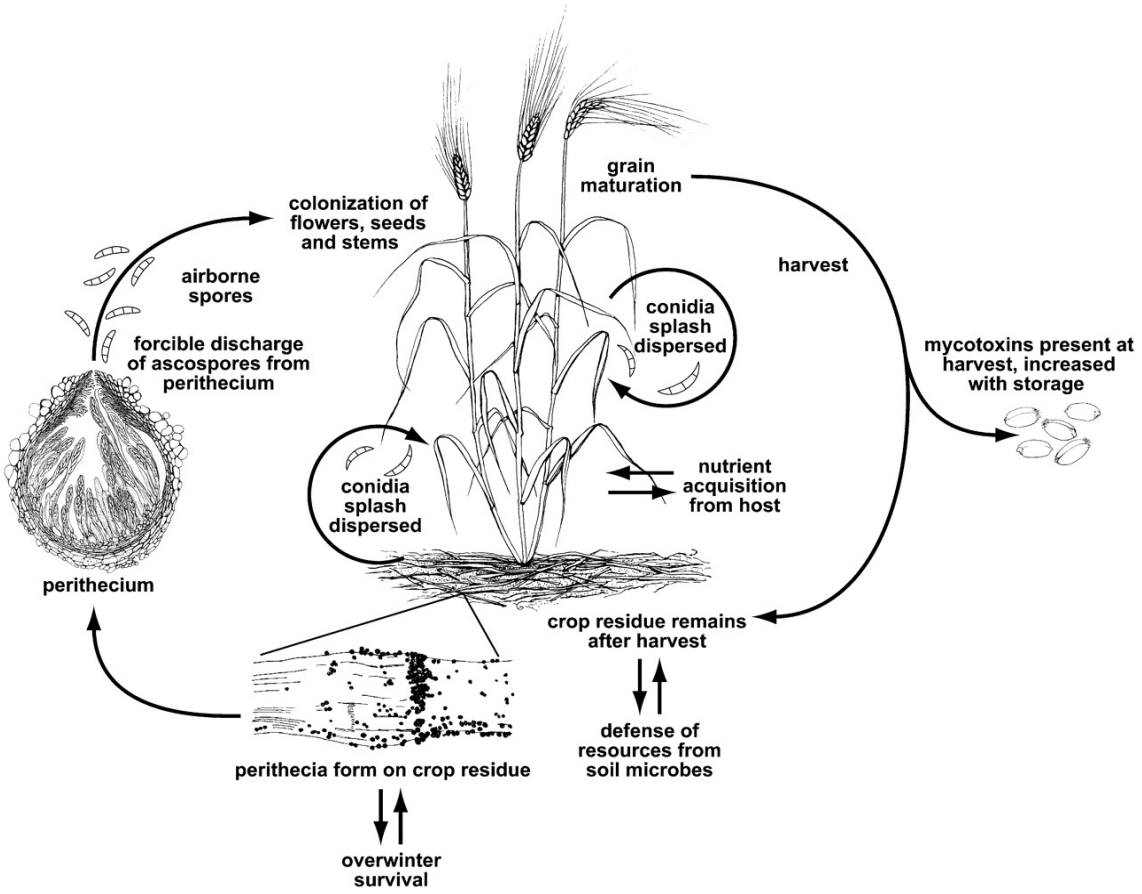

Figure 5. The life cycle of *F. graminearum* (sexual phase, *G. zeae*), causal agent of *Fusarium* head blight on wheat (Trail, 2009). Details of specific aspects of the cycle are discussed in the text.

F. graminearum produces several mycotoxins, including the trichothecene deoxynivalenol (DON), the phytoestrogenic zearalenone, fusarin C, and aurofusarin among others (Trail, 2009). Therefore, primary economic and health consequences of the *Fusarium* disease are due to mycotoxin contamination. To protect the food and feed supply many countries imposed maximum mycotoxin levels (van Egmond *et al.,* 2007). DON is a potent protein biosynthesis inhibitor and causes vomiting, as such this mycotoxin is known as vomitoxin. When ingested in sufficient quantities, DON affects the digestive system and major organ function in humans and animals (Snijders, 1990). DON is the only mycotoxin shown to be a virulence factor, causing tissue necrosis (Proctor *et al.*, 1995). DON allows the fungus to propagate from florets crossing the rachis node into the wheat rachis (Jansen *et al.*, 2005).

In the life cycle of *F. graminearum*, infection of a wheat spike is initiated by airborn ascospores and conidia landing on flowering spikelets during anthesis (Figure 5). Wind currents can pick them up and and transport them across great distances. The infection may also proceed through bird or insect damaged kernels (Sutton, 1982). Germination of *F. graminearum* usually takes place within 6-12 h of plant contact and hyphae initially grow intercellular and

asymptomatically to form hyphal networks on the surface of floral tissues (Bushnell *et al.,* 2003). Afterwards hyphae and bulbous infection hyphae are found at 48-72 h on inoculated, detached wheat florets (Rittenour and Harris, 2010). Subsequently, compound infection structures such as, lobate appressoria and infection cushions penetrate the floret tissue (Boenisch and Schäfer, 2011). Finally, *F. graminearum* spreads through vascular tissues in the rachilla and rachis propagating from floret to floret (Bushnell *et al.,* 2003).

1.7. Infection structures of *F. graminearum*

During plant invasion, a network of vegetative hyphae or mycelia is formed by all filamentous fungi to acquire nutrients from host plants. Under the control of regulatory genetic networks fungi build developing complexes such as three-dimensional structures for the generation, protection, and dispersal of spores. Several expression studies performed with the ascomycetes *F. graminearum*, *N. crassa*, and *Sordaria macrospora* reveal the developmental regulation of gene expression on a larger scale (Wang *et al.*, 2009). The penetration process of *F. graminearum* has been observed and described in many studies. *F. graminearum* initially colonizes the surface of wheat florets without immediate penetration (Bushnell *et al.*, 2003). *F. graminearum* can enter tissue of wheat and barley by natural openings, such as stomata (Pritsch *et al.*, 2000; Bushnell *et al.*, 2003; Boddu *et al.*, 2006; Trail, 2009), or penetrate epidermal cell walls with short infection hyphae (Wanjiru *et al.*, 2002; Cuomo *et al.*, 2007; Bluhm *et al.*, 2007; Kikot *et al.*, 2009). In some studies, the penetration of *F. graminearum* is indicated as a pathogen that does not form different types of appressoria (Mendgen *et al.*, 1996; Cuomo *et al.*, 2007; Bluhm *et al.*, 2007; Kikot *et al.*, 2009). However, other publications showed lobed, highly septate, and corralloid hyphal structures. These microscopy images demonstrated various infection structures which might be involved in penetration of glumes (Pritsch *et al.*, 2000; Boddu *et al.*, 2006; Rittenour and Harris, 2010). Recent work demonstrated the colonization of the flower leaves by so called runer hyphae of *F. graminearum*, followed by the development of multicellular infection structures, called lobate appressoria and infection cushions (Boehnisch and Schaefer, 2011) (Figure 6).

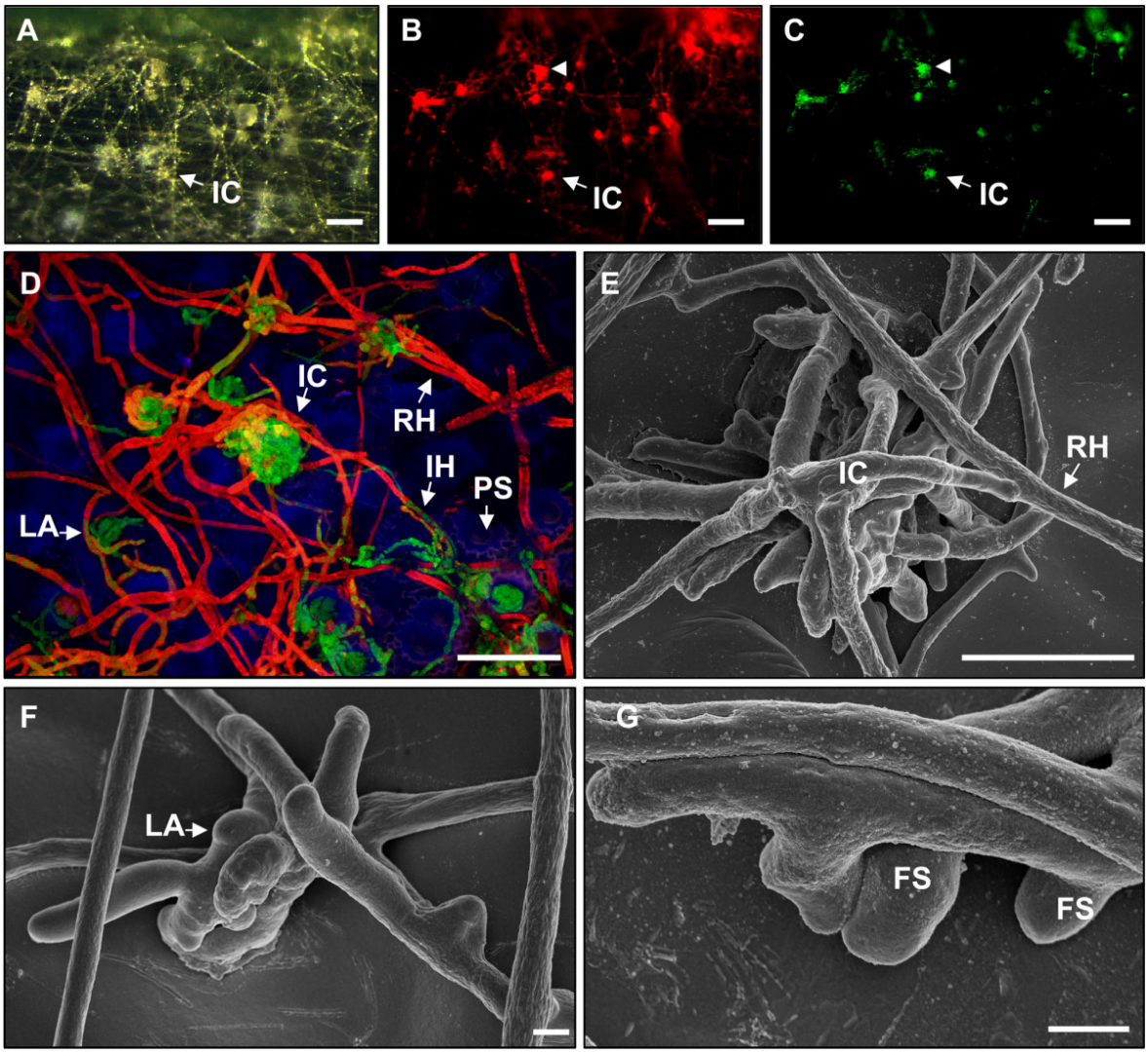

Figure 6. Infection structures and TRI5 induction of *F. graminearum* TRI5prom::GFP on wheat cv Nandu. **(A-C)** White light and fluorescence micrographs of infection cushions on palea at 8 dpi using MZFLIII microscope, scale bars = 100 µm. **(A)** Natural appearance of the inoculated surface of palea. **(B)** Infection cushions are visible by dsRed fluorescence. **(C)** GFP fluorescence demonstrates *TRI5* induction in infection structures. **(D)** Laser scanning microscopy of GFP inductive fungal structures (white arrowhead in B and C). Overlay image of individually detected dsRed and GFP fluorescence of the fungus as well as blue plant autofluorescence. The image represents a maximum intensity projection of a z-stack, scale bar = 50 µm. **(E-G)** Scanning electron micrographs of different infection structures on glume at 8 dpi. **(E)** Infection cushion, scale bar = 50 µm. **(F)** Lobate appressorium, and **(G)** foot structures, scale bars = 2 µm. Abbreviations: FS Foot structures, IC infection cushion, IH infection hypha, LA lobate appressorium, PS papillae silica cell, RH runner hyphae (Boenisch and Schäfer, 2011).

In addition, specific trichothecene induction in infection structures was demonstrated by different imaging techniques (Figure 6 A-D) eventhough trichothecenes production was proven not to be essential for infection structure development. All infection structures developed from epiphytic runner hyphae. Compound appressoria including lobate appressoria (Figure 6 F) and infection cushions (Figure 6 E) were observed on inoculated caryopses, paleas, lemmas, and glumes of susceptible and resistant wheat cultivars (Boenisch and

Schäfer, 2011).

1.8. Hypusination of eIF5A in *F. graminearum*

The important role of the hypusine biosynthesis pathway has been reported for the first time in a plant pathogen. The transcriptional level of *F. graminearum* DHS, the first enzyme necessary for the biosynthesis of hypusine, is up-regulated during the pathogenic interaction of *F. graminearum*- wheat. The external application of guanylhydrazone CNI-1493, a compound that inhibits fungal DHS activity, reduced *F. graminearum* disease symptoms in both wheat and maize without affecting kernel development (Woriedh *et al.*, 2011). However, until now studies about eIF5A and its hypusine modification are still limited in plant pathogenic fungi. Most evidence for the essential nature of eIF5A and its deoxyhypusine/hypusine modification has been obtained from gene mutation, gene disruption or knock down studies in the yeast *S. cerevisiae* and higher eukaryotes (Frigieri *et al.,* 2008). Mutations of eIF5A and DHS revealed the essentiality of these genes for cell viability, cell growth, differentiation and proliferation efficiency in yeast. However, the *Lia1* (DOHH) gene is not essential in yeast (Dias *et al.,* 2008; Park, 2010). In *F. graminearum*, DHS and DOHH genes are essential indicating full hypusination of eIF5A is necessary for cell viability (Woriedh *et al.*, 2011; Martinez-Rocha *et al.*, 2016). In addition, overexpression of DHS or DOHH genes produced opposite phenotypes. While DHS oeverexpressing mutant (DHSoex) is hypervirulent towards wheat, DOHH overexpressing mutant (DOHHoex) is avirulent. DHSoex invades wheat plant faster and produces more infection structures than the wild type strain. On the contrary, DOHHoex is not able to produce infection structures or penetrate wheat florets. In addition, DOHHoex presents overproduction of reactive oxygen species (ROS), reduction of DON production and increased sexual reproduction. A double DHSoex/DOHHoex overexpressing mutant caused similar FHB symptoms as the wild type. For the first time new insights on the impact of the two enzymes involved in eIF5A activation and the life cycle of a plant pathogen have been provided, highlighting the various functions of differently modified eIF5A (Martinez-Rocha *et al.*, 2016).

1.9. Combination of laser microdissection and RNA-Seq in study of plant-pathogen interactions

Using high-throughput methods, such as EST sequencing and microarray hybridization, the expression analyses in fungi were carried out at different time points including developing

mycelia and infection structures on articfical surfaces. Additionally the comparison between wild-type strains and mutants can also be accomplished. However, until now the results have not been satisfactory. One reason is difficult separation of the tissues; infection structures or fruiting bodies of ascomycetes are often surrounded by or embedded in vegetative mycelium. Another reason is that the tiny size especially in the early stages of development (<50 µm) leads to a difficult sample collection. Therefore the gene evaluation is not specific to the tissue in question (Teichert *et al.*, 2012).

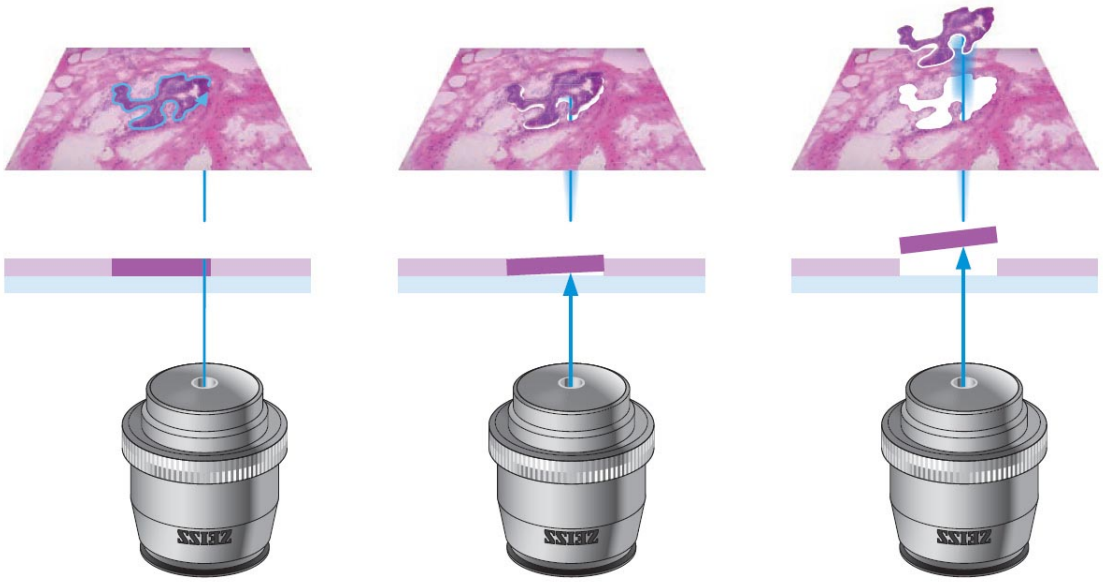

Figure 7. The laser cutting and laser catapulting processes (PALM company). Laser Microdissection and Pressure Catapulting (LMPC) technology from Carl Zeiss and developed by PALM made non-contact sampling possible. The key function is the laser catapult: The specimen is microdissected by a focused laser beam. Then a defined laser pulse transports the cut piece of the specimen out of the object plane into a collection device.

To date advances of technology provide specific tools to solve those limitations. For example, laser microdissection (LM) has become an important tool for isolating individual cells from fungi, animal or plant tissues (Figure 7). The LM approach has been successfully used to study the transcriptional reprogramming of host cells during plant–microbe interactions, such as nitrogen-fixing bacteria (Damiani *et al.,* 2012, Roux *et al.,* 2014), arbuscular mychorrhizal (Balestrini *et al.,* 2007, Gaude *et al.,* 2012), phytoplasma (Santi *et al.,* 2013) and ectomychorrhizal fungi (Hacquard *et al.,* 2013).

In case of phytopathogenic fungi this technique has been used to isolate both fungal and host plant cells after pathogen infection. It is applying to study the growth of phytopathogenic or symbiotic species *in planta* and for the analysis of gene expression differences in single, neighboring hyphae (Tang *et al.,* 2006; Tremblay *et al.,* 2008; Fosu-Nyarko *et al.,* 2010; de Bekker *et al.,* 2011; Berruti *et al.,* 2013; Balestrini *et al.*, 2014; Lenzi *et al.,* 2015, Klug *et al.,* 2015). In LM, sample preparation is a critical step involving fixing samples with appropriate

fixatives to preserve the integrity of the cell morphology and target metabolites (e.g., RNA). After marking the cells in high accuracy, sample sections are dissected by a laser focused through a microscope. Afterwards LM samples are collected into a protective (e.g., RNAse-free) medium or particular container for subsequent sample preparation. For example, isolated RNA can then be subjected to gene expression studies such as quantitative RT-PCR, microarray analysis or next generation after a linear RNA amplification process (Fosu-Nyarko *et al.*, 2010).

RNA-Seq using "Next Generation Sequencing" technologies provides a far more precise measurement of transcript levels and their genes compared to other methods such as microarrays (Wang *et al.*, 2009). In RNA-Seq experiments, alignment to a reference genome is performed with millions of short sequence reads and the number of reads that fall into a particular genomic region is recorded, as read count data. In addition to mRNA transcripts, RNA-Seq can look at different populations of RNAs to include total RNA, microRNA (miRNA), small interfering RNAs (siRNA), long noncoding RNAs (lncRNA), or messenger RNA (mRNA), and ribosomal profiling (Maher *et al.*, 2009).

The combination of LM and RNA-seq has been firstly applied to the analysis of fungal organ-specific transcriptomes by Teichert *et al.,* (2012). They established an LM protocol for isolating protoperithecia (young fruiting bodies that are more-or-less spherical without a differentiated neck) of *S. macrospora*, and used amplified RNA from the microdissected samples in subsequent RNA-seq analysis (Teichert *et al.*, 2012). LM was used to accurately cut stomata cells and surrounding areas of grapevine leaves infected with *Plasmopara viticola* at early stages of infection. This combined method shows the efficiency in the survey of site-specific regulation of transcriptional response (Lenzi *et al.,* 2016).

Taken together, combination of RNA-seq and LM is a powerful methodology for understanding the molecular processes underlying the development of multicellular organisms. It can isolate precisely single cells from heterogeneous tissues or specific cell groups and also allows single-cell gene expression analyses (Emmert-Buck *et al.,* 1996).

1.10. Transcriptome profiling of *F. graminearum* during infection

As a result of its devastation in the field, *F. graminearum* is one of the most intensively studied fungal pathogens (Goswami and Kistler, 2004). Its genome has been sequenced and annotated by Cuomo *et al.* (2007). Lately due to the development of technology for exploring the transcriptome of this pathogen, many studies have been performed under a variety of different

stages of infection on wheat, barley and maize (Sieber *et al.*, 2014; Harris *et al.*, 2016). A large number of candidate enzymes involved in secondary metabolite biosynthesis as well as unknown metabolites exhibited strong gene expression correlation during infection and presumably play a role in virulence (Sieber *et al.*, 2014). Furthermore, gene expression profiles of *F. graminearum* were undertaken during the early developmental stages of conidia germination (Seong *et al.*, 2008); under different conditions in culture, like nitrogen or carbon starvation, DON-inducing and non- inducing conditions (Gardiner *et al.*, 2009a) and during growth on complete media.

In *F. graminearum* global transcriptome profiling during infection of barley spikes and wheat spikes, stalks, crown, and coleoptiles has been performed using Affymetrix gene chips (Güldener *et al.*, 2006; Stephens *et al.*, 2008; Guenther *et al.*, 2009; Lysøe *et al.*, 2011; Zhang *et al.*, 2012). Studies profiling gene expression during the initial 196 h after inoculation have detected 10007 probe sets in wheat and 7777 probe sets in barley (Lysøe *et al.*, 2011). Comparison of gene expression profiles from *F. graminearum* infected spikes to those from mycelium grown under different *in vitro* conditions identified from 416 to 799 genes expressed specifically *in planta* (Güldener *et al.*, 2006; Guenther *et al.*, 2009; Lysøe *et al.*, 2011). In another study 344 genes preferentially expressed *in planta* were identified comparing fungal transcriptomes from laser-captured hyphae growing within the wheat coleoptile and in culture grown mycelium (Zhang *et al.,* 2012). Analyses revealed 67 gene clusters coding for potential secondary metabolites. Additionally 20 gene clusters with unknown metabolites display strong gene expression correlation *in planta* and presumably play a role in virulence (Sieber *et al.*, 2014).

The transcriptome data of *F. graminearum* was also compared with a variety of approaches; during pathogenic growth in barley infection (Güldener *et al.*, 2006), during early wheat infection (Stephens *et al.*, 2008; Guenther *et al.*, 2009; Lysoe *et al.*, 2011b; Erayman *et al.*, 2015), as well as examination of mycelia at distinct growth stages inside of wheat coleoptiles (Zhang *et al.*, 2012). Recently, comparisons of *F. graminearum* transcriptomes were performed on living or dead wheat heads to differentiate substrate-responsive and defense-responsive genes (Boedi *et al.*, 2016). Those studies indicated fungal genes which are directly associated with pathogenicity and expressed during infection. However, some fungal genes expressed during infection may not be correlated to pathogenic processes but simply responding to a specific plant tissue while others may be directly involved in the pathogenic process (Boedi *et al.*, 2016).

A recent study from Harris *et al.* (2016) compared the transcriptome of *F. graminearum* during early infection (up to 4 d post-inoculation) on barley, maize, and wheat using custom oligomer microarrays. This study identified 69 *F. graminearum* genes as preferentially expressed in developing maize kernels relative to wheat and barley spikes. These host-specific differences demonstrate the genomic flexibility of *F. graminearum* to adapt to a range of hosts (Harris *et al.*, 2016).

1.11. Aim of the study

This thesis is focused on the role of posttranslational hypusination of the eukaryotic translation initiation factor 5A (eIF5A) in *Zea mays* and *Fusarium graminearum* trough the regulation of the biosynthetic enzymes deoxyhypusine synthase (DHS) and deoxyhypusine hydroxylase (DOHH).

Studying maize, I aim to:

Firstly, investigate the role of DHS in *Zea mays* development and fungal resistance. Therefore, DHS1-silencing and overexpressing T3 lines were generated. They were used to:

(1) Survey the relative expression of genes in the eIF5A pathway.
(2) Characterize the phenotype of the DHS-silencing and DHS-overexpressing transgenic lines.
(3) Test the resistance of transgenic maize towards the leaf pathogens *Bipolaris sorokiniana, Cochliobolus heterostrophus,* and *Colletotrichum graminicola.*
(4) Determine the transcriptional changes of defense genes in these transgenic lines during fungal infection.

Studying *F. graminearum*, I aim to:

(1) Transcriptionally characterize the *F. graminearum* strains differing in their hypusination of eIF5A during early wheat infection.
(2) Analyse infection structure formation of wild type (WT), DHS- and DOHH overexpressing mutants (DHSoex and DOHHoex)
(3) Prepare and collect infection structures, isolate mRNA and produce optimal LD-PCR from low amounts of fungal material.
(4) Analyse differential gene expression in DOHHoex compared to WT and determine the transcripts which are missing in an avirulent mutant and may play an important role in infection cushion formation and subsequent infection.
(5) Analyse differential gene expression in DHSoex compared to WT and find out the transcripts which are necessary in a hypervirulent mutant.
(6) Analyses differential gene expression during early infection and growth in culture.

2. Materials and Methods

2.1. Chemicals and reagents

Reagents

All reagents used in this study were purchased from the following companies, unless stated otherwise. Specific reagents used in this study are listed in Table 1. Specific Kits for RNA extraction and cDNA libraries preparation are listed in Table 2.

Table 1. List of reagents

Reagents	Company	Location
LightCycler® 480 SYBR Green I Master	Roche	Germany
Trizol pEQGold	Thermo Fisher Scientific	Germany
One Taq 2x Master Mix with Standard Buffer	New England Bio Labs	Germany
SuperScript II RNase H Reverse Transcriptase	Thermo Fisher Scientific	Germany
RevertAid H Minus Reverse Transcriptase	Thermo Fisher Scientific	Germany
Liquid Cover Glass	Zeiss	Germany
Tween 20	Carl Roth	Germany
Sucrose and fructose	Carl Roth	Germany
Phenol	Carl Roth	Germany
Chloroform	Carl Roth	Germany
Ethanol	Carl Roth	Germany
Yeast extract	Carl Roth	Germany
DifcoTM granulated Agar	Becton Dickinson	USA
Peptone	Becton Dickinson	USA

Table 2. List of kits

Kits	Company	Location
Dynabeads® Oligo (dT)25	Thermo Fisher Scientific	Germany
SMARTer™ Pico PCR cDNA Synthesis Kit	Clontech	USA
NucleoSpin Exctract II columns of a PCR clean-up Gel extraction Kit	Machery & Nagel	USA
NucleoSpin Plant	Machery & Nagel	USA
Advantage 2 PCR Kit - Cat. Nos. 639206 & 639207	Clontech	USA
End-It DNA End-Repair Kit	Thermo Fisher Scientific	Germany
RNeasy Micro Kit	Qiagen	USA

2.2. Biological samples

2.2.1. Fungal strains

Fungal strains for maize infection

The *Colletotrichum graminicola* strain was kindly provided by Dr. Richard O´Connell from INRA-AgroParisTech, France.

Table 3. Fungal strains used for maize infection

Name	Host plant	Conidiation medium
*C. heterostrophus C4-GFP**	Maize	CMA (See 2.4)
*B. sorokiniana-GFP**	Wheat, maize	CMA (See 2.4)
*C. graminicola-GFP**	Wheat, maize	Half-strength oat meal (See 2.4)

*The PIGPAPA vector was used to introduce the EGFP protein in the fungal strains in order to visualize the infection ratio in the different maize lines studied (Horwitz *et al.*, 1999).

Fungal strains for wheat infection

All mutants are in the genetic background of the *F. graminearum* wild type strain Fg-8/1 Schwabe (teleomorph: *Gibberella zeae* [Schwein] Petch) commonly found on fields in Europe. The strain was isolated and kindly provided by Prof. Dr. Thomas Miedaner (Landessaatzuchtanstalt, Hohenheim, Germany) (Miedaner *et al.*, 2000). The used wild type strain will be named in the following as WT.

To produce constitutively GFP expressing strains for histological studies the eGFP reporter gene was introduced into the wild type strain, and the overexpressing mutants, DHSoex and DOHHoex. The wild type strain and the overexpressing mutants were transformed by plasmid mediated homologous integration as described previously (Maier *et al.*, 2006).

Table 4. *F. graminearum* strains used for wheat infection and transcriptome production.

Name	Genetic bacground	Phenotype	References
WT-GFP	Wild type Fg. 8/1	Wild type	Miedaner *et al.*, 2000
DHSoex-GFP	Deoxy hypusine synthase gene overexpressed under the gpdA promoter	Hypervirulent	Martinez-Rocha, *et. al.*, 2016
DOHHoex-GFP	Deoxy hypusine hydroxylase under the gpd1 promoter	Non-virulent	Martinez-Rocha, *et. al.*, 2016

2.2.2. Maize lines

The maize lines used for this study were produced by Mayada Woriedh and Conni Staerkel during their PhD thesis with the help of DNA Cloning Services, University of Hamburg and S. Amati, University of Hamburg. During this study, a T3 generation for each line was produced and used for further experiments.

Table 5. Maize lines used in this study.

Name of maize line	Inserted construct	Reference	Renamed line	Generation (produced during this study)
WT HiIIA	-		WT	-
DHS-RNAi-M1.1	DHS-RNAi	Woriedh, M. PhD Thesis, 2010	Si-1	T3
DHS-RNAi-M1.2	DHS-RNAi		Si-2	T3
DHS-RNAi-M4.1	DHS-RNAi		Si-3	T3
DHSoe-HiIIBxM10-13b	DHS-Oe	Stärkel, C. PhD Thesis, 2011	Oe-1	T3
DHSoe-M4.1	DHS-Oe		Oe-2	T3

2.2.3. Wheat plants

In this study, the spring wheat (*Triticum aestivum* L.) cultivar Nandu (EWDB, Accession no. RICP 01C0203421) was used for fungal infection studies. Wheat plants were grown in plastic pots at 18 - 20°C, 60% relative humidity, and a photoperiod of 16 h. At the early stages of anthesis (GS - growth stage 61 - 65 according to Zadoks *et al.*, 1974) wheat plants were transferred to a growth chamber (Weiss-Technik) and cultivated under 16 h illumination and a temperature of 18°C at day, and 16°C at night.

2.3. Primers

All oligonucleotide primers used in this study were designed using Oligo program (Primer Analysis Software - version 6.45, USA). This software calculates hybridization temperature and secondary structure of an oligonucleotide based on the nearest neighbor ΔG (change in free energy) values. Primers were generally 20 - 40 nucleotides in length and had a GC content of 40 - 60 %. All primers are listed in 5´- 3´ direction.

The following primers were used in this study:

T**able 6. Primers for Maize DHS verification of plasmid insertion.**

Name	Sequence (5'→ 3')	Description
Cre_F	CCATCGCTCGACCAGTTTAG	Forward primer *Cre*
Cre_R	TCGACCAGGTTCGTTCACTC	Reverse primer *Cre*
Bar_F	GGTCTGCACCATCGTCAACC	Forward primer *Bar*
Bar_R	ACCACGTCATGCCAGTTCC	Reverse primer *Bar*

Table 7. Primers to verify heat shock efficiency in the maize DHS RNAi lines.

Name	Sequence (5'→ 3')	Description
CS Ubi int F	CCTGTTGTTTGGTGTTACTTCTG	Forward primer *Ubi*
CS spacer GUS 3' R	ACCAACGCTGATCAATTCCA	Reverse primer *Spacer*

Table 8. Primers to verify heat shock efficiency in the maize DHS overexpression lines.

Name	Sequence (5'→ 3')	Description
CH_mDHS1_F	ATTTCCTATCCGGTTCAGTCC	Forward primer *DHS*
CH_mUbi1_R	TTAGCCCTGCCTTCATACGC	Reverse primer *Ubi*

Table 9. Primers for maize *DHS1, DHS2, DOHH, eIF5A1, eIF5A2* and *eIF5A3* qPCR.

Name	Sequence (5'→ 3')	Description
CS_Maize_DHS1_qF	GGCATACAAGAATAACATCCCT	Forward primer *DHS* (GenBank: NM_001155612)
CS_Maize_DHS1_qR	CTCCACCAAGAACTATAATCCC	Reverse primer *DHS* (GenBank: NM_001155612)
CH_ZmDHS2_qF	GTGCTCACGCTTTCTGCTGT	Forward primer *DHS2* (GenBank: NP_001130806.1)
CH_ZmDHS2_qR	ACCCCCAGCAGTCGTAACAA	Reverse primer *DHS2* (GenBank: NP_001130806.1)
CH_ZmDOHH_qF	CCACTTCACCCTTTCTCTCA	Forward primer *DOHH* (GenBank: NP_001130218.1)
CH_ZmDOHH_qR	AGCATCTCCACCATCATTCC	Reverse primer *DOHH* (GenBank: NP_001130218.1)
CH_ZmeIF5A1_qF	GATGACCTCAGGCTTCCGAC	Forward primer *eIF5A1* (GenBank: NC_024460.1)
CH_ ZmeIF5A1_qR	GTTCTTGCCCCCGATCTCCT	Reverse primer *eIF5A1* (GenBank: NC_024460.1)
CH_ZmeIF5A2_qF	CCGCATGTGAACCGTACTGA	Forward primer *eIF5A2* (GenBank: NC_024460.1)
CH_ZmeIF5A2_qR	CTGGACAGTCACAACAAGATC	Reverse primer *eIF5A2* (GenBank: NC_024460.1)
CH_ZmeIF5A3b_qF	ATCGTCATCAAGAACCGCC	Forward primer *eIF5A3* (GenBank: NM_001112136)
CH_ZmeIF5A3b_qR	TCTATGGCAACAAAGTGGCA	Reverse primer *eIF5A3* (GenBank: NM_001112136)
CH_18SrRNA_mai_1F	CCTGCTGCCTTCCTTGGATG	Forward primer *18SrRNA* (GenBank: U42796)
CH_18SrRNA_mai_1R	GATGGTACGTGCTACTCGGATAACC	Reverse primer *18SrRNA* (G

		enBank: U42796)
CH_ZmGAPc_F	CTGGTTTCTACCGACTTCCTTG	Forward primer GAPc (GenBank: EU953063)
CH_ZmGAPc_R	CGGCATACACAAGCAGCAAC	Reverse primer GAPc (GenBank: EU953063)

Table 10. Primers for Maize defense genes qPCR.

Name	Sequence (5'→ 3')	Description
CH_ZmPal_Fw	CGAGGTCAACTCCGTGAACG	Forward primer *Pal* (GenBank: L77912)
CH_ZmPal_Rev	GCTCTGCACGTGGTTGGTGA	Reverse primer *Pal* (GenBank: L77912)
CH_ZmHpl _Fw	TACGAGATGCTGCGGATG	Forward primer *Hpl* (GenBank: AY540745)
CH_ ZmHpl_Rev	CTCGAAGTCGTCGTAGCG	Reverse primer *Hpl* (GenBank: AY540745)
CH_ ZmGsl_F_2	CCAGGCAATGATGATGTTAG	Forward primer *Gsl* (GenBank: XM_008676820)
CH_ ZmGsl_R_2	GGGGTTAAAACACTGAATGC	Reverse primer *Gsl* (GenBank: XM_008676820)

ZmPal: *Zea mays* phenylalanine ammonia-lyase known SA-responsive (Morris *et al.*, 1998; Farag *et al.*, 2005).

ZmHpl: Zea mays hydroperoxide lyase known JA-responsive (Feussner and Wasternack, 2002; Nemchenko *et al.*, 2006).

ZmGsl known 1.3-beta-glucan synthase-responsive.

Table 11. Primers for amplification of specific fungal strains genes.

Name	Sequence (5'→ 3')	Description
CH_Coll_ITS1_F	AACCCTTTGTGAACGTACCTA	Forward primer (GenBank: AJ536217)
CH_Coll_ITS1_R	TTACTACGCAAAGGAGGCT	Reverse primer (GenBank: AJ536217)
CH_Coch_gpd_F	CCCTCGCCTGACGCCCCCAT	Forward primer (GenBank: X63516)
CH_Coch_gpd_R	CGAGGACACGGCGGGAGTAA	Reverse primer (GenBank: X63516)
CH_Bipo_URP_F	GGTCCGAGACAACCAACAA	Forward primer (GenBank: HM543724)
CH_Bipo_URP_R	AAAGAAAGCGGTCGACGTAA	Reverse primer (GenBank: HM543724)

The author's initials are abbreviated by "CS" or "CH" for primer ordering according to current laboratory practices. Primers were ordered from MWG Operon, Hamburg, Germany.

2.4. Media and culture conditions.

CM medium (Leach, Lang *et al.,* 1982):

- Solution A (100x): 100 g/l $Ca(NO_3)_2$ x 4 H_2O.

- Solution B (100x): 20 g/l KH_2PO_4; 25 g/l $MgSO_4$ x $7H_2O$; 10 g/l NaCl (sterilized by filtration).

- Solution C: 20% (w/v) Glucose (sterilized by filtration through 0.2 μm filter).

- Suspension D (100x): 60 g/l H_3BO_3; 390 mg/l $CuSO_4$ x $5H_2O$; 13 mg/l KI; 60 mg/l $MnSO_4$ x H_2O; 51 mg/l $(NH_4)_6Mo_7O_{24}$ x $4H_2O$; 5.48 g/l $ZnSO_4$ x $7H_2O$; 932 mg/l $FeCl_3$ x 6 H2O; 2ml Chloroform (added for sterilization of the solution).

- Solution E: 1 g Yeast extract; 0.5 g Casein, hydrolyzed by enzymatic cleavage; 0.5 g Casein, hydrolyzed by acid degradation.

To prepare 1 liter of CM, 10 ml of solution A was added to 929 ml H_2O and was sterilized in the autoclave. For solid CM media, 16 g/l granulated agar was supplemented before autoclaving. Then 10 ml of the solution B, 50 ml of the solution C, 1 ml of the suspension D and the complete solution E were added. For selection of the transformants, 40-100 μg ml^{-1} Hygromycin B was added to the solid medium.

CMA (Complete media)

To prepare 1 liter of CMA media, these components are as follows:

50 ml	20X Nitrale salts (see below)
1 ml	Trace elements (see below)
10 g	D-Flucose
2 g	Peptone
1 g	Yeast extract
1 g	Casamino acids
1 ml	Vitamin solution
15 g	Agar
pH = 6.5 (w/NaOH)	Autoclave

20X Nitrale salts

120 g	$NaNO_3$
10.4 g	KCl

10.4 g	$MgSO_4.7H_2O$ (5.2 g if anhydrous)
30.4 g	KH_2PO_4
H_2O to 1 l	Autoclave

Trace elements

80 ml	H_2O
2.2 g	$ZnSO_4.7H_2O$
1.1 g	H_3BO_3
0.5 g	$MnCl_2.4H_2O$
0.5 g	$FeSO_4.7H_2O$
0.17 g	$CoCl_2.6H_2O$
0.16 g	$CuSO_4.5H_2O$
0.15 g	$Na_2MoO_4.2H_2O$
5 g	Na_4EDTA

Half-strength oat meal

Oatmeal agar (Difco BD, USA) was used for this preparation.

36.25 g of the powder was suspended in 1 liter of purified water and mixed thoroughly. Afterward it was heated with frequent agitation and boiled for 1 minute to completely dissolve the powder. Finally, medium was autoclaved at 121°C for 15 minutes.

Water agar

Granulated agar 20 g

Distilled water 1000 ml

SNA medium (Nirenberg, 1981)

Components of 1 l SNA are as follows:

1 g	KH_2PO_4
1 g	KNO_3
0.5 g	$MgSO_4$ x 7H2O
0.5 g	KCl
0.2 g	Glucose
0.2 g	Saccharose
1 l	H_2O
16 g	granulated agar (used for solid agar plate)

2.5. General molecular methods

2.5.1. DNA extraction

2.5.1.1. DNA extraction from plant material

DNA was isolated from plant material following the cetyl trimethyl ammonium bromide - CTAB protocol (Pallota *et al.*, 2000). In short, ca. 300 mg leaf material were put in a screw cap tube and frozen in liquid nitrogen after adding two steel spheres to each tube. The samples were ground in the Retsch mill at highest speed for 3 minutes and kept under liquid nitrogen before further processing. To each tube 900 µl CTAB-Lysis buffer (1 M Tris-HCl pH 8.0, 5 M NaCl, 0.5 M EDTA pH 8.0, CTAB, H_2O) were added and the samples were vortexed thoroughly and incubated for 15 minutes at 65°C. Subsequently, the samples were centrifuged for 10 minutes at 13.000 rpm and room temperature. The supernatant was pipetted into a new 2 ml-tube. 900 µl of chloroform were added to each tube. Samples were mixed vigorously or the tubes were inverted 10 times, spun for 10 minutes at 13000 rpm, and the supernatant was transferred to a fresh tube. Next, 750 µl isopropanol were added to each sample and inverted 25 times, followed by 25 minutes of incubation at -20°C. All samples were centrifuged for 30 minutes at 4°C. The supernatant was discarded and pellets were washed once with 500 µl 70% ethanol, then air dried and resuspended in 50 - 100 µl of DEPC water or TE buffer, with 10 µg/ml RNAse.

2.5.1.2. DNA extraction from fungal material

Fungal DNA was extracted with CTAB method (Cubero *et al.,* 1999).

2.5.2. RNA extraction from plant material

RNA was efficiently isolated according to the following Trizol protocol (pEQGold, Invitrogen). 200 mg of dried leaf material (lyophilized samples) were ground under liquid nitrogen in a Retsch Mill, extracted with 1 ml Trizol and centrifuged at full speed (13000 rpm) for 5 min. Supernatant was pipetted into a new tube and mixed with 200 µl of chloroform. Tubes were shaken vigorously by hand (or votex) for 15 seconds and incubated at RT for 3 minutes. Then tubes were centrifuged at 13000 rpm for 15 min at 4°C. The upper aqueous phase was transferred to a new tube and was added 1 volume of isopropanol. Tubes were mixed thoroughly by inverting several times and incubated at -20°C for 25 minutes. The mixture was then centrifuged for 30 min at full speed and 4°C, and the pellet washed with 70% ethanol, air dried, and resolved in 40 µl DEPC water. RNA integrity was examined on nanodrop and agarose gel.

2.5.3. PCR

OneTaq 2X Master Mix with standard buffer was used in all Polymerase Chain Reaction (PCR) processes. The following guidelines are provided by the company to ensure a successful PCR.

Component	25 µl reaction
10 µM Forward Primer	1 µl
10 µM Reverse Primer	1 µl
Template DNA	variable
OneTaq 2X Master Mix with Standard Buffer	12.5 µl
Nuclease-free water	to 25 µl

Step	Temp	Time
Initial denaturation	94°C	30 seconds
30 Cycles	94°C	15 - 30 seconds
	45 - 68°C	15 - 60 seconds
	68°C	1 minute/kb
Final extension	68°C	5 minutes
Hold	4 - 10°C	

2.5.4. cDNA synthesis

Before cDNA synthesis, 2µg of RNA were treated with Dnase to avoid DNA contamination. Afterward synthesis of cDNA was carried out using components from Fermentas, St. Leon-Rot, Germany. For RT-PCR, SuperScript II RNase H Reverse Transcriptase (Invitrogen, Germany) was used, according to the manufacturer's instructions. The resulting single-stranded cDNA was later used as a template for quantitative real-time PCR (qRT-PCR) reactions.

2.5.5. Expression analysis by Quantitative Real Time PCR (qPCR)

QPCR was conducted in a Roche Light Cycler 480, using Roche SYBR Green Master Mix. Transcript levels of the target genes were normalized against β-tubulin (fungi) or 18s (maize) gene expression. The qRT-PCR reactions were carried out using gene-specific primers (Table

9, 10, 11) and a dilution 1:20 of cDNA prepared as mentioned in section 2.5.4 in a final volume of 10 µl. The PCR program was as follows: incubation for 2 min at 50°C, then 2 min at 95°C, followed by up to 40 cycles of denaturation at 94°C for 30 s, annealing at 55 - 58°C for 30 s and extension at 72°C for 15 s, followed by a melting curve analysis in order to check the specificity of fragment amplification. All of the measurements were repeated twice, each with three replicates and using at least two independent mutant strains and the wild type. Relative changes in gene expression were calculated using the relative expression software tool-Multiple Condition Solver REST-MCS version 2 (REST-348, Michael W. P., 2001)

2.6. Methods used for Maize plants

2.6.1. Heat shock conditions in maize

Heat shock induction was used to activate the RNAi construct. The process used to induce the heat shock promoter in maize is described in Figure 8.

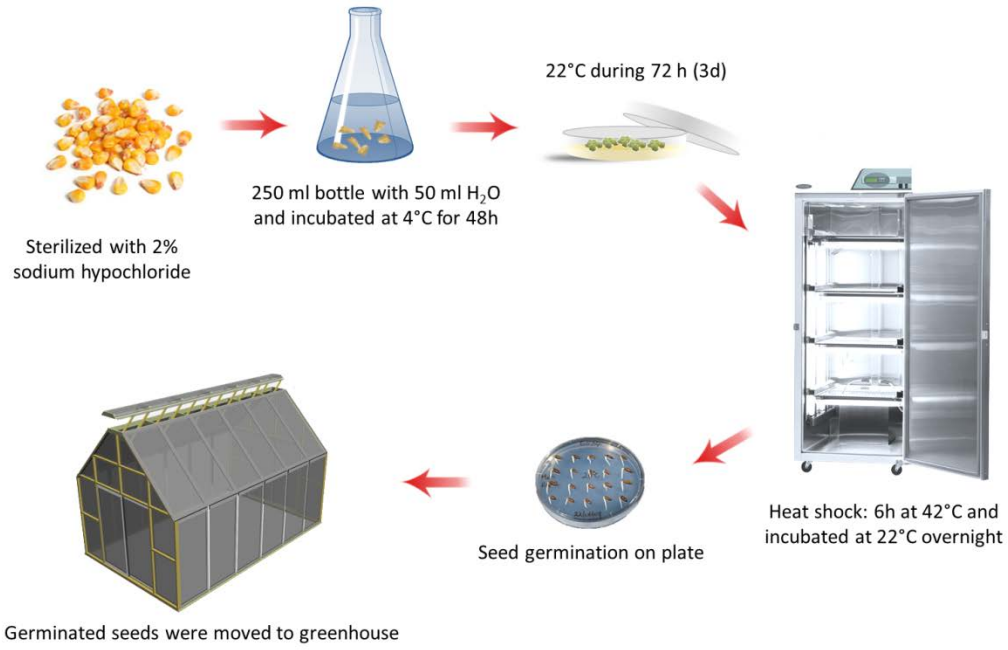

Figure 8. Heat shock proceeding in maize. The seeds of each T1 generation lines of maize were surface sterilized with 2% sodium hypochlorite for 25 minutes, washed with sterile water and placed in a 250 ml bottle with 50 ml H_2O (bottle was closed) and incubated at 4°C for 48 hours. After that, the grains were placed between two filter papers on a Petri dish. Add 4 ml of water to each filter paper. The plates were sealed with parafilm and placed at 22°C during 72 hours (3 days) to allow pre-germination of the seeds. For the next 4 days, the Petri dishes were placed in a chamber with 42°C, 80% humidity for 6 hours following this the plates were incubated at 22°C over night. In the 5th day after heat shock the seeds were transferred to soil in the greenhouse, each germling seed was potted in a small tray with a red tag (line, date and owner).

2.6.2. Temperature stress in maize

Before applying temperature stress conditions, maize plants were grown until the third leaf was fully developed at 25/22°C (day/night) in the greenhouse with a 12-hour photoperiod, a light intensity of 300 μmol m^2 and a relative humidity of 60/70% (day/night). Temperature stress was performed in a growth chamber where all conditions were controlled. The experiment was conducted with two different conditions, cold-stress at a temperature of 6 - 8°C and heat-stress at a temperature of 40 - 42°C.

2.6.3. Fungal conidia production for maize infection

C. graminicola was cultured on half-strength oatmeal agar (Difco) at 23°C for 2 weeks under continuous light. Falcate spores were collected by adding 10 ml of sterile water and rubbing the surface of the culture gently with a plastic minipestle. The conidial suspension was filtered through filter and the conidia were washed x3 in sterile water. The concentration of conidia was adjusted to $5x10^6$ spores per milliliter after the third wash. For leaf inoculations, 0.01% Tween-20 was added to the spore suspensions.

Conidia of *C. heterostrophus* C4, and *B. sorokiniana* were produced on CMA agar plates at 22°C for 2 weeks under near-UV light (TLD 36 W-08; Philips, Eindhoven, The Netherlands) and white light (TL 40 W-33 RS; Philips), harvested from plates with sterile water and a sterile glass rod. Conidia were counted with Fuchs-Rosenthal haemocytometer, and adjusted to a concentration of 50 conidia per μl.

2.6.4. Maize leaf infection with fungal strains

The maize leaf assay was carried out with detached leaves of 6 weeks old maize plants. From the middle of the leaves, 8 cm long sections were taken, surface sterilized and placed in Petri dishes with a moist sterile filter paper. One 10 μl drop of the conidia suspension (see section 2.6.3) containing 0.01 mM Tween 20 was carefully placed in the middle of each leaf section. The plates were then sealed carefully with parafilm without disturbing the drop. The plates were kept at 24°C and 16 hours for 7 days. The diameter of developing lesion was measured and the samples were used for microscope checking.

2.6.5. Histology of fungal infection in maize lines

The epidermal and sub-epidermal invasion of maize leaf infected with the fungal strains *C. heterostrophus C4-GFP*, *B. sorokiniana-GFP* and *C. graminicola-GFP* were studied by macroscopic analysis with a Leica MZFLIII fluorescence stereomicroscope and confocal laser-scanning microscope LSM 780 (Zeiss, Germany). Cross sections were produced by hand cutting with

a razor blade and immediately transferred onto a glass slide by tweezers. Microscopy of sections was performed in water. GFP fluorescence of fungal GFP expressing strains was excited at 488 nm by using an argon laser.

In some experiments, visualization of plant cell walls was observed by additional aniline blue staining of cross sections. Aniline blue was excited at 405 nm by using a diode laser.

2.6.6. gDNA quantification of fungal material in infected maize lines

To determine the presence of *C. heterostrophus C4-GFP*, *B. sorokiniana-GFP* and *C. graminicola-GFP* on maize leaves, infected plants at 6 dpi were collected and immediately frozen in liquid nitrogen. The cutting area was measured around 2 cm^2 and covered inoculated point. The endophytic content was analyzed in three independent experiments on 3 samples per line.

Genomic DNA was extracted from maize leaves using NucleoSpin Plant (Machery & Nagel, USA). Real-time quantitative PCR analysis was performed using a Roche Light Cycler 480, according to the manufacturer's guide. Quantification of fungal DNA was performed using Roche SYBR Green Master Mix, 100 ng of genomic DNA and 10 µM of specific primers for fungi (Table 11). Real-time PCR conditions were optimized to 40 cycles consisting of incubation for 2 min at 50°C, then 2 min at 95°C, followed by up to 40 cycles of denaturation at 94°C for 30 s, annealing at 55 - 65°C for 30 s and extension at 72°C for 15 s. Each reaction was performed in triplicate.

2.6.7. Statistical analysis.

Descriptive statistics including the mean and the standard error of the mean (SE) along with the Tukey range test for multiple comparison procedures in conjunction with an ANOVA were used to determine significant differences. $P < 0.05$ was considered significant.

2.7. Methods used for *F. graminearum* infection and transcriptomics

2.7.1. Conidia production

Conidia production of *F. graminearum* wild type strain and overexpressing mutants DHSoex-GFP and DOHHoex-GFP was performed on SNA agar plates. Plates were inoculated with a plaque of mycelium or 10 µl conidial suspension of $1x10^5$ conidia/ml and incubated at 18°C for 10 - 12 days under illumination with 16 h normal halogen light and 8h long wave UV light per day. Conidia were washed from the plate surface by rinsing the agar twice thoroughly with 2 ml H_2O cooled on ice. Afterwards, the amount of conidia were counted in a Fuchs-Rosenthal counting chamber and the concentration was adjusted to stock

solutions of 100 conidia per µl. Aliquots of 50, 500, and 1000 µl were stored at -70°C until use.

2.7.2. Inoculation of wheat spike and detached wheat glume

The susceptible spring wheat cultivar Nandu - *Triticum aestivum* (Lochow-Petkus, Bergen-Wohlde, Germany) was used for the bioassay with detached glumes. Plants were cultivated in a growth room at 20°C, with a photoperiod of 16 h light and 60% relative humidity, and then transferred to infection chambers with optimized conditions (16 h illumination and a temperature of 18°C at day, and 16°C at night).

Spike infection and detached wheat glume infection assays were prepared according to Boenisch and Schäfer (2011). Wheat spikes were inoculated at two of the middle florets between lemma and palea with 10 µl of 500 conidia suspension. Ten spikes were used for each assay. Each assay was repeated at least three times. For the detached wheat glume assay, spikelets of wheat plants were taken at anthesis to isolate glumes. Glumes were detached from the floret with razor blades and washed with 0.01% (v/v) Tween 20 with shaking with a magnetic stirrer for 10 minutes. Glumes were washed with sterilized water 3 times. The washing step was included to remove wheat pollen and dust from the glume surface. Subsequently glumes were placed in Petri dishes (92 × 16 mm) on 1.6% (w/v) granulated agar. Three Petri dishes containing 60 biological replicates of at least six floret organs represented one independent experiment. The adaxial side of glumes was inoculated with 5 µl sterile water containing 20 conidia per µl. 10 µl pure water was used as a negative control. After inoculation, the Petri dishes were sealed with Parafilm and incubated in a growth chamber at conditions described in section 2.2.3.

2.7.3. Macroscopical studies of fungal infection on wheat glume

To further understand the interaction between plant and fungi, macroscopic studies of inoculated wheat glumes were carried out using a Leica MZFLIII fluorescence stereomicroscope. The presence of infection structures on the whole surface of wheat glume tissues was studied and investigated after inoculation with different strains of *F. graminearum*. All stages of fungal development and wheat penetration were described in detail up to 3 weeks by Boenisch and Schäfer (2011). Based on that description, infected glumes were checked directly in Petri dishes without preparation. Using a Leica GFP3 filter set with an excitation filter at 470/40 nm and a band pass filter transmitting light at 525/50 nm, as well as with a GFP2 filter set with an excitation filter at 480/40 nm and a long pass filter at 510 nm, GFP fluorescence was observed in all GFP transformed strains being used. Using the

fluorescence stereomicroscope MZFLIII living GFP expressing hyphae were easily distinguished from plant tissue. Infection structures of different strains of *F. graminearum* were determined and marked for the further purposes. Under normal light conditions, inclined reflected light of an external halogen lamp KL 1500 Electronic was used to visualize plant necrosis as well as the mycelium.

2.7.4. Microscopic analysis and histology of infected wheat glumes

The confocal laser-scanning microscope LSM 780 was used to investigate the plant-pathogen interactions. Infected wheat glumes with different strains of *F. graminearum* were dissected by hand to produce cross sections. Subsequently, cross sections were transferred onto a glass slide by tweezers and then spread with a drop of water. A coverslip was placed over the drop of water and all bubbles were removed. GFP fluorescence of all used GFP expressing strains was excited at 488 nm by using an argon laser.

2.7.5. Scanning electron microscopy (SEM)

Inoculated glumes of wheat were prepared for scanning electron microscopy. Fixation of the samples was conducted by Elke Wölken (Cell Biology of Plants and Phycology, Biocenter Klein Flottbek, University of Hamburg). Samples were fixed according to a protocol described by Huang *et al.* 2008 using 4% (v/v) glutaraldehyde in 50 mM phosphate buffer and post-fixed with 1% (w/v) osmium tetroxide. Instead of ethanol, acetone was used in the graded series. Afterwards critical-point drying was performed by Karen Dehn (Biodiversity, Evolution and Ecology of Plants - BEE, Biocenter Klein Flottbek). At the critical-point drying, acetone was replaced by liquid carbon dioxide. Dried samples were mounted on stubs with carbon tabs and Ponal Classic. After at least 48 hours of drying in a desiccator, the samples were sputter-coated with gold using apparatus SCD 050. The scanning electron microscope SEM LEO 1525 was used operating at 6 kV. Preparation of the samples was carried out depending on the purpose. To get an insight into the epidermis, the dried glumes were cut freehand with a razor blade before decal on the sample plate.

2.7.6. Laser capture microdissection (LCM)

Laser capture microdissection is a method used for isolating specific cells of interest. In this study, this method was used to isolate different infection structures formed on wheat flower leaves by different mutants of *F. graminearum* (Figure 9).

For laser capture microdissection (LCM) glumes were inoculated with 5 µl of 2 x 10^4 conidia per ml suspension of WT-GFP, DHSoex-GFP or DOHHoex-GFP mutants and incubated as

described in section 2.7.2. Glumes at 9 - 10 dpi were taken for isolation of 1 - 2 mm^2 tissue samples containing infection cushions and runner hyphae. Samples were collected by a sterilized razor blade and immediately transferred to a new tube containing 99% ethanol, and kept on ice. After collection of 20 - 30 specimens per sample, the ethanol was gently removed and samples were lyophilized overnight. Samples were then stored at -80°C. The next step was done immediately the day after to avoid unexpected degradation. The transfer of infection structures from glume to glass slides was performed under sterilized conditions. Glass slides, tweezers and platform used in this method were sterilized by ethanol 70% and by being left in drying oven at 200°C overnight. Afterwards infection structures were transferred from the glume surface on RNase-free glass slides at room temperature. The glass slides were covered with Liquid Cover Glass, a resin containing solution of isopropanol. This solution was spread on glass using a RNase-free tip and dried at room temperature for 4 - 5 min. For testing the adhesive, a gloved finger was used to check the sticky surface. Subsequently 4 - 6 individual tissue samples were put on one glass slide and used for LCM. The glumes were pressed by a handle of a forcipe with its inoculated side on the sticky glass slide. The glume was carefully removed with tweezers in one quick pull. This was necessary to be sure that all infection structures were kept on the slide. The coverslip with the fungal infection structures was placed correctly into the holding tray of the inverse microscope PALM MicroBeam in order to guarantee an accurate function and comfortable work. Identification and isolation of runner hyphae and infection cushion was done by bright field microscopy in air with a 20 x objective. Through CCD video camera infection structures were selected in real time by using the auto-LPC-function (freehand circle for infection cushions and/or line marking for runner hyphae) of the PALM Robo software. To be able to precisely cut the tissue and reliably catapult it, the laser focus has to be set accurately to optimal values under right conditions. Catapulting points for the UV-A laser (λ 355 nm) was set within the selected area or along the selected line automatically by the software. The following settings were used: Curtting energy 32 at a focus of 63, catapulting at delta 25 of the cutting energy and a focus of -2. The selection of the respective tissues using PALM microscope was done for 1 hour at room temperature (20°C). An adhesive cap of a 500 µl eppendorf tube was used to capture all of selected elements after catapulting upwards (against gravity). The presence of either infection cushions or runner hyphae in the cap was verified by a so-called „Cap Check“, using a 5x and 20x objective. After catapulting, the collection tubes were carefully removed from the tube holder and stored at -80°C until mRNA isolation was performed (see section 2.7.9). To avoid contamination by the respective unwanted tissue,

runner hyphae and infection cushions were collected on separate days.

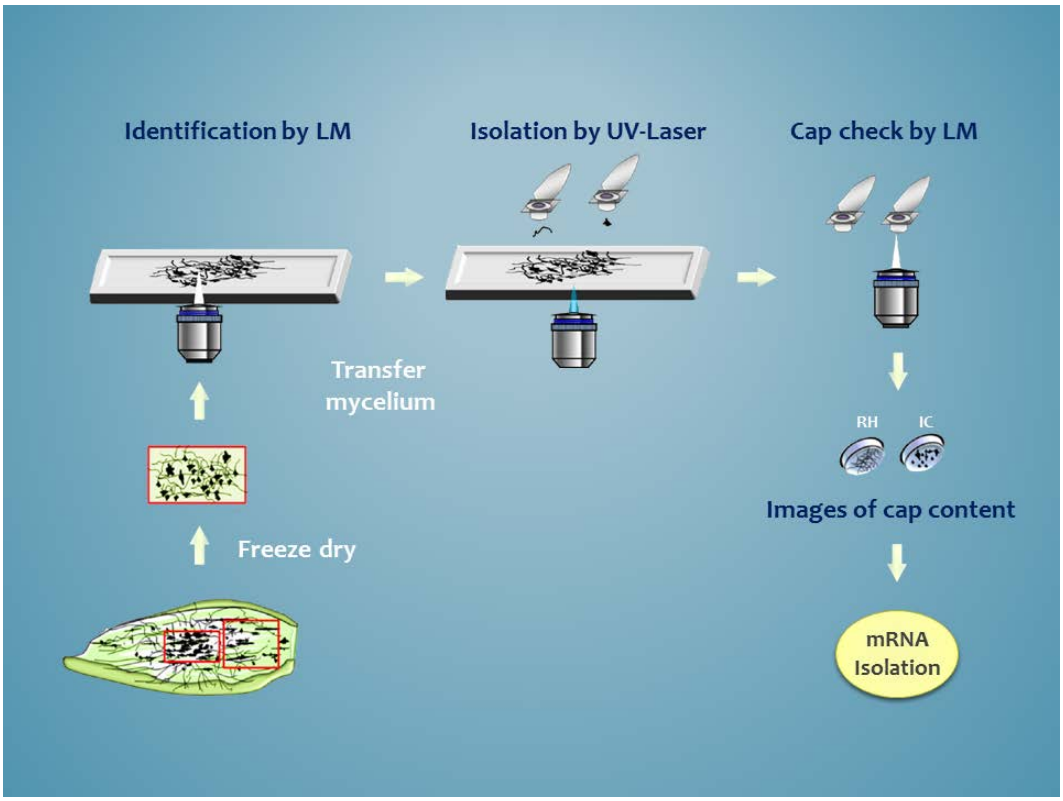

Figure 9. Scheme of the isolation of infection cushions and runner hyphae by laser capture microdissection (LCM). Small samples of glumes containing runner hyphae (RH) and infection cushions (IC) were dehydrated by ethanol, lyophilized and transferred onto an adhesive microscopy slide. RH and ICs were identified and selected by light microscopy (LM). Afterwards ICs and RH were isolated into individual adhesive caps by UV-laser impulses. The content of the cap after isolation of RH and IC was controlled by LM of the tube caps, by a so- called "cap check" (modified from Boenisch PhD Thesis, 2013).

2.7.7. Total RNA isolation from fungal mycelia

$5x10^5$ conidia of *F. graminearum* WT-GFP were incubated in an Erlenmeyer flask with 25 ml liquid CM medium for 3 days at 28°C. Mycelium was harvested by Gaze sieves and washed with sterile water 3 times prior to incubation in 99% ethanol for 1 hour on ice. Afterwards the mycelium was lyophilized overnight. Samples were then stored at -80°C. The lyophilized mycelium (0.1 mg) was homogenized in the Retsch mill at highest speed for 3 minutes and kept under liquid nitrogen before further processing. Afterwards mycelium was used for total RNA isolation with the RNeasy Micro Kit. Total RNA was eluted from RNeasy MiniElute spin columns with 14 µl of RNase-free water (Qiagen, Kit supplement). Total RNA of mycelium was diluted 1:10 before carrying out the first-strand synthesis.

2.7.8. Infection structures and runner hyphae preparation for transcriptome analysis

This method was established by Dr. M. J. Boenisch during her PhD thesis (2013). Figure 10 provides an overview of the workflow to achieve expression patterns from runner hyphae

and infection cushions following laser capture microdissection. By using dynabead oligo $(dT)_{25}$ kit, isolation of mRNA from infection cushions and runner hyphae was performed. Next, entire mRNAs bound on beads were used for first-strand synthesis by SMART (switching mechanism at 5' end of the RNA transcript)-PCR. Thereby, ss cDNAs were provided, which served as templates for ds cDNA synthesis by long distance PCR (LD-PCR). The amplified cDNA libraries were purified and sent to the next generation sequencing facility at the Heinrich Pette Institute (Hamburg, Germany), where Illumina sequencing was performed. The resulting sequencing data were mapped to the reference genome of *F. graminearum* and used for differential expression analysis by Dr. Ulrich Güldener (Institute of Bioinformatics and Systems Biology, Munich, Germany).

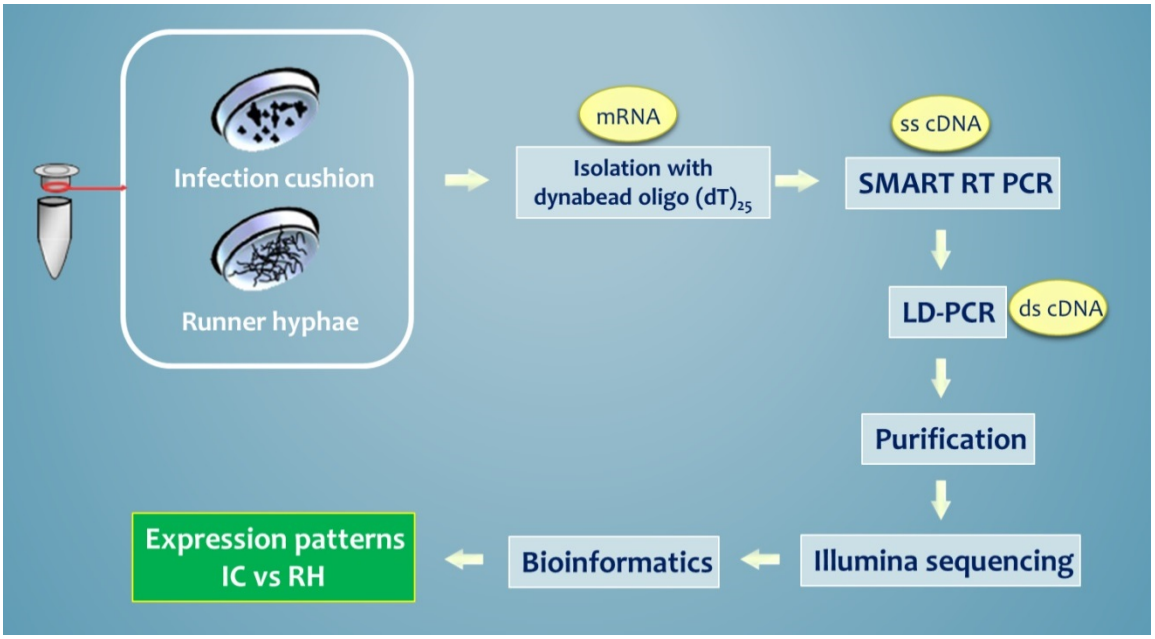

Figure 10. Scheme of the methodical workflow performed to provide expression data from runner hyphae and infection cushions isolated by laser microdissection. Isolation of mRNA from infection cushions and runner hyphae with magnetic beads was performed. The mRNAs were used for first-strand synthesis by SMART-PCR. Thereby ss cDNAs were provided, which served as templates for ds cDNA synthesis by LD-PCR. The resulting cDNA libraries were purified and sequenced by Illumina Sequencing. The resulting sequencing data were mapped to the reference genome of *F. graminearum* and used for differential expression analysis (modified from Marike Boenisch, PhD thesis, 2013).

2.7.9. mRNA isolation

Before using Dynabeads Oligo$(dT)_{25}$ from the mRNA direct Kit, the stock was resuspended thoroughly. Subsequently, 15 µl of beads was transferred to a RNase-free 1.5 ml microcentrifuge tube and placed on a magnet. After 30 seconds the supernatant was removed and the beads were washed with 50 µl lysis/binding buffer using a magnet and pipette. The lysis/binding buffer was removed by placing the suspension on the magnet for 30 seconds, or until the suspension was clears. Cell lyses was performed with 50 µl lysis/binding

buffer in collection tubes from LCM containing infection cushions or runner hyphae. The tube with the cap downwards was vortexed for 1 min at room temperature. Afterwards the washed beads were added to the cell lysate and were resuspended thoroughly by pipetting. To allow the polyA tail of the mRNA to hybridize to the oligo$(dT)_{25}$ on the beads the tube was incubated on a roller for 10 min at room temperature. The magnet was used to separate the beads from the solution between each washing step. The supernatant was removed and the beads/mRNA complex was washed twice with 50 µl washing buffer A and then twice with 50 µl washing buffer B. After removing the supernatant the beads/mRNA complex was suspended in 3 µl H_2O and transferred into a 200 µl PCR tube for first-strand cDNA synthesis by SMART-PCR (section 2.7.10).

Dynabeads Oligo$(dT)_{25}$

Approx. 5 mg beads per ml were supplied in PBS pH 7.4, containing 0.02% NaN_3 as a preservative. The used beads had a size of 2.8 µm ± 0.2 µm in diameter, a surface area of 3-7 m^2/g and a density of approx. 1.6 g/cm^3. 1 mg of the beads has the capacity to bind up to 2 µg of mRNA.

Lysis/binding buffer

100 mM	Tris-HCl, pH 7,5
500 mM	LiCl
10 mM	EDTA, pH 8
1%	LiDS
5 mM	dithiothreitol (DTT)

Washing buffer A

100 mM	Tris-HCl, pH 7,5
0.15 M	LiCl
1 mM	EDTA
1%	LiDS

Washing buffer B

10 mM	Tris-HCl, pH 7,5
0.15 M	LiCl
1 mM	EDTA

2.7.10. First-strand synthesis by SMART-PCR

The SMARTer™ Pico PCR cDNA Synthesis Kit was used to perform the first-strand ss

cDNA synthesis with the beads/mRNA complex from infection cushions and runner hyphae. For the SMART (**s**witching **m**echanism **a**t 5' end of the **R**NA **t**ranscript) PCR 1 µl 3' SMART CDS - Primer II A (12 µM) were added to 3 µl beads bound to mRNA isolated from runner hyphae or infection cushions, and incubated at 72°C for 2 min in a PCR cycler Primus. Then 6 µl Mastermix was added to a total volume of 10 µl per reaction. The PCR was performed at 42°C for 90 min with a following termination step at 72°C for 10 min. PCR tubes were placed on ice for 10 min and subsequently LD (long distance)-PCR was performed (section 2.7.11.).

1x Mastermix for 10 µl SMART-PCR reaktions:

2 µl	5x First-Strand buffer
0.25 µl	DTT (100 mM)
1 µl	dNTP Mix (10 mM)
1 µl	SMARTer II A Oligonucleotide (12 µM)
0.25 µl	RNase Inhibitor
1 µl	SMARTScribe™ Reverse Transcriptase (100 U)
0.5 µl	H_2O
Total volume	6 µl

5x first-strand buffer:

250 mM	Tris-HCl (pH 8.3)
375 mM	KCl
30 mM	$MgCl_2$

3' SMART CDS Primer II A sequence

5'-AAGCAGTGGTATCAACGCAGAGTACT(30)N-1N-3'

SMARTer II A Oligonucleotide sequence

5'-AAGCAGTGGTATCAACGCAGAGTACXXXXX-3'

2.7.11. Amplification of cDNA by LD-PCR

According to the recommendation of the SMARTer™ Pico PCR cDNA Synthesis Kit, Advantage 2 PCR Kit was used to amplify the single stranded cDNA (ss cDNA) produced by SMART PCR (previous section). The optimal number of LD-PCR cycles was determined to ensure the cDNA remained in the exponential phase of amplification. The optimal number of cycle for runner hyphae and infection cushions was checked by two test LD-PCR reactions. First PCR was performed with a 50 µl LD-PCR reaction using 1 µl template and determined the optimal cycle within 15, 18, 21, 24, 27, 30 and 32 cycles by electrophoresis of

1.2 % agarose gels in 1x TAE. By an additional 25 µl LD-PCR reaction with 0.5 µl template the optimal cycle was determined for each cycle between the two cycles that showed the strongest increase of PCR product in the 50 µl reactions. After determination of the optimal cycle number for both tissues, the remaining first strand reaction of each tissue was cycled to one cycle below the where plateau was reached. The LD-PCR products were pooled and a 2 µl aliquot was loaded on a 1.2 % agarose gels in 1x TAE to determine the amount of synthesised cDNA. The remaining cDNAs were used for purification (section 2.7.12) and 5' phosphorylation of cDNAs (section 2.7.13).

LD-PCR Protocol for 50 µl reactions

After 1 µl template was added to 49 µl of a 1x Mastermix the PCR was performed in a thermal cycler (Primus) as follows:

1. 95°C 1 min
2. 95°C 15 sec ⎫
3. 65°C 30 sec ⎭ 15 cycles
4. 68°C 6 min
5. Pause at 68°C and transfer 5 µl from the 15-cycle PCR for agarose gel analysis.
6. Three additional cycles were run with the remaining PCR mixture and 5 µl transferred from the 18-cycle PCR for agarose gel electrophoresis. This step was repeated until 32 cycles.

1x Mastermix (for 50 µl PCR reactions)

5 µl	10x Advantage 2 PCR buffer
1 µl	dNTP Mix (10 mM)
1 µl	5' PCR Primer II A (12 µM)
1 µl	10x Advantage 2 Polymerase Mix
41 µl	H_2O
49 µl	Total volume

10x Advantage 2 PCR Buffer

400 mM	Tricine-KOH pH 8.7
150 mM	KOAc
35 mM	$Mg(OAc)_2$
37.5 µg/ml	BSA
0.05 %	Tween
0.05 %	Nonidet-P40

10x Advantage 2 Polymerase Mix

The mix contains a TITANIUM Taq DNA Polymerase, a proofreading polymerase, and TaqStart Antibody (1.1 µg/µl) in the following storage buffer:

10 %	Glycerol
3 mM	Tris-HCl pH 8,0
15 mM	KCl
0,01 mM	EDTA

2.7.12. Purification of cDNA libraries

In order to remove salts, primers, enzymes and other remaining substances from LD-PCR reaction containing the cDNA libraries of infection cushions and runner hyphae a purification step through silica membranes was performed. Following the recommendation of the SMARTer™ Pico PCR cDNA Synthesis Kit, NucleoSpin Exctract II columns of a PCR clean-up Gel extraction Kit were used according to the manufactures instructions. 5 - 10 µg cDNA of each tissue type were purified in two columns and the elution step was performed twice with 35 µl NE Buffer (5 mM Tris/HCl pH 8.5) per column. Finally, the elution volume per column was 68 µl (1 µl dead volume per column) and thus 136 µl of purified cDNA from infection cushions and runner hyphae were obtained in total. The purified cDNAs were further 5´-phosphorylated (section 2.7.13).

2.7.13. End-it-Reaction

The End-It DNA End-Repair Kit was used to provide 5´-phosphorylated, blunt-ended cDNAs from infection cushions and runner hyphae according to the manufactures protocol. Two End-it-Reactions of 100 µl total volume were preformed each with 68 µl purified cDNA (5-10 µg) of runner hyphae or infection cushions.

End-It-Reaction protocol

68 µl	cDNA in NE Buffer (5 mM Tris/HCl pH 8,5)
5 µl	10x End-Repair buffer
5 µl	dNTP Mix
5 µl	ATP
1 µl	End-Repair Enzyme Mix
16 µl	H_2O
100 µl	Total volume

The End-It-Reaction was incubated at room temperature for 45 minutes and then stopped by heating at 70°C for 10 minutes.

The blunt-ended cDNAs from infection cushions and runner hyphae were purified with the PCR clean-up Gel extraction Kit as described in section 2.7.12 above to remove all substances remaining from the End-it-Reaction. The elution of cDNAs was performed twice with 25 µl per column. Afterwards, the cDNAs of each sample were pooled and the amount of blunt-ended and purified cDNAs for each tissue was determined by electrophoresis of 1.2 % agarose gels. Finally, 1 µg of the blunt-ended and purified cDNAs were used for next generation sequencing (section 2.7.14).

2.7.14. RNA-seq mapping and quantification

Total RNA was sequenced by the next generation sequencing facility at Heinrich-Pette-Institute, Hamburg, Germany. The genome of *F. graminearum* and FGDB annotation version 3.2 was retrieved from http://www.helmholtz-muenchen.de/en/ibis/institute/groups/fungal-microbial-genomics/resources/index.html (Wong *et al.*, 2011). RNA-seq reads were mapped on the reference genome using tophat2 (v2.0.8). The interval for allowed intron lengths was set to min 20 nt and max 1 kb (Kim *et al.*, 2013; Trapnell *et al.*, 2009). Cufflinks were used to determine the abundance of transcripts in FPKM (**F**ragments **P**er **K**ilobase of exon per **M**illion fragments mapped) and calculated differentially expressed genes using cuffdiff (Trapnell *et al.*, 2010; Trapnell *et al.*, 2012). The gene models were included as raw junctions. Genes with a minimum of two fold increase or decrease in expression ($|\log2 \text{ of the FPKM values } +1| \geq 1$) between the two experimental conditions were considered as regulated. Significant differentially regulated genes of no functional annotation were manually re-visited.

2.7.15. Functional classification

Genes with a minimum of two fold increase or decrease in expression between the two experimental conditions were analysed for overrepresented functions. Using the FunCat catalogue of protein function (Ruepp *et al.*, 2004) in combination with Fisher's exact test (Fisher, 1922) and the MGSA-R package (Bauer *et al.*, 2010). Resulting p-values were corrected for multiple testing using the Benjamini Hochberg procedure (Benjamini and Hochberg, 1995).

3. Results

3.1. Characterization of maize deoxyhypusine synthase by silencing or overexpressing the coding gene *ZmDHS1*

3.1.1 *In silico* analyses of *ZmDHS* sequence alignment

Using the NCBI BLAST server, homologues of DHS proteins were identified by BLASTP and TBLASTN searches (Altschul *et al.,* 1997) in the non-redundant protein and EST databases respectively (Figure 11). The alignment was performed using the CLUSTAL W program.

Two genes of DHS in *Zea mays* were identified and they were called *ZmDHS1* and *ZmDHS2*. According to previous PhD work concerning DHS, *ZmDHS1* has a protein coding of 370 aa with a predicted molecular mass of 40.74 kDa and displayed a homology of 90% to wheat, 91% to rice and 72% to *A. thaliana* (Woriedh, 2010). *ZmDHS2* has a translated coding of 379 aa with a predicted molecular mass of 41.74 kDa and a homology of 84% to wheat, 83% to rice and 67% to *A. thaliana*, respectively. The amino acid identity between *ZmDHS1* and *ZmDHS2* is 84%. *ZmDHS1* has the highest similarity to DHS genes in other species. Therefore *ZmDHS1* was chosen in this study as an interesting candidate for silencing and overexpressing in maize.

To determine the importance of DHS in maize plants, silencing and overexpressing lines were created in previous studies (Woriedh, 2010; Stärkel, 2011).

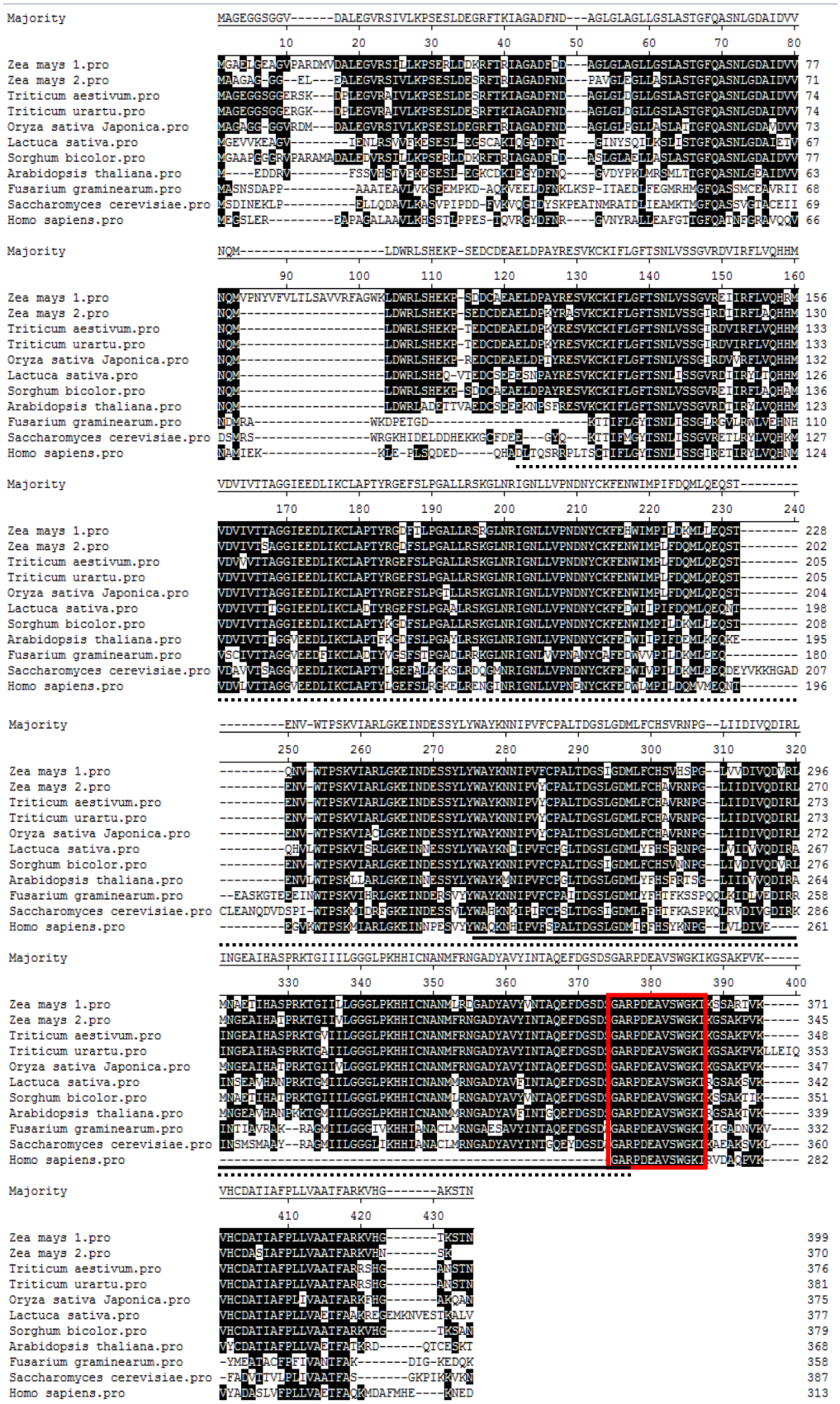

Figure 11. Alignment of the predicted amino acid sequence of DHS proteins from *Zea mays* and several organisms. The amino acids in black boxes are those identical to the consensus sequence. Genebank accession numbers, GU735677 DHS1 protein from *Zea mays*; GU735678 DHS2 protein from *Zea mays*; ACP28134.1 *Triticum aestivum* DHS; EMS56183.1 *Triticum Urartu* DHS; AAP44695.1 *Oryza sativa Japonica* DHS; AAU34016.1

Lactuca sativa DHS; EES10596.1 *Sorghum bicolor* DHS; AF296078 *Arabidopsis thaliana* DHS*;* GU809212 *Fusarium graminearum* DHS*;* P38791.1 *Saccharomyces cerevisiae*; P49366.1 *Homo sapiens* DHS. Underlined amino acids refer to the spermidine binding site (276–379). Underdoted refer to the NAD binding site from serine 121 to aspartic acid 379. The active center of the DHS protein from glutamine 360 to lysine 366 is indicated with a red box.

3.1.2. Confirmation of heat shock and recombination of the DHS RNAi and DHS overexpressing construct in maize by PCR

The heat shock elements of the regulatory region enhance the expression of the ubiquitin protein in response to temperature stress. Inducible promoters are an elegant way to start gene expression at specific time points or in certain plant organs. One of the major advantages of inducible systems is that the gene of interest is exclusively expressed at the desired locations or developmental stages. This method avoids possible side effects of the construct early during the regeneration phase as well as false positive phenotypes unrelated to the physiological trigger of the intended gene expression.

T1 seeds were produced by crossing regenerated transgenic T0 plants as the male or female parent with maize inbred line HiIIA, HiIIB (M. Woriedh, PhD thesis, 2010 and C. Stärkel, PhD thesis, 2011). Plants were back-crossed, outcrossed rather than self-pollinated to keep the transgene hemizygous and, thus, to potentially increase the stability of transgene expression, resulting in T2 seed that is hemizygous for each transgene insertion. Activation of Cre-lox system of selected plants was performed by heat shock to induce the RNAi and overexpressed *ZmDHS1* gene following the method in section 2.6.1. The method and the verified strategy are described in Figure 12. The construct is inducible with heat shock, which activates the cre-recombinase that cuts at the lox sites and moves the *ZmDHS1* gene behind the ubiquitin promoter. After the DNA extraction (Section 2.5.1.1), PCR using specific primers (Section 2.3, Table 7 and 8) was performed to verify heat shock efficiency in transgenic maize lines. A size of 797 bp in the DHS silencing maize lines (SI-1, SI-2, SI-3) and a fragment of 633 bp in the DHS overexpression maize lines (OE-1 and OE-2) confirmed the excision of the geneticin gene by the Cre-recombinase (Figure 12).

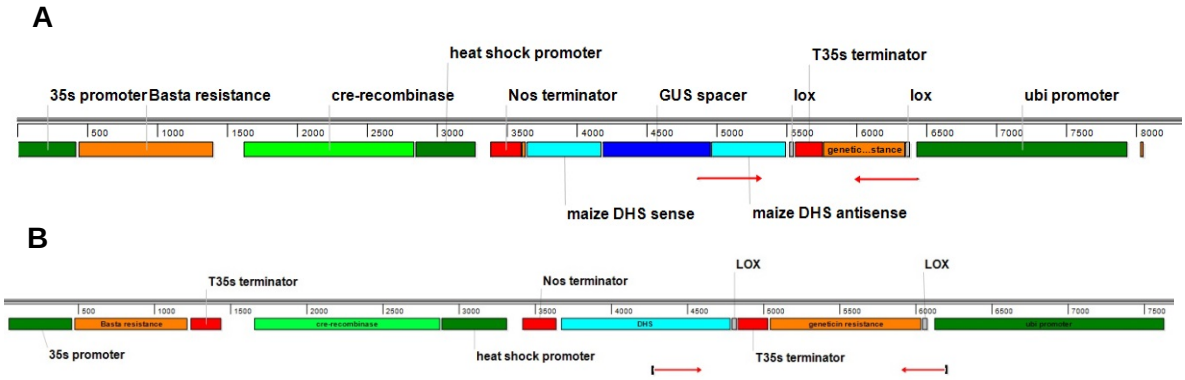

Figure 12. Schematic representation of the strategy to verify the heat shock efficiency. (A) Amplification of fragments with a size of 797 bp confirm the excision of the geneticin gene by the Cre-recombinase in the DHS silencing maize lines. **(B)** A fragment of a size 633 bp for the DHS overexpression maize lines. Red arrows indicate the primers used for the confirmation of the excision.

All transgenic seedling maize plants from T3 generation were verified to avoid the presence of non-transgenic plants or without Cre-lox activation. Each transgenic line had 20 plantlets, the verification was performed with all transgenic lines. The following plants with recombinant bands were chosen to perform further essays. For example in Figure 13, the DHS silencing line SI-1-3 and the DHS overexpressing line OE-2-2 were not chosen because of the missing band.

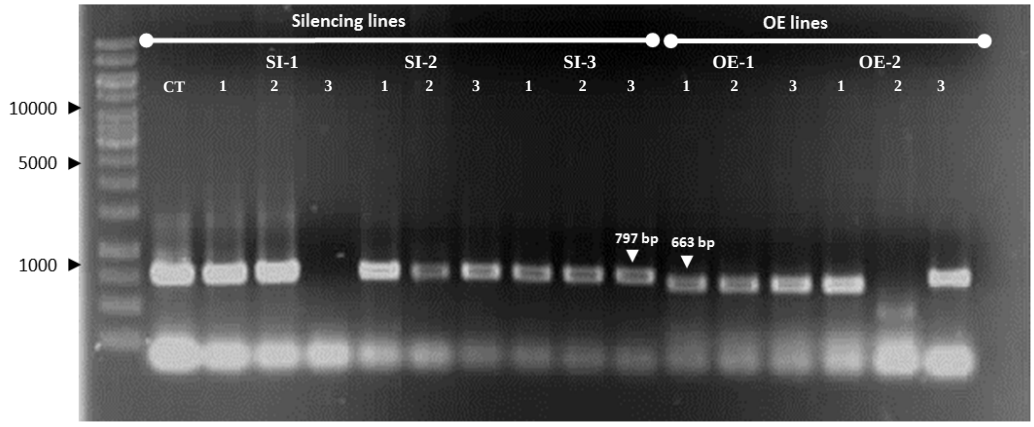

Figure 13. Verification of the introduction of constructs and Cre-lox activation in the recombinant maize lines. All of the plants - except SI-1 (3) of silencing lines (SI-1; SI-2 and SI-3) contained the recombinant band of 797 bp using primers CS_Ubi_int_F and CS_spacer_Gus_R in PCR. Overexpressing lines (OE-1 and OE-2) showed the recombinant band of 633 bp using primers CH_mDHS_1F and CH_mUbi_1R except OE-2 (2). The non-recombinant size was 1.5 kb and 1.9 kb with silencing and overexpressing lines, respectively. CT is control. PCR was conducted with 40 cycles using the Onetaq 2X master mix with standard buffer (New England BioLabs).

3.1.3. Relative expression of *ZmDHS1* and *ZmDHS2* in DHS silencing and DHS overexpressing lines

After verification of the lines containing the correct construct, expression analysis for *ZmDHS1* were carried out. Isolated RNA from transgenic plants was used to make cDNA

and run qRT-PCR (Section 2.5.2). qRT-PCR using the SYBR Green master mix (Roche) was conducted with primers CH_18SrRNA_mai_1F/R and CS_Maize_DHS_qF/R (Table 9) in order to determine the expression level of DHS in silencing and overexpressing maize lines of the T3 generation. Plant material was harvested at 1 month of age. Using 18SrRNA as a reference gene and the wild type cDNA as the standard, a 5.2, 6.09 and 8.90 fold decreases were determined for silencing lines SI-1, SI-2 and SI-3, respectively. On the contrary, a 50.32 fold increase of transcript was determined for line OE-1 and 60.44 fold increase for line OE-2 (Figure 14).

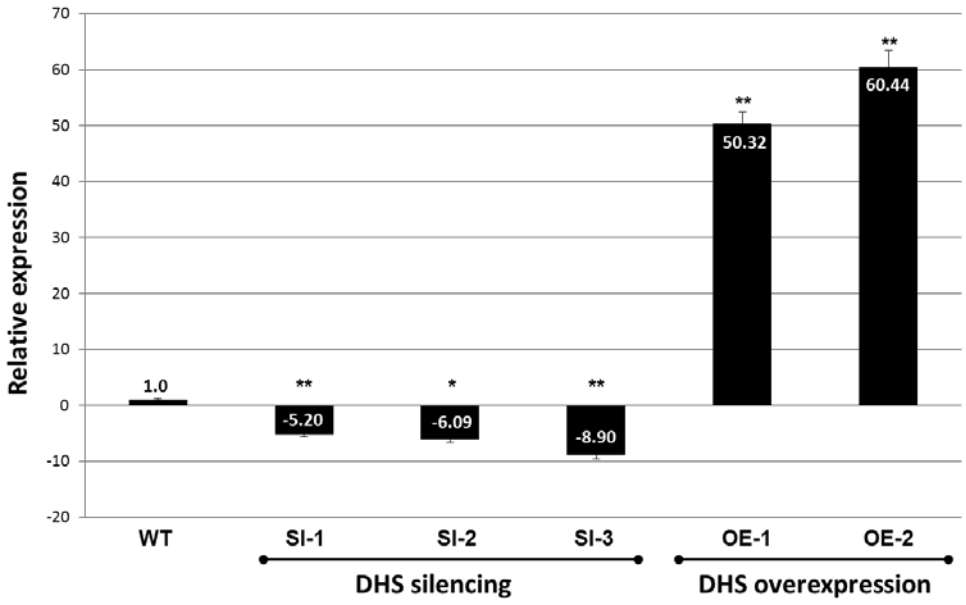

Figure 14. Relative expression levels of *ZmDHS1* in DHS silencing or DHS overexpressing lines. Silencing lines showed a decrease on DHS expression level. DHS expression level was increased in overexpressing lines. Line OE-2 has the highest increase of 60.44 fold, line OE-1 the second highest of 50.32 fold. Quantitative RT-PCR was performed with three biological and three technical replicates. The wild type expression was set at 1. The diagram was compiled using the relative expression software tool-Multiple Condition Solver REST-MCS version 2 (REST-348, Michael W. P., 2001). Quantitative RT-PCR was performed in triplicate, with three replicates each. Wild-type expression was set at 1. Error bars indicate standard deviations calculated from data per triplicate samples and are representative of three independent experiments. Significance with respect to wild type: *$p < 0.05$, **$p < 0.01$, ****$p < 0.0001$ (calculated with ANOVA-Bonferroni-Holm).

The expression results provide strong evidence for the activation of the silencing and overexpressing DHS constructs in maize plants.

In addition, expression of the second DHS gene *ZmDHS2* was determined using specific primers (Table 10).

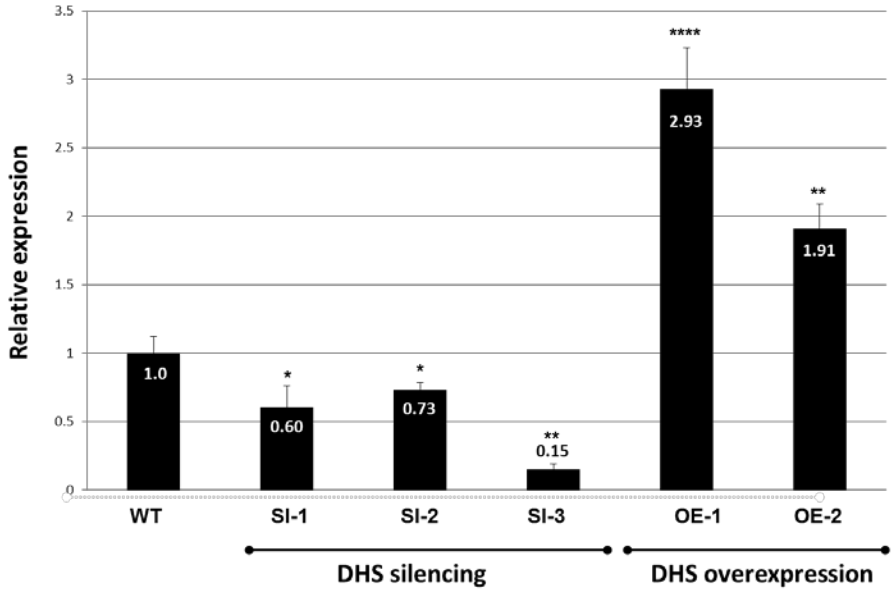

Figure 15. Relative expression of *ZmDHS2* in DHS silencing and DHS overexpressing lines. Expression of DHS2 was down-regulated in all silencing lines compared to the wild type. On the contrary, DHS2 expression was up-regulated in DHS overexpressing lines, approximate 2-fold time in OE-2 and 3-fold time in OE-1. Quantitative RT-PCR was performed three times, with three biological and technical replicates. The wild type expression was set at 1. The diagram was compiled using the relative expression software tool-Multiple Condition Solver REST-MCS version 2 (REST-348, Michael W. P., 2001). Quantitative RT-PCR was performed in triplicate, with three replicates each. Wild-type expression was set at 1. Error bars indicate standard deviations calculated from data per triplicate samples and are representative of three independent experiments. Significance with respect to wild type: *$p < 0.05$, **$p < 0.01$, ****$p < 0.0001$ (calculated with ANOVA-Bonferroni-Holm).

When the expression of *ZmDHS1* was down-regulated, expression of *ZmDHS2* was down-regulated in all silencing lines compared to the wild type (~2 times in SI-1 and SI-2; ~5 times in SI-3) (Figure 15). *ZmDHS2* expression was up-regulated in DHS overexpressing lines, approximate 2-fold time in OE-2 and 3-fold time in OE-1.

3.1.4. Relative expression of eIF5A genes in DHS silencing and DHS overexpressing lines

DHS execute the first enzymatic step for the modification of the eukaryotic translation initiation factor 5A (eIF5A). Using BLAST analysis three genes of eIF5A were identified in *Z. mays* and these genes were named *ZmeIF5A-1*, *-2*, and *-3*. To determine if the difference in *ZmDHS1* expression has an effect in *ZmeIF5A* expression levels, samples from plants carrying the silencing or overexpressing constructs were grown and collected at 1 month of age. qRT-PCR using the SYBR Green master mix (Roche) was conducted using eIF5A-1, -2 and -3 specific primers (Table 10).

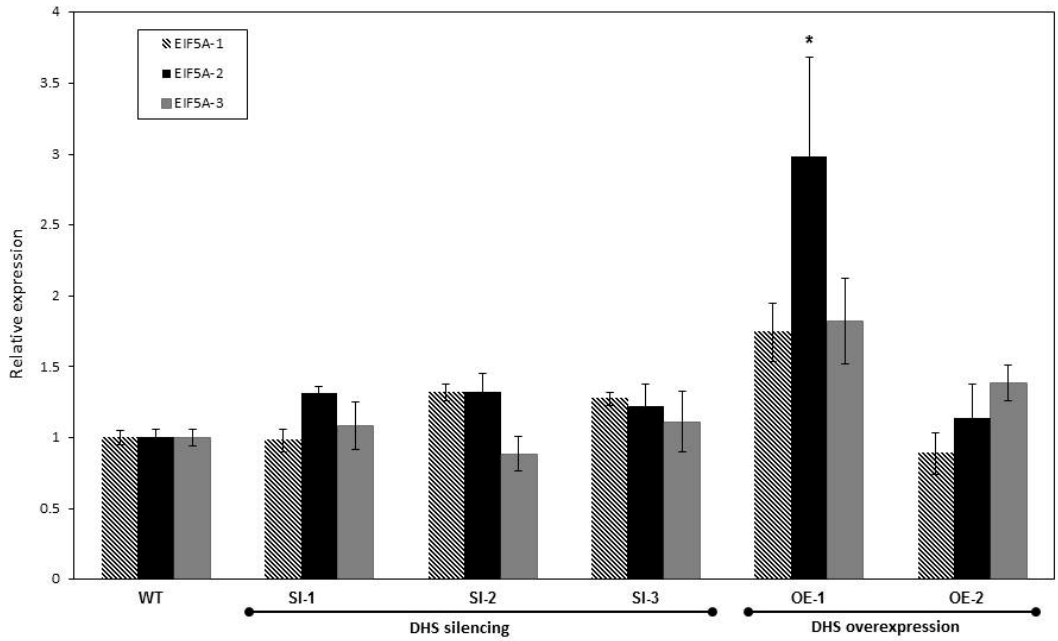

Figure 16. Relative expression levels of *ZmeIF5A-1*, *ZmeIF5A-2* and *ZmeIF5A-3* in DHS silencing or DHS overexpressing lines. No significant difference was found in the expression of ZmeIF5A-1, ZmeIF5A-2 and ZmeIF5A-3 in silencing lines SI-1, SI-2, SI-3 and overexpressing line OE-2 compared to the wild type. Expression of the *ZmeIF5A-2* gene was up-regulated in overexpressing line OE-1 compared to the wild type. Quantitative RT-PCR was performed, with three biological and three technical replicates. The wild type expression was set at 1. The diagram was compiled using the relative expression software tool-Multiple Condition Solver REST-MCS version 2 (REST-348, Michael W. P., 2001). Quantitative RT-PCR was performed in triplicate, with three replicates each. Wild-type expression was set at 1. Error bars indicate standard deviations calculated from data per triplicate samples and are representative of three independent experiments. Significance with respect to wild type: *$p < 0.05$, **$p < 0.01$, ****$p < 0.0001$ (calculated with ANOVA-Bonferroni-Holm).

The wild type cDNA was used as the standard and 18SrRNA was used as a reference gene. No significant difference was found in the expression of *ZmeIF5A-1*, *ZmeIF5A-2* and *ZmeIF5A-3* in silencing lines SI-1, SI-2, SI-3 and overexpressing line OE-2 compared to the wild type. However, expression of the the *ZmeIF5A-2* gene was up-regulated in the overexpressing line OE-1 compared to the wild type (Figure 16). These results suggested that eIF5A genes are not co-expressed or expressed at different levels of *ZmDHS1* transcription.

3.1.5. Relative expression levels of *ZmDOHH* in DHS silencing and DHS overexpressing lines

DOHH is the second enzyme necessary to activate eIF5A. Relative quantification of *ZmDOHH* in DHS silencing and DHS overexpressing lines was surveyed (Section 2.5.2 and 2.5.5). No significant difference was found in the expression of *ZmDOHH* in silencing lines SI-1, SI-2, SI-3 and overexpressing line OE-2 compared to the wild type. However, expression of the *ZmDOHH* gene was slightly up-regulated in the overexpressing line OE-1 (Figure 17).

This result suggests that expression of *ZmDHS1* does not have an effect on the expression of *ZmDOHH*.

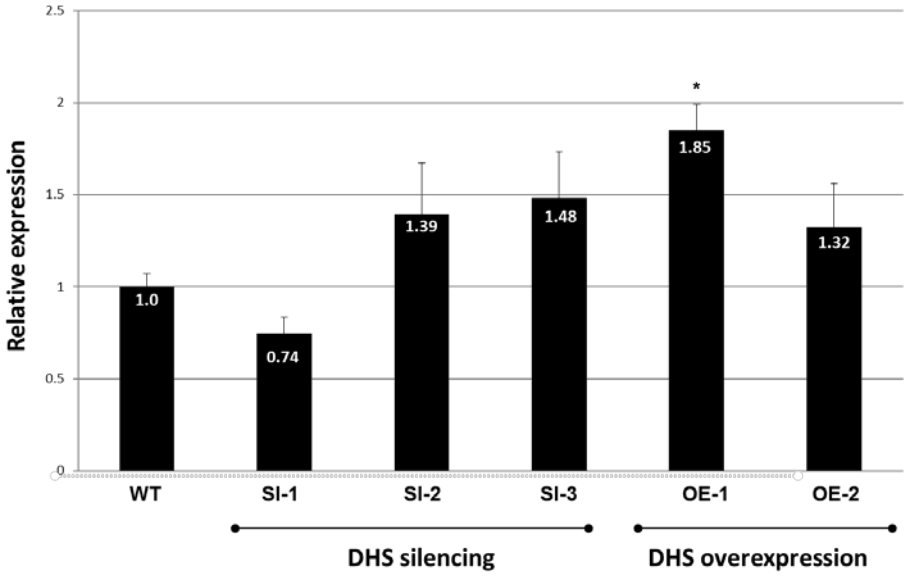

Figure 17. Relative expression of *ZmDOHH* in DHS silencing and DHS overexpressing lines. No significant difference was found in the expression of *ZmDOHH* compared to the wild type. Quantitative RT-PCR was performed three times, with three biological and technical replicates. The wild type expression was set at 1. The diagram was compiled using the relative expression software tool-Multiple Condition Solver REST-MCS version 2 (REST-348, Michael W. P., 2001). Quantitative RT-PCR was performed in triplicate, with three replicates each. Wild-type expression was set at 1. Error bars indicate standard deviations calculated from data per triplicate samples and are representative of three independent experiments. Significance with respect to wild type: *p < 0.05, **p < 0.01, ****p < 0.0001 (calculated with ANOVA-Bonferroni-Holm).

3.1.6. Phenotypic analysis of maize silencing and overexpressing DHS lines

Twenty plants of each transgenic line at T3 generation were grown in the greenhouse and observed for their growth behavior and development. The plant height, number of leaves, as well as the length and width of leaves were measured every 6 days for 4 months. Cobs were pollinated and the number of seeds was counted after harvest. During that time, the rate of flower, pollen and cob formation in all of transgenic lines were also observed. The data were analysed and compared to each other in order to determine if there is any difference.

3.1.6.1. Germination of maize kernels from the DHS silencing and overexpressing lines

The purpose of this experiment is to provide an overview about the impact of DHS silencing or overexpression on seeds germination. After heat shock induction, the seeds were moved to the greenhouse and the percentage of germination was estimated. The viability of a population of seeds was based on the survival and shooting formation of the plants. The equation to calculate the germination percentage is: GP = seeds germinated/total seeds x 100. The experiment was extended over a period of eight days to allow the last seed germination. The

percentage of germination of 5 lines of transgenic maize plants and the wild type line (HiII-A) is shown in Figure 18.

After several days of sowing, (conditions in Section 2.6.2) seeds absorbed water and began to swell. When enough water had been absorbed and the soil temperature was favorable, germination occurred. In our experiment, there were no significant differences between the wild type and the transgenic plant lines in percentage of germination. The silencing lines SI-1, SI-2 and SI-3 as well as the overexpressing line OE-1 showed 100% germination in comparison to the wild type. The overexpressing line OE-2 showed 70% of germination in comparison to the wild type (Figure 18 A). The overexpressing line OE-2 showed a slower mesocotyl elongation. In addition, this line also showed slower shoot formation than the others (Figure 18 B).

The study revealed that in some cases with the increase of *ZmDHS1* level, the germination rate was slightly decreased.

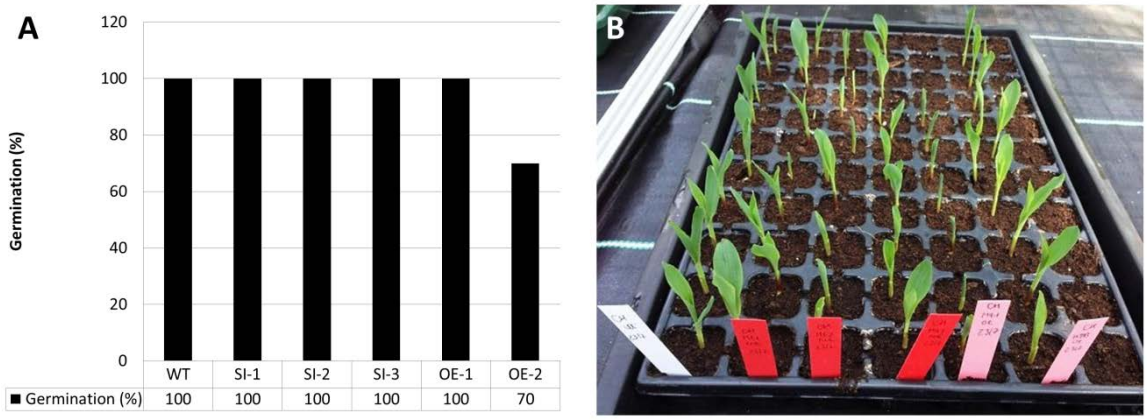

Figure 18. Germination rate of transgenic seeds from silencing or overexpressing DHS lines in comparison to the wild type. The plants were grown in the greenhouse with 25/22°C (day/night) and a 12-hour photoperiod. The percentage of germination was determined after 8 days of sowing. (**A)** Graph indicating the percentage of germination of 10 seeds per line. Wild type, silencing lines SI-1; SI-2; SI-3 and overexpressing line OE-1 showed 100% of germination. Overexpressing line OE-2 had 70% of germination. (**B)** Representative picture of germinated plants. From left to right: wild type (white label), DHS silencing line (red label) SI-1; SI-2; SI-3, DHS overexpressing line (pink label) OE-2; OE-1. The experiment was performed three times with ten plants per line.

3.1.6.2. The height of DHS silencing and overexpressing maize plants

The height of the germinated seedlings of all transgenic DHS lines and the wild type was measured during 10 weeks and recorded every week. After 10 weeks of measurement, a statistically pronounced significant effect was found in DHS silencing and overexpressing lines (Figure 19). The time course showes the height measured for the whole growing season (10 Weeks).

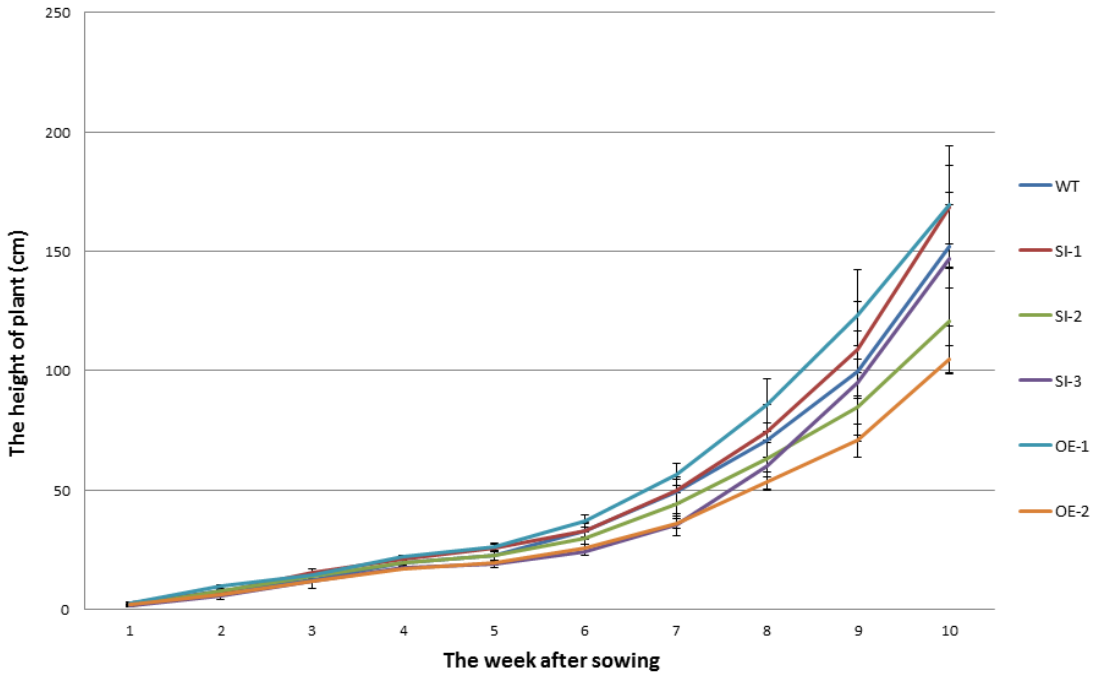

Figure 19. Height of transgenic maize plants during the 10-weeks period after sowing. The color lines showed the growth trend of different lines. The experiment was performed three times with ten plants per line.

Two lines, one silencing (SI-1) and one overexpressing (OE-1) line grew faster and had a significant difference of height compare to the wild type. Overexpressing line OE-1 showed the highest length (Table 12). During the growth and development period, this overexpressing line showed the fastest growth rate compared to the others. The silencing line SI-1 growth was faster than wild type and had the approximate height of overexpressing line OE-1 at the tenth week of growth (ten plants per line).

Table 12. The height (cm) of transgenic maize plants during 10 weeks after sowing.

Weeks	1	2	3	4	5	6	7	8	9	10
WT	2.57	7.63	12.27	19.20	22.35	32.61	49.10	70.90	99.50	152.00
SI-1	2.28	7.26	15.53	20.91	25.61	33.00	49.72	74.61	109.06	168.67
SI-2	1.42	7.65	13.83	19.24	22.33	29.75	43.95	63.05	84.70	120.80
SI-3	1.26	5.71	11.50	17.29	18.90	23.90	35.35	60.00	94.8	146.70
OE-1	2.48	9.54	14.38	22.09	26.30	36.90	56.25	85.50	123.4	169.50
OE-2	1.76	6.24	11.71	17.13	19.46	25.50	35.86	53.57	70.64	104.57

The silencing line SI-2 and overexpressing line OE-2 presented a smaller height in comparison to wild type. The silencing line SI-3 showed an interesting growth rate. After seven weeks the growth increased rapidly and nearly reached the height of wild type after 10 weeks. Before the seventh week, this line grew significantly slower than the wildtpye. At that time the height was as high as overexpressing line OE-2. The data also showed a contrasting result in

overexpressing line OE-2 which had higher *ZmDHS1* level of transcription (Figure 14). This overexpressed DHS maize line grew slowly and had a dwarf phenotype in comparison to wild type. The average heights (cm) of the germinated seedlings of maize in all the lines are shown in Table 12. Even though there are differences in growth rate, most plants developed normally and formed normal leaves and ear (Figure 20).

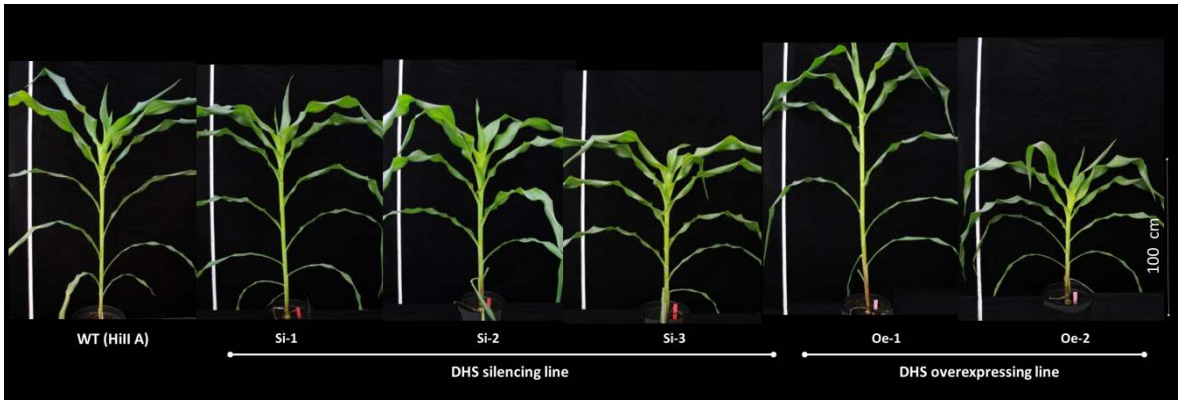

Figure 20. The height of transgenic maize plants after 8 weeks of culture. From the left to the right of picture: wildtype, DHS silencing line SI-1; SI-2; SI-3, DHS overexpressing line OE-1; OE-2; respectively (Ten plants per line, 3 repetitions).

3.1.6.3. The stages of growth of DHS silencing and overexpressing maize transgenic plants

After the rough germination stage, since breaking through the soil surface to maturity, maize will undergo several growth stages. These stages are separated into two groups: vegetative and reproductive. The time point, used to separate these two groups, is the appearance of silks. Figure 21 below is showing respective growth stages of maize.

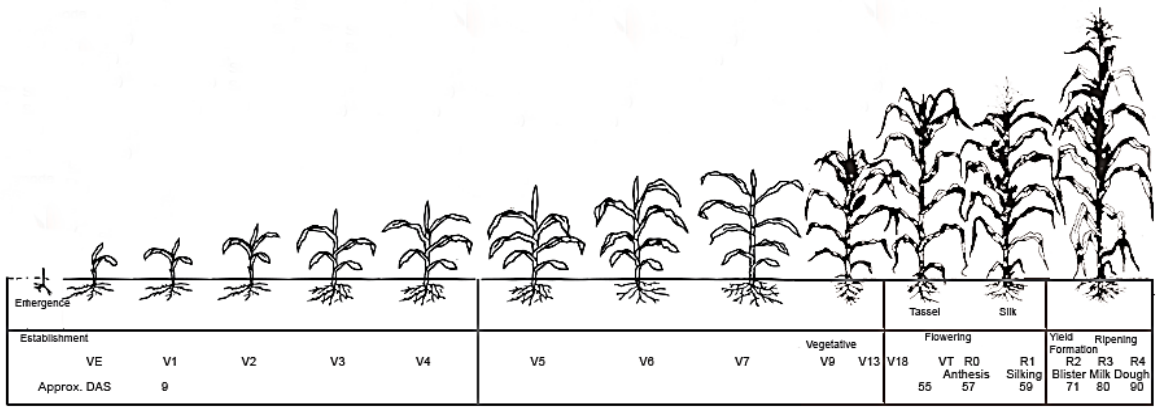

Figure 21. Maize growth stages. Vegetative Stages: VE – Emergence, V1 - First Leaf, V2 - Second Leaf, …, V6 - Sixth Leaf, V10 - Tenth Leaf, V(n) - nth Leaf, VT – Tassle. Reproductive Stages: R1 – Silking, R2 – Blister, R3 – Milk, R4 – Dough, R5 – Dent, R6 - Black Layer (Physiological Maturity) (Ritchie, 1993).

In the vegetative stage, the numbers of leaves that are completely developed determine the stage of the plant. To understand more about the growth and development of transgenic plants, we make a comparison of the number of leaves on the silencing and overexpressing

DHS maize lines. Observation of the number of leaves was performed from the first week until the last week of the vegetative stage (Table 13).

Table 13. The percentage of plants that have reached the respective leaf numbers during the vegetative stage. After 6, 7 and 8 weeks a certain amount of plants of each line had reached V8, V10, and V12 respectively. The columns show the percentage of plants that have reached the respective growth stage.

	6 weeks	7 weeks	8 weeks
Line	Number of leaves 8 – 9 (V8)	10 – 11 (V10)	12 – 13 (V12)
WT	90%	100%	100%
SI-1	90%	100%	100%
SI-2	80%	100%	100%
SI-3	50%	30%	50%
OE-1	100%	100%	100%
OE-2	50%	20%	40%

During this time there were no significant differences between wild type compared to DHS silencing lines SI-1 and SI-2. These lines had the same number of leaves and went to the next stage in the same time compared to wild type. All plants in these two lines had 10 – 11 leaves (V10) and were ready to move to reproductive stage. Plants of the DHS overexpressing line OE-1 grew faster and full development was achieved 1 vegetative stage earlier than the wild type. Although plants from wild type and OE-1 line looked similar in phenotype they were not at the same vegetative stage. While the wild type plants were still in V9, overexpressing line OE-1 plants were considered in V10 already. OE-1 overexpressing line reached V10 in 6 weeks meanwhile wild type reached it in 7 weeks.

There were two lines, DHS silencing line SI-3 and DHS overexpressing line OE-2, which were low and high in DHS level expression, respectively, and showed slow growth in the vegetative stage. The number of leaves was less than wild type in the same time. They reached the new stage of vegetative growth with less than 50% of total plants and needed 8 weeks to reach V10 (Table 13).

3.1.6.4. The width and length of transgenic maize leaves (12 weeks)

The width and length of maize leaves in the transgenic plants (Figure 22 A, B), silencing line SI-2 showed a wider leaf (~10 cm) compared to the wild type (7.5 cm) (Figure 22 A). An increase in width of leaf was observed in over expressing line OE-1. Overexpressing line OE-2 had a smaller leaf width (6.5 cm) compared to the wild type (Figure 22 A). There were no significant differences in the length of DHS silencing lines SI-1, SI-2 and SI-3 as well as DHS overexpressing line OE-1 (Figure 22 B). Due to slow growth and dwarf phenotype showed in

section 3.1.6.2, there was a big difference in the width and length of overexpressing line OE-2 in comparison to the others. The leaves of overexpressing line OE-2 (78 cm) were smaller and shorter than wild type leaf (88 cm).

The width and length were recorded showing that silencing line SI-2 and overexpressing line OE-1 had bigger leaves compared to wild type. No significant difference was observed in silencing lines SI-1 and SI-3.

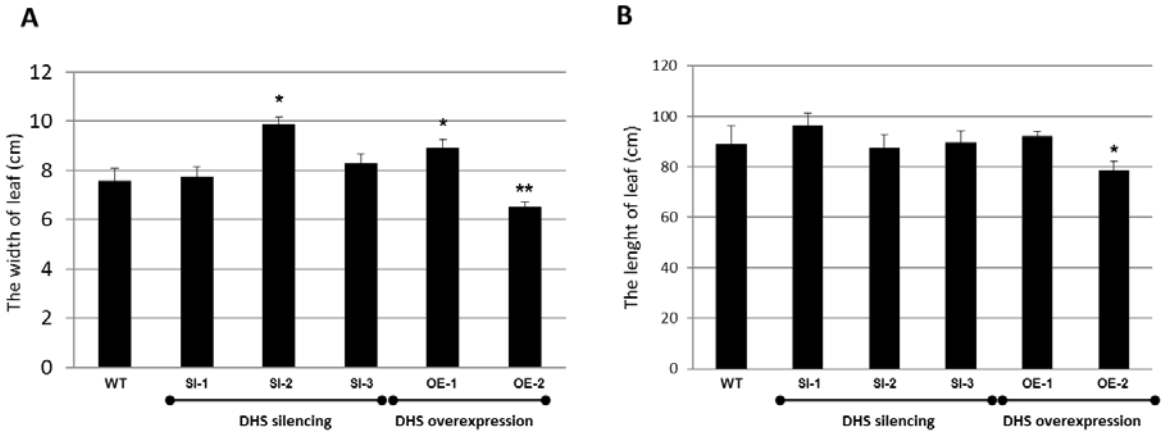

Figure 22. Comparison of width and length of transgenic maize leaves (12 weeks). The width (cm) and the lenght (cm) of leaves from silencing and overexpressing DHS transgenic lines were compared to the wild type. 20 plants per each line were used in the comparison. (**A)** Silencing line SI-2 showed a wider leaf (~10 cm) compared to the wild type (7.5 cm). An increase in width of leaf was observed in over expressing line OE-1. Overexpressing line OE-2 had a less wide leaf (6.5 cm) compare to the wild type. (**B)** There were no significant differences in the lenght of DHS silencing lines (SI-1, SI-2 and SI-3) or DHS overexpressing line OE-1 compared to the wild type. The leaf of overexpressing line OE-2 (78 cm) was smaller than wild type leaf (88 cm). The experiment was performed with ten plants per line, 3 repetitions. Significance with respect to wild type: *$p < 0.05$, **$p < 0.01$, ****$p < 0.0001$ (calculated with ANOVA-Bonferroni-Holm).

3.1.6.5. Reproductive stages of DHS silencing and overexpressing maize plants

At V10 and VT reproductive stages, tassel formation starts to become visible. In 80% of the overexpressing line OE-1 plants the tassel was formed after 9 weeks. Plants from overexpressing line OE-2 did not show any tassel (Table 14). Silencing lines SI-1; SI-2 and SI-3 formed tassel earlier than wild type. The percentage of plants showing the tassel is 45%, 20% and 50%, respectively. Interestingly all plants showed tassel after 10 weeks even OE-2 plants. In this period the tassel was completely extended; however, silks were not yet visible (Table 14).

Table 14. Percentage of plants showing tassel formation in reproductive stages.

	9 weeks	10 weeks
WT	10%	100%
SI-1	45%	100%
SI-2	20%	100%
SI-3	50%	100%
OE-1	80%	100%
OE-2	0%	100%

After tassel formation, nutrient and water accumulation also increased greatly enough for the requirement of the next reproductive stages. However, there were some plants in both silencing and overexpressing lines showing no pollen formation phenotype. Especially, silencing line SI-2 had only 30% plant showing pollen formation. The tassel in this silencing line was formed but did not blossom. The SI-1 and SI-3 silencing lines showed no difference in pollen formation phenotype in comparison to the wild type. Overexpressing line OE-2 also had 10% of plant without showing pollen formation. The overexpressing line OE-1 showed faster pollen formation. At 11 weeks, overexpressing line OE-1 had 100% pollen formation in comparison with the 90% of the wild type (Table 15).

Table 15. Percentage of plant showing pollen formation in reproductive stages.

	10 weeks	11 weeks	12 weeks	13 weeks
WT	50%*	90%	100%	100%
SI-1	40%	80%	100%	100%
SI-2	0%	20%	30%	30%
SI-3	60%	90%	100%	100%
OE-1	90%	100%	100%	100%
OE-2	0%	30%	70%	90%

*(Ten plants per line, 3 repetitions)

Subsequently silks appeared and were visible outside the husks. The silks have the purpose of capturing pollen that falls from the tassel. The captured pollen grain moves down the silk to the ovule, where pollination occurs. In our experiment, all plants were self-pollinated and the cobs were covered with a bag. The pollination was performed manually and equally to avoid unexpected mistakes. Environmental conditions are very important during this growth stage. Abiotic stress during this time can cause poor pollination or kernel set. Lack of moisture can cause the silks to become too dry and can greatly limit their ability to transfer pollen. Therefore these conditions were checked every day in the greenhouse to make sure that they were suitable for kernel formation. Wild type and overexpressing lines did not show any

significant difference at this stage. On the contrary, the percentage of kernel formation was quite low in the silencing lines. Silencing line SI-2 produced just 20% of plants with kernels. The percentage was 50% and 82% in silencing lines SI-3 and SI-1, respectively. These results showed that DHS silencing in maize reduced the kernels formation ratio. No abnormal phenotypes were observed in the kernels. The shape of all kernels was similar to the wild type.

Table 16. Percentage of cob formation.

	10 weeks	11 weeks	12 weeks
WT	0%	90%	100%
SI-1	30%	77%	82%
SI-2	0%	20%	20%
SI-3	0%	50%	50%
OE-1	0%	90%	100%
OE-2	0%	85%	100%

The stage of physiological maturity occurs when the kernel has achieved its peak (55 to 65 days after silking) dry matter accumulation. After this last stage, all kernels were harvested and grains were counted.

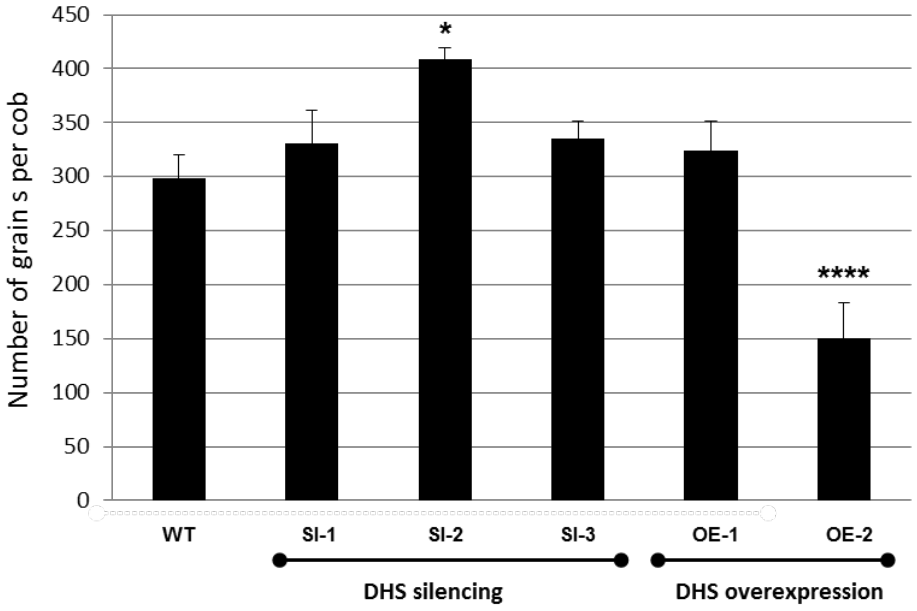

Figure 23. The number of grains per cob on different transgenic maize plants. SI-2 has the highest number of grains per cob (408 grains). OE-2 shows the lowest number of grains per cob (150 grains). The number of grains in wild type is ~300 grains. There are no big differences in number of grains of SI-1, SI-3 and OE-1 compared to wild type. From the left to the right: wild type, DHS silencing line SI-1; SI-2; SI-3, DHS overexpressing line OE-1; OE-2; respectively. Ten cobs per line were used to count the number of grains (except SI-2, SI-3 and OE-2 which developed 2, 5, 7 cobs, respectively). Significance with respect to wild type: *$p < 0.05$, **$p < 0.01$, ****$p < 0.0001$ (calculated with ANOVA-Bonferroni-Holm).

Even though the percentage of kernel formation in the silencing line SI-2 was not high, the cob gained a considerable amount of grains (2 cobs). The number of grains per cob was highest (408 grains) in comparison to the other lines (Figure 23). Overexpressing lines OE-2 did not produce many grains (150 grains). The number of grains in this line was the half of the number of grains in wild type (~300 grains). No significant difference in number of grains was observed in the other lines (Figure 23).

3.1.7. Fungal infection of transgenic maize leaves

Detached leaves of transgenic maize lines were infected with the fungal maize pathogens, *Collectotrichum graminicola, Cochliobolus heterostrophus* C4 and *Bipolaris sorokiniana* as described in material and methods (Section 2.6.4). The relative necrotic lesion diameter of the inoculated leaf was determined as a scale for the disease severity of each fungus. The experiment was repeated 3 times and significant differences in resistance could be observed under the given conditions.

The 3 fungal species constantly induced necrotic lesions on infected wild type and DHS silencing lines leaves. In case of *C. graminicola* and *C. heterostrophus* C4 inoculation, there were no significant differences in the length of the lesion in DHS silencing lines compared to the wild type. With *B. sorokiniana* inoculation silencing line SI-2 and SI-3 showed more necrotic lesions compared to the wild type. On the contrary, the two DHS overexpressing lines revealed a resistance to fungi. The 3 fungal species produced less necrotic lesions in both lines compared to the wild type. *C. graminicola* induced almost no necrotic lesion in overexpressing line OE-2 (Figure 24).

In general, this experiment showed that overexpression of DHS in maize increased the resistance against fungi.

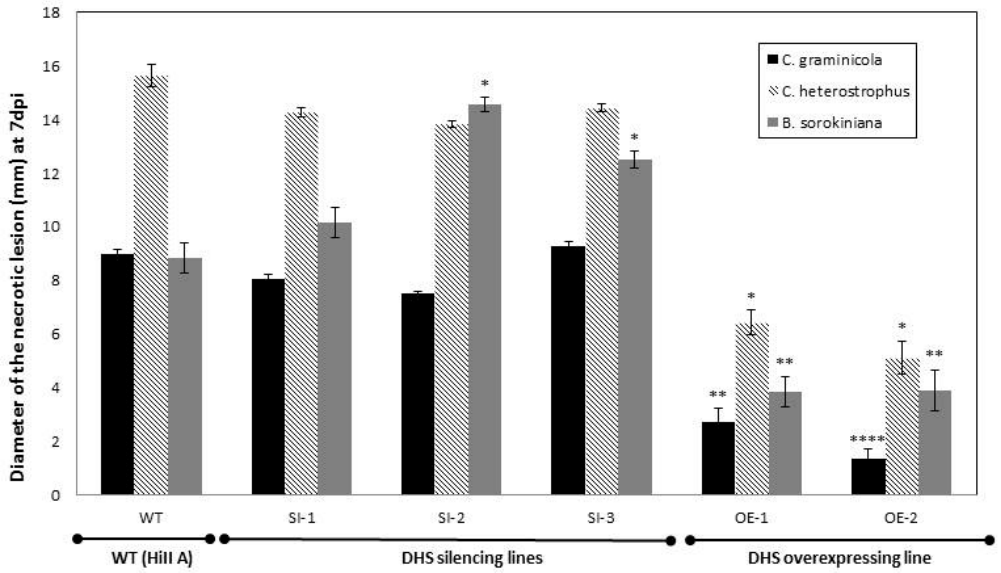

Figure 24. Fungal pathogenicity test on maize leaves of WT, DHS silencing and DHS overexpressing lines. In this assay, the pathogenicity of different fungi (*C. graminicola*, *C. heterostrophus*, and *B. sorokiniana*) was tested on detached leaf sections of 6 weeks old WT, DHS silencing and DHS overexpressing lines. The significant difference in the size of the lesions could be found in the transgenic lines compared to the wild type. In this assay maize DHS overexpressing plants (T3) show a strong resistance to *C. graminicola*, *C. heterostrophus*, and *B. sorokiniana*. Quantitative RT-PCR was performed three times, with three replicates each. Error bars indicate standard deviations calculated from data per triplicate samples and are representative of three independent experiments. Significance with respect to wild type: *$p < 0.05$, **$p < 0.01$, ****$p < 0.0001$ (calculated with ANOVA-Bonferroni-Holm).

3.1.7.1. Macroscopic and microscopic analysis of fungal colonization on transgenic maize leaves

The macroscopic analysis of inoculated detached leaves of maize revealed an epiphytic growth of all 3 fungal species used in our pathogenicity test. Figures 25 to 27 showed how *C. graminicola*, *C. heterostrophus*, and *B. sorokiniana* were able to colonize the mesophyll of maize leaves in a similar manner. The DHS silencing lines as well as the wild type show susceptibility to all fungal strains. DHS overexpressing lines were more resistant against the fungi. The EGFP signal from the mycelia coincided with the necrotic area.

Lesions caused by *C. graminicola* did not show a clear necrotic area on bright field pictures. However, macrographs produced with the Leica MZFLIII fluorescence stereomicroscope showed a detectable necrotic lesion on each leaf (Figure 25). The lesion formation was strongly reduced on the leaves of the DHS overexpressing lines infected with *C. heterostrophus* and *B. sorokiniana* (Figure 26 and 27). Macrographs in Figure 26 provided evidence of reduced necrosis and fungal growth in the overexpressing lines. While on silencing line leaves, the necrotic lesions and colonization of *C. heterostrophus* were constantly observable on the

inoculated point. No big difference in lesions size was observed on leaves of the silencing lines compared to wild type (Figure 26).

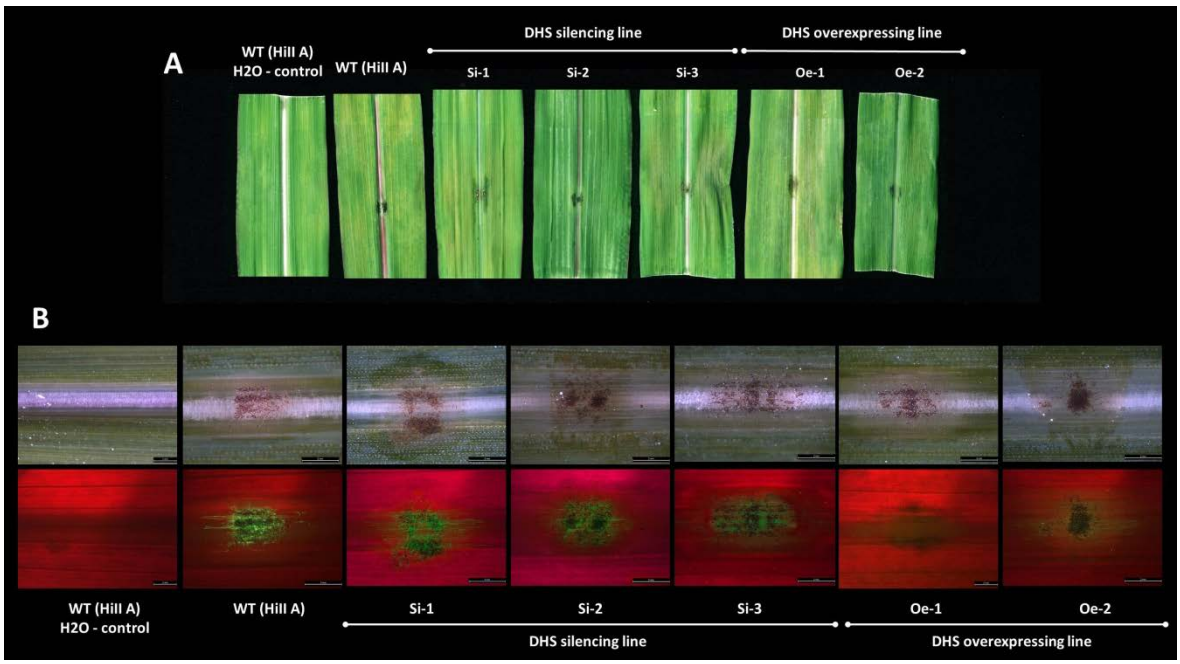

Figure 25. Infection of maize leaves by the fungal pathogen *C. graminicola M.1001-GFP*. Detached leaves of DHS silencing and DHS overexpressing lines were inoculated with droplets (10 µl) containing 100 conidia per µl. Leaves were incubated at 22°C. Photos are representative for disease phenotypes at 6 days post-inoculation. (**A)** Necrotic area at inoculated point was visible by bright field. (**B)** GFP fluorescence of the mycelium due to constitutive GFP expression. Scale bar = 2 mm. The maize infections were performed with 9 leaves for each line and 3 independent experiments (n = 27).

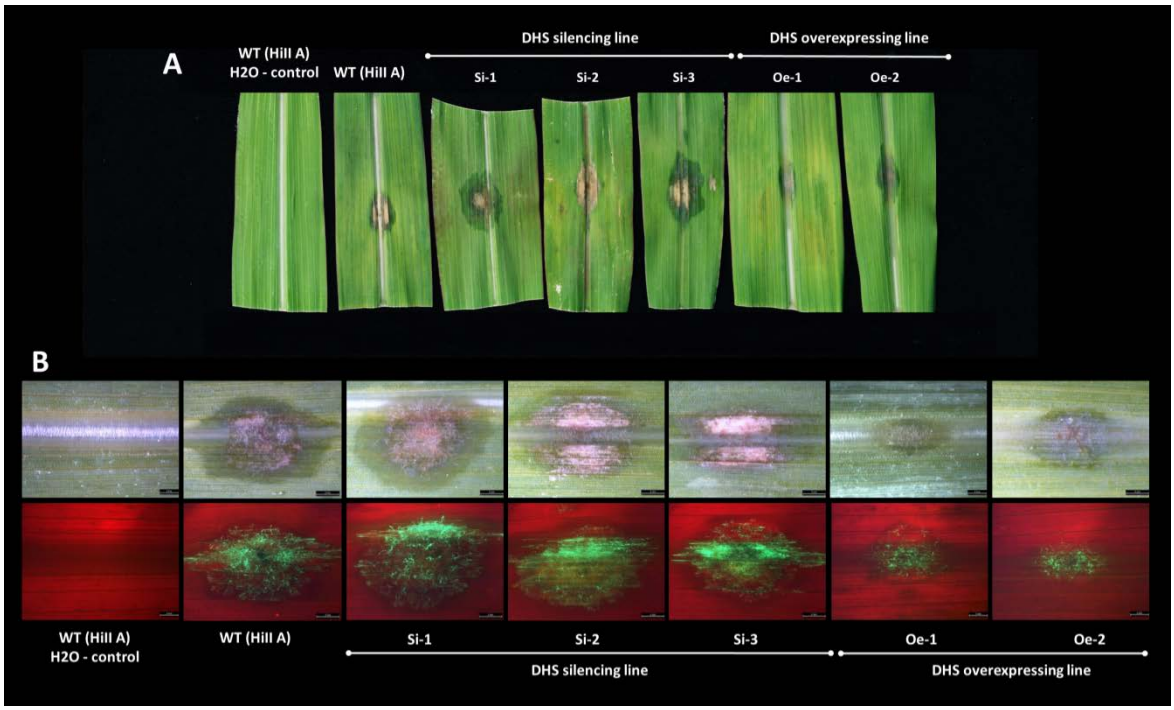

Figure 26. Infection of maize leaves by the fungal pathogen *C. heterostrophus C4-GFP*. Detached leaves of DHS silencing and DHS overexpressing lines were inoculated with droplets (10 µl) containing 100 conidia per µl. Leaves were incubated at 22°C. Photos are representative for disease phenotypes at 6 days post-inoculation. (**A)** Necrotic area at inoculated point was visible by bright field. (**B)** GFP fluorescence of the mycelium due to

constitutive GFP expression. Scale bar = 2 mm. The maize infections were performed with 9 leaves for each line and 3 independent experiments (n = 27).

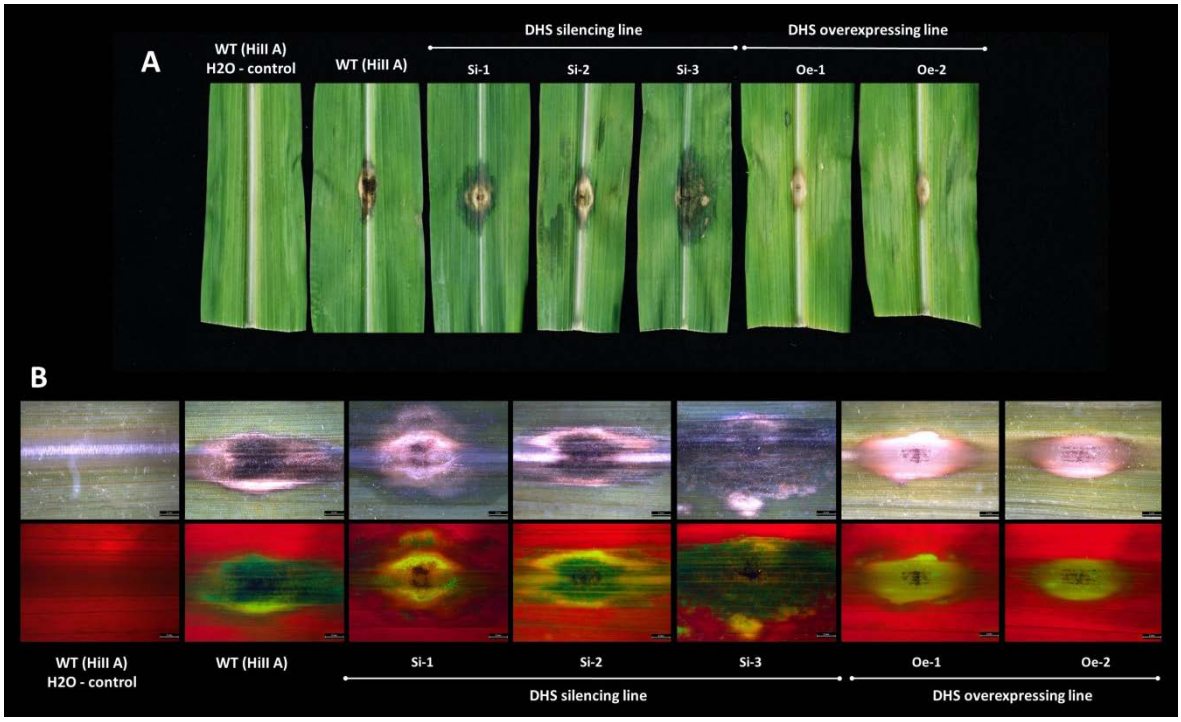

Figure 27. Infection of maize leaves by the fungal pathogen *B. sorokiniana*. Detached leaves of DHS silencing and DHS overexpressing lines were inoculated with droplets (10 µl) containing 100 conidia per µl. Leaves were incubated at 22°C. Photos are representative for disease phenotypes at 6 days post-inoculation. (**A)** Necrotic area at inoculated point was visible by bright field. (**B)** GFP fluorescence of the mycelium due to constitutive GFP expression. Scale bar = 2 mm. The maize infections were performed with 9 leaves for each line and 3 independent experiments (n = 27).

B. sorokiana produced a strong necrotic lesion on the silencing line SI-3. This fungus also induced significantly varying levels of chlorotic lesions in silencing lines SI-1, SI-2 and wild type. A significant difference was found in the size of the chlorotic lesions between DHS overexpressing lines and the other lines (Figure 27). The lesion was smaller and mycelia were less visible than wild type and DHS silencing lines (Figure 27).

The necrotic lesions were observed underneath by dark colour area of plant cells where the GFP signal correlated with the presence of mycelia and specialized hyphal infection structures. Micrographs from cross sections of infected leaves revealed an epiphytic and endophytic growth of the three fungal pathogens (Figure 28). According to the confocal pictures, the growth of *C. graminicola* M.1001, *C.heterostrophus* C4 and *B. sorokiana* were strongly decreased in DHS overexpressing lines. In these lines, all fungi only grew superficially and did not extend colonization in mesophyll. No subcuticular growth was observed below the epidermis and inside the mesophyll cells of infected plants.

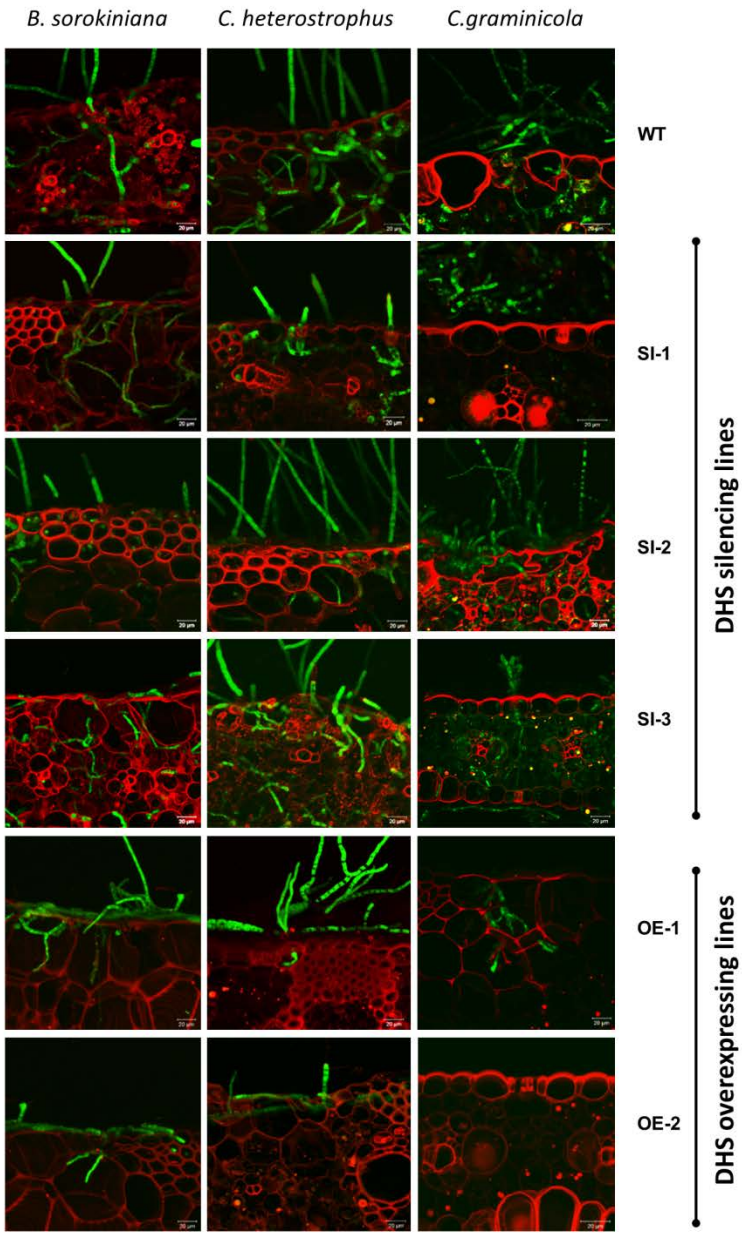

Figure 28. Laser scanning microscopy of *C. graminicola*, *C. heterostrophus* C4 and *B. sorokiniana* on transgenic *Zea mays* leaves. Detached leaves of *Zea mays* were inoculated with 10 µl droplets containing 50 conidia per µl of fungi. Micrographs from leaf cross sections are representative for 6 days post-inoculation (dpi); micrographs showing overviews of the fungal penetration in different transgenic maize lines. Mycelium on leaf surfaces and inside the leaf tissue was visualized by GFP fluorescence at 488 nm by using an argon laser. Scale bars=20 µm.

Successful penetration of the plant cell wall and colonization of the host tissue were readily visible in other maize lines. The growing hyphae of *C. graminicola* M.1001, *C.heterostrophus* C4 and *B. sorokiana* were detected inside the mesophyll and also the aerial hyphae rapidly formed outside the host tissue (Figure 28). All the pathogen also became subcuticular after penetration. This was followed by colonization of the epidermal and the mesophyll cells. The histology of infection was found to be similar in the wild type (Figure 28).

3.1.7.2. DHS overexpression in maize plant reduces fungi DNA content in inoculated maize leaves

In order to evaluate the efficacy of resistance on the DHS overexpressing lines fungal growth of inoculated maize plants was quantified by determining the amount of fungal gDNA by real-time PCR. Genomic DNA of each fungus and plant were extracted from inoculated leaves point and the DNA content was determined and compared to wild type in both DHS silencing and overexpressing plants (Section 2.6.6).

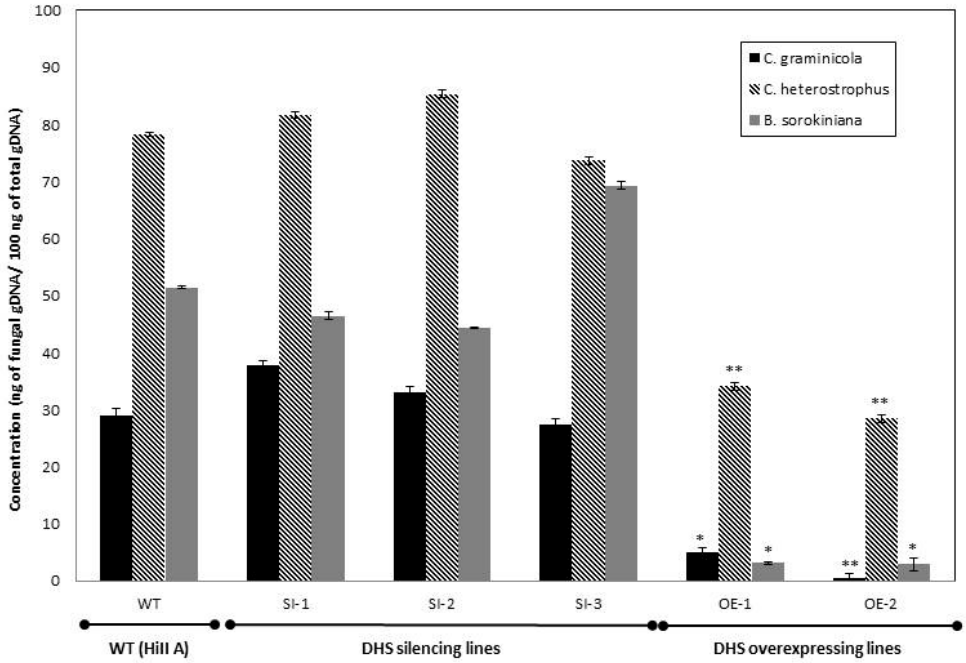

Figure 29. Fungal DNA content (*C. graminicola*, *C. heterostrophus*, and *B. sorokiniana)* of infected maize leaves. Amount of fungal DNA was quantified by real-time PCR at 6 days post inoculation. Samples were collected from 2 cm² of infection site. Each bar represents fungal DNA content/100 ng total DNA of three independent experiments. The endophytic content was analyzed in three independent experiments on 3 samples per line. Significance with respect to wild type: *$p < 0.05$, **$p < 0.01$, ****$p < 0.0001$ (calculated with ANOVA-Bonferroni-Holm).

Although, no significant differences were observed on fungal DNA content in silencing lines compared to the wild type, a significant difference was detected in DHS overexpressing plants (OE-1 and OE-2) (Figure 29). As shown in Figure 29, the genomic DNA content from all fungal species, in the overexpressing lines was much less than in the wild type and the silencing lines. These results showed that DHS overexpression in maize plants strongly reduced the fungal infection, while DHS silencing seemed to be ineffective against fungal infection.

3.1.8. Effects of DHS silencing and overexpression on defense-related genes expression in maize

To elucidate the role of *ZmDHS1* in the plant defence response, the expression of defense-related genes was determine by qRT-PCR. The leave samples were collected following the method in section 2.6.4. A set of defense related-genes were selected (*ZmPal, ZmHpl* and *ZmGs1*) and their expression was determined and compared between the wild type and the transgenic maize lines (Table 10). The transcriptional changes of defense genes were also compared before and after fungal infection with the two fungal pathogens that produced more disease, *C. heterostrophus*, and *B. sorokiniana*.

3.1.8.1. Regulation of *ZmPal* on DHS silencing and overexpressing maize lines

In the SAR pathway, PAL is a key regulatory enzyme and jasmonic acid/ethylen (JA/ET) signaling pathway activates its expression (Kato *et al.*, 2000). The *ZmPal* transcript was 2 to 3 fold up-regulated in all DHS silencing lines compared to the wild type (Figure 30 A). No significant difference was observed in overexpressing line OE-1. However, there was a slight transcript reduction of *ZmPal* in overexpressing line OE-2 compared to wild type. After infection with *B. sorokiniana*, the transcript level of *ZmPal* decreased in all mutant lines except DHS silencing line SI-1, which was not different to the wild type (Figure 30 B, black bars). DHS overexpressing lines showed a strong down-regulation compared to wild type. Expression of *ZmPal* showed opposite results on leaves infected with *C. heterostrophus*. Up-regulation of *ZmPal* was observed in all transgenic lines compared to the wild type. Specifically the transcript level of *ZmPal* in silencing line SI-1 was higher than wild type and overexpressing lines. Transcript levels of *ZmPal* were nearly the same between the overexpressing line OE-1 and OE-2 (Figure 30 B, striped bars).

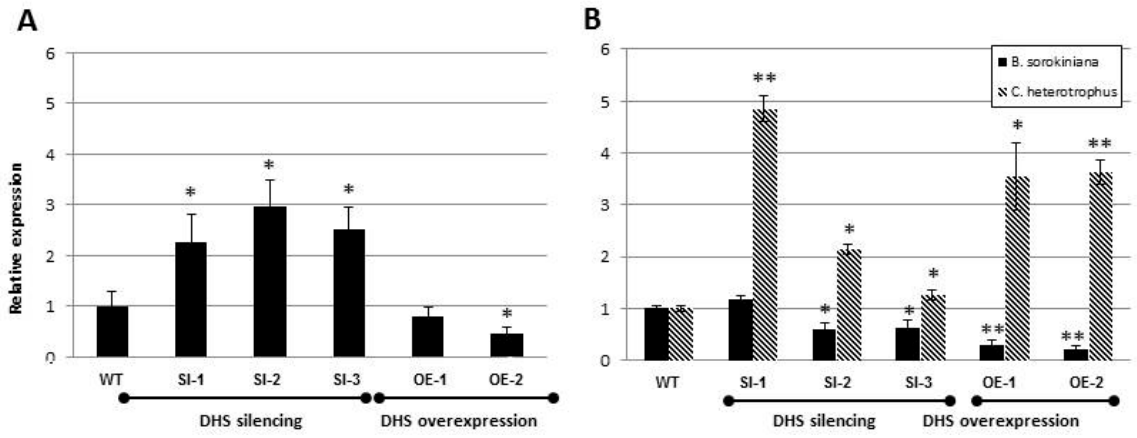

Figure 30. Relative expression of *ZmPal* gene by qPCR in DHS silencing and DHS overexpressing lines. (A) Expression of *ZmPal* before fungal inoculation. No significant difference was observed in the expression of *ZmPal* in overexpressing line OE-1 compared to the wild type. The expression of *ZmPal* was 2 to 3

fold up-regulated in all DHS silencing lines compared to the wild type. Expression of *ZmPal* was slightly down-regulated in overexpressing line OE-2 compared to wild type. **(B)** Expression of *ZmPal* after inoculation with *B. sorokiniana* (black bars) and *C. heterotrophus* (striped bars). After infection with *B. sorokiniana,* the transcript level of *ZmPal* decreased in all transgenic lines, except DHS silencing line SI-1, which was similar to the wild type). Expression of *ZmPal* was up-regulated compared to the wild type on leaves infected with *C. heterotrophus*. Quantitative RT-PCR was performed three times, with three biological and technical replicates. The wild type expression was set at 1. The diagram was compiled using the relative expression software tool-Multiple Condition Solver REST-MCS version 2 (REST-348, Michael W. P., 2001). Significance with respect to wild type: *p < 0.05, **p < 0.01, ****p < 0.0001 (calculated with ANOVA-Bonferroni-Holm).

3.1.8.2. Regulation of *ZmHpl* on DHS silencing and DHS overexpressing maize lines

ZmHpl is a key regulatory enzyme and controls JA-responsive pathways in plant (Feussner and Wasternack, 2002; Nemchenko *et al.*, 2006). The result revealed that *ZmDHS1* influences hydroperoxide lyase gene (*ZmHpl*) expression. Expression of *ZmHpl* was increased in almost all transgenic lines without infection (27.3-fold in SI-2, 6.3-fold in SI-3 and 5.4 fold in OE-1). In the silencing line SI-1 expression of *ZmHpl* was remarkably increased 50 fold compared to the wild type. Up-regulation was also observed in silencing lines Si-2, SI-3 and overexpressing lines OE-1. There was no difference between overexpressing line OE-2 and the wild type (Figure 31 A).

After infection with *B. sorokiniana*, transcript level of *ZmHpl* was down-regulated in SI-3 and OE-1. No significant differences in *ZmHpl* expression were detectable in the other lines (Figure 31 B). On the other hand, the infection with *C. heterotrophus* clearly affected the expression of *ZmHpl*. Expression of *ZmHpl* in DHS overexpressing line OE-1 and OE-2 was up-regulated approximately 3 and 6 times, respectively, compared to the wild type. Silencing lines showed no differences in the expression of *ZmHpl* compared to the wild type (Figure 31 C).

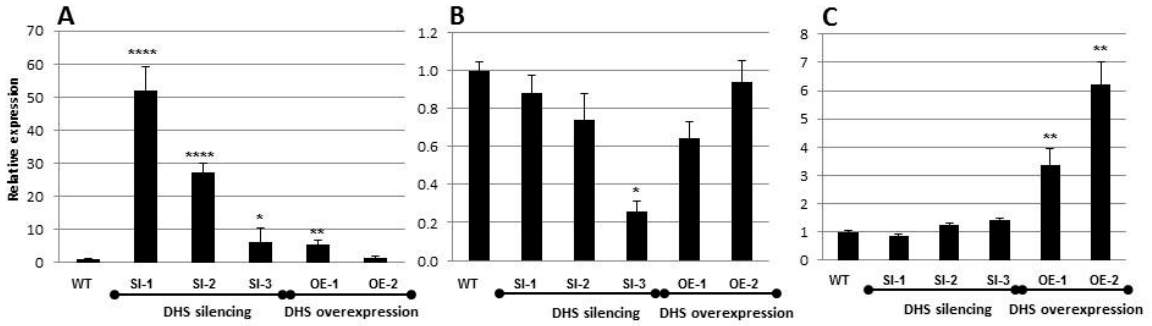

Figure 31. Relative expression of *ZmHpl* gene by qPCR in DHS silencing and DHS overexpressing lines. (A) Expression of *ZmHpl* before fungal inoculation. All transgenic lines showed an increase in *ZmHpl* expression levels in comparison to wild type, except the OE-2 overexpressing line which was similar to the wild type. (**B)** Expression of *ZmHpl* after inoculation with *B. sorokiniana*. The transcript level of *ZmHpl* was decreased in the silencing line SI-3 and in the overexpressing line OE-1. No significant difference was observed in the other lines compared to the wild type. (**C)** Expression of *ZmHpl* after inoculation with *C. heterotrophus*. In overexpressing lines, expression of *ZmHpl* was up-regulated compared to the wild type. Quantitative RT-PCR was performed three times, with three biological and technical replicates. The wild type expression was set at 1.

The diagram was compiled using the relative expression software tool-Multiple Condition Solver REST-MCS version 2 (REST-348, Michael W. P., 2001). Significance with respect to wild type: *p < 0.05, **p < 0.01, ****p < 0.0001 (calculated with ANOVA-Bonferroni-Holm).

3.1.8.3. Regulation of *ZmGsl* on DHS silencing and DHS overexpressing maize lines

In higher plants, 1-3-β-glucan or callose is a component of specialized cell walls or cell wall-associated structures at particular stages of growth and differentiation. Callose synthases produce high levels of callose increasing resistance to several different biotic stresses. It is also deposited at cell plates during cytokinesis. In addition, callose can be deposited at plasmodesmata (PD) to regulate the cell-to-cell movement of molecules by controlling the size exclusion limit (SEL) of PD (Chen and Kim, 2009).

In order to determine whether or not *ZmDHS1* is involved in 1-3-β-glucan synthesis, qRT-PCR was used to verify the glucan synthase gene in DHS silencing and overexpressing lines. In *Arabidopsis thaliana*, twelve genes encoding putative callose synthase have been identified (Verma and Hong, 2001). However there is only one gene encoding putative callose synthase in maize.

The result showed a connection between *ZmDHS1* and 1-3-β-glucan synthase (*ZmGsl*) in transcript level. There was a 3-4-fold increase in the expression of 1-3-β-glucan synthase in the overexpressing lines compared to the wild type before infection (Figure 32 A). No significant difference was observed in the expression of *ZmGsl* in silencing lines compared to the wild type (Figure 32 A). After infection with *B. sorokiniana* the expression of 1-3-β-glucan synthase was also up-regulated in overexpressing lines compared to the wild type. There were no significant differences in the expression of *ZmGsl* in the silencing lines compared to the wild type. In the cases of leaves infected with *C. heterotrophus*, two lines (SI-3 and OE-1) had a decrease in the expression of 1-3-β-glucan synthase compared to the wild type (Figure 32 B). The other lines had no significant difference in the transcript level of 1-3-β-glucan synthase compared to the wild type.

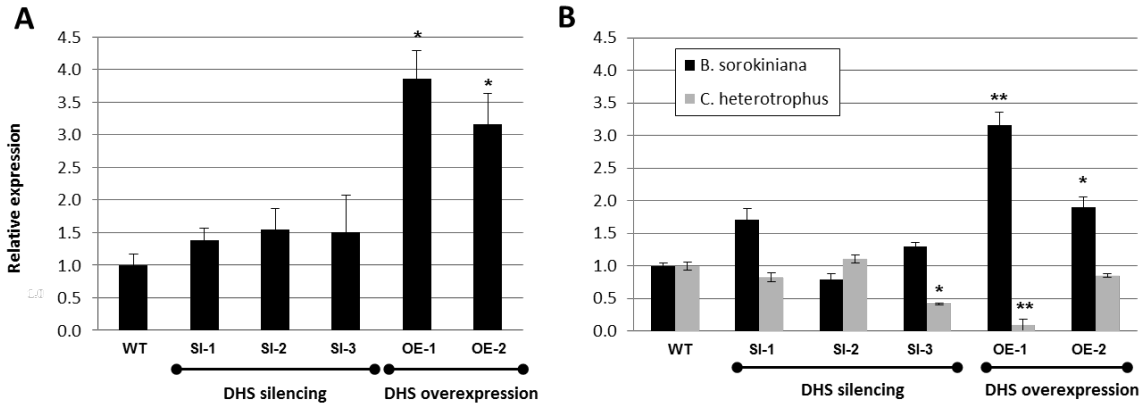

Figure 32. Relative expression of *ZmGsl* in DHS silencing and DHS overexpressing lines. (A)

Expression of 1-3-β-glucan synthase before fungal inoculation. No significant difference in *ZmGsl* expression was observed in silencing lines compared to the wild type. The expression of *ZmGsl* was 3 to 4 times- up-regulated in DHS overexpressing lines compared to the wild type. **(B).** Expression of 1-3-β-glucan synthase after inoculation with *B. sorokiniana* (black bars) and *C. heterotrophus* (grey bars). After infection with *B. sorokiniana* the expression of *ZmGsl* was also up-regulated in the overexpressing lines compared to the wild type. There were no significant differences in the expression of *ZmGsl in the* silencing lines compared to the wild type. After infection with *C. heterotrophus* two lines (SI-3 and OE-1) had a decrease in the expression of *ZmGsl* compared to the wild type. The other lines had no significant difference in the transcript level of *ZmGsl* compared to the wild type. Quantitative RT-PCR was performed three times, with three biological and technical replicates. The wild type expression was set at 1. The diagram was compiled using the relative expression software tool-Multiple Condition Solver REST-MCS version 2 (REST-348, Michael W. P., 2001). Significance with respect to wild type: *$p < 0.05$, **$p < 0.01$, ****$p < 0.0001$ (calculated with ANOVA-Bonferroni-Holm).

3.2. Expression profiles of *Fusarium graminearum* wild type and overexpressing mutants DHSoex and DOHHoex during early wheat infection

Continuing with the study of eIF5A-hypusine biosynthesis in a different system, the pathogenicity of *F. graminearum* towards wheat was surveyed by infecting the spring wheat cultivar Nandu with mutants of *F. graminearum* overexpressing DHS (DHSoex) or DOHH (DOHHoex) and the wild type strain (WT). All strains used in this part of the study are carrying a constitutive expressed GFP gene (Section 2.2.1).

3.2.1. Pathogenicity assay of wild type and overexpressing mutants DHSoex and DOHHoex on wheat spikes.

To determine the pathogenic development of wild type**,** DHSoex and DOHHoex, point inoculation assays on wheat spikes were performed. Wheat spikes were infected with a conidial suspension of 200 c/ml of WT strain and the overexpressing mutants DHSoex and DOHHoex.

Figure 33. Pathogenicity assay on wheat. Two central wheat spikelets were inoculated with a conidial suspension of 200 c/ml of the WT, DHSoex and DOHHoex and incubated for 10 days. The inoculation points are indicated with black asterisks. The infection of DHSoex strain proceeded faster and spread further compared to the wild type infection. No disease symptoms were observed with the DOHHoex strain and the infection stopped in the inoculated spikelet. The wild type infection caused typical symptoms for *Fusarium* head blight disease. Water was used as a negative control. The wheat infections were performed with 10 spikes for each treatment and 3 independent experiments (n = 30).

After 10 days of inoculation the DHSoex mutant showed an increase in virulence compared to the wild type. On the contrary, the mutant DOHHoex caused nearly no disease symptoms and strongly reduced virulence compared to the wild type. The results provided evidence that DOHH overexpression in *F. graminearum* does not produce infection on wheat spikes (Figure 33).

3.2.2. Expression analysis of *FgDHS*, *FgDOHH* and *FgEIF5A1* on the overexpressing mutants and wild type of *F. graminearum*

The expression of *FgDHS* and *FgDOHH* gene during wheat infection was determined by qPCR analysis. The expression of *FgDHS* and *FgDOHH* was up-regulated as expected in the respective overexpressing mutant compared to the wild type. There were no significant differences in the expression of *FgDOHH* and *FgeIF5A* compared to the wild type in DHSoex. With DOHHoex, *FgDHS* and *FgeIF5A* showed a similar result, no significant difference compared to the wild type (Figure 34).

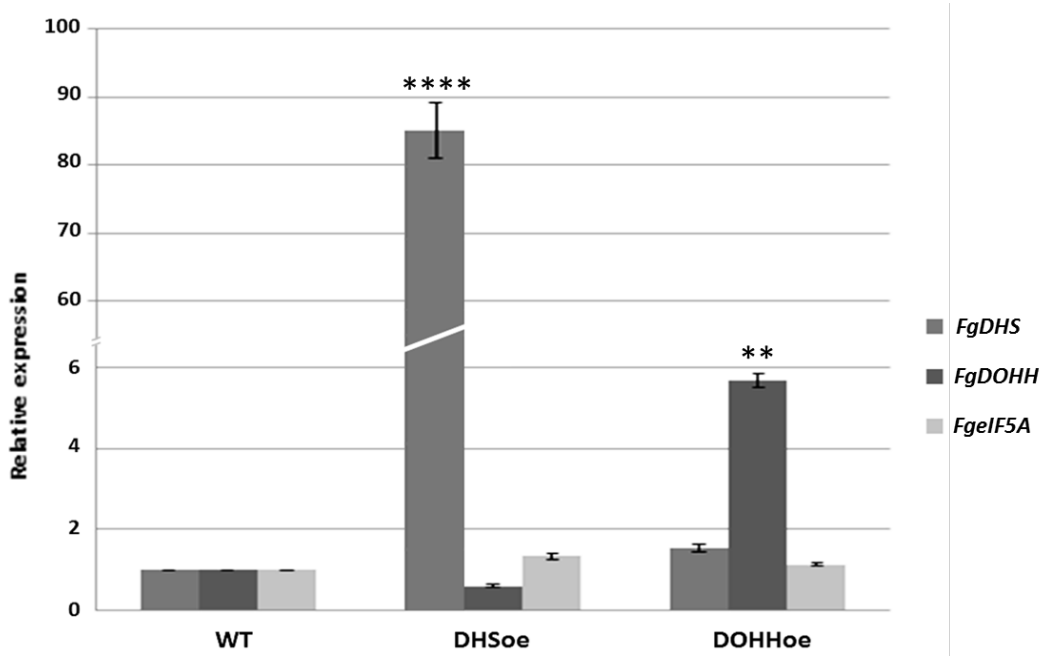

Figure 34. Relative expression of *FgDHS*, *FgDOHH* and *FgeIF5A* genes during wheat infection. Gene expression was determined by qPCR using cDNA derived from DHSoex, DOHHoex mutants and the WT strain during wheat infection at 10 dpi. Tubulin was used as normalizer and water as a negative control. *FgDHS* and *FgDOHH* expression are up regulated in the respective overexpressing strains. Quantitative RT-PCR was performed three times, with three biological and technical replicates. The wild type expression was set at 1. The diagram was compiled using the relative expression software tool-Multiple Condition Solver REST-MCS version 2 (REST-348, Michael W. P., 2001). Significance with respect to wild type: *p < 0.05, **p < 0.01, ****p < 0.0001 (calculated with ANOVA-Bonferroni-Holm).

3.2.3. Comparison of infection structure formation in wild type, DHSoex and DOHHoex on wheat glumes

In previous studies, the overproduction of infection structures on DHSoex mutant and the lack of infection structures on the DOHHoex mutant of *F. graminearum* was determined (Martinez-Rocha *et al.*, 2016). Therefore in the presented work, macroscopy study was focused in detail on the initial infection stages of these mutants compared to wild type. During the infection assays with detached floret organs, infection structures of WT, DHSoex, DOHHoex were identified and compared by stereomicroscopy, confocal laser scanning microscopy and scanning electron microscopy.

3.2.3.1. Bioimaging infection structure formation

All mutants were studied during initial infection stages from 7 to 11 days post inoculation. While the DHSoex exhibited a more severe infection of wheat glumes; the DOHHoex was unable to cause disease symptoms of the inoculated glumes (Figure 35).

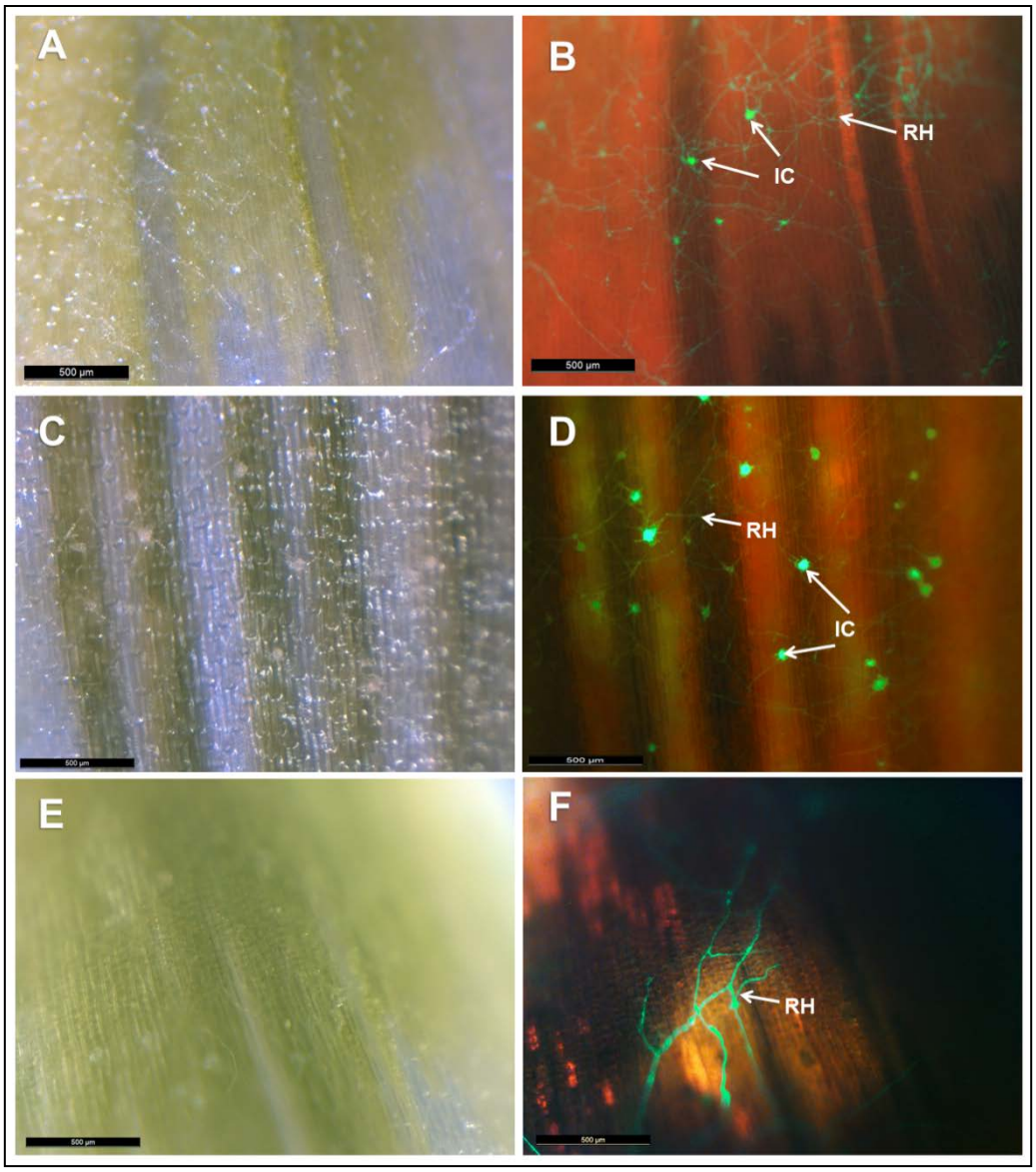

Figure 35. Infection structures of *F. graminearum* on wheat glumes at 9 dpi. Wheat glumes infected with theWT strain **(A, B)**, the DHSoex mutant **(C, D) or the** DOHHoex mutant **(E, F).** Bright-field images of the glume surface inoculated with *F. graminearum* **(A, C, E)**. Infection cushion and runner hyphae grew on a glume with GFP detection **(B, D, F)**. The formation of infection cushions (IC) was increased after 9 dpi compared to WT. DOHHoex mutant did not produce any infection structures when compared to DHSoex or WT. Scale bar = 500 µm. ***Abbreviations: RH*** *Runner hyphae;* ***IC*** *Infection cushion.* Micrographs were taken with a fluorescence stereomicroscope (MZFLIII, Leica) and are representative of 10 infected glumes.

Homogenous hyphal networks were observed on glumes inoculated with the DHSoex mutant or the wild type strain after 7 dpi. No disease symptoms were observed at this stage I. From 7 to 10 dpi, compound appressoria, infection cushion and foot structures of DHSoex and wild type, which characterize infection stage II, were formed and expanded to the whole glume surface. Remarkably the DHSoex mutant showed bigger infection cushions and the amount of infection cushion was slightly higher compared to the wild type at the same time of infection (Figure 35 A-D). Generally, infection stage II of the DHSoex mutant occurred 2-3 days earlier when compared to the wild type.

During infection stage I germination of conidia and colonization of the plant surface of the DOHHoex mutant was similar to the wild type. Growth and development of DOHHoex mycelium on glumes was monitored daily by fluorescence stereomicroscopy. The DOHHoex mutant did not produce foot structures or compound appressoria, such as lobate appressoria and infection cushions during stage II. In addition, no necrosis was observed even after 14 dpi. In figure 35 (E, F) runner hyphae of the DOHHoex mutant are visible, growing on the surface of a glume at 9 dpi.

3.2.3.2. Microscopic analysis of infection structure formation

To observe more details of the early infection phase of the wild tpe and overexpressing mutants, confocal laser scanning microscopy (CLSM) and scanning electron microscopy (SEM) were used. The formation of infection structures was increased in the DHSoex mutant in comparison to the wild type strain when grown on wheat glumes (Figure 36, 37, 38). DHSoex mutant exhibited all infection stages similar to the wild type. However, the penetration process occurred 2-3 days earlier compared to the wild type juged by the appearecence of the different types of appressoria.

Using CLSM, the mycelium and infection structures of the mutants were visible on the plant due to constitutively expressed GFP in the hyphal cytoplasm (Figure 36). Microscopic analysis revealed no differences between the DHSoex mutant and WT regarding the germination of conidia and colonization of the runner hyphae on the glume surface during stage I of infection.

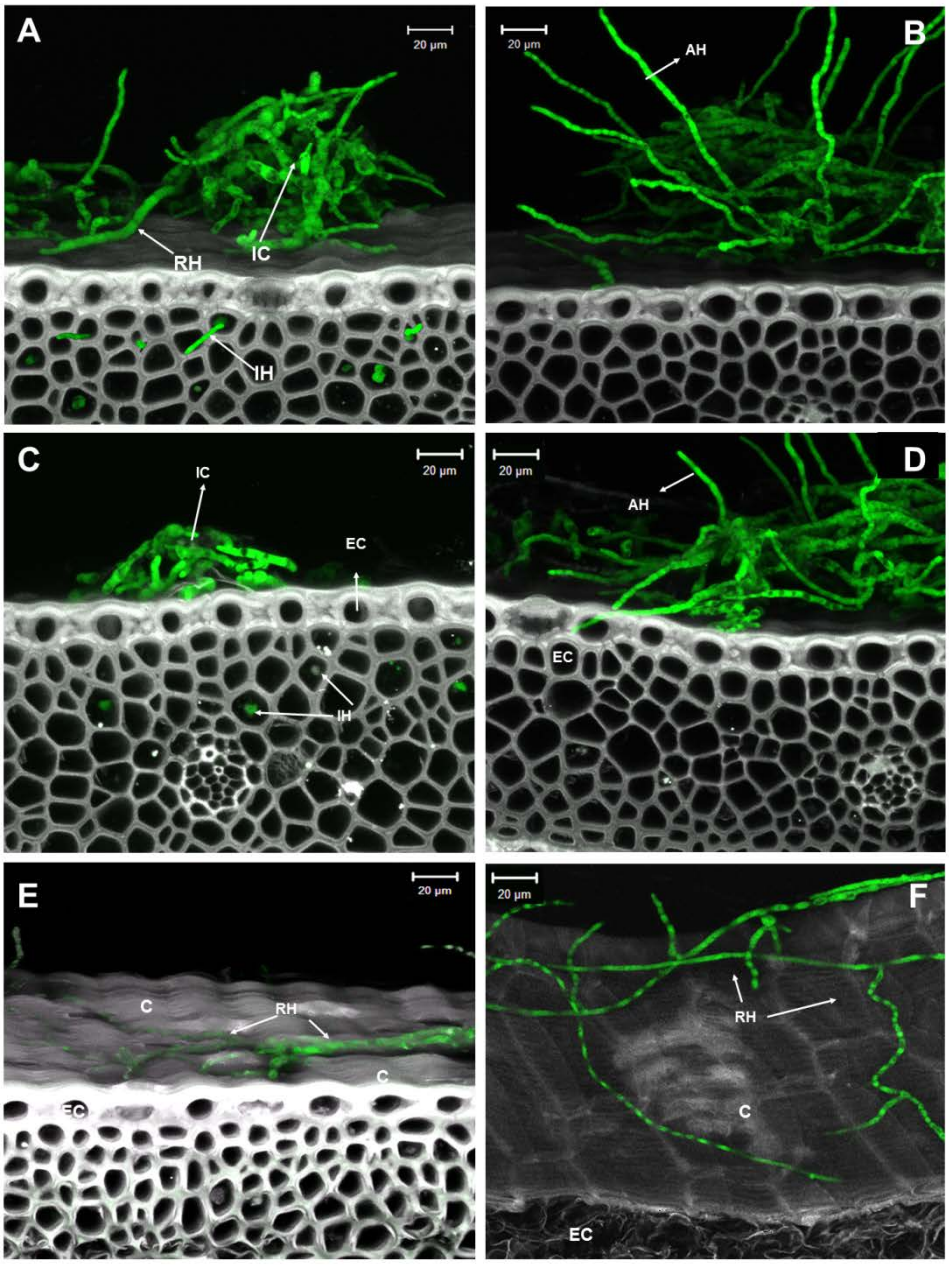

Figure 36. Confocal laser scanning microscopy (CLSM) images of infection structures on wheat glume cross sections. Wheat glumes infected with the WT strain **(A, B)**, with the DHSoex mutant **(C, D)** or the DOHHoex mutant **(E, F)**. **(A, C)** Infection cushion formed on glumes by WT and DHSoex, respectively. **(B, D)** Aerial hyphae of WT and DHSoex grown on glumes after 9 days of inoculation. **(E, F)** The DOHHoex mutant only produced runner hyphae on glumes. **(E)** Weak GFP signal showed the dying part of runner hyphae. The DOHHoex mutant did not produce any infection structures when compared to DHSoex or WT. Scale bar = 20 µm. ***Abbreviations:*** ***RH*** *Runner hyphae;* ***IC*** *Infection cushion;* ***IH*** *Intracellular hyphae;* ***EC*** *Epidermal cell;* ***C*** *Plant cuticle;* ***AH*** *Aerial hyphae.*

In stage II appressoria, infection cushions and runner hyphae were observed in WT and DHSoex (Figure 36 A, B, C, D). During infection stage III, the DHSoex mutant caused necrosis earlier than WT after 8-10 dpi. The entire tissue of glumes was necrotic, and aerial hyphae were also clearly observed (Figure 36 B, D).

The DOHHoex mutant did not produce infection structures. No intracellular hyphae of the DOHHoex mutant were visible in a cross section of glumes. A reduction of GFP fluorescence in the mycelium was observed starting at 6 dpi (Figure 36 E, F).

By using SEM, clear pictures of infection structures from wild type and the overexpressing mutants were obtained by scanning electron microscopy (SEM) and revealed all types of infection structures including infection cushions (IC), foot structures and runner hyphae (RH) (Figure 37 A-D). Figure 37 A, C and E show typical RH of wild type and overexpressing mutants growing on glume. A closed-up view from complex IC of wild type and DHSoex on glumes from upper view can be observed in Figure 37 B and D, while no IC is observed for DOHH (Figure 37 F).

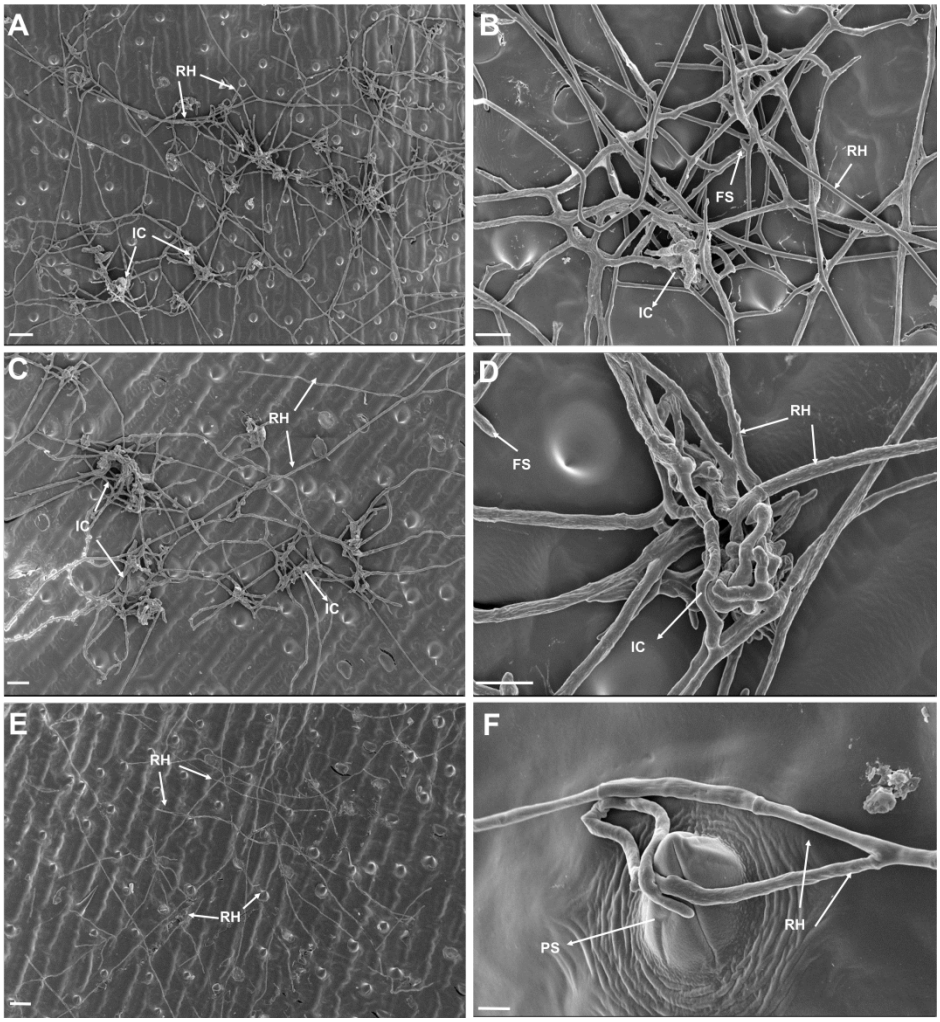

Figure 37. Infection structures of *F. graminearum* on wheat glumes at 9 dpi observed with SEM. Wheat glumes infected with the WT strain **(A, B)**, with the DHSoex mutant **(C, D)** or the DOHHoex mutant **(E, F)**. **(A, C)** Typical infection cushion and runner hyphae of WT and DHSoex grew on glume from upper view. **(B, D)** Complex infection cushion of WT and DHSoex on glumes. **(E, F)** Runner hyphae of DOHHoex on glume from upper view and closed-up view. Scale bar = 20 μm (**A, C, E**) or 10 μm (**B, D, F**). *Abbreviations: **RH** Runner hyphae; **IC** Infection cushion; **IH** Intracellular hyphae; **PS** Papillae silica cell; **FS** Foot structure.*

Not only infection structures above epidermal tissue but also intracellular hyphae of wild type and DHSoex are observed in Figure 38 A to D demonstrating that penetration occurs at IC. No intracellular hyphae of the DOHHoex mutant were visible (Figure 38 E, F). These results demonstrate that the DOHHoex mutant does not form infection cushions and it does not penetrate the epidermal cells of wheat glumes. In DOHHoex the stage I of infection is similar to the wild type, stage II does not exist and stage III is not shown as described in the wild type.

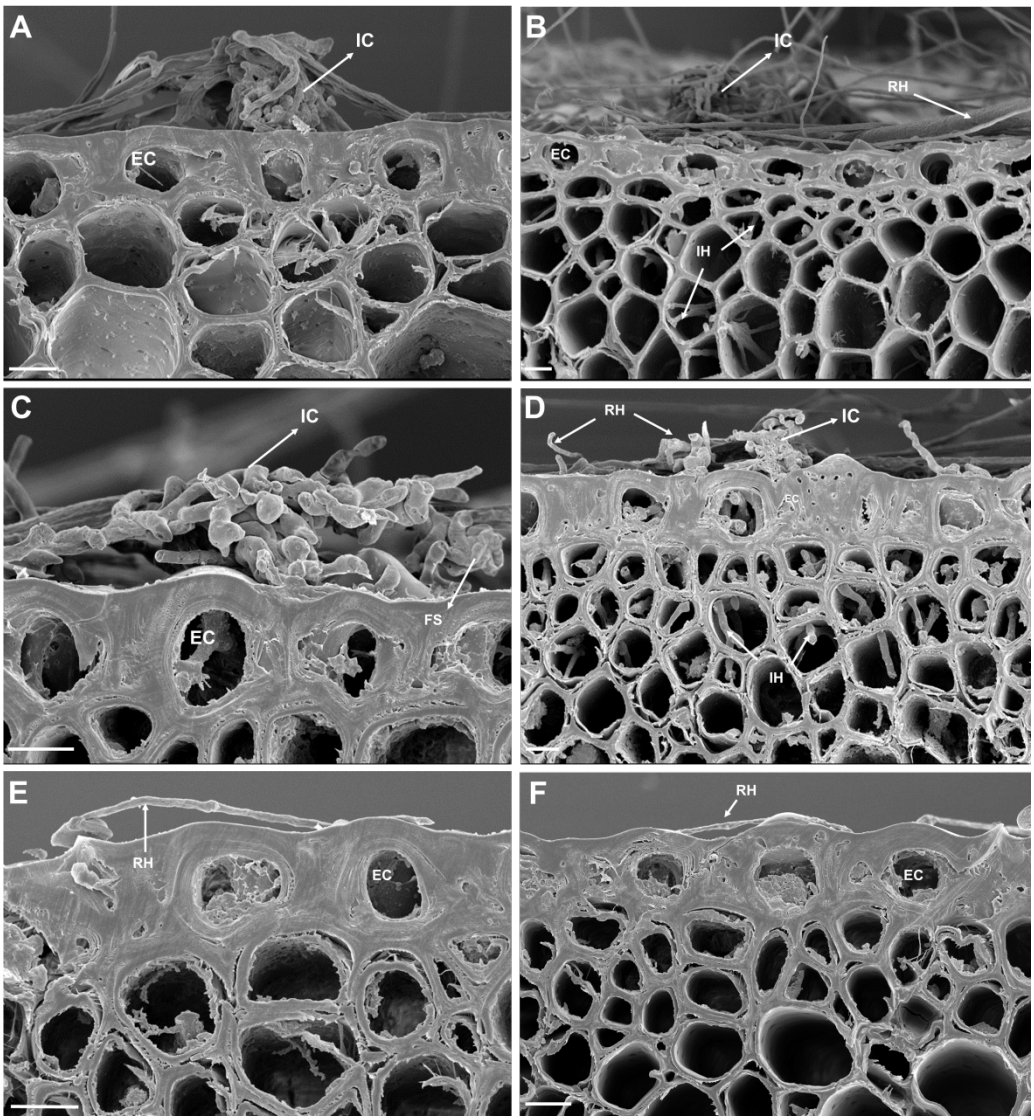

Figure 38. Cross sections of infection structures of *F. graminearum* on wheat glumes at 9 dpi using SEM. Wheat glumes infected with the WT strain **(A, B)**, with the DHSoex mutant **(C, D)** or the DOHHoex mutant **(E, F)**. **(A, C)** Epidermal invasion by infection cushions formed by the WT and DHSoex mutant. **(B, D)** Overview of runner hyphae, complex infection cushion and intracellular hyphae of WT and DHSoex in a cross section of glume. **(E, F)** Runner hyphae of DOHHoex in a cross section of glume. Scale bar = 20 µm. ***Abbreviations: RH*** *Runner hyphae;* ***IC*** *Infection cushion;* ***IH*** *Intracellular hyphae;;* ***EC*** *Epidermal cell.*

Stomata penetration could be observed during stage II in wild type and DHSoex mutant by SEM studies (Figure 39 A, B). The DOHHoex mutant could not build up any infection

structures during stage II; hence no penetration was recorded even after 14 dpi. Using CLSM, stomata penetration of DOHHoex hyphae was observed (Figure 39 C).

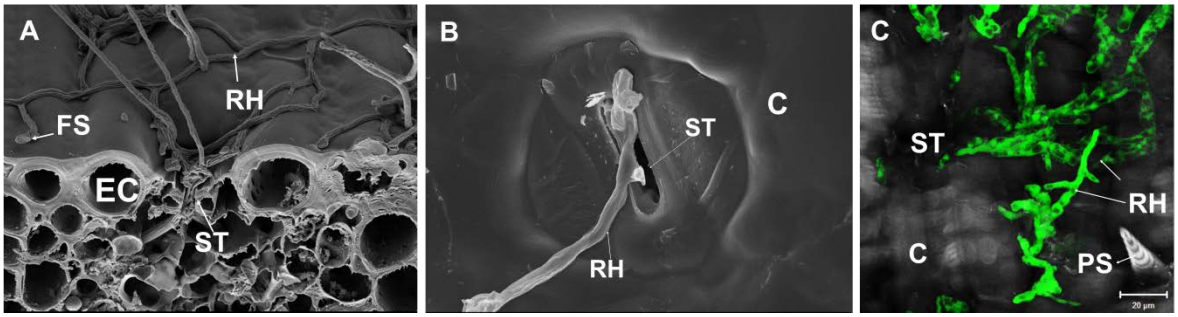

Figure 39. Stomata penetration of wheat glumes. (A) SEM micrograph of runner hyphae of WT entering the glume through stomata in a cross section. **(B)** SEM micrograph of runner hyphae of DHSoex going through a stomatal pore. **(C)** CLSM micrograph of runner hyphae of DOHHoex mutant going through stomata of wheat plant. Scale bar = 10 µm. ***Abbreviations: RH*** *Runner hyphae;* ***EC*** *Epidermal cell;* ***C*** *Plant cuticle;* ***PS*** *Papillae silica cell;* ***ST*** *stomata;* ***FS*** *Foot structure.*

3.2.4. Collection of infection structures, mRNA isolation and optimal LD-PCR from fungal material grown on wheat glumes

In order to determine the genes responsible for the clear differences in infection structures produced by the DHSoex and DOHHoex mutants and the wild type, a transcriptome analysis was performed. Following the frame work of sample isolation by laser capture microdissection (LCM) (Section 2.7.6), runner hyphae (RH) and infection cushions (IC) from WT and DHSoex as well as RH from DOHHoex were collected. After selection and excition, laser impulses catapulted the samples against gravity in separate adhesive caps. The amount and the excised area of RH and IC of the different mutants and the wild type are described in Table 17.

Table 17. Amount and area of collected RH and IC.

Sample name	Replicate 1		Replicate 2		Replicate 3	
	Number of elements	Area of all elements (µm²)	Number of elements	Area of all elements (µm²)	Number of elements	Area of all elements (µm²)
Runner hyphae of WT (WT_RH)	1,021	1,520,123	987	1,490,456	1,005	1,516,374
Infection cushion of WT (WT_IC)	460	1,484,038	477	1,512,314	562	1,532,782
Runner hyphae of DHSoex (DHS_RH)	965	1,542,607	987	1,513,918	953	1,483,378
Infection cushion of DHSoex (DHS_IC)	419	1,534,500	423	1,509,354	400	1,490,235

Runner hyphae of DOHHoex (DHS_RH)	1,145	1,498,545	1,216	1,512,224	1,134	1,500,985

Isolation of mRNAs from these samples was performed using the dynabead oligo $(dT)_{25}$ kit (Material and Methods section 2.7.8). Subsequently, first- strand synthesis of mRNAs was performed by SMART-PCR. Thereby ss cDNAs were provided, which served as templates for ds cDNA synthesis by LD-PCR as described in Material and methods section 2.7.11.

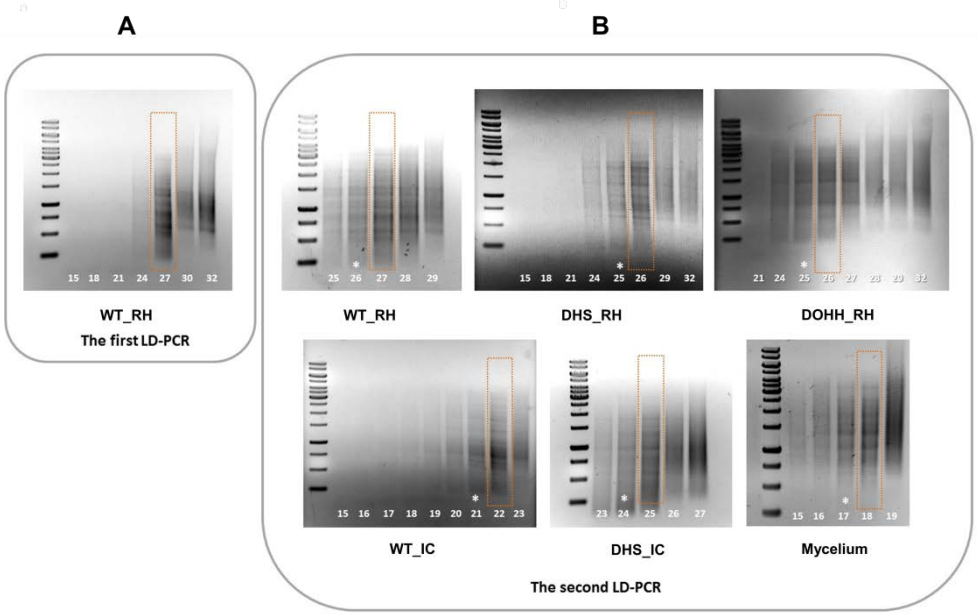

Figure 40. Determination of the optimal LD-PCR cycle for exponential amplification of cDNA libraries. **(A)** Example of the first LD-PCR for WT- RH. 5 µl of cDNA at different cycles were separated by electrophoresis on a 1.2% agarose gel in 1X TAE buffer (**B)** With the second LD-PCR, the optimal number of cycles for exponential phase of amplification were determined. In all samples appears a smear between 0.5 and 5 kb size. The best cycle was chosen for synthesis of ds cDNA.

In order to determine the quality of the produced libraries as well as the optimal number of amplification cycles with exponential phase, the cDNA libraries from RH and IC of WT, DHSoex- and DOHHoex were separated in agarose gels by electrophoresis as described in section 2.7.11 (According to the protocol in M. Boenisch University of Hamburg PhD thesis, 2013). After 2 rounds of LD-PCR per sample, the optimal number of cycles for exponential phase of amplification was selected: 26 for WT-RH, 21 for WT-IC, 25 for DHS-RH, 24 for DHS_IC, 25 for DOHH_RH and 17 for mycelium (Figure 40).

3.2.5. Transcriptome sequencing of infection cushions and runner hyphae

The produced cDNA libraries were sequenced using Illumina Plattform at the Heinrich-Pette-Institute (Section 2.7.14). Statistics and quality assessment of the sequenced data was

performed. Table 18 shows the total number of RAW (unprocessed) reads and the remaining trimmed reads from cDNA libraries of mycelia, runner hyphae and infection cushions.

Table 18. The number of raw reads and the remaining trimmed reads per sample.

Replicate	Type I	Type II	Raw Reads	Trimmed Reads	% Trimmed Reads
1	WT	Myc	23,821,986	23,784,701	99.84%
2	WT	Myc	24,929,593	24,790,152	99.44%
3	WT	Myc	27,703,434	27,595,045	99.61%
1	WT	IC	28,546,547	27,821,924	97.46%
2	WT	IC	30,079,787	29,716,292	98.79%
3	WT	IC	29,280,120	28,912,143	98.74%
1	WT	RH	29,226,814	28,906,107	98.90%
2	WT	RH	21,596,160	21,238,090	98.34%
3	WT	RH	30,281,192	29,925,276	98.82%
1	DHS	IC	24,913,780	24,507,804	98.37%
2	DHS	IC	21,887,232	21,751,474	99.38%
3	DHS	IC	24,510,671	24,243,119	98.91%
1	DHS	RH	22,199,124	21,778,039	98.10%
2	DHS	RH	26,339,260	26,169,407	99.36%
3	DHS	RH	39,380,966	39,236,502	99.63%
1	DOHH	RH	27,530,382	27,293,508	99.14%
2	DOHH	RH	28,495,262	28,401,309	99.67%
3	DOHH	RH	35,180,565	35,032,380	99.58%

At first, the overall similarity between samples was determined. Figure 41 visualizes sample-to-sample distances using a principal components analysis (PCA). In this ordination method, the data points (mycelia, IC and RH samples) are projected onto the 2D plane such that they spread out in the two directions. The x-axis is the direction that separates the data points the most (*PC1)*. The y-axis is a direction that separates the data the second most (*PC2*). The percentage of the total variance that is contained in the direction is printed in the axis label. A close proximity between sample points resembles a close relation. In our cDNA libraries, each data point of WT mycelia and WT-IC is close together, meaning the distances between samples in those tissues are approximately equal. In other tissues the distances between samples is not significantly different.

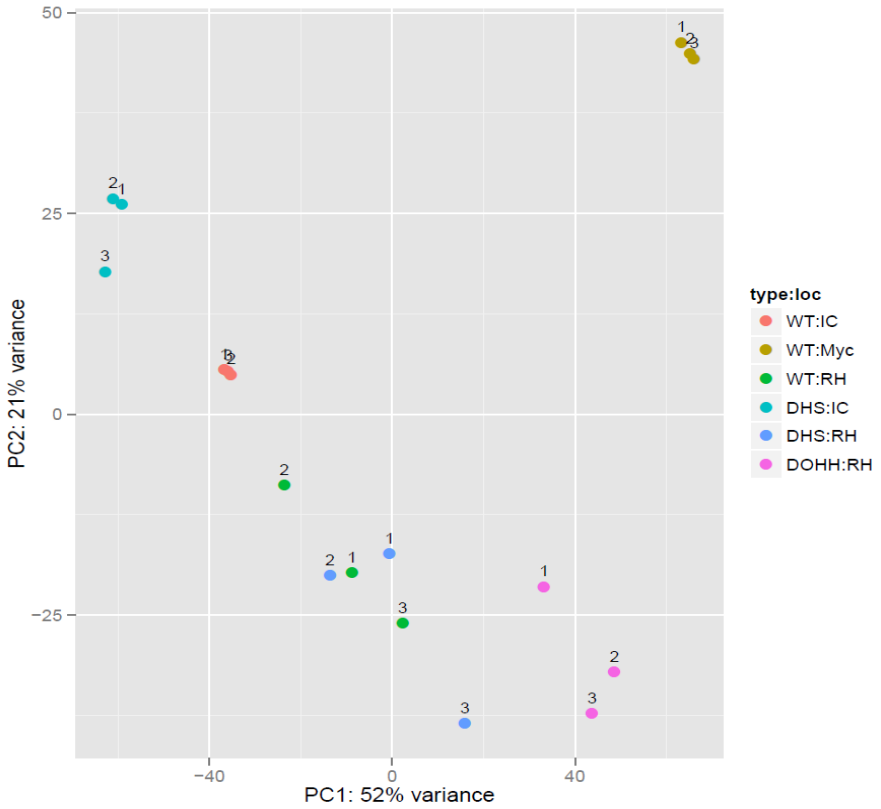

Figure 41. Visualization sample-to-sample distances of cDNA libraries. The data points (each sample corresponds to a color), are projected onto the 2D plane such that they spread out in the two directions. The x-axis is the direction that separates the data points the most (*PC1)*. The y-axis is a direction that separates the data the second most (*PC2*). All samples of WT mycelia and WT-IC are quite similar in this study. The distances between samples in other tissue is not significantly different. Each unique combination of treatment is given its own color.

For the analysis of the data the trimmed reads were mapped against the reference-genome of *F. graminearum*, obtained from the Helmholtz Zentrum München, with the STAR-software. Afterwards differential expression was determined with the "R-Bioconductor" Package "DESeq2". De-novo-assembly of the transcripts was done with the 'Trinity Transcriptome Assembler', and the resulting transcripts were annotated with "blastn" and the "nt" database (Data provided by the Heinrich-Pette-Institute).

3.2.6. Differential expression analyses

The analysis of the differentially expressed genes in the wild type and the overexpressing mutants were divided into three main parts:

Part I, comparison of the differentially expressed genes between DOHHoex and wild type, Part II, comparison of the differentially expressed genes between DHSoex and wild type and Part III, comparison of the differentially expressed genes during culture growth conditions and during early infection conditions.

Specific gene categories were defined for detailed comparisons of gene expressions. The categories were: Transcription factors (TF), Glycoside hydrolases (GH), Secondary metabolite (SM), ROS-related, Transporter (TP), Effectors, Fungal cell wall remodeling enzymes (FCWRE), Protein kinase (PK), and Plant Cell wall degrading enzymes (PPCWDE).

Several secondary metabolites produced by *F. graminearum* are essential factors for its defence and virulence, though the function of most of them is unknown. The expression of genes encoding secondary metabolite biosynthetic (SMB) gene clusters (Zhang *et al.*, 2012), including the well characterized mycotoxin pathways of the trichothecenes (Alexander *et al.*, 2009), and the red pigment aurofusarin (Malz *et al.*, 2005) were compared between wild type and the different mutants.

3.2.6.1. Part I: Comparison of differentially expressed genes between DOHHoex and wild type

The DOHHoex mutants of *F. graminearum* were unable to produce infection structures and subsequently to infect wheat spikes (see 3.2.3). Due to these findings we considered the comparison of this mutant to wild type the most interesting one (DOHH_RH to WT_RH and/or WT_IC), because it might indicate which genes are specifically regulated during infection structure formation and subsequent plant tissue penetration.

The Venn diagrams in Figure 42 show the results of this comparison between DOHH_RH and WT_RH and WT_IC. There are 1050 up regulated genes in comparison to WT_RH vs DOHH_RH and 902 up regulated genes when WT_IC vs DOHH_RH are compared (Figure 42 A, Appendix Figure 1). 495 genes are upregulated in WT runner hyphae (WT_RH) as well as in infection cushions (WT_IC) compared to DOHHoex runner hyphae (DOHH_RH). 555 genes are specifically unregulated in WT_RH, whereas 407 genes are specifically upregulated in WT_IC. Part B of the figure shows the down regulated genes. 483 genes are down regulated in the comparison of WT_RH vs DOHH_RH and 1064 are down regulated comparing WT_IC vs DOHH_RH (Appendix Figure 2). In this comparison 329 down regulated genes are the same in WT_RH and WT_IC. Discarding the similar genes in both tissues we have 154 down regulated genes specifically in WT_RH and 735 down regulated genes only in WT_IC.

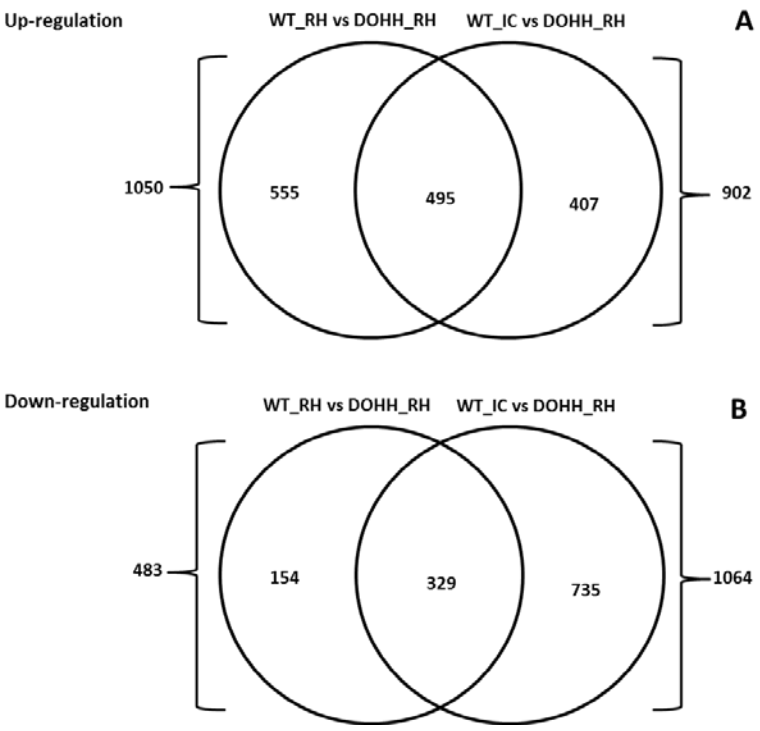

Figure 42. Venn diagrams displaying the differentially expressed, overlapped and unique genes upon different infection structures of *F. graminearum* wild type compared to runner hyphae of DOHHoex. (A) Displays the number of up-regulated genes in WT_RH and WT_IC compared to DOHH_RH. **(B)** Displays the number of down-regulated genes in WT_RH and WT_IC compared to DOHH_RH. Significance was set at $P < 0.05$, with a fold-change of 2 (log2 scale).

Comparison between WT_RH and DOHH_RH

The results from the WT_RH and DOHH_RH comparison revealed that from all 12579 significantly expressed genes, 179 genes are specifically transcribed in DOHH_RH representing 1.29% of the transcribed genome. However there are 1116 genes only transcribed in WT_RH representing 8% of the transcribed genome (Table 19). The comparison also showed the number of up and down regulated genes (Table 19, Figure 43).

Table 19. Number of expressed genes in WT_RH compared to DOHH_RH in different major categories.

	Genes expressed	Not expressed genes	Up regulated genes Log2>2	Down regulated genes Log2>2	In DOHH_RH		In WT_RH	
					Genes expressed only in DOHH-RH	Log2>2	Genes expressed only in WT_RH	Log2>2
Total	12579	1247	1050	483	179	15	1116	142
TF	866	26	29	44	5	0	26	4
GH	248	18	60	3	3	0	29	6
SM	478	84	52	17	17	0	69	6
ROS-related	997	52	102	42	11	0	69	7
TP	639	40	43	65	6	0	47	5
Effector	551	38	120	13	9	1	93	18
FCWRE	90	13	20	5	1	0	9	2
PK	191	18	7	9	2	0	13	1
PCWDE	217	9	59	3	1	0	33	7

The data demonstrated that in WT_RH the number of up regulated genes was higher than down regulated genes in the following categories: effectors, ROS-related, GH, secondary metabolite clusters, FCWRE and PCWDE. The number of down regulated genes was higher than up regulated genes in TF, TP and PK categories (Figure 43).

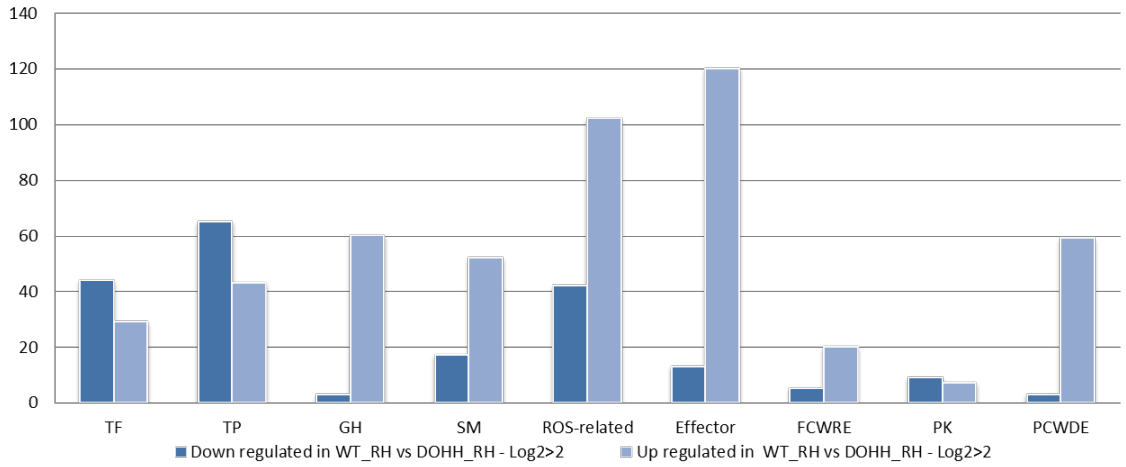

Figure 43. Up and down regulated genes (Log 2>2) in WT_RH compared to DOHH_RH. Regulated genes of wild type runner hyphae compared to DOHH runner hyphae grouped in functional categories transcription factor (TF), transporter (TP), glycoside hydrolase (GH), secondary metabolite (SM), ROS-related, effector, fungal cell wall remodeling enzymes (FCWRE), protein kinase (PK), cell wall degrading enzymes (CWDE). Differentially up-regulated genes are represented by pale blue colors; dark blue colors show down-regulated genes. The y-axis is the number of genes which were expressed in the samples.

To understand what makes WT_RH different from DOHH_RH we focused on the genes only expressed in WT_RH (missing genes in DOHHoex). There are 1116 genes only expressed in WT_RH compared to DOHHoex from which 142 genes have a Log2>2. A description in different major categories is shown in Figure 44. More than 50% of the uniquely expressed genes are uncategorized.

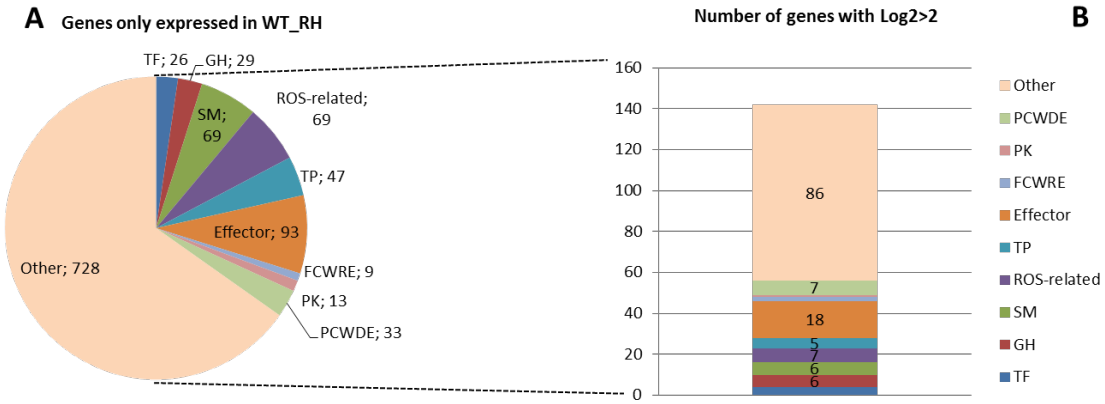

Figure 44. Pie graph of genes only expressed in WT_RH compared to DOHH_RH. (A) Genes expressed only in WT_RH compared to DOHH_RH arranged in different categories. **(B)** Genes only expressed in WT_RH and up-regulated in comparison to DOHH_RH (Log2>2).

Based on the analysis described in Figure 42, 77 genes only expressed in WT_RH, which were not shared in WT_IC, were chosen for further analysis (Appendix Table 1). There are sixty seven genes which encode for uncharacterized proteins (Appendix Table 1) and ten genes are described in the *F. graminearum* database (Table 20). In this analysis, there are some genes with high expression (Log2>5) such as *FGSG_03177, FGSG_12402, FGSG_15635*, and *FGSG_16406*. Data also show 7 genes that belong to SM gene cluster such as C37 (*FGSG_16114, FGSG_12294, FGSG_15339, FGSG_13421* and *FGSG_04441*), C11 (*FGSG_15074*) and C15 (*FGSG_00322*). The numbers in Table 20 show the Log2 of FPKM numbers (Fragments per Kilobase of Exon per Million Fragments Mapped) in comparison between WT_RH and DOHH_RH.

Table 20. Ten genes which are only expressed in WT_RH compared to DOHH_RH.

FGSG_Number	WT_RH vs DOHH_RH Log2	Description	Gene_cluster
FGSG_11202	3.402	probable guanylate kinase (ident 100.0%)	
FGSG_03177	5.698	related to amidase (ident 100.0%)	
FGSG_12402	5.815	related to flavoprotein (ident 34.4%)	
FGSG_04665	3.066	related to fumarate reductase flavoprotein subunit precursor (ident 100.0%)	
FGSG_07716	2.141	related to G protein coupled receptor like protein (ident 100.0%)	
FGSG_04709	2.224	related to multidrug resistant protein (ident 100.0%)	
FGSG_16114	3.99	related to multidrug transporter (yeast bile transporter) (ident 52.1%)	C37
FGSG_03706	2.312	related to non-ribosomal peptide synthetase (ident 66.5%)	
FGSG_07557	2.037	related to transcription co-repressor GAL80 (ident 100.0%)	
FGSG_01831	3.316	related to trihydrophobin precursor (ident 100.0%)	

The numbers in Table 21 show the Log2 of FPKM number. The number 0 is defined as no expression of a gene. Data of plant cell wall degrading enzymes revealed 59 up regulated genes in WT_RH compared to DOHH_RH, namely xylanases, cellulases and glucanases comprising the majority (Table 21). In this PCWDE category are 7 genes not expressed in DOHH_RH (Log2 = 0). Moreover, 12 genes (*FGSG_03628, FGSG_08046, FGSG_02202, FGSG_03624, FGSG_06463, FGSG_11036, FGSG_08911, FGSG_00184, FGSG_04930, FGSG_11098, FGSG_06445* and *FGSG_11048*) with high level of up-regulation (Log2>5) in WT-RH were also recorded (Table 21).

Table 21. Fifty nine PCWDE genes are up regulated in WT_RH compared to DOHH_RH.

FGSG_Number	Enzyme class	Enzyme substrate	Enzyme subclass	WT_RH vs DOHH_RH	log2 FPKM DOHH_RH	log2 FPKM WT_RH
FGSG_06605	cellulase	cellulose	beta glucosidase	2.807	4.943	7.750
FGSG_04953				2.460	3.679	6.139
FGSG_00767				2.043	3.505	5.548
FGSG_00571		cellulose	cellulase percursor	4.124	4.041	8.165
FGSG_03628			Cellulose breaking down enhancer	8.682	1.304	9.986
FGSG_03742				4.726	3.377	8.103
FGSG_01621				3.389	4.628	8.016
FGSG_03695				4.384	2.721	7.105
FGSG_06397				4.826	1.623	6.449
FGSG_02202			endo-1,4-beta-glucanase	7.215	1.485	8.700
FGSG_11488		cellodextrin	Cellobiohydrolase	2.935	2.155	5.090
FGSG_03632				4.566	0.224	4.790
FGSG_08253		Cellobiose	Cellobiose dehydrogenase	3.513	0.727	4.241
FGSG_11098	cellulase/hemicellulase	cellulose/hemicellulose	beta-1,3-glucan binding protein	5.263	1.614	6.877
FGSG_01570	cutinase	cutin	conserved hypthetical protein	2.501	5.634	8.136
FGSG_02342			cutinase 1 percursor	2.786	6.553	9.339
FGSG_03624	hemicellulase	Xylan	endo-1,4-beta-xylanase	6.679	3.391	10.070
FGSG_11049			acetylxylan esterase	4.951	1.661	6.612
FGSG_11229				2.831	3.739	6.570
FGSG_03867				3.689	1.846	5.535
FGSG_11112				3.587	0.000	3.587
FGSG_00783				2.199	0.277	2.476
FGSG_04930			endo-1,4-beta-xylanase	5.304	5.753	11.057
FGSG_08046				7.520	2.426	9.946
FGSG_08911				5.515	1.612	7.126
FGSG_02341				3.112	0.274	3.386
FGSG_00184			endo-1,4-beta-xylanase A	5.422	3.354	8.776
FGSG_02651			endo-1,4-beta-xylanase B	3.061	0.072	3.133
FGSG_11487		hemicellulose	alpha mannosidase	3.485	0.316	3.801
FGSG_06445			arabinose	5.152	0.000	5.152
FGSG_10999		MLG[c]	Endo-1,3(4)-β-glucanase	4.223	4.205	8.429
FGSG_11304				2.386	3.881	6.267
FGSG_15917			Endo-β-1,4-glucanase	4.661	0.000	4.661
FGSG_11258	ligninase	lignin	chloroperoxidase	2.246	5.122	7.368
FGSG_11037				4.070	0.428	4.497
FGSG_00032				2.551	0.000	2.551
FGSG_03194	pectinase	HG,RGII primary chain	endopolygalacturonase	2.302	1.776	4.078
FGSG_11011			PGU1 - Endo-polygalacturonase	2.123	2.406	4.529
FGSG_08946			exopolygalacturonase	3.440	1.486	4.926
FGSG_07625			Pectin/Pectate lyase	2.435	5.071	7.506

FGSG_06463				6.654	0.076	6.730
FGSG_03003				3.790	1.915	5.704
FGSG_03002				2.728	1.947	4.675
FGSG_07207				3.362	0.000	3.362
FGSG_11366		Pectin/ Xylan side chain	arabinanase	3.091	3.021	6.113
FGSG_11048				5.137	4.798	9.935
FGSG_00096				3.253	2.923	6.175
FGSG_07551				2.866	2.780	5.646
FGSG_02386				3.643	1.845	5.488
FGSG_03483				3.477	0.728	4.205
FGSG_09291				2.222	0.031	2.253
FGSG_01607		Pectin side chain	beta-galactosidase	2.343	0.404	2.747
FGSG_07794				2.117	0.000	2.117
FGSG_03406		Pectin	pectinesterase	4.398	2.914	7.312
FGSG_03530				2.769	0.000	2.769
FGSG_04848			rhamnogalacturonan acetylesterase	4.943	0.084	5.027
FGSG_11036	Phenolic	Ferulic acid	Feruloyl esterase	5.743	2.633	8.376
FGSG_12548				3.122	4.279	7.401
FGSG_11428				4.917	0.417	5.334

A survey on fungal cell wall remodeling genes revealed 20 up regulated genes in WT_RH compared to DOHH_RH (Table 22). In this category 2 genes (*FGSG_06451* - related to levanase and *FGSG_11037* - encoded endoglucanase I precursor) were missed in DOHH_RH and 2 genes (*FGSG_08253* - related to endo-1,4-beta-glucanase and *FGSG_11098* - related to beta-1,3-glucan binding protein) had high levels up-regulation in WT_RH.

Table 22. Twenty fungal cell wall remodeling enzyme genes (FCWRE) are up regulated in WT_RH compared to DOHH_RH.

FGSG_Number	WT_RH vs DOHH_RH	log2 FPKM DOHH_RH	log2 FPKM WT_RH	Description
FGSG_00184	4.223	4.205	8.429	uncharacterized protein
FGSG_02262	3.495	4.131	7.626	related to endo-1,3-beta-glucanase (ident 52.3%)
FGSG_02339	3.317	2.835	6.152	related to SUC2 - invertase (sucrose hydrolyzing enzyme) (ident 100.0%)
FGSG_02354	2.741	7.354	10.094	related to class V chitinase (ident 49.2%)
FGSG_02651	2.386	3.881	6.267	related to endo-1,3-beta-glucanase (ident 100.0%)
FGSG_03212	3.856	8.605	12.461	related to endochitinase (ident 100.0%)
FGSG_04654	2.097	4.288	6.385	related to agglutinin isolectin 1 precursor (ident 100.0%)
FGSG_04704	3.163	0.086	3.249	related to glucoamylase precursor (ident 100.0%)
FGSG_06451	3.756	0.000	3.756	related to levanase (ident 100.0%)
FGSG_06549	2.747	2.611	5.358	related to chitin binding protein (ident 100.0%)
FGSG_06550	2.488	1.527	4.015	related to chitin synthase (ident 100.0%)
FGSG_06873	2.255	3.243	5.498	related to CRH1 - family of putative glycosidases might exert a common role in cell wall organiza (ident 100.0%)

FGSG_08253	7.215	1.485	8.700	related to endo-1,4-beta-glucanase (ident 100.0%)
FGSG_08415	2.050	2.295	4.345	uncharacterized protein
FGSG_10235	2.441	9.297	11.738	related to rasp f 7 allergen (ident 100.0%)
FGSG_10922	2.671	2.846	5.517	uncharacterized protein - related to extracellular cellulase CelA/allergen Asp F7-like, putative (ident 59.2%)
FGSG_11037	4.661	0.000	4.661	probable endoglucanase 1 precursor (ident 100.0%)
FGSG_11098	5.263	1.614	6.877	related to beta-1,3-glucan binding protein (ident 100.0%)
FGSG_11205	3.612	10.064	13.676	probable SnodProt1 precursor (ident 100.0%)
FGSG_11496	3.174	6.962	10.136	uncharacterized protein

In the comparison between WT_RH and DOHH_RH 77 genes were only expressed in WT_RH. The profound differences in the expression of CWDE and FCWRE genes could be the answer for the differences in phenotype we observed between mycelium growth of WT and DOHHoex on plant flower leaves.

Comparison between WT_IC and DOHH_RH

The comparison between WT_IC and DOHH_RH showed that from all 12662 significantly expressed genes, 196 genes were only transcribed in DOHH_RH representing 1.41% of the transcribed genome and 1199 genes only transcribed in WT_RH representing 8.67% of the transcribed genome (Table 23). This comparison also focused on the genes expressed exclusively in WT_IC compared to DOHH_RH. The purpose of this part is to look for candidate genes involved in IC formation and virulence in *F. graminearum*.

The number of up and down regulated genes in WT_IC compared to DOHH_RH is shown in Figure 45. Up regulated genes in WT_IC showed a high number of expressed genes in PCWDE, FCWRE, effector, GH and SM compared to DOHH_RH. The number of down regulated genes was higher than up regulated genes in the TF and TP categories.

Table 23. Overview of the number of expressed genes in WT_IC compared to DOHH_RH in different major categories.

	Genes expressed	Not expressed genes	Up regulated genes Log2>2	Down regulated genes Log2>2	In DOHH_RH		In WT_IC	
					Genes only expressed in DOHH_RH	Log2>2	Genes only expressed in WT_IC	Log2>2
Total	12662	1164	902	1064	196	29	1199	147
TF	866	26	27	72	2	0	26	2
GH	256	10	81	8	1	0	37	14
SM	488	74	73	36	12	0	79	12
ROS-related	1001	48	109	99	12	1	73	13
TP	652	27	74	89	7	0	60	9
Effector	558	31	106	63	12	2	100	29
FCWRE	93	10	19	9	0	0	12	4
PK	195	14	6	8	1	0	17	1
PCWDE	219	7	80	10	1	0	35	17

The data demonstrate that in WT_IC the number of up regulated genes was higher than down regulated genes in categories such as GH, SM clusters, ROS-related, effectors, FCWRE and PCWDE. The number of down regulated genes was higher than up regulated genes in the TF, TP and PK categories.

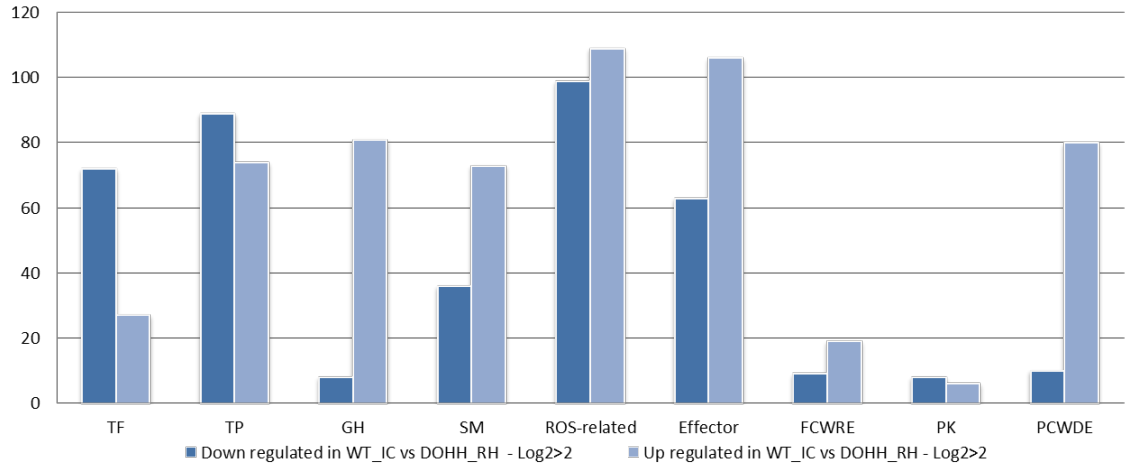

Figure 45. Up and down regulated genes in WT_IC compared to DOHH_RH. The statistical significance of gene induction (x axis) shows some functional categories (from the left to the right: transcription factor (TF), transporter (TP), glycoside hydrolase (GH), secondary metabolite (SM), ROS-related, effector, fungal cell wall remodeling enzymes (FCWRE), protein kinase (PK), cell wall degrading enzymes (PCWDE), respectively. Differentially up-regulated genes are represented by pale blue colors; dark blue colors are down-regulated genes. The y-axis gives the number of genes expressed in the samples.

Figure 46 shows the genes exclusively expressed in WT_IC compared to DOHH_RH. All of the genes with Log2>2 are shown in Figure 46 B. However, among these genes are some genes also expressed in WT_RH (Figure 42). Therefore, to reduce the high number of candidate genes we subtracted these genes.

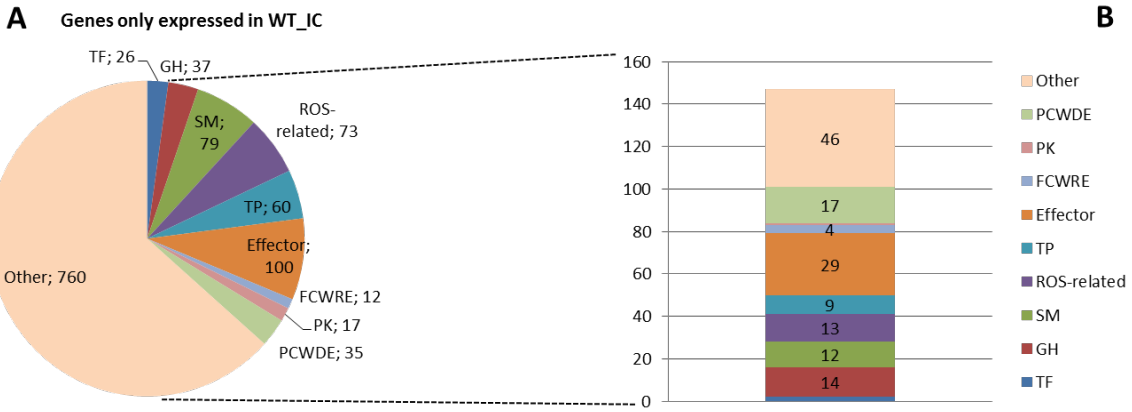

Figure 46. Pie graph of genes only expressed in WT_IC compared to DOHH_RH. (A) Genes only expressed in WT_IC compared to DOHH_RH with different categories. **(B)** Number of up regulated genes (147

genes) only expressed WT_IC and up-regulated in comparison to DOHH_RH (Log2>2). Significance was set at $P < 0.05$, with a fold-change of 2 (Log2 scale).

In a new analysis, 82 genes only expressed in WT_IC (Appendix Table 2) were chosen from 147 genes only expressed in WT_IC. Among them some genes were identified as putative virulence factors. Six genes encode proteins from the C37 cluster (*FGSG_10611, FGSG_17400, FGSG_10613, FGSG_10612, FGSG_10614* and *FGSG_17401*) (Table 24 and Appendix Table 2). One gene is a C15 and one other gene is C11 a cluster gene. All of these clusters have been described in reports of Ma *et al.* (2010) and Zhang *et al.* (2012). The C37 (FG3_40) and C40 (FG3_54) clusters are required for virulence (Zhang *et al.*, 2012). There were 4 genes showing a highly expressed level (Log2>5) (*FGSG_09085* - cellobiose dehydrogenase, *FGSG_12440* - lysine permease, *FGSG_15254* and *FGSG_16366* – encoded uncharacterized protein). Forty two of these 82 genes encode for uncharacterized proteins (Appendix Table 2). Table 24 shows 40 specifically expressed and up-regulated genes in WT_IC compared to DOHH_RH - Log2>2. These genes were described in the *F. graminaerum* database (Table 24).

Table 24. Forty genes specifically expressed and up-regulated in WT_IC compared to DOHH_RH - Log2>2.

FGSG_Number	Log2 FPKM WT_IC	Description	SM_Cluster
FGSG_06098	3.402	probable arginosuccinate synthetase (ident 100.0%)	
FGSG_09085	5.698	probable cellobiose dehydrogenase (ident 100.0%)	
FGSG_12440	5.815	probable lysine permease (ident 100.0%)	
FGSG_15973	3.066	probable neutral amino acid permease (ident 100.0%)	
FGSG_04864	2.141	probable pectate lyase (ident 100.0%)	
FGSG_11208	2.224	probable Xyloglucanase (ident 65.0%)	
FGSG_10611	3.99	related to 6-hydroxy-d-nicotine oxidase (ident 100.0%)	C37
FGSG_16895	2.312	related to acetylxylan esterase (ident 50.0%)	
FGSG_10986	2.037	related to alcohol oxidase (ident 100.0%)	
FGSG_04678	3.316	related to beta-mannanase (ident 100.0%)	
FGSG_03605	2.37	related to bifunctional 4-hydroxyphenylacetate degradation enzyme (ident 100.0%)	C15
FGSG_17091	2.659	related to capsule-associated protein (ident 100.0%)	
FGSG_07668	3.115	related to Carboxypeptidase 2 (ident 42.9%)	
FGSG_00773	2.324	related to copper transport protein (ident 100.0%)	
FGSG_10634	3.791	related to cutinase 1 precursor (ident 100.0%)	
FGSG_16565	2.603	related to CYB2 - Lactate dehydrogenase cytochrome b2 (ident 100.0%)	
FGSG_17400	3.044	related to cytochrome P450 monooxygenase (ident 100.0%)	C37
FGSG_07887	2.597	related to dehydrogenase/reductase (ident 36.7%)	
FGSG_08042	2.531	related to dihydroxyacetone kinase (ident 100.0%)	
FGSG_03918	4.335	related to endoglucanase (ident 100.0%)	

FGSG_04773	2.847	related to endoglucanase IV precursor (ident 100.0%)	
FGSG_09137	2.472	related to hydrolases or acyltransferases (alpha/beta hydrolase superfamily) (ident 35.9%)	
FGSG_11215	2.412	related to hydroxylase (ident 100.0%)	
FGSG_05793	2.89	related to integral membrane protein pth11 (ident 100.0%)	
FGSG_03790	2.748	related to metalloprotease MEP1 (ident 100.0%)	
FGSG_11528	2.825	related to monophenol monooxygenase (tyrosinase) (ident 100.0%)	
FGSG_10474	2.683	related to myo-inositol transport protein ITR1 (ident 100.0%)	
FGSG_00118	4.56	related to neutral amino acid permease (ident 100.0%)	
FGSG_03568	4.7	related to O-methyltransferase B (ident 100.0%)	
FGSG_03888	3.17	related to ornithine aminotransferase (ident 100.0%)	
FGSG_10613	4.549	related to para-hydroxybenzoate polyprenyltransferase precursor (ident 100.0%)	C37
FGSG_03131	3.304	related to pectate lyase L precursor (ident 100.0%)	
FGSG_16173	2.208	related to phosphoenolpyruvate phosphomutase (ident 53.9%)	
FGSG_10561	3.106	related to RF2 protein (ident 100.0%)	
FGSG_10612	3.204	related to salicylate hydroxylase (ident 100.0%)	C37
FGSG_07662	2.47	related to TAM domain methyltransferase (ident 33.6%)	
FGSG_12522	2.255	related to TAM domain methyltransferase (ident 40.1%)	
FGSG_04589	3.589	related to tetracenomycin polyketide synthesis O-methyltransferase tcmP (ident 100.0%)	C11
FGSG_07993	2.846	related to xylan 1,4-beta-xylosidase (ident 100.0%)	
FGSG_03609	3.539	related to xylosidase/glycosyl hydrolase (ident 50.7%)	

80 CWDE genes are upregulated in WT_IC, out of which 17 genes are specifically expressed in WT_IC (Table 25). Most of the cell wall degrading enzymes show high transcription level in WT_IC.

Table 25. Eighty PCWDE genes are up regulated in WT_IC (compared to DOHH_RH).

Enzyme class	Enzyme substrat	Enzyme subclass	FGSG_Number	WT_IC vs DOHH_RH	log2 FPKM DOHH_RH	log2 FPKM WT_IC
cellulase	cellulose	beta glucosidase	FGSG_00767	3.508	3.505	7.013
			FGSG_03410	3.086	0.997	4.083
			FGSG_03858	2.007	3.870	5.876
			FGSG_04953	2.608	3.679	6.287
			FGSG_08609	2.750	0.599	3.348
			FGSG_02632	4.587	0.121	4.708
		cellulase percursor	FGSG_01621	4.254	4.041	8.295
		cellulose binding	FGSG_08003	4.495	1.240	5.735
		Cellulose breaking down enhancer	FGSG_03632	2.182	1.623	3.805
			FGSG_03695	7.607	1.304	8.911
			FGSG_04773	2.847	0.000	2.847
			FGSG_06397	3.680	3.377	7.057

			FGSG_08011	4.284	0.546	4.830
			FGSG_11488	5.825	2.721	8.546
		endo-1,4-beta-glucanase	FGSG_08253	7.727	1.485	9.212
		endoglucanase	FGSG_03918	4.335	0.000	4.335
	cellodextrin	Cellobiohydrolase	FGSG_00571	5.479	2.155	7.634
			FGSG_03628	6.832	0.224	7.055
	Cellobiose	Cellobiose dehydrogenase	FGSG_03742	3.824	0.727	4.552
			FGSG_04872	4.195	1.777	5.972
			FGSG_05983	4.666	2.190	6.856
			FGSG_09085	5.698	0.000	5.698
Cellulose /hemicellulase	Cellulose /hemicellulose	beta-1,3-glucan binding protein	FGSG_11098	5.586	1.614	7.200
cutinase	cutin	cutinase 1 percursor	FGSG_10634	3.791	0.000	3.791
	hemicellulose	alpha mannosidase	FGSG_04930	4.236	0.316	4.552
		arabinose	FGSG_08046	4.616	0.000	4.616
		beta mannanase	FGSG_04678	3.316	0.000	3.316
		beta mannosidase	FGSG_13861	2.286	0.634	2.920
	MLG[e]	Endo-1,3(4)-β-glucanase	FGSG_00184	3.566	4.205	7.772
			FGSG_02651	2.543	3.881	6.424
			FGSG_03788	3.418	0.921	4.339
			FGSG_07772	5.004	1.172	6.176
		Endo-β-1,4-glucanase	FGSG_11037	6.301	0.000	6.301
	xyloglucan	Endo-β-1,4-glucanase	FGSG_05851	2.008	4.316	6.324
			FGSG_11208	2.224	0.000	2.224
hemicellulase	Xylan	endo-1,4-beta-xylanase	FGSG_03624	7.815	3.391	11.206
		acetylxylan esterase	FGSG_00783	3.110	0.277	3.387
			FGSG_03867	3.013	1.846	4.859
			FGSG_11049	6.424	1.661	8.085
			FGSG_11112	4.957	0.000	4.957
		xylan 1,4-beta-xylosidase	FGSG_07993	2.846	0.000	2.846
		endo-1,4-beta-xylanase	FGSG_06445	7.736	2.426	10.162
			FGSG_10411	2.567	1.826	4.393
			FGSG_10999	8.001	1.612	9.613
			FGSG_11304	6.584	0.274	6.858
			FGSG_11487	5.233	5.753	10.987
		endo-1,4-beta-xylanase A	FGSG_15917	6.264	3.354	9.618
		endo-1,4-beta-xylanase B	FGSG_11258	5.156	0.072	5.228
ligninase	lignin	chloroperoxidase	FGSG_02341	3.955	0.428	4.382
			FGSG_00032	3.773	0.000	3.773

pectinase	HG,RGII primary chain	endopolygalacturonase	FGSG_03194	2.111	1.776	3.887
		PGU1 - Endo-polygalacturonase	FGSG_11011	3.122	2.406	5.528
		exopolygalacturonase	FGSG_07551	4.922	1.486	6.408
		Pectin/Pectate lyase	FGSG_02386	2.977	5.071	8.048
			FGSG_03131	3.304	0.000	3.304
			FGSG_03483	6.860	0.076	6.936
			FGSG_03713	4.278	1.673	5.951
			FGSG_04864	2.141	0.000	2.141
			FGSG_07794	4.997	0.000	4.997
			FGSG_09291	5.277	1.915	7.191
	Pectin side chain	beta-galactosidase	FGSG_00096	5.282	0.000	5.282
			FGSG_11048	5.092	0.404	5.496
	Pectin/ Xylan side chain	arabinanase	FGSG_08946	5.215	3.021	8.237
			FGSG_03002	3.747	1.845	5.592
			FGSG_03609	3.539	0.000	3.539
			FGSG_05824	2.521	0.898	3.419
			FGSG_06463	4.131	2.923	7.053
			FGSG_07207	2.471	0.728	3.199
			FGSG_07542	2.087	4.781	6.868
			FGSG_07625	4.829	4.798	9.627
			FGSG_07639	5.139	1.516	6.656
			FGSG_07695	2.488	2.357	4.845
	RGI	Pectin/Pectate lyase	FGSG_00989	2.255	2.296	4.552
			FGSG_04689	2.768	0.381	3.148
	Pectin	pectinesterase	FGSG_03406	5.352	2.914	8.267
			FGSG_03530	3.534	0.000	3.534
		rhamnogalacturonan acetylesterase	FGSG_04848	4.731	0.084	4.816
Phenolic	Ferulic acid	Feruloyl esterase	FGSG_11036	5.012	2.633	7.645
			FGSG_11428	6.051	0.417	6.468
			FGSG_12548	2.564	4.279	6.844

Additionally, 19 fungal cell wall remodeling genes show high expression in WT_IC compared to DOHH_RH. Most of them encode for glucanases. There are 4 genes only expressed in WT_IC (*FGSG_11037* - endoglucanase I precursor, *FGSG_03609* - related to xylosidase/glycosyl hydrolase, *FGSG_06451* - related to levanase and *FGSG_10561* - related to release factor - *RF2* protein) (Table 26).

Table 26. Nineteen fungal cell wall remodeling genes are up regulated in WT_IC compared to DOHH_RH.

FGSG_Number	WT_IC vs DOHH_RH	log2 FPKM DOHH_RH	log2 FPKM WT_IC	Description
FGSG_08253	7.727	1.485	9.212	related to endo-1,4-beta-glucanase (ident 100.0%)
FGSG_11037	6.301	0	6.301	probable endoglucanase I precursor (ident 100.0%)
FGSG_11098	5.586	1.614	7.2	related to beta-1,3-glucan binding protein (ident 100.0%)
FGSG_07772	5.004	1.172	6.176	related to mixed-linked glucanase precursor MLG1 (ident 100.0%)
FGSG_06550	4.208	1.527	5.735	related to chitin synthase (ident 100.0%)
FGSG_00184	3.566	4.205	7.772	uncharacterized protein
FGSG_03609	3.539	0	3.539	related to xylosidase/glycosyl hydrolase (ident 50.7%)
FGSG_06451	3.477	0	3.477	related to levanase (ident 100.0%)
FGSG_03788	3.418	0.921	4.339	uncharacterized protein
FGSG_06549	3.381	2.611	5.992	related to chitin binding protein (ident 100.0%)
FGSG_10922	3.214	2.846	6.06	uncharacterized protein - related to extracellular cellulase CelA/allergen Asp F7-like, putative (ident 59.2%)
FGSG_10561	3.106	0	3.106	related to RF2 protein (ident 100.0%)
FGSG_04704	2.957	0.086	3.043	related to glucoamylase precursor (ident 100.0%)
FGSG_11496	2.57	6.962	9.533	uncharacterized protein
FGSG_02262	2.563	4.131	6.694	related to endo-1,3-beta-glucanase (ident 52.3%)
FGSG_02651	2.543	3.881	6.424	related to endo-1,3-beta-glucanase (ident 100.0%)
FGSG_07695	2.488	2.357	4.845	related to xylosidase/glycosyl hydrolase (ident 51.9%)
FGSG_00952	2.318	2.635	4.952	related to chitinase (ident 100.0%)
FGSG_05851	2.008	4.316	6.324	related to endoglucanase I precursor (ident 100.0%)

Reactive oxygen species (ROS) play an essential role in pathogen–plant interactions. We analyzed ROS related fungal gene expression and compared to DOHHoex mutants to determine whether the eIF5A pathway contributes to increased or reduced ROS levels and if the increased virulence of the DHSoex mutants coincides with altered ROS levels.

The selection of enzymes which are involved in extracellular ROS production and scavenging is based on the database from Zhang (2012). Intracellular ROS (e.g., in mitochondria and peroxisomes) are not included in the survey because they are more closely correlated to cell metabolism and protection against excess self generated ROS and are not directly relevant to plant–pathogen interactions (Zhang *et al.*, 2012). In this study, the transcriptome data showed that there was no considerable difference in the transcription of genes encoding for extracellular ROS-producing enzyes between WT_IC and DOHH_RH (Figure 47).

NoxA and NoxB expression in WT_IC are slightly up-regulated compared to DOHH_RH. Among extracellular ROS production *FGSG_10677, FGSG_11032* and *FGSG_09093* genes showed significantly up-regulation in WT_IC compared to DOHH_RH. There was no big difference observed for other genes from this class (Figure 47). In the extracellular hydrogen

peroxide gene class *FGSG_02341, FGSG_ 00032* and *FGSG_12369* genes also showed up-regulation in WT_IC compared to DOHH_RH.

			WT_IC vs DOHH_RH	log2 FPKM DOHH_RH	log2 FPKM WT_IC
Extracellular ROS production	Galactose oxidase	FGSG_09093	3.370	3.404	6.774
	NOXA	FGSG_00739	0.504	5.323	5.827
	NOXB	FGSG_10807	1.029	4.838	5.867
	Peroxisomal amine oxidase	FGSG_10677	6.590	1.668	8.258
	D-amino-acid oxidase	FGSG_13617	0.547	5.493	6.040
	Galactose oxidase	FGSG_11032	5.117	0.481	5.598
	Amine oxidase	FGSG_06053	0.126	4.703	4.829
	Monomeric sarcosine oxidase	FGSG_02924	-0.667	2.078	1.411
	NOXC	FGSG_11195	-0.589	1.820	1.232
Extracellular H2O2 scavenging enzymes	Peroxidase	FGSG_04434	-3.136	10.550	7.414
	Chloroperoxidase	FGSG_02341	3.955	0.428	4.382
	Chloroperoxidase	FGSG_03436	-0.412	3.253	2.841
	Chloroperoxidase	FGSG_00032	3.773	0.000	3.773
	CAT	FGSG_12369	3.453	5.058	8.511
	CAT	FGSG_06733	-1.035	1.335	0.300
Extracellular O_2^- scavenging enzymes	SOD	FGSG_08721	1.222	10.428	11.650
	SOD	FGSG_00576	0.253	7.548	7.800

Figure 47. Expression of key regulator genes in ROS pathway in WT_IC compared to DOHH_RH.

Interestingly we have observed 9 genes belonging to the aurofusarin cluster which are up regulated in DOHH_RH (comparison between DOHH_RH and WT_IC) (Table 27).

Table 27. Nine aurofusarin genes are up regulated in DOHH_RH compared to WT_IC.

FGSG_Number	Gene name	Description	DOHH_RH vs WT_IC	log2 FPKM DOHH_RH	log2 FPKM WT_IC
FGSG_02320	aurRI	pathway specific binuclear zinc cluster transcription factor for the aurofusarin gene cluster (ident 100.0%)	2.131	6.172	4.041
FGSG_02321	aurO	oxidoreductase that catalyses the conversion of dimeric 9-hydroxyrubrofusarin to aurofusarin (ident 100.0%)	3.409	8.056	4.647
FGSG_02322	aurT	aurofusarin/rubrofusarin efflux pump AFLT (ident 100.0%)	2.586	8.562	5.976
FGSG_02324	PKS12	polyketide synthase that catalyse the condensation of one acetyl-CoA and six malonyl-CoA resultin (ident 100.0%)	3.654	3.882	0.228
FGSG_02325		uncharacterized protein	4.853	6.207	1.354
FGSG_02326	aurJ	o-methyltransferase that catalyse the methylation of nor-rubrofusarin resulting in formation of r (ident 100.0%)	4.018	6.285	2.267
FGSG_02327	aurF	flavin depend monooxygenase that catalyses the oxidation of rubrofusarin to 9-hydroxyrubrofusarin (ident 100.0%)	4.478	6.746	2.268
FGSG_02328	gip1	laccase that catalyse the dimerization of two 9-hydroxyrubrofusarin in C7 positions (ident 100.0%)	3.657	5.32	1.663
FGSG_02329		uncharacterized protein	3.159	6.285	3.126

TRI genes belonging to the trichothecene biosynthesis pathway play an important role in the pathogenic process. Our analysis indicated that all TRI genes were highly expressed in WT_IC

compared to DOHH_RH (Table 28). Ten TRI genes have a high expression in WT_IC in comparison to DOHH_RH.

Table 28. TRI genes in comparison between WT_IC and DOHH_RH.

FGSG_Number	Gene name	Description	WT_IC vs DOHH_RH	log2 FPKM WT_IC	log2 FPKM DOHH_RH
FGSG_03534	Tri3	probable cytochrome P450 (ident 100.0%)	7.329	7.581	0.252
FGSG_16251	Tri6	trichodiene oxygenase (cytochrome P450) (ident 100.0%)	6.302	6.454	0.152
FGSG_00071	Tri1	regulatory protein (ident 100.0%)	5.972	10.488	4.516
FGSG_03535	Tri4	trichothecene efflux pump (ident 100.0%)	5.852	9.933	4.081
FGSG_03539	Tri9	Trichodiene synthase (ident 100.0%)	5.582	11.298	5.716
FGSG_03543	Tri14	putative trichothecene biosynthesis gene (ident 100.0%)	5.399	9.38	3.981
FGSG_03541	Tri12	trichothecene biosynthesis positive transcription factor (ident 100.0%)	5.296	6.147	0.851
FGSG_03540	Tri11	trichothecene 3-O-esterase (ident 100.0%)	5.278	7.734	2.456
FGSG_03537	Tri5	related to TRI7 - trichothecene biosynthesis gene cluster (ident 100.0%)	5.164	9.508	4.344
FGSG_03542	Tri13	isotrichodermin C-15 hydroxylase (ident 100.0%)	5.138	5.353	0.215
FGSG_03532	Tri8	cytochrome P450 monooxygenase (ident 100.0%)	4.83	8.901	4.07
FGSG_07896	Tri101	uncharacterized protein	4.269	10.279	6.01
FGSG_03533	Tri7	trichothecene 15-O-acetyltransferase (ident 100.0%)	3.313	3.394	0.081
FGSG_03538	Tri10	trichothecene 3-O-acetyltransferase (ident 100.0%)	2.958	5.385	2.427
FGSG_00070	Tri16	probable alpha-glucoside transport protein (ident 100.0%)	0.223	3.12	2.898

These data show that DOHHoex did not activate many virulence related genes such as CWDE and TRI genes. The expression of genes possibly involved in IC formation was decreased and could be the explanation of the mutant's inability to form infection structures.

3.2.6.2. Part II: Comparison of differentially expressed genes between wild type and DHSoex

In section 3.2.3 the infection process of DHSoex mutant was described and compared to the one of WT on inoculated glumes. DHSoex showed similar formation of infection structures to WT. However, the DHSoex mutant showed bigger infection cushions and a slightly higher amount compared to the WT at the same stage (time point) of infection. The infection of this mutant showed stronger penetration than the WT. The molecular basis of this difference might be answered by the comparison between WT and DHSoex transcriptomes. In addition, the results could reveal more candidate genes involved in pathogenicity.

Comparison between WT_RH and DHS_RH

During stage II of infection, WT and DHSoex RH (runner hyphae) exhibited very similar development. Nevertheless, a number of genes are differentially regulated between WT_RH and DHS_RH (Table 29; Appendix Figure 3). WT_RH has many up-regulated genes in comparison to DHS_RH, especially in effector and PCWDE genes (Figure 48). There are 833 (6.02%) genes only expressed in WT_RH and 191 (1.38%) genes only expressed in DHS_RH. Among the 191 genes which are only expressed in DHS_RH (Figure 49), there are 6 genes with Log2>2 and most of them are genes that encode for unknown proteins (Figure 49 B).

Table 29. Overview of the number of expressed genes in DHS_RH compared to WT_RH in different functional categories.

DHS_RH vs WT_RH	Genes expressed	Not expressed genes	Up regulated genes Log2>2	Down regulated genes Log2>2	In DHS_RH		In WT_RH	
					Genes only expressed in DHS_RH	Log2>2	Genes only expressed in WT_RH	Log2>2
Total	12591	1235	154	505	191	6	833	56
TF	866	26	5	7	5	0	18	0
GH	251	15	8	20	6	0	11	0
SM	471	91	14	24	10	0	49	0
ROS-related	997	52	25	29	11	0	53	1
TP	640	39	30	11	7	0	33	0
Effector	553	36	10	62	11	0	49	5
FCWRE	92	11	3	7	3	0	4	0
PK	192	17	0	1	3	0	6	0
PCWDE	218	8	7	25	2	0	11	0

In DHS_RH the number of down regulated genes was higher than up regulated genes in categories such as TF, GH, SM, ROS-related, effectors, FCWRE and PCWDE. The number of up regulated genes was higher than down regulated genes only in the TP category (Figure 48).

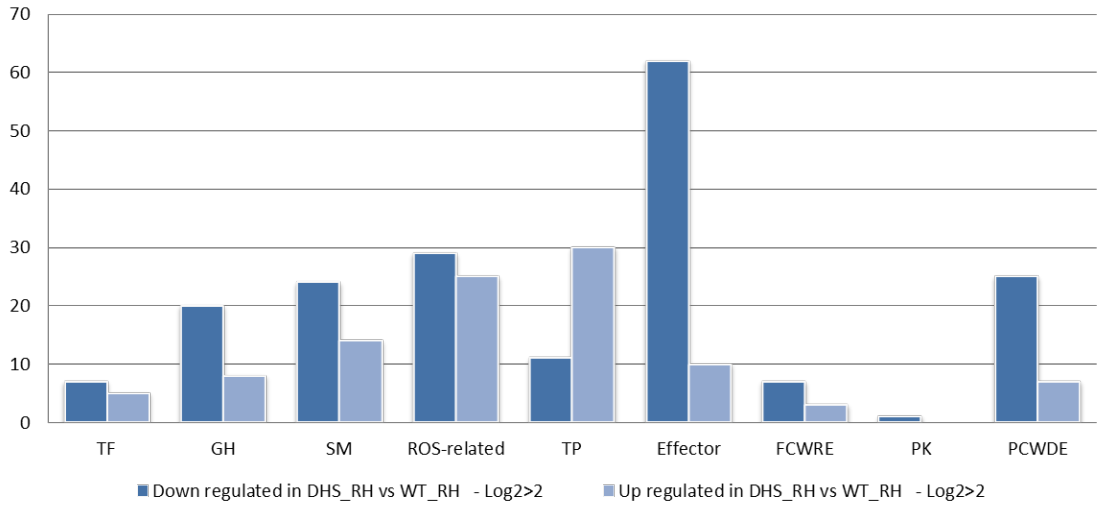

Figure 48. Up and down regulated genes in DHS_RH compared to WT_RH. The statistical significance of gene induction (x axis) shows some functional categories (from the left to the right: transcription factor (TF),

transporter (TP), glycoside hydrolase (GH), secondary metabolite (SM), ROS-related, effector, fungal cell wall remodeling enzymes (FCWRE), protein kinase (PK), plant cell wall degrading enzymes (PCWDE), respectively. Differentially up-regulated genes are represented by pale blue colors; dark blue colors are down-regulated genes. The y-axis is the number of genes which were expressed in the samples.

To understand what makes DHS_RH different from WT_RH we focused on the genes solely expressed in DHS_RH (missing genes in WT_RH). 191 genes were only expressed in DHS_RH compared to WT_RH from which only 6 genes have a Log2>2. These 6 genes encode uncharacterized proteins. Figure 49 shows the genes exclusively expressed in DHS_RH compared to WT_RH.

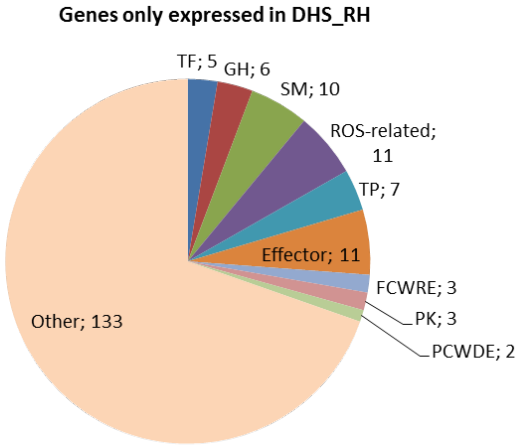

Figure 49. Pie graph of genes only expressed in DHS_RH in comparison to WT_RH. Number of genes exclusively expressed in DHS_RH compared to WT_RH in different functional categories.

The results from this comparison showed that DHSoex has inactivated genes; however this mutant was still fully pathogenic.

Comparison between WT_IC and DHS_IC

The DHSoex mutant could form bigger and more infection cushions than WT and penetrated the plant tissues faster during infection stage II. We compared expressed genes in IC of the DHSoex mutant and WT to understand the molecular background (Appendix Figure 4). The results in table 30 show the overview of the difference in number of expressed genes in WT_IC and DHS_IC. From 12689 significantly expressed genes, 223 genes are only transcribed in DHS_IC representing 1.61% of the transcribed genome and 811 genes only transcribed in WT_IC representing 5.86% of the transcribed genome (Table 30). The total genes only expressed in WT_IC (811 genes) is more than the total genes only expressed in DHS_IC (223 genes). However the genes with Log2>2 from genes only expressed in WT_IC (35) are less than genes only expressed in DHS_IC (39). WT_IC had 811 genes which were only expressed in WT_IC, but just 35 genes were significantly up-regulated (Table 30).

Table 30. Overview of the number of expressed genes in DHS_IC compared to WT_IC in different functional categories.

DHS_IC vs WT_IC	Genes expressed	Not expressed genes	Up regulated genes Log2>2	Down regulated genes Log2>2	In DHS_IC		In WT_IC	
					Genes only expressed in DHS_IC	Log2>2	Genes only expressed in WT_IC	Log2>2
Total	12689	1137	844	423	223	39	811	35
TF	866	26	12	16	2	0	23	1
GH	257	9	66	5	2	0	7	0
SM	486	76	58	26	10	4	57	1
ROS-related	1000	49	71	41	11	0	51	1
TP	651	28	49	29	6	0	36	1
Effector	559	30	116	22	13	3	57	5
FCWRE	94	9	11	2	1	0	5	0
PK	195	14	2	4	1	0	11	0
PCWDE	221	5	86	3	3	0	4	0

844 genes were up regulated in DHS_IC compared to WT_IC (Figure 50). In DHS_IC the number of up regulated genes was higher than down regulated genes in categories TF and PK. The number of down regulated genes was higher than up regulated genes in GH, SM, ROS-related, TP, effectors, FCWRE and PCWDE categories (Figure 50). Interestingly, DHS_IC had 86 up regulated PCWDE genes and only 3 ones were down regulated.

In this comparison (Figure 50 and 51) we focused on the genes solely expressed in DHS_IC. These genes could be involved in the hyper virulence process.

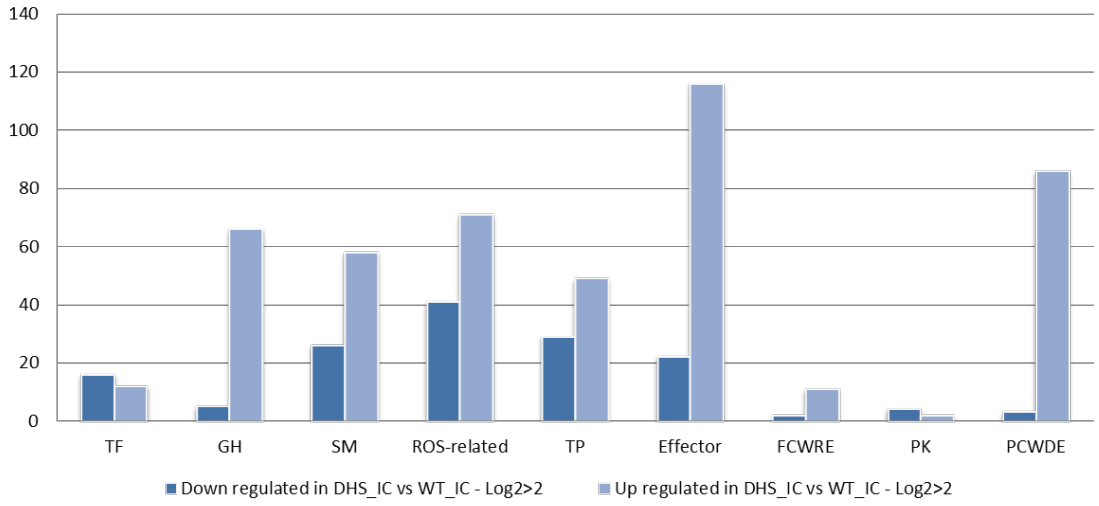

Figure 50. Up and down regulated genes in DHS_IC compared to WT_IC. The statistical significance of gene induction (x axis) shows some functional categories (from the left to the right: transcription factor (TF), transporter (TP), glycoside hydrolase (GH), secondary metabolite (SM), ROS-related, effector, fungal cell wall remodeling enzymes (FCWRE), protein kinase (PK), plant cell wall degrading enzymes (PCWDE), respectively. Differentially up-regulated genes are represented by pale blue colors; dark blue colors are down-regulated genes. The y-axis gives the number of genes which were expressed in the samples.

To figure out what makes DHS_IC different from WT_IC we focused on the genes solely expressed in DHS_IC (missing genes in WT_IC). Figure 51 shows the genes exclusively expressed in DHS_IC compared to WT_IC. All of the genes with Log2>2 are shown in Figure 51 B.

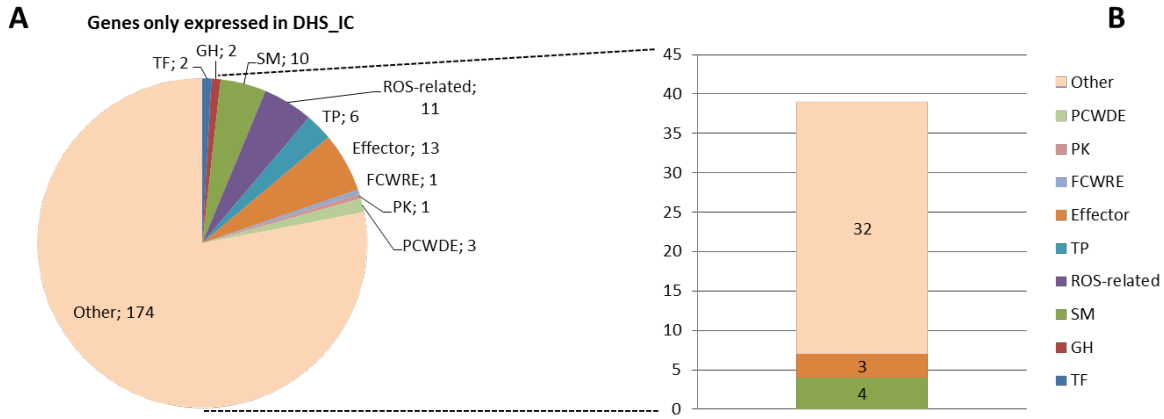

Figure 51. Pie graph of genes solely expressed in DHS_IC in comparison to WT_IC. (A) Genes expressed in DHS_IC compared to WT_IC in different categories. **(B)** Number of up regulated genes expressed DHS_IC and up-regulated in comparison to WT_IC (Log2>2). Significance was set at $P < 0.05$, with a fold-change of 2 (Log2 scale).

Out of 223 genes exclusively expressed in DHS_IC there were 39 genes significantly up regulated (Appendix Table 3). The majority of them were uncharacterized proteins (Appendix Table 3) and 5 genes had high expression with Log2>5 (*FGSG_03048* - related to dTDP-glucose 4,6-dehydratase, *FGSG_04850*, *FGSG_07755*, *FGSG_12581* and *FGSG_13701* - encoded uncharacterized protein). Table 31 shows 3 genes (in total 39 genes) which were described in *F. graminaerum* database. Thirty-six uncharacterized proteins were listed in Appendix Table 3.

Table 31. Three genes in 39 genes are only expressed, up-regulated and described (Log2>2) in DHS_IC compared to WT_IC.

Locus	log2 DHS_IC	Description
FGSG_03048	5.535	related to dTDP-glucose 4,6-dehydratase (ident 100.0%)
FGSG_17495	2.528	related to GNT1 – N-acetylglucosaminyltransferase transferase capable of modification of N-linked (ident 100.0%)
FGSG_03840	3.057	related to spore coat protein SP96 precursor (ident 100.0%)

Secondary metabolites are important virulence factors and the comparison indicates many cluster genes involving in pathogenicity. In 58 up regulated genes of SM there was a cluster showing extremely high expression in DHS_IC such as butenolide - C31 (Table 32).

Table 32. Seven butenolide (C31) genes are up regulated in DHS_IC compared to WT_IC.

FGSG_Number	Description	DHS_IC vs WT_IC	log2 WT_IC	log2 DHS_IC
FGSG_08082	related to GNAT family N-acetyltransferase (ident 35.6%)	8.895	0.284	9.179
FGSG_08081	related to gibberellin 20-oxidase (ident 100.0%)	8.393	2.599	10.992
FGSG_08079	probable benzoate 4-monooxygenase cytochrome P450 (ident 100.0%)	7.446	0.284	7.73
FGSG_08083	related to glutamic acid decarboxylase (ident 100.0%)	6.407	0.056	6.463
FGSG_08084	related to monocarboxylate transporter 4 (ident 100.0%)	5.105	0.046	5.151
FGSG_08077	related to flavin oxidoreductase (ident 100.0%)	2.651	5.388	8.038
FGSG_08078	related to general amidase (ident 100.0%)	2.318	5.099	7.417

Other cluster genes such as C11, C14, C16 (TRI), C21, and C40 also showed high expression level in DHS_IC compared to WT_IC (Table 33). Table 33 gives an overview of the up regulated genes in comparison between DHS_IC and WT_IC. All genes in this table are above the threshold of Log2>2.

Table 33. Fifty-one secondary SM genes are up regulated in DHS_IC compared to WT_IC.

FGSG_Number	Description	Cluster	Metabolite	DHS_IC vs WT_IC	log2 WT_IC	log2 DHS_IC
FGSG_04588	polyketide synthase (ident 100.0%)	C11		2.725	0.910	3.635
FGSG_04589	related to tetracenomycin polyketide synthesis O-methyltransferase tcmP (ident 100.0%)	C11		3.382	3.589	6.972
FGSG_04590	related to isotrichodermin C-15 hydroxylase (cytochrome P-450 monooxygenase CYP65A1) (ident 100.0%)	C11		3.368	3.168	6.536
FGSG_04591	probable farnesyltranstransferase (al-3) (ident 100.0%)	C11		4.054	3.185	7.239
FGSG_04592	related to light induced alcohol dehydrogenase Bli-4 (ident 100.0%)	C11		3.202	4.568	7.771
FGSG_04593	related to para-hydroxybenzoate polyprenyltransferase precursor (ident 100.0%)	C11		4.414	3.390	7.803
FGSG_04595	related to hydroxylase (ident 100.0%)	C11		2.910	3.231	6.141
FGSG_04596	related to O-methyltransferase (ident 100.0%)	C11		3.655	5.113	8.767
FGSG_16087	related to integral membrane protein (ident 45.2%)	C11		4.034	3.876	7.910
FGSG_16088	related to 3-ketoacyl-acyl carrier protein reductase (ident 100.0%)	C11		3.055	4.905	7.960
FGSG_03728	uncharacterized protein	C14		3.658	1.452	5.110
FGSG_03729	related to salicylate 1-monooxygenase (ident 100.0%)	C14		2.553	0.792	3.345
FGSG_03731	uncharacterized protein - related to synaptic vesicle transporter SVOP and related transporters (major facilitator superfamily) (ident 45.3%)	C14		2.791	2.917	5.708
FGSG_03732	related to transporter protein HOL1 (ident 100.0%)	C14		2.509	0.240	2.749
FGSG_16238	related to gentisate 1,2-dioxygenase (ident 44.3%)	C15	Zearalenone	2.477	1.341	3.818
FGSG_03535	trichodiene oxygenase (cytochrome P450) (ident 100.0%)	C16	Tri4	2.464	9.933	12.396
FGSG_03530	acetylesterase, trichothecene gene cluster (ident	C16	OrfB	2.992	3.534	6.526

	100.0%)					
FGSG_03533	related to TRI7 - trichothecene biosynthesis gene cluster (ident 100.0%)	C16	Tri7	3.575	3.394	6.968
FGSG_03539	uncharacterized protein	C16	Tri9	3.819	11.298	15.117
FGSG_03540	isotrichodermin C-15 hydroxylase (ident 100.0%)	C16	Tri11	2.089	7.734	9.823
FGSG_03542	probable cytochrome P450 (ident 100.0%)	C16	Tri13	4.508	5.353	9.862
FGSG_03543	putative trichothecene biosynthesis gene (ident 100.0%)	C16	Tri14	2.253	9.380	11.632
FGSG_16251	trichothecene biosynthesis positive transcription factor (ident 100.0%)	C16	Tri6	3.251	6.454	9.704
FGSG_16340	related to phytoene dehydrogenase AL-1 (carotenoid biosynthesis protein al-1) (ident 100.0%)	C18	Orcinol/ orsellinic acid	2.109	3.726	5.836
FGSG_04692	related to Tri201 - trichothecene 3-O-acetyltransferase (ident 100.0%)	C21	Triacetylfusarinine	2.259	5.715	7.974
FGSG_04693	related to integral membrane protein PTH11 (ident 100.0%)	C21	Triacetylfusarinine	3.518	4.924	8.442
FGSG_04696	uncharacterized protein	C21	Triacetylfusarinine	2.942	1.267	4.209
FGSG_12583	uncharacterized protein	C21	Triacetylfusarinine	3.886	0.284	4.171
FGSG_05796	uncharacterized protein	C23	Trichothecene	4.335	0.918	5.252
FGSG_06452	related to deacetylase (ident 100.0%)	C24		3.200	10.074	13.274
FGSG_08411	related to ARCA protein (ident 100.0%)	C28	Carotenoid	2.284	0.117	2.402
FGSG_15133	uncharacterized protein	C3		2.928	1.200	4.129
FGSG_12001	putative protein (EST hit) (ident 100.0%)	C3		2.377	0.524	2.902
FGSG_10543	uncharacterized protein	C36		2.125	3.983	6.108
FGSG_13782	putative protein (EST hit) (ident 100.0%)	C36		3.085	3.013	6.098
FGSG_10990	related to AM-toxin synthetase (AMT) (ident 100.0%)	C40		2.040	6.684	8.724
FGSG_10993	related to selenocysteine lyase (ident 100.0%)	C40		2.120	7.034	9.153
FGSG_11455	uncharacterized protein	C41		4.656	1.118	5.774
FGSG_11320	uncharacterized protein - related to Protein moaF (ident 32.1%)	C43		2.153	0.000	2.153
FGSG_15645	uncharacterized protein	C43		2.099	0.000	2.099
FGSG_06506	uncharacterized protein - related to chitin binding protein (ident 51.8%)	K10		3.764	1.967	5.731
FGSG_16670	uncharacterized protein	K10		2.040	0.000	2.040
FGSG_10397	uncharacterized protein - related to trichodiene synthase (Sesquiterpene cyclase) (ident 25.2%)	K15	Culmorin	3.395	6.971	10.365
FGSG_17383	related to short-chain dehydrogenase/reductase family protein, putative (ident 40.1%)	K16		2.523	1.966	4.489
FGSG_17495	related to GNT1 - N-acetylglucosaminyltransferase transferase capable of modification of N-linked (ident 100.0%)	K17		2.528	0.000	2.528
FGSG_01676	uncharacterized protein	K2		2.700	2.760	5.460
FGSG_03968	related to cellulose binding protein CEL1 (ident 100.0%)	K4		2.393	2.441	4.834
FGSG_03969	uncharacterized protein	K4		2.682	7.720	10.402
FGSG_16176	uncharacterized protein	K4		2.927	3.261	6.188
FGSG_03342	related to lipase/esterase (ident 42.0%)	K6		3.479	3.600	7.079
FGSG_06445	probable endo-1,4-beta-xylanase (ident 100.0%)	K9		3.139	10.162	13.301

In DHS_IC the most significantly up regulated genes group in the category of putative PCWDEs. Many PCWDEs that target major components of the plant cell wall such as pectin, cellulose, hemicellulose and cutin are highly up-regulated in DHS_IC in comparison to WT_IC (Figure 52). Firstly, the PCWDEs that target pectin, the major component of intercellular middle lamella, were surveyed. The expression of PCWDEs that putatively cleave the primary chains of pectin, including endo- and exopolygalacturonases, petin/pectate lyases, and rhamnogalacturonate lyases, were activated in WT_IC and DHS_IC and showed highest expression in DHS_IC.

DHS_IC up-regulates genes coding for secreted enzymes which cleave and digest the primary chain of pectin, the pectin side chains and the remaining main chains of cell wall components. In the case of cellulose, an important structural component of the primary cell wall, the expression of cellulose-targeting enzyme genes displayed up-regulation in DHS_IC. Xylanase enzymes which degrade the linear polysaccharide beta-1,4-xylan into xylose, breaking down hemicellulose, were also highly up-regulated (~3-4 times fold) in DHS_IC. Putative feruloyl esterases and cutinases, which can release cell wall–bound ferulic acids and degrade cutin layer, respectively, also displayed increased expression during infection of DHS_IC (Figure 52).

			Gene ID	CAZY type	DHS_IC vs WT_IC	log2 WT_IC	log2 DHS_IC
Pectin	Pectin primary chain cleavage						
		Exopolygalacturonase	FGSG_07551	GH28	2.058	6.408	8.466
		Endo-polygalacturonase	FGSG_11011		3.029	5.528	8.557
		Pectate lyase 1	FGSG_09291	PL1	2.513	7.191	9.704
		Rhamnogalacturonase	FGSG_11143	PL4	2.670	1.629	4.299
			FGSG_00989	PL4	2.416	4.552	6.968
	Pectin side chain cleavage						
		Unsaturated rhamnogalacturonyl hydrolase	FGSG_03143	GH105	5.487	0.908	6.395
		α-L-fucosidase	FGSG_11254	GH29	3.595	2.596	6.191
		β-galactosidase	FGSG_03343	GH35	1.323	2.492	3.814
		Arabinogalactan endo-1,4-beta-galactosidase	FGSG_11048	GH53	3.199	5.496	8.695
	Pection modification						
		Pectinesterase	FGSG_03530	CE12	2.992	3.534	6.526
			FGSG_04848	CE12	4.180	4.816	8.996
Cellulose		Endocellulase	FGSG_11184	GH5	2.927	4.602	7.529
			FGSG_03795	GH5	3.733	4.888	8.620
		Cellulose breaking-down enhancer	FGSG_03632	GH61	3.393	3.805	7.198
			FGSG_03695	GH61	2.950	8.911	11.861
			FGSG_08011	GH61	4.093	4.830	8.923
			FGSG_04773	GH61	2.829	2.847	5.676
		Cellulose-binding protein	FGSG_08003	CBM1	-0.958	5.735	4.777
Hemicellulose	Xylan						
		Xylanase	FGSG_11304	GH10	3.460	6.858	10.318
			FGSG_07993	GH3	2.580	2.846	5.425
			FGSG_03624	GH11	2.904	11.206	14.110
		Acetylxylan esterase	FGSG_11049	CE1	3.668	8.085	11.753
			FGSG_11548	CE5	6.590	0.842	7.432
	MLG						
		Endo-1,3(4)-β-glucanase	FGSG_00184	GH16	-0.311	7.772	7.461
			FGSG_04768	GH16	2.480	1.677	4.157
			FGSG_07772	GH16	-2.153	6.176	4.023
	Xyloglucan						
		Endo-β-1,4-glucanase	FGSG_11208	GH74	4.117	2.224	6.340
Pectin & Xylan side chain		Arabinanase	FGSG_07625	GH62	2.561	9.627	12.188
			FGSG_03003	GH43	3.086	3.804	6.890
			FGSG_03609	GH43	3.571	3.539	7.110
			FGSG_03905	GH43	2.394	4.406	6.799
			FGSG_07639	GH43	2.289	6.656	8.944
			FGSG_03049	GH43	2.768	1.240	4.008
			FGSG_11366	GH43	4.204	1.927	6.131
			FGSG_06463	GH51	2.008	7.053	9.062
			FGSG_03813	GH54	3.304	0.762	4.067
Phenolics		Feruloyl esterase	FGSG_11036	CE1	2.723	7.645	10.368
			FGSG_11428	CE1	2.896	6.468	9.364
Cutin		Cutinase	FGSG_10634		1.528	3.791	5.319

Figure 52. Targeted plant cell wall components of the encoded PCWDEs. Comparison between DHS_IC and WT_IC.

By changing the activated level of DHS enzyme, it could regulate *F. graminearum* virulence. To understand this we checked PCWDE genes in a comparison between DHS_IC and WT_IC. Table 34 is showing 86 PCWDE genes which are up regulated in DHS_IC compared to WT_IC.

Table 34. Eighty-six PCWDE genes are up regulated in DHS_IC compared to WT_IC.

Enzyme class	Enzyme substrat	Enzyme subclass	FGSG_Number	DHS_IC vs WT_IC	log2 WT_IC	log2 DHS_IC
Cellulase	Cellobiose	Cellobiose dehydrogenase	FGSG_03742	2.079	4.552	6.63
			FGSG_04872	2.484	5.972	8.457
	Cellodextrin	Cellobiohydrolase	FGSG_03628	2.077	7.055	9.132
	Cellulose	Beta glucosidase	FGSG_03387	2.399	1.173	3.571
			FGSG_04913	2.279	2.314	4.593
			FGSG_08609	2.413	3.348	5.762
		Cel1 protein percursor	FGSG_16018	6.117	2.373	8.489
		Cellulose breaking down enhancer	FGSG_02202	2.199	6.266	8.466
			FGSG_03632	3.393	3.805	7.198
			FGSG_03695	2.95	8.911	11.861
			FGSG_03968	2.393	2.441	4.834
			FGSG_04681	2.456	0.571	3.027
			FGSG_04773	2.829	2.847	5.676
			FGSG_06397	2.044	7.057	9.101
			FGSG_08011	4.093	4.83	8.923
			FGSG_11488	2.548	8.546	11.094
		Endo-1,4-beta-glucanase	FGSG_08253	2.053	9.212	11.265
		Hypothetical protein	FGSG_11184	2.927	4.602	7.529
Cutinase	Cutin	Conserved hypthetical protein	FGSG_01570	2.775	6.965	9.74
		Cutinase 1 percursor	FGSG_02342	2.744	7.339	10.082
			FGSG_03457	3.454	6.874	10.329
Phenolic	Ferulic acid	Feruloyl esterase	FGSG_11036	2.723	7.645	10.368
		Feruloyl esterase	FGSG_11428	2.896	6.468	9.364
Hemicellulase	Hemicellulose	Beta mannanase	FGSG_04678	2.454	3.316	5.77
			FGSG_11066	2.893	0.746	3.639
		Arabinose	FGSG_07640	3.108	1.997	5.105
		Alpha galactosidase	FGSG_02059	4.277	5.318	9.594
	Lignin	Chloroperoxidase	FGSG_02341	2.869	4.382	7.251
	MLG[c]	Endo-1,3-beta-glucanase	FGSG_04768	2.48	1.677	4.157
		Endo-β-1,4-glucanase	FGSG_11037	3.919	6.301	10.22
	Xylan	Xylan 1,4-beta-xylosidase	FGSG_07993	2.58	2.846	5.425
		Endo-1,4-beta-xylanase A	FGSG_15917	3.212	9.618	12.831
		Endo-1,4-beta-xylanase B	FGSG_11258	2.71	5.228	7.938

		Endo-1,4-beta-xylanase	FGSG_03624	2.904	11.206	14.11
			FGSG_06445	3.139	10.162	13.301
			FGSG_10999	2.596	9.613	12.209
			FGSG_11304	3.46	6.858	10.318
			FGSG_11487	2.715	10.987	13.702
			FGSG_13189	4.258	1.478	5.736
		Acetylxylan esterase	FGSG_03867	3.399	4.859	8.258
			FGSG_11049	3.668	8.085	11.753
			FGSG_11112	2.107	4.957	7.064
			FGSG_11548	6.59	0.842	7.432
		Xylanase	FGSG_01748	2.108	0.194	2.302
	Xyloglucan	Endo-β-1,4-glucanase	FGSG_05851	2.095	6.324	8.419
			FGSG_11208	4.117	2.224	6.34
Pectinase	**HG,RGII primary chain**	Endopolygalacturonase	FGSG_03194	2.181	3.887	6.068
		PGU1 - Endo-polygalacturonase	FGSG_11011	3.029	5.528	8.557
		Exopolygalacturonase	FGSG_07551	2.058	6.408	8.466
		Pectin/Pectate lyase	FGSG_01607	4.522	3.588	8.11
			FGSG_02386	2.656	8.048	10.704
			FGSG_02977	5.714	1.005	6.718
			FGSG_03131	2.247	3.304	5.552
			FGSG_03483	3.013	6.936	9.949
			FGSG_03908	5.806	0.6	6.406
			FGSG_04864	4.283	2.141	6.424
			FGSG_09291	2.513	7.191	9.704
			FGSG_11163	5.604	0.69	6.293
	Pectin	Pectinesterase	FGSG_03406	3.349	8.267	11.616
			FGSG_03530	2.992	3.534	6.526
		Rhamnogalacturonan acetylesterase	FGSG_04848	4.18	4.816	8.996
		Pectinesterase	FGSG_07533	3.205	1.81	5.014
			FGSG_11280	2.712	3.689	6.401
	Pectin side chain	Alpha-L-arabinanase	FGSG_03598	2.267	4.018	6.285
		Alpha-L-fucosidase	FGSG_11254	3.595	2.596	6.191
		Beta-galactosidase	FGSG_03904	2.024	1.401	3.425
			FGSG_11048	3.199	5.496	8.695
			FGSG_12461	2.343	4.186	6.529
		Hypothetical protein	FGSG_03054	2.18	3.11	5.29
		Unsaturated rhamnogalacturonyl hydrolase	FGSG_03143	5.487	0.908	6.395
	Pectin/Xylan side chain	Arabinanase	FGSG_03002	2.674	5.592	8.266
			FGSG_03003	3.086	3.804	6.89
			FGSG_03049	2.768	1.24	4.008
			FGSG_03609	3.571	3.539	7.11
			FGSG_03813	3.304	0.762	4.067
			FGSG_03905	2.394	4.406	6.799

			FGSG_05824	2.33	3.419	5.749
			FGSG_06463	2.008	7.053	9.062
			FGSG_07625	2.561	9.627	12.188
			FGSG_07639	2.289	6.656	8.944
			FGSG_07695	3.216	4.845	8.061
			FGSG_11366	4.204	1.927	6.131
			FGSG_11468	2.45	6.31	8.76
			FGSG_00989	2.416	4.552	6.968
	RGI	Pectin/Pectate lyase	FGSG_06117	2.448	3.687	6.135
			FGSG_11143	2.67	1.629	4.299

In this study, the transcriptome data showed that the transcript levels in genes encoding for extracellular ROS-producing enzymes had no considerable difference in DHS_IC compared to WT_IC (Figure 53).

		FGSG_Number	DHS_IC vs WT_IC	Log2 WT_IC	Log2 DHS_IC
Extracellular ROS production	Galactose oxidase	FGSG_09093	1.712	6.774	8.486
	NOXA	FGSG_00739	1.375	5.827	7.201
	NOXB	FGSG_10807	1.744	5.867	7.611
	Peroxisomal amine oxidase	FGSG_10677	-2.996	8.258	5.262
	D-amino-acid oxidase	FGSG_13617	0.364	6.040	6.404
	Galactose oxidase	FGSG_11032	-0.559	5.598	5.039
	Amine oxidase	FGSG_06053	-0.097	4.829	4.732
	Monomeric sarcosine oxidase	FGSG_02924	0.182	1.411	1.593
	NOXC	FGSG_11195	-0.979	1.232	0.253
Extracellular H_2O_2 scavenging enzymes	Peroxidase	FGSG_04434	0.629	7.414	8.044
	Chloroperoxidase	FGSG_02341	2.869	4.382	7.251
	Chloroperoxidase	FGSG_03436	1.630	2.841	4.471
	Chloroperoxidase	FGSG_00032	-0.814	3.773	2.960
	CAT	FGSG_12369	1.799	8.511	10.310
	CAT	FGSG_06733	0.563	0.300	0.863
Extracellular O_2^- scavenging enzymes	SOD	FGSG_08721	0.069	11.650	11.719
	SOD	FGSG_00576	-0.024	7.800	7.776

Figure 53. Expression of key regulator genes in ROS pathway in infection cushion of WT and DHSoex.

NoxA and *NoxB* expression in DHS_IC was slightly up-regulated compared to WT_IC. Among extracellular hydrogen peroxide and superoxide genes, *FGSG_02341* gene showed significant up-regulation in DHS_IC compared to WT_IC. Other genes from this class exhibit no considerable difference (Figure 53). Additionally the data recorded 59 other ROS-related genes in DHS_IC which were up-regulated in comparison to WT_IC (Table 35).

Table 35. Fifty-nine of ROS-related genes are up regulated in DHS_IC compared to WT_IC.

FGSG_Number	Description	DHS_IC vs WT_IC	log2 WT_IC	log2 DHS_IC
FGSG_02882	probable iron-dependent peroxidase (ident 62.5%)	4.457	0.363	4.820
FGSG_02880	related to nitrate reductase (NADPH) (ident 100.0%)	3.856	2.745	6.601
FGSG_13829	related to cysteine dioxygenase type I (ident 100.0%)	3.499	2.366	5.865
FGSG_02974	probable catalase 2 (ident 100.0%)	3.472	4.393	7.865
FGSG_02881	probable catalase isozyme P (ident 100.0%)	3.368	0.446	3.814
FGSG_03593	related to 6-hydroxy-D-nicotine oxidase (ident 100.0%)	3.317	0.415	3.732
FGSG_08037	related to protocatechuate 3,4-dioxygenase beta subunit (ident 46.9%)	3.279	4.173	7.452
FGSG_12519	probable aspartate aminotransferase, cytoplasmic (ident 100.0%)	3.088	3.188	6.276
FGSG_11272	probable ABC1 transport protein (ident 100.0%)	2.887	2.240	5.127
FGSG_02341	related to chloroperoxidase (ident 100.0%)	2.869	4.382	7.251
FGSG_12573	related to 3-hydroxybutyryl-CoA dehydratase (ident 100.0%)	2.846	3.777	6.623
FGSG_02852	probable maleylacetoacetate isomerase (ident 100.0%)	2.727	3.578	6.305
FGSG_17598	related to O-methylsterigmatocystin oxidoreductase (ident 100.0%)	2.702	7.081	9.783
FGSG_12599	related to trichodiene oxygenase cytochrome P450 (ident 100.0%)	2.690	1.698	4.388
FGSG_07483	uncharacterized protein	2.662	2.646	5.308
FGSG_12821	related to glutathione S-transferase III (ident 100.0%)	2.661	4.052	6.714
FGSG_07590	related to taurine dioxygenase (ident 100.0%)	2.659	1.389	4.048
FGSG_11260	related to dehydrogenase (ident 100.0%)	2.636	1.088	3.724
FGSG_01767	related to pisatin demethylase (ident 100.0%)	2.617	3.143	5.760
FGSG_03696	related to maackiain detoxification protein 1 (ident 100.0%)	2.565	1.225	3.790
FGSG_09124	related to NADPH-dependent beta-ketoacyl reductase (rhlG) (ident 100.0%)	2.540	2.655	5.195
FGSG_01816	related to theta class glutathione S-transferase (ident 100.0%)	2.534	1.910	4.444
FGSG_09103	related to gibberellin 20-oxidase (ident 100.0%)	2.517	0.690	3.207
FGSG_02266	related to short-chain alcohol dehydrogenase (ident 100.0%)	2.507	0.336	2.843
FGSG_04826	mannitol dehydrogenase (ident 100.0%)	2.503	5.620	8.123
FGSG_10587	related to peroxisomal amine oxidase (copper-containing) (ident 100.0%)	2.492	4.613	7.104
FGSG_07303	related to gibberellin 20-oxidase (ident 100.0%)	2.464	3.501	5.965
FGSG_00172	related to glutathione transferase omega 1 (ident 100.0%)	2.454	5.022	7.475
FGSG_01812	probable CYB2 - lactate dehydrogenase cytochrome b2 (ident 100.0%)	2.441	3.434	5.875
FGSG_06518	related to short-chain alcohol dehydrogenase (ident 100.0%)	2.440	1.193	3.632
FGSG_03348	related to monophenol monooxygenase (tyrosinase) (ident 73.8%)	2.434	1.359	3.793
FGSG_07683	related to alcohol/sorbitol dehydrogenase (ident 100.0%)	2.429	5.085	7.514
FGSG_02668	related to linoleate diol synthase (ident 100.0%)	2.377	7.051	9.429
FGSG_11162	uncharacterized protein	2.358	1.278	3.636
FGSG_16338	probable delta-1-pyrroline-5-carboxylate dehydrogenase (ident 100.0%)	2.356	3.073	5.429
FGSG_04214	related to formaldehyde dehydrogenase (ident 100.0%)	2.349	3.752	6.101
FGSG_16373	related to sarcosine oxidase (ident 77.1%)	2.329	0.325	2.654
FGSG_16843	probable alcohol oxidase (ident 93.9%)	2.326	8.698	11.024
FGSG_03936	probable UGA2 - succinate semialdehyde dehydrogenase (ident 100.0%)	2.324	2.849	5.174
FGSG_04969	related to salicylate 1-monooxygenase (ident 100.0%)	2.321	0.978	3.299
FGSG_06068	related to benzoate 4-monooxygenase cytochrome P450 (ident 100.0%)	2.259	5.334	7.594
FGSG_00053	probable AAD14 - strong similarity to aryl-alcohol reductase (ident 100.0%)	2.226	3.344	5.569

FGSG_02267	related to 15-hydroxyprostaglandin dehydrogenase (ident 100.0%)	2.220	3.930	6.150
FGSG_17148	related to L-amino-acid oxidase (ident 62.1%)	2.218	3.457	5.675
FGSG_17337	related to acyl-coa dehydrogenase, long-chain specific precursor (ident 100.0%)	2.209	4.692	6.901
FGSG_09341	related to fumarate reductase (ident 100.0%)	2.175	3.099	5.274
FGSG_03935	related to short-chain alcohol dehydrogenase (ident 100.0%)	2.175	3.936	6.111
FGSG_00669	related to multidrug transporter (yeast bile transporter) (ident 100.0%)	2.129	2.030	4.159
FGSG_12373	related to fructosyl amino acid oxidase (ident 100.0%)	2.123	4.187	6.311
FGSG_01523	probable D-xylose reductase (ident 100.0%)	2.119	9.750	11.869
FGSG_02758	related to DNA damage response protein (ident 100.0%)	2.112	8.106	10.218
FGSG_16526	related to CTT1 - Catalase T, cytosolic (ident 100.0%)	2.089	1.774	3.863
FGSG_00012	related to benzoate 4-monooxygenase cytochrome P450 (ident 100.0%)	2.073	1.047	3.121
FGSG_00200	related to alcohol oxidase (ident 100.0%)	2.071	5.652	7.722
FGSG_00071	cytochrome P450 monooxygenase (ident 100.0%)	2.034	10.488	12.522
FGSG_02753	related to pyridoxine 4-dehydrogenase (ident 100.0%)	2.017	5.254	7.271
FGSG_07765	related to isotrichodermin C-15 hydroxylase (cytochrome P-450 monooxygenase CYP65A1) (ident 100.0%)	2.015	5.027	7.042
FGSG_10193	probable cytochrome b5 (ident 100.0%)	2.011	8.633	10.644
FGSG_09684	related to flavin oxidoreductase (ident 100.0%)	2.007	2.371	4.378

Infection cushions of DHSoex showed a bigger size than IC of WT. Comparison of fungal cell wall remodeling genes of DHS_IC and WT_IC indicated that many genes that encode for glucanases are up regulated in DHS_IC (Table 36).

Table 36. Eleven fungal cell wall remodeling genes are up regulated in DHS_IC compared to WT_IC.

FGSG_Number	Description	DHS_IC vs WT_IC	log2 WT_IC	log2 DHS_IC
FGSG_11037	probable endoglucanase I precursor (ident 100.0%)	3.919	6.301	10.220
FGSG_06506	uncharacterized protein - related to chitin binding protein (ident 51.8%)	3.764	1.967	5.731
FGSG_03609	related to xylosidase/glycosyl hydrolase (ident 50.7%)	3.571	3.539	7.110
FGSG_03813	probable alpha-L-arabinofuranosidase (ident 100.0%)	3.304	0.762	4.067
FGSG_07695	related to xylosidase/glycosyl hydrolase (ident 51.9%)	3.216	4.845	8.061
FGSG_05757	probable rAsp f 9 allergen (ident 100.0%)	3.037	6.361	9.398
FGSG_11205	probable SnodProt1 precursor (ident 100.0%)	2.733	9.896	12.629
FGSG_04768	related to endo-1,3-beta-glucanase (ident 100.0%)	2.480	1.677	4.157
FGSG_04060	related to extracellular cellulase CelA/allergen Asp F7-like, putative (ident 54.1%)	2.250	3.441	5.690
FGSG_05851	related to endoglucanase I precursor (ident 100.0%)	2.095	6.324	8.419
FGSG_08253	related to endo-1,4-beta-glucanase (ident 100.0%)	2.053	9.212	11.265

These results suggest that overexpression of DHS leads to a higher transcription of putative viruelence genes of *F. graminearum* in comparison to WT. An upregulation was especially recorded in secondary metabolite gene clusters, ROS related genes, plant cell wall degraded enzymes, and fungal cell wall remodeling enzymes.

3.2.6.3. Part III: Differential expression analyses of the expressed genes during early infection and expressed genes in culture.

In order to compare the expression of genes necessary for fungal growth during in culture conditions (mycelia) and during early plant infection, transcriptomics data from the two different conditions were analysed. The expressed genes during infection were taken from all genes expressed in IC or RH of WT and overexpressing mutants grown in wheat florets. Expressed genes in mycelia were from the wild type strain grown on CM media. Table 37 provides a schematic overview of the expressed genes.

Table 37. Overview of the number of the expressed genes during infection and in culture in different major categories.

	Total number of genes	Expressed genes	Not expressed genes	Up regulated genes *in planta* vs Myc - Log2>2	Down regulated genes *in planta* vs Myc - Log2>2	Non-regulated genes *in planta* vs Myc	In plant infection		In culture	
							Genes only expressed *in planta*	Log2>2	Genes only expressed in Myc	Log2>2
Total	13826	13231	595	3093	2417	7721	539	139	199	9
TF	892	875	17	115	150	610	7	3	3	0
TP	266	666	13	214	147	305	14	5	7	0
GH	562	261	5	127	48	86	10	6	3	0
SM	1049	528	34	166	96	266	33	13	22	0
ROS-related	179	1027	22	387	170	470	40	11	12	0
Effector	589	585	4	251	120	214	43	17	9	0
FCWRE	103	97	6	38	19	40	3	0	2	0
PK	209	199	10	26	27	146	6	0	1	0
PCWDE	226	223	3	140	29	54	11	8	2	0

The expressed genes were recorded by the expression of genes in culture and all of infection structures from WT, DHSoex and DOHHoex mutant (96% of all genes). The genes which were not expressed in any sample (4% in the whole genome) are most likely expressed under specific conditions such as mating and ascospore formation or environmental stress. Numbers of expressed genes in planta and in mycelia are shown in different major categories as previously described (Figure 54). During in culture growth, 5834 genes (Log_2 (FPKM)>4) or 8832 genes (log_2(FPKM)>2) were expressed. Out of which 199 genes were only expressed in culture. 7948 genes (log_2(FPKM)>4) or 10619 genes (log_2(FPKM)>2) were expressed during infection (including all RH and IC of mutants and WT) with 539 genes only expressed during infection).

During infection 3093 genes were up regulated (22.37%), 2417 down regulated genes (17.48%) and 7721 non regulated genes (55.84%) in comparison to expressed genes in culture (Table 37; Appendix Figure 5 and 6). Figure 54 shows the differentially up and down regulated genes which were expressed during infection and compared to mycelia. In our data, some genes did not express in WT but in DHSoex or DOHHoex. In 13231 total expressed genes there were

832 genes which transcript in mycelia, RH and IC of WT but not in DHSoex. 1768 genes were expressed in mycelia, IC and RH (WT and DHSoex) but not in DOHHoex. Furthermore some genes are only activated in IC but not in RH. We determined 524 genes which were only expressed in mycelia (398 genes), WT_IC (247 genes) and DHS_IC (156 genes) but not in RH of WT, DHSoex and DOHHoex.

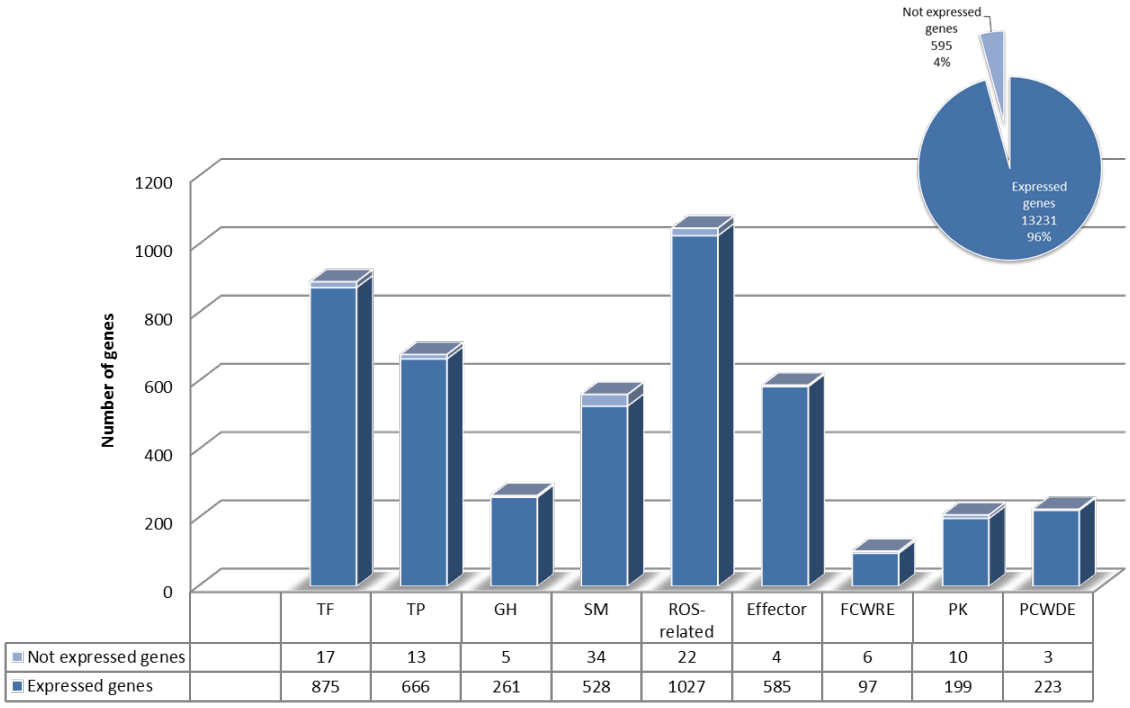

Figure 54. Number of expressed and non-expressed genes during infection and in culture. The pie graph in the right corner shows the expressed and non-expressed genes in all infection structures (IS) of the WT strain, DHSoex or DOHHoex overexpressing mutants and WT grown in culture. The number of expressed genes per each is shown in the column graph, with pale bleu representing non-expressed genes and blue representing expressed genes. From the left to the right: transcription factor (TF), transporter (TP), glycoside hydrolase (GH), secondary metabolite (SM), ROS-related, effector, fungal cell wall remodeling enzymes (FCWRE), protein kinase (PK), plant cell wall degrading enzymes (PCWDE), respectively.

Compared to expressed genes during culture, the number of up-regulated genes during plant infection was higher than the down regulated ones in almost all categories. In PCWDE the number of up-regulated genes was 5 fold higher than the down-regulated genes. In other categories such as GH, ROS-related, secondary metabolism, FCWRE and effectors the number of up-regulated genes was 2-3 fold higher than down-regulated genes. No big difference was recorded in protein kinase (PK) between up and down-regulation (Figure 55).

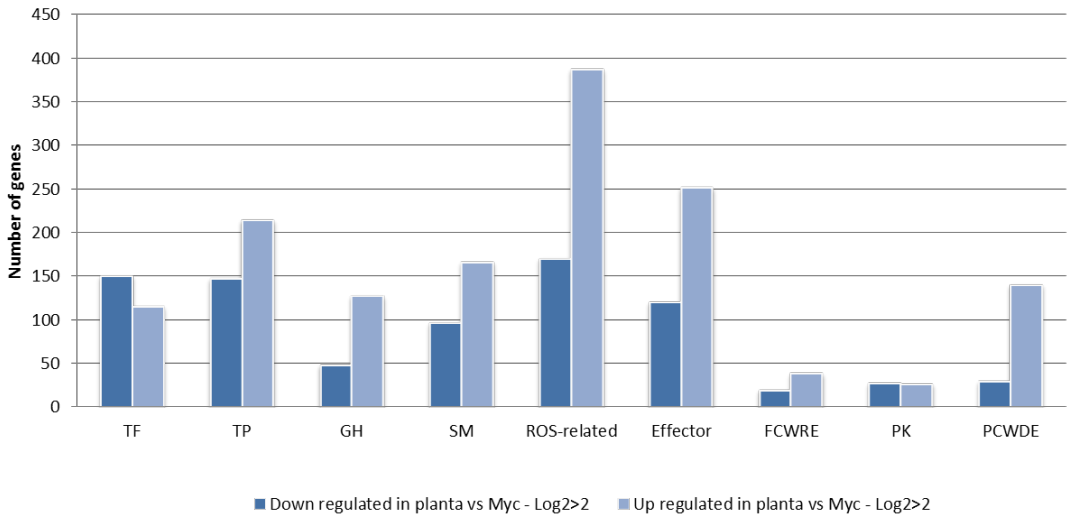

Figure 55. Up and down regulated genes expressed in plant infection compared to mycelia in culture. Genes expressed in IC or RH of WT and overexpressing mutants during infection of wheat florets compared to genes expressed in mycelia of the wild type strain grown on CM media. The statistical significance of gene induction (x axis) shows some functional categories (from the left to the right: transcription factor (TF), transporter (TP), glycoside hydrolase (GH), SM, ROS-related, effector, fungal cell wall remodeling enzymes (FCWRE), protein kinase (PK), plant cell wall degrading enzymes (PCWDE) and other, respectively). Differentially up-regulated genes are represented by pale blue colors; dark blue colors are down-regulated genes. The y-axis gives the number of genes which were expressed in the samples.

539 genes, 3.9% of the whole genome, were actived solely during infection. Those genes are representing the specific interaction of the fungal pathogen with the host. The expressed genes in planta were recorded by the expression of genes in all infection structures (RH or IC) from WT, DHSoex and DOHHoex mutant but not in mycelium (Figure 56 A).

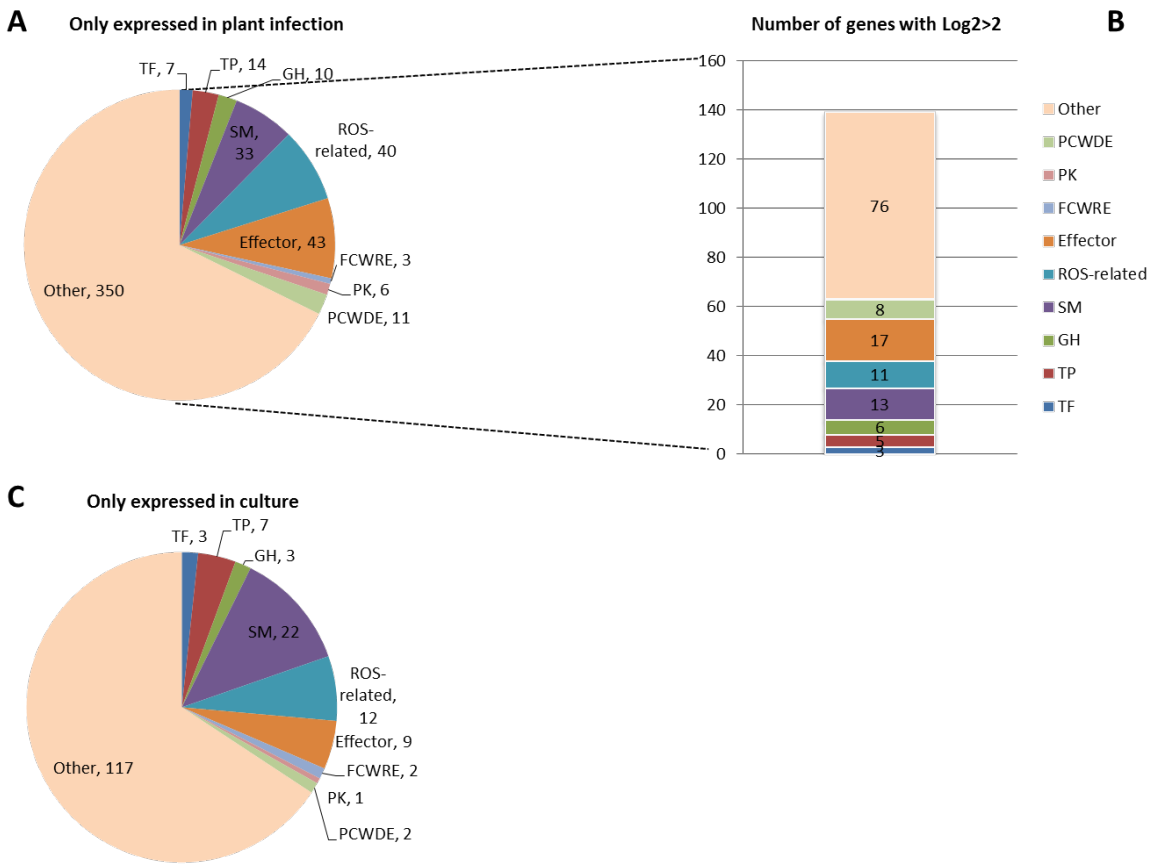

Figure 56. Pie graph of genes only expressed in plant infection or in culture and number of differentially up regulated genes. (A) Genes only expressed in plant infection with different categories. **(B)** Number of up regulated genes only expressed of in plant infection with Log2>2. **(C)** Genes only expressed in culture with different categories. Number of genes only expressed in plant infection is higher than number of genes only expressed in mycelium. The differentially up regulated genes with Log2>2 in plant infection (139) is much more than in mycelium (15).

199 genes, 1.44% of all genes, were only expressed in mycelium (missing during infection condition) as showed in Figure 56 C. However, in 199 genes only 9 have a Log2>2 in mycelia expression. All of the 9 genes encode for unidentified proteins (*FGSG_03937, FGSG_10618, FGSG_12965, FGSG_13425, FGSG_15100, FGSG_15300, FGSG_15412, FGSG_15758,* and *FGSG_17535*).

Genes who were specifically activated during the interaction of the pathogen with its host plant are possibly indispensable for successful infection. Therefore, the 539 genes which were only expressed during infection were analysed in greater detail. 139 genes were up regulated above the threshold of Log2>2 (Figure 52 B). Details of each gene were described in Table 38. The numbers in Table 58 shows the Log2 of FPKM numbers. The number 0 is defined as no expression of a gene.

In 139 up regulated genes only expressed in plant infection, there are 96 genes encoding for uncharacterized proteins (Appendix Table 4). The data in Table 38 revealed some interesting

genes which are expressed in specific tissue of the wild type strain or the overexpressing mutants. These genes have been known and described in *F. graminaerum* database. The data shows that there are 2 genes only expressed in DOHH_RH (*FGSG_15234, FGSG_15492*), 9 genes only expressed in RH of WT, DHSoex and DOHHoex (*FGSG_01714, FGSG_11682, FGSG_15196, FGSG_15234, FGSG_15457, FGSG_15492, FGSG_15183, FGSG_15208, FGSG_15530*), 14 genes only expressed in IC of WT and DHS (*FGSG_17388, FGSG_04850, FGSG_09127, FGSG_12581, FGSG_15197, FGSG_15386, FGSG_15417, FGSG_15453, FGSG_15517, FGSG_15556, FGSG_16158, FGSG_16382, FGSG_12185, FGSG_15254*) and 8 genes only expressed in DHS_IC (*FGSG_04850, FGSG_12581, FGSG_15197, FGSG_15386, FGSG_15453, FGSG_15517, FGSG_16158, FGSG_16382*) (Table 38, Appendix Table 4).

In the transcription factor (TF) category, all of the genes are not expressed in DOHH_RH and highly up-regulated In DHS_IC compared to mycelia (Table 38, TF). Interestingly, 6 genes in the GH category are highly up-regulated in DHS_IC but not in other tissues compared to mycelia. These genes are suggested to play a role in hypervirulence activation of DHSoex. Thirteen genes in secondary metabolites which belong to a variety of gene clusters are recorded. These cluster genes such as C31 (Butenolide), C16 (Tri), C11, K4 have known as a key in pathogenicity of *F. graminaerum* (Table 38, SM). However in this comparison these single genes are specifically activated during plant infection. It is suggested that these genes are distinctive and important in plant infection.

According to my data, in 17 effector genes only expressed in plant infection (Log2>2) there are 13 genes which encode uncharacterized protein. Therein, at least 11 effector genes have no transcription in DOHH_RH and 14 effector genes are highly up-regulated compared to mycelia (Table 38, Effector; Appendix Table 4). In the PCWDE category, there is a contrast of gene expression between RH and IC of WT and mutants. High up-regulation of these genes is shown in IC of WT and DHSoex compared to mycelia. The level of up-regulated genes in DHS_IC is obviously higher than in WT_IC and it can explain the hypervirulence of DHSoex (Table 38, PCWDE).

Table 38. Up regulated genes only expressed in plant infection vs Myc - Log2>2.

	DOHH_RH	WT_RH	DHS_RH	WT_IC	DHS_IC	Description	Cluster
TF							
FGSG_03794	0.000	0.046	0.938	0.169	3.894	uncharacterized protein	
FGSG_08080	0.000	2.103	0.876	1.865	3.847	uncharacterized protein	
FGSG_00154	0.000	3.789	1.008	2.768	5.666	uncharacterized protein	

TP							
FGSG_07584	3.438	0.750	1.167	0.489	1.893	related to DAL5 - Allantoate and ureidosuccinate permease	
FGSG_04709	0.000	2.475	0.215	0.000	0.000	related to multidrug resistant protein	
FGSG_16391	0.321	0.980	2.453	2.590	1.362	hypothetical protein	
FGSG_00118	0.000	0.025	0.091	4.560	0.134	related to neutral amino acid permease	
FGSG_08055	0.710	1.018	2.322	3.677	4.196	related to neutral amino acid permease	
GH							
FGSG_03384	0.000	0.025	0.091	0.770	2.206	probable exopolygalacturonase	
FGSG_03908	0.000	0.000	0.647	0.600	6.406	probable pectate lyase 1	
FGSG_04681	0.000	0.153	0.000	0.571	3.027	probable endoglucanase IV precursor	
FGSG_07533	0.162	1.327	0.423	1.810	5.014	conserved hypothetical protein	
FGSG_04773	0.000	1.917	0.348	2.847	5.676	related to endoglucanase IV precursor	
FGSG_04864	0.000	0.064	0.000	2.141	6.424	probable pectate lyase	
SM							
FGSG_03969	8.367	9.400	10.315	7.720	10.402	uncharacterized protein	K4
FGSG_02325	6.207	5.274	6.393	1.354	0.000	uncharacterized protein	C7
FGSG_03728	1.195	0.529	0.000	1.452	5.110	uncharacterized protein	C14
FGSG_08080	0.000	2.103	0.876	1.865	3.847	uncharacterized protein	C31 Butenolide
FGSG_01784	1.303	4.078	1.352	2.678	0.000	related to phosphatidylinositol/phosphatidylcholine transfer protein (ident 100.0%)	K3
FGSG_03493	0.000	0.707	2.260	1.216	0.000	uncharacterized protein	K5
FGSG_04667	0.779	2.037	1.605	2.725	2.839	related to sulfonate dioxygenase (ident 100.0%)	C10
FGSG_06449	1.744	1.617	2.002	1.558	2.808	probable fumarylacetoacetate hydrolase (ident 100.0%)	C24
FGSG_15645	1.374	2.843	1.179	0.000	2.099	uncharacterized protein	C43
FGSG_03531	0.117	2.579	1.307	4.067	4.242	monooxygenase (ident 100.0%)	C16 Tri
FGSG_03542	0.215	6.968	4.460	5.353	9.862	probable cytochrome P450 (ident 100.0%)	C16 Tri
FGSG_04589	0.000	0.972	1.364	3.589	6.972	related to tetracenomycin polyketide synthesis O-methyltransferase tcmP (ident 100.0%)	C11
FGSG_08082	0.273	3.334	0.115	0.284	9.179	related to GNAT family N-acetyltransferase (ident 35.6%)	C31 Butenolide
ROS-related							
FGSG_00078	3.524	0.790	0.394	0.065	0.869	related to aldo/keto reductase (ident 100.0%)	
FGSG_13196	6.243	1.048	3.422	0.902	0.000	related to 3-oxoacyl-(acyl-carrier-protein) reductase (ident 100.0%)	
FGSG_03348	0.000	0.653	0.000	1.359	3.793	related to monophenol monooxygenase (tyrosinase) (ident 73.8%)	
FGSG_03728	1.195	0.529	0.000	1.452	5.110	uncharacterized protein	C14
FGSG_02917	1.737	2.764	2.535	1.599	1.123	related to cellobiose dehydrogenase (ident 100.0%)	
FGSG_03546	1.569	1.944	2.789	0.851	0.000	putative 3-hydroxyacyl-CoA-dehydrogenase (ident 100.0%)	
FGSG_04667	0.779	2.037	1.605	2.725	2.839	related to sulfonate dioxygenase (ident 100.0%)	C10
FGSG_11568	2.108	2.208	2.928	1.665	2.844	related to monooxigenase (ident 100.0%)	
FGSG_13514	1.274	2.188	2.963	1.557	3.013	related to pyridoxine 4-dehydrogenase (ident 100.0%)	
FGSG_03436	3.253	1.748	1.169	2.841	4.471	related to chloroperoxidase (ident 100.0%)	
FGSG_03531	0.117	2.579	1.307	4.067	4.242	monooxygenase (ident 100.0%)	C16 Tri

Effector						
FGSG_17159	2.380	3.581	5.326	3.405	4.144	related to mannosyltransferase
FGSG_03209	0.025	1.824	1.961	4.223	4.168	triacylglycerol lipase II precursor
FGSG_08002	1.192	2.091	0.155	5.239	4.057	glucan 1,4-alpha-glucosidase
FGSG_04818	0.065	3.205	0.285	1.288	0.000	triacylglycerol lipase precursor
PCWDE						
FGSG_02917	1.737	2.764	2.535	1.599	1.123	related to cellobiose dehydrogenase (ident 100.0%)
FGSG_03384	0.000	0.025	0.091	0.770	2.206	probable exopolygalacturonase (ident 100.0%)
FGSG_03908	0.000	0.000	0.647	0.600	6.406	probable pectate lyase 1 (ident 100.0%)
FGSG_04681	0.000	0.153	0.000	0.571	3.027	probable endoglucanase IV precursor (ident 100.0%)
FGSG_07533	0.162	1.327	0.423	1.810	5.014	uncharacterized protein - related to pectin methylesterase family protein (ident 43.6%)
FGSG_04773	0.000	1.917	0.348	2.847	5.676	related to endoglucanase IV precursor (ident 100.0%)
FGSG_03436	3.253	1.748	1.169	2.841	4.471	related to chloroperoxidase (ident 100.0%)
FGSG_04864	0.000	0.064	0.000	2.141	6.424	probable pectate lyase (ident 100.0%)
Other						
FGSG_06692	11.046	14.132	11.906	8.631	9.548	probable DDR48 - heat shock protein (ident 100.0%)
FGSG_13046	6.314	10.880	4.292	4.988	5.530	putative protein (EST hit) (ident 100.0%)
FGSG_11405	2.643	2.532	2.242	1.364	0.053	related to alkaline protease (oryzin) (ident 100.0%)
FGSG_16233	0.284	1.488	1.460	2.439	4.924	related to ATO2 - Integral membrane protein, involved in ammonia production (ident 100.0%)
FGSG_16565	0.000	0.466	1.135	2.603	3.149	related to CYB2 - Lactate dehydrogenase cytochrome b2 (ident 100.0%)
FGSG_03504	0.472	4.144	3.580	3.976	6.468	related to integral membrane protein (ident 100.0%)
FGSG_07839	3.602	0.878	3.680	0.290	0.243	related to integral membrane protein PTH11 (ident 100.0%)
FGSG_10678	0.041	2.244	1.232	2.858	0.033	related to IQ calmodulin-binding motif protein (ident 46.8%)
FGSG_00061	0.670	3.485	0.000	0.272	3.478	related to KP4 killer toxin (ident 100.0%)
FGSG_16282	2.737	3.375	3.425	2.489	2.363	related to L-fucose permease (ident 100.0%)
FGSG_11566	2.900	1.142	3.330	0.718	1.191	related to oxidoreductase (ident 40.2%)
FGSG_03886	0.838	1.130	0.878	1.995	5.078	related to phospholipase C (ident 100.0%)
FGSG_16658	1.446	2.791	1.700	1.646	2.176	related to RTM1 protein (ident 100.0%)
FGSG_12920	4.515	4.313	0.769	2.501	4.121	related to stress responsive A/B barrel domain protein (ident 45.1%)
FGSG_17467	1.491	2.142	3.463	0.808	1.590	related to zinc finger transcription factor (ident 71.6%)

In summary, out of 13231 expressed genes 3093 genes were up regulated (22.37%) and 2417 genes down regulated (17.48%) during infection compared to in culture growth. 539 genes were exclusively expressed during infection and 199 genes solely expressed in culture. From the infection specific genes 139 genes were strongly expressed (log2>2). From the in culture specific genes 9 were expressed with a log2>2.

4. Discussion

4.1. Characterization of maize deoxyhypusine synthase (*ZmDHS1*)

Hypusine biosynthesis requires the interactions of three proteins, eIF5A, DHS and DOHH. The three proteins are highly conserved in all eukaryotes suggesting a vital cellular function of hypusine-eIF5A (Park *et al.,* 2010).

The first part of this study focused on the elucidation of the maize deoxyhypusine synthase *ZmDHS1,* the first enzyme in the biosynthetic pathway of hypusine formation. In previous studies, the *ZmDHS1* gene was silenced (M. Woriedh, PhD Thesis, University of Hamburg, 2010) and overexpressed (C. Stärkel, PhD Thesis, University of Hamburg, 2011).

In this study, transgenic maize plants from T3 generation were generated and verified to avoid the presence of non-transgenic plants or without Cre-lox activation. The *ZmDHS*1 gene expression results provide a strong evidence of activation of the silencing and overexpressing DHS constructs in the transgenic maize plants. However, two genes of DHS in maize were found, therefore we decided to study the similarity of the two genes as well as the correlation of DHS expression to other essential genes for hypusine biosynthesis. In addition, the physiological analysis of the silenced or overexpressed DHS maize plants as well as resistance to fungal plant pathogens, were assessed.

4.1.1. Sequence conservation of *ZmDHS1* and *ZmDHS2*

The genes *ZmDHS1* and *ZmDHS2* in maize share 84% identity in their amino acid sequence; with *ZmDHS1* having a higher similarity to DHS amino acid sequences in other species. DHS amino acid sequences are particularly conserved in the C-terminal active site of the enzyme (Figure 34). The active site of the DHS protein which includes a conserved region from glutamine 360 to lysine 366 has been determined in several reports (Yan *et al*, 1996; Joe *et al*, 1995). Lately, DHS cDNA from several plants have been cloned and compared together. Arabidopsis (*Arabidopsis thaliana*), tomato (*Solanum lycopersicum*), wheat (*Triticum aestivum* L.), maize (*Zea mays*), canola (*Brassica* ssp.) and tobacco (*Nicotiana tabacum*) share a high sequence similarity (Ober and Hartmann, 1999a; Wang *et al*., 2001; 2003; 2005; Woriedh, 2010). DHS proteins are conserved not only among plants but also in different species including yeast, human (*Homo sapiens*), *Caenorhabditis elegans,* mouse (*Mus musculus*) and the filamentous fungus *Neurospora crassa* (Wolff and Park, 1999). The identity among the human, wheat, and maize DHS amino acid sequence is 60%. Similar physical and catalytic properties from several species were shared apart from sequence similarity of DHS. The enzymes exhibit cross-species reactivities with heterologous eIF5A precursors (Kang *et al*., 1995; Yan *et al*., 1996). The

charged amino acid, ASP 352, located at the bottom of the active site tunnel is responsible for binding to spermidine, CNI-1493 and the GC7 inhibitor, is highly conserved (Umland *et al*, 2004). Moreover Gly 350 is within hydrogen-binding distance of the guanidinium group in all DHS proteins (Njuguna *et al*, 2006). The amino acid residues predicted to be involved in the binding of NAD are also highly conserved in all species. This discovery suggests maintenance of a fundamental cellular function of eIF5A and DHS through evolution (Wolff *et al*, 2007). In all examind species so far, the DHS protein shows a strict specificity toward its substrate protein eIF5A, and it also exhibits a narrow specificity toward spermidine (Wolff *et al.,* 2007). The high similarity of maize DHS amino acid sequence with other characterized DHS enzymes suggests that DHS in maize could have a strict specificity toward its substrate.

4.1.2. The correlation of DHS expression in eIF5A pathway of maize

The correlations of DHS expression in eIF5A pathway of *Zea mays* were investigated. Genes of eIF5A have been determined in various other eukaryotic organisms, such as yeast, amphibians, humans, mammals and plants. The same is true for DHS, after characterization of DHS genes in a variety of eukaryotic organisms, such as *S. cerevisiae*, *N. crassa*, and mammals, the importance of the hypusine/deoxyhypusine modification in cellular proliferation has been assessed and established, but little work has been done with plants (Schnier *et al.*, 1991; Chen and Liu, 1997; Nishimura *et al.*, 2005; Park, 2006; Frigieri *et al.*, 2007). Moreover, the correlations of DHS expression to other genes which are essential for hypusine biosynthesis have not been reported. Therefore we examine a possible co-transcriptional regulation of DHS, DOHH and eIF5A genes in DHS silencing and overexpressing maize plants.

4.1.2.1. *ZmDHS1* and *ZmDHS2* show a transcriptional co-expression

The expression of *ZmDHS1* as well as the *ZmDHS2* genes was analyzed in the silencing and overexpressing transgenic mutants performed in *ZmDHS1*. The low expression of the *ZmDHS1* gene in the silencing lines SI-1, SI-2 and SI-3 demonstrated a strong silencing of this gene. The SI-3 line exhibits the strongest silencing of *ZmDHS1*. According to previous results, lines SI-1 and SI-2 showed multiple integrations of the plasmid, while line SI-3 had a single integration (Stärkel, 2011). The expression levels of *ZmDHS1* in the silencing lines can be affected by various factors during transformation. It has been proposed that different positions of transgene integration can lead to variability of transgene expression level among transformants (Day *et al.*, 2000). However, in another report, the analysis of a small number of single-copy T-DNA transformants reveal that transgene transcript levels are not affected by position effects (Hobbs *et al.*, 1990). Direct proportionality between expression level and

transgene copy number has been recorded (Ku *et al.*, 1999), whereas a correlation between silencing and high transgene doses and/or repeat arrangements of transgenes has been described by several other studies (Hobbs *et al.*, 1990; Jorgensen *et al.*, 1996; Que *et al.*, 1997). Transgene dose affects the silencing susceptibility rather than the interaction of alleles at the same locus. Furthermore, promoterless copies or copies of the *GUS* gene under the control of the weak nopaline synthase promoter failed to trigger silencing (Schubert *et al.*, 2004).

The high expression of the *ZmDHS1* gene in the overexpressing OE-1 and OE-2 mutants demonstrated the integration and functionality of the constructs in these lines. There is only one copy introduced in these lines (Stärkel, 2011). The results of *ZmDHS2* expression in the silencing and overexpressing *ZmDHS1* transgenic maize lines suggested a transcriptional co-expression between *ZmDHS1* and *ZmDHS2* genes. In addition to the high identity in amino acid sequence of the DHS maize genes (84% similarity), the similarity at a nucleotide level was surveyed. The analysis showed similarity among the two sequences (80%). The construct of silencing and overexpressing lines is based on the nucleotide sequence of *ZmDHS1* therefore ability to have a transcriptional co-expression could be explained by the high similarity at a nucleotide level. Until now, there are no reports about the transcriptional co-expression between two DHS genes. However, a gene co-expression network can be constructed by looking for pairs of genes which show a similar expression pattern across samples, since the transcript levels of two co-expressed genes rise and fall together across samples. Gene co-expression networks are also controlled by the same transcriptional regulatory program, functionally related, or members of the same pathway or protein complex (Weirauch, 2011).

To date no study describes the function of different *ZmDHS* genes. Are both of them involved in hypusine biosynthesis? Or do they have transcriptional co-regulation? Further experiments in *ZmDHS-2* gene of maize could answer these questions. In my study, the results suggest that after changing the expression of *ZmDHS1,* the expression of *ZmDHS2* is affected in a similar manner; therefore a possible transcriptional co-regulation could be feasible.

4.1.2.2. *ZmDHS1* has no effect on the expression of *ZmDOHH* and *ZmeIF5A* genes

The results from relative expression quantification of *ZmDOHH* and *ZmeIF5A* genes have revealed that in general, the adjustment in expression of *ZmDHS1* does not influence the transcriptional expression of *ZmDOHH* and the three genes of *ZmeIF5A*. Nevertheless, there is an exception in overexpression line OE-1. In this line, a slight up-regulation in the expression of *ZmDOHH*, *ZmeIF5A*-1and *ZmeIF5A*-3 is observed, but most of all, up-regulation of the *ZmeIF5A*-2.

Wang *et al.* (2001) reported that tomato DHS mRNA and eIF5A mRNA are up-regulated in parallel in response to drought and chilling stress and coincided with the onset of flower and fruit senescence. Park *et al.* (2010) reported that eIF5A and the two modification enzymes evolved in an independent manner without a co-evolutionary linkage between them. Recently, in a study about eIF5A hypusine biosynthesis in *F. graminearum* it has been reported that no transcriptional co-expression has been recorded among the genes necessary for hypusine biosynthesis and their substrate eIF5A. In *F. graminearum*, the regulatory effect of DHS and DOHH towards eIF5A is only at a translational level under the studied conditions (Martinez-Rocha *et al.*, 2016).

In maize, the expression of *ZmDHS1* has no strong effect on the expression of *ZmDOHH* and *ZmeIF5A* genes at a transcript level. However, in one *ZmDHS1* overexpressinge line, a slight upregulation of *ZmDOHH* and *ZmeIF5A-2* genes was observed.

4.1.3. *ZmDHS1* overexpression affected the germination of maize plant

In plant propagation, seed germination is a critical developmental period that plays a vital role. Understanding the main biochemical processes, especially information concerning gene expression, within this important period is necessary to reveal the success of germination. In maize, the germination of maize plants was decreased in the DHS overexpression line OE-2. Interestingly, this overexpression line showed the highest up-regulation of DHS in comparison to wild type and others.

During the seed germination the coleoptile, which is a protective sheath over the mesocotyl, is seen first when emergence occurs. Mesocotyl elongation is very sensitive to soil temperatures, if the soil temperatures are either too cool or too hot, the elongation will be slown down and further emergence will be delayed (Ritchie *et al.*, 1993). The effect of soil temperature and water can be eliminated on the seeds of overexpressing line OE-2, whereas the germination conditions remained the same as the control plants and silencing lines which did not show an effect in germination.

During germination, the flow of genetic information is initially based on the translation of stored mRNAs; afterward, coupled transcription–translation takes place, as de novo transcription of many mRNAs is required to complete the entire germination process effectively (Hayes and Jones, 2000). Additionally, during early germination of maize, mRNAs degradation is recorded in endosperm of grains, while translation is reinitiated based on the stored mRNAs within the scutellum and embryonic axis (Holdsworth *et al.,* 2008). In the germination period, energy metabolism resumes, repair processes are activated, ribosomes are synthesized and the cell cycle is initiated, whereas events associated with seed maturation are

suppressed. These changes might be reflected in the patterns of gene expressions, which quickly switch from a germinative to a developmental program (Bewley, 1997, Bradford *et al.,* 2000). eIF5A hypusination and its pathway had been involved in the plant germination process. A specific up-regulation of eIF5A transcripts at 24h of germination indicated the importance of this protein during this fast growth period in maize (Jiménez-López *et al.*, 2011). Indeed, available data also indicates that in plants, as in other eukaryotic organisms, eIF5A is involved in many cellular functions, and reduction of the eIF5A level has been shown to have a dramatic effect on growth and development in *Arabidopsis* (Łebska *et al.,* 2010). However, levels of *ZmeIF5A* transcripts in the overexpressing line OE-2 were similar to the control line. Therefore this is not the main reason for the reduction of germination rate. Furthermore, participation of polyamines in the control of cell division during seed germination has been well investigated. Spermidine and spermine have been directly related to the germination process (Sepúlveda *et al.*, 1988). During hypusination of eIF5A, the role of spermidine is quite strict and it can only be replaced by very few structurally similar analogues (Byers *et al.*, 1994; Chattopadhyay *et al.*, 2003). It is suggested that when the amount of DHS protein is produced beyond the requirement of the hypusination pathway, it could interfere in other mechanisms regarding to spermidine and influence the germination process.

Moreover, regarding hormone participation in many plant species, ethylene is known to promote seed germination (Beaudoin *et al.,* 2000; Linkies *et al.,* 2009). In overexpressing line OE-2, a reduction of *PAL* transcript (section 3.1.8.2) was observed. *PAL* is a key regulatory enzyme involved in JA/ ET signaling pathway in plants. Therefore, the reduction of *Pal* transcript could be an important factor in reduction of germination.

In conclusion, high level of *ZmDHS1* overexpression can affect the germination rate of maize by changing mechanisms regarding to spermidine and JA/ ET signalling pathway. On the contrary silencing *ZmDHS1* does not interfere in the germination rate of maize.

4.1.4. DHS plays an important role in growth and development of maize

Full-length cDNAs for DHS and eIF5A were isolated from a number of plants and recombinant plant DHS could catalyse the formation of deoxyhypusinated recombinant plant eIF5A. Pleiotropic effects were observed in recombinant DHS plants (Ober and Hartmann, 1999a, b; Wang *et al.*, 2003; 2005). The present study indicates that alterations in the biosynthesis of hypusine, promoted by the DHS in *Zea mays*, resulted in a wide variety of phenotypes affecting many biological processes related with growth and development (control

the height of plant, the number and the length of leaves, the formation of pollen, kernel and grain).

Constitutive suppression of DHS in *Arabidopsis*, canola and tomato showed pleiotropic effects including enhanced growth, enhanced tolerance to drought stress and delay in the onset of leaf and fruit senescence. At high levels of constitutive suppression of DHS, delayed bolting, stunted reproductive growth and male sterility were recorded (Wang *et al.*, 2003, 2005). Recently, a study on DHS inactivation in Arabidopsis showed several aspects of plant biology such as control of flowering time, the aerial and root architecture and root hair phenotypes (Belda-Palazón *et al.*, 2016).

In *Arabidopsis*, suppression of DHS resulted in more rootmass, bigger leaves and enhanced seed yield (Wang *et al.*, 2003). Duguay *et al* (2007) showed that the dominant phenotypic traits of the DHS-suppressed plants exhibited a dramatic enhancement of both vegetative and reproductive growth (Duguay *et al.*, 2007).

Those phenotypes are also observed in some DHS silencing lines of maize. DHS silencing line SI-3 clearly shows the bigger leaves and enhanced seed yield. During the vegetative stage, the growth and development of DHS silencing line SI-1 are faster than wild type.

Table 39. Correlation of the degree of DHS suppression and overexpression to the strength of phenotypes (Ten plants per line, 3 repetitions).

	Level DHS silencing/overexpresing	Height (cm)	Number of leaves	Leaf width (cm)	Pollen (%)	Kernel (%)	Grain (%)
SI-1	↓	↑↑↑	n.c.	n.c.	n.c.	↓	↑
SI-2	↓↓	↓↓	n.c.	↑↑↑	↓↓↓	↓↓↓	↑↑↑
SI-3	↓↓↓	n.c.	↓↓	↑	n.c.	↓↓	↑
OE-1	↑↑	↑↑↑	↑	↑↑	↑	n.c.	↑
OE-2	↑↑↑	↓↓↓	↓↓	↓↓	↓	n.c.	↓↓↓

Note: strength of phenotypes compared to wild type: ↑ weak, ↑↑ medium, ↑↑↑ strong, - no change, ↓ weak, ↓↓ medium, ↓↓↓ strong, n.c. no change

Effects of DHS silencing in maize not only appears in the vegetative stage but also in reproductive stages. The percentage was 50% and 82% in silencing lines SI-3 and SI-1, respectively. Especially DHS silencing line SI-2 which has a low rate of pollen and kernel formation. Several studies reported that DHS plays an essential role in flower development leading to seed formation (Wang *et al.*, 2005, Duguay *et al.*, 2007). DHS is strongly expressed in developing flower buds and open flowers, concomitant with the growth and differentiation phase as well as the senescent phase (Duguay *et al.*, 2007). Constitutive suppression of DHS in *Arabidopsis* resulted in curtailed reproductive growth and male sterility (Wang *et al.*, 2005). Lower levels of constitutive DHS suppression in *Arabidopsis* showed enhanced growth

resulting in higher seed yield in the absence of obvious negative pleiotropic effects such as delayed bolting and stunted reproductive development (Wang *et al.*, 2003) and are similar to some of the phenotypes reported in this work. It is suggested that the strength of these phenotypes is correlated with the degree of DHS suppression (Wang *et al.*, 2003). The results in this study are in agreement with some of the observed traits; moreover, the phenotypes of DHS silencing lines are variable and unpredicted (Table 39). The augmented seed yield in the silencing DHS lines SI-2 correlates with an increase in leaf biomass, but delay in flowering and male sterility, all of which could be unexpected to contribute to an increase in seed formation (Table 39).

Mostly the studies in plant DHS focus on suppression or silencing. Until now, overexpression of DHS in plants has not been recorded. In this work, maize DHS overexpressing lines with different degrees of DHS overexpression developed a variety of phenotypes in both vegetative and reproductive stages (Table 39). DHS overexpressing line OE-1 showed an outstanding growth and development resulting in a higher plant, bigger leaves, and earlier formation of tassel and pollen. However, DHS overexpressing line OE-2, which has the highest level of *ZmDHS1* overexpression, showed an opposite result. A reduction of growth and development has been recorded in both vegetative and reproductive stages. This line has smaller leaves, shorter stem, lower seed yield and late formation of pollen in comparison to wild type. These unexpected results in both overexpressing lines showing opposite phenotypes could be explained due to their variance in level of *ZmDHS1* expression. But because there is only limited knowledge of DHS protein functions in plants, other elements with significant effect in the plant growth and development cannot be discarded. The results suggest that overexpression of DHS in plants might change several aspects of plant biology.

Recently, an atypical role of the *Arabidopsis* eIF5A-2 gene has been determined, it acts as part of the cytokinin receptor machinery that controls cytokinin signalling activity involved in development of root vasculature (Ren *et al.*, 2013). Furthermore the alterations in auxin and cytokinin homeostasis have been correlated with shoot and root alterations, these results are also observed in mutants defective in spermidine biosynthesis (Cui *et al.*, 2010). Relative quantification of *ZmeIF5A2* expression in DHS overexpressing lines OE-1 showed a slight up-regulation of the eIF5A-2 gene compared to the wild type, which may lead to the production of more eIF5A-2 protein affecting the plant phenotype. This could explain why overexpression of *ZmDHS1* in line OE-1 is able to enhance growth and development. Even though there is no evidence on alterations of eIF5A protein levels due to *ZmDHS1* expression, it seems that the slightly increasd eIF5A transcription could lead to the phenotype alteration.

eIF5A, as a highly conserved gene, regulates cell division, cell expansion, cell differentiation, and cell death in a variety of organisms; therefore it plays a critical role in growth and development (Thompson *et al.*, 2004). Additionally, eIF5A genes regulate stress responses, stem xylem development, programmed cell death, and leaf senescence (Thompson *et al.*, 2004; Feng *et al.*, 2007; Hopkins *et al.*, 2008; Liu *et al.*, 2008b; Ma *et al.*, 2010). Mutations in eIF5A-2, also known as Fumonisin B1-resistant12 (FBR12), cause severe defects in plant growth and development and eventually seedling lethality (Feng *et al.*, 2007). In particular, Arabidopsis eIF5A-1 and FBR12/eIF5A-2 genes affect stem xylem development (Feng *et al.*, 2007; Liu *et al.*, 2008b). Moreover, pumpkin (*Cucurbita maxima*) eIF5A genes interact with phloem proteins, implying a possible role in the regulation of the sieve tube system (Ma *et al.*, 2010). Study on plant gene expression has determined that different eIF5A genes are preferentially expressed in specific tissues and transcript levels can be regulated by plant developmental stages or various environmental stresses (Dresselhaus *et al.*, 1999; Chou *et al.*, 2004).

The connection between the alterations in *ZmDHS1* and enhanced growth is not clear at present, but it may be related to eIF-5A genes in specific plant tissues. It is suggested that the pleiotropic effects by alterations in *ZmDHS1* expression are on the one hand related to differential functions of different eIF-5A genes and on the other hand to the spermidine-dependent hypusination pathway. Belda-Palazón *et al.* (2016) knocked-down the DHS enzyme in *Arabidopsis* and provided a holistic view of the biological relevance of the spermidine-dependent hypusination pathway for plant growth and development. This study uncovered that ancient axis spermidine/eIF5A had assumed central biological functions as well as specific functionalities in the evolutive adaptation of the eukaryotic cell that still remain to be carefully detailed in most of the organisms and in particular in plants (Belda-Palazón *et al.*, 2016).

In consequence, specific levels of *ZmDHS1* are necessary in specific tissues and at specific times for the optimal growth and development of maize plants.

4.1.5. DHS overexpression in maize and prospects for fungal resistance

Plant breeders try to improve host resistance by many approaches. My study represents the first step toward understanding the effects of eIF5A pathway modification in resistance to fungal plant pathogens.

The majority of eIF5A-hypusine studies in plants focus on the importance in regulation of basic cellular processes. By overexpressing *ZmDHS1* gene of maize, we strongly increased the resistance of maize towards the leaf pathogens *Bipolaris sorokiniana*, *Cochliobolus heterostrophus*, and *Colletotrichum graminicola*. We transformed the fungal strains to express GFP and monitored

the fungal infection with fluorescent stereomicroscope and confocal laser scanning microscopy. The infection became clearly restricted in the DHS-overexpressing lines compared to wild type or DHS-silencing lines inoculated with *B. sorokiniana* and *C. heterostrophus*, but not with *C. graminicola*. Quantification of fungal infection by qPCR demonstrated the reduced amount of fungi mostly on the surface of leaves of DHS-overexpressing lines in comparison to DHS-silencing lines and wild type, in spite of the different infection behaviour of the tested fungi.

To understand the constitutive and inducible defenses against the leaf pathogens *B. sorokiniana* and *C. heterostrophus*, expression analyses of a set of defense-related genes were carried out. The analysed genes were: *ZmPal*, known for SA-response (Morris *et al.*, 1998; Farag *et al.*, 2005), *ZmHpl*, known for JA-response (Feussner and Wasternack, 2002; Nemchenko *et al.*, 2006) and *ZmGsl* (1-3-beta-glucan synthase) known for callose deposition response.

PAL and *HPL* genes have also been surveyed and showed an interesting result. Both genes are well investigated in plant defense systems of monocots and dicots. *PAL* is a key enzyme in phenylpropanoid metabolism and is involved in plant response to biotic and abiotic stresses. *PAL* expression is reported to be activated by the *JA/ ET* signalling pathway and it is a key regulatory enzyme in the *SAR* pathway (Kato *et al.*, 2000; Shoresh *et al.*, 2005). *PAL* is involved in the first enzymatic step in the pathway of the phenylpropanoid biosynthesis (Yalpani *et al.*, 1993; Ribnicky *et al.*, 1998), leading to the formation of several antimicrobial compounds such as phytoalexins (Hahlbrock, 1989) and may be correlated in reinforcing the cell wall structure by deposition of phenolic compounds (Koike *et al.*, 2001; Saldajeno *et al.*, 2008). Furthermore, there was a report that *ZmPal* expression was upregulated in maize primed with *Trichoderma virens* which resulted in a higher resistance to *C. graminicola*, suggesting an important role for *PAL* also in systemic resistance mediated maize defense (ISR) (Djonovic *et al.*, 2007). Beside its role in plant defence responses, the hydroperoxide lyase *HPL* is also involved in the production of antimicrobial compounds (Nakamura and Hatanaka, 2002) and wound-related substances (Matsui, 2006). In a study about the interaction of fungi and plants, *ZmHpl* transcription is reported to correlate with an increased resistance to the fungal pathogen (Yedidia *et al.*, 2003; Djonovic *et al.*, 2007; Shah, 2009).

ZmDHS1 alteration in maize influences the expression of *ZmPal1* and *ZmHpl* genes. In DHS silencing lines there is an up-regulation of *PAL* and *HPL* compared to wild type, before fungal infection. However, during the infection of *B. sorokiniana* and *C. heterotrophus* the expression of *PAL* and *HPL* did not show evident changes compared to wild type. The alteration of *ZmPAL* and *ZmHPL* genes expression before fungal infection may be involved in the change of plant hormones such as *SA, JA* and *ABA*. Furthermore, this change in

expression without a pathogen attack may render susceptible the maize plants instead of enhancing the resistance against the fungal infections. On the contrary, DHS-overexpressing lines did not produce a high up-regulation of *ZmPAL* and *ZmHPL* before fungal infection. Nevertheless, the overexpressing lines produced an up-regulation of *ZmPAL* and *ZmHPL* (3.3 to 6.2 times compared to wild type) during *C. heterotrophus* infection, but a down-regulation during *B. sorokiniana* infection. The lack of up-regulation in these two genes before infection seems to be the key point in the successful resistance towards *C. heterotrophus* and *B. sorokiniana.* An early and rapid perception of the invading pathogen can lead to induction and mobilization of biochemical and structural defence-related mechanisms resulting in a successful plant defence. During early defence response, papillae formation is a crucial factor that contributes to the plant's innate immunity (Jones and Dangl, 2006; Schwessinger and Ronald, 2012). 1-3-β-glucan plays an important role enhancing the deposition of papillae (Aist, 1976). The papilla or cell wall thickening is a complex structure formed between the plasma membrane and the inside of the plant cell wall acting as a physical barrier (Stone, 1992). This barrier slows down the invasion of pathogens and lengthens the time for an induction of other defence responses that may require gene activation and expression (Lamb and Dixon, 1997; Brown *et al.*, 1998; Boller and Felix, 2009). Interestingly, similar expression of 1-3-β-glucan synthase *ZmGsl1* was recorded in the DHS-silencing lines compared to wild type. However, an up-regulation in the same *ZmGsl1* gene was recorded in the DHS-overexpressing lines compared to wild type before fungal inoculation. After fungal infection with *B. sorokiana*, *ZmGsl1* still had an increased expression in comparison to wild type. Up-regulation in this gene before infection seems to be the key point in the successful resistance towards *C. Heterotrophus* and *B. sorokiniana.* It is suggested that up-regulation *ZmGsl1* gene in transcript level improves the resistance of cell wall.

In conclusion, silencing *ZmDHS1* does not have an impact on resistance towards fungal pathogens, even though expression profiles of key genes such as *ZmPal* and *ZmHpl* were up-regulated before fungal infection. This suggests that hormone signalling pathways may be altered leading to physiological alterations, but not pathogen resistance. It seems that the silencing of DHS transcript is not strong enough to produce meaningful differences between the DHS-silencing lines and the wild type. Therefore, if the necessary amount of DHS protein is still being produced, the eIF5A-deoxyhypusine is produced as well. Hence hypusine-eIF5A conducts the essential processes for cell survival and does not enhance resistance towards fungal pathogens.

Overexpression of *ZmDHS1* produced an enhanced resistance towards fungal pathogens as well as physiological changes on maize plants. The lack of up-regulation in *ZmPAL* and

ZmHPL genes before infection seems to be the key point in the successful resistance towards *C. heterotrophus* and *B. sorokiniana*. The enhanced resistance of DHS overexpressing lines may come from the upregulation of the *ZmGs1* (β-1-3-glucan synthase) gene transcript level before and also after infection. A physical barrier of callose produced prior to infection may contribute to slow down the fungal growth and in consequence allow the defence response of the plant to act.

4.2. Expression profiles of *Fusarium graminearum* wild type and overexpressing mutants DHSoex and DOHHoex during early wheat infection.

4.2.1. Development of infection structures in WT, DHSoex and DOHHoex of *F. graminearum*

Many studies investigated the biology of the development of infection structures of plant pathogenic fungi. Several plant pathogenic fungi form specialized structures called appressoria to breach the intact cuticles of their plant hosts (Dean *et al.*, 2005). During initial infection, hyphal cells undergo a morphological change to form single-celled structures or compound appressoria (Armentrout and Downer, 1986). There are two types of compound appressoria, lobate appressoria and infection cushions and they are described as multicellular types of appressoria, formed by irregular shaped hyphae (Emmett and Parbery, 1975). Both types of compound appressoria are built by *F. graminearum* to penetrate the plant tissue with their morphology being similar to other fungal plant pathogens such as *Botrytis cinerea* (Huang *et al.*, 1999; Tenberge, 2004), *Rhizoctonia solani* (Demirci and Döken, 1998; Pannecoucque and Höfte, 2009), and *Sclerotinia sclerotiorum* (Emmett and Parbery, 1975; Huang *et al.*, 2008).

Colonization by *F. graminearum* of wheat floret tissues has been described in detail (Wanjiru *et al.*, 2002; Bushnell *et al.*, 2003; Jansen *et al.*, 2005; Ilgen *et al.*, 2009; Brown *et al.*, 2010; Boenisch and Schäfer, 2011). In the present work, infection structure formation between WT and two overexpressing mutants (DHSoex-hypervirulent and DOHHoex- avirulent) was investigated and evaluated. Observations on wheat glumes showed that all types of infection structures including infection cushions, lobate appressoria, foot structures, infection hyphae, and intracellular hyphae were formed in the WT and DHSoex mutant.

Boenisch and Schäfer (2011) described distinguishing features in three successive infection stages (stage I - III) of *F. graminearum* on wheat florets. During stage I, no disease symptoms are observed. This is compatible with previous conclusion in wheat and barley, where conidia of *F. graminearum* initially germinate, form runner hyphae and expand without producing symptoms on the exterior surfaces of floret tissues, and don´t penetrate the epidermis

immediately (Kang and Buchenauer, 2000; Bushnell *et al.*, 2003; Goswami and Kistler, 2004). The first infection structures are infection hyphae and they are described in detail for different *Fusarium* species by ultrastructural studies using TEM and SEM (Kang and Buchenauer, 2000; Wanjiru *et al.*, 2002; Kang *et al.*, 2005).On wheat glumes runner hyphae and infection hyphae of WT and DHSoex are detectable on glume surfaces during stage I. After 7 dpi, both the WT and DHSoex mutant showed characteristics of infection stage II such as foot structures, lobate appressoria, and infection cushions. Interestingly, DHSoex mutant produced bigger infection cushions and the number of compound appressoria was higher compared to the WT at the same time of infection. Complex infection structures formed by WT and DHSoex were determined by SEM and CLSM images.

As described in previous publications (Pritsch *et al.*, 2000; Bushnell *et al.*, 2003; Boddu *et al.*, 2006), *F. graminearum* tends to enter floret tissues via natural openings, wounded cells and direct penetration via infection hyphae and this also is recorded by SEM and CLSM in this work with WT and DHSoex. Boenisch and Schäfer (2011) provided evidence that infection hyphae, infection cushions, and lobate appressoria directly penetrate epidermal cells. After removing those infection structures in the outer epidermal cell wall, penetration pores underneath were detectable and showed penetration pegs in infection cushions. The DHSoex mutant is hypervirulent and forms more and bigger infection cushions suggesting more penetration pegs could be presented underneath DHS infection cushions (DHS_IC). However, we were not able to evaluate the actual number of penetration pegs in WT or DHSoex during this stage.

Infection stage II of DHSoex mutant occurred 2 -3 days earlier than in WT. Necrotic lesions surrounding big infection cushions were observed at 9 dpi in case of WT and 7 dpi in case of DHS. Armentrout and Downer (1987) also observed the same symptom on cotton hypocotyls infected with *R. solani,* necrotic lesions appeared when infection cushions were fully developed (Armentrout and Downer, 1987). The investigation demonstrated infection structure formation on the glume surface during stage II of WT and DHSoex but not in DOHHoex mutant. The DOHHoex mutant showed an expansion of runner hyphae without development of infections structure and without penetration of the cuticle. After 12 days post inoculation the runner hyphae of DOHHoex seemed to degenerate suggesting that the DOHHoex mutant could not take up nutrients from the host plant. Glumes were colonized by runner hyphae, but showed no infection cushions and caused no necroses before 14 dpi. After 14 dpi some necrotic tissues were observed on the glume surface but mainly at the place of wounded glume. However this symptom did not spread out to the entire surface.

The results, demonstrate that development of compound appressoria and virulence in *F. graminearum* is regulated through the eIF5A-hypusine pathway. In a recent publication the overexpression of DHS or DOHH in *F. graminearum* led to hypervirulent or hypovirulent phenotypes, while the overexpression of both genes led to a similar phenotype as the wild type (Martinez-Rocha *et al.*, 2016). Balance in the expression of the two biosynthetic enzymes is required for proper function of eIF5A, for cell viability and fungal proliferation. Infection structure formation and pathogenicity in wheat and maize are completely inhibited by overexpression of DOHH. On the contrary, DHS overexpression led to more infection structure formation and hypervirulence towards wheat (Martinez-Rocha *et al.*, 2016).

In this study, the results have provided more evidence regarding the function of the eIF5A-hypusine during the initial steps of plant-fungal interaction and infection structure formation on wheat glumes. However, until now nothing is known about the molecular basis for infection structure formation and penetration of *F. graminearum*. Therefore, by transcription analysis and comparison to wild type development during early wheat infection we further investigated what caused the increased formation of infection structures and hypervirulence of DHSoex mutant. We could also find out the lack of infection structures formation and avirulence in DOHHoex. Moreover, transcriptome of mycelium was used to detect plant specific gene expression or respective repression.

4.2.2. Comparative gene expression of hypervirulent and avirulent mutants during the early infection of *F. graminearum*

In this study, combination of laser microdissection and RNA-Seq was used to determine the differentially transcribed genes from various specific structures such as the expanding runner hyphae (RH) and the penetrating infection cushions (IC) without including the plant. The completely annotated genome of *F. graminearum* was available (Cuomo *et al.*, 2007; Ma *et al.*, 2010; Wong *et al.*, 2011) and a whole genome oligo-nucleotide microarray (Güldener *et al.*, 2006). We have performed a one to one comparison of the transcriptome of runner hyphae of wild type, DHSoex (WT_RH vs DHS_RH) and DOHHoex mutants (WT_RH vs DOHH_RH), infection cushions from the wild type, DHSoex (WT_IC vs DHS_IC) and DOHHoex mutants (WT_IC vs DOHH_RH) during infection.

The results showed a significant difference between the transcriptomes of WT, DHSoex and DOHHoex. To analyze the differences between the mutants and the wild type, we focused on the differentially expressed genes as well as the only expressed genes in one or another strain. The results from each comparison have revealed that not only the total expression but also the number of up-regulated genes in IC were higher than in RH suggesting that IC are specific

structures for penetration and require specific expressed genes for host manipulation during penetration.

4.2.2.1. General comparison of differentially expressed genes between DOHHoex and wild type

By changing the eIF5A pathway many genes have been turned off or turned on and affected the pathogenicity process of *F. graminearum*. A significant variation in the number of genes with detectable expression was analyzed in sets of functional categories in RH and IC of *F. graminearum*. First of all, analysis of the differentially expressed genes between WT and the avirulent DOHHoex mutant revealed that, the number of up-regulated as well as the only expressed genes in WT_RH was higher than the down-regulated or only expressed genes in DOHH_RH (Table 19). The majority of the up-regulated or only expressed genes in WT_RH encode for PCWDE, GH, putative effectors, secondary metabolite and ROS-related enzymes, categories involved during the initial infection process.

Comparison between WT_IC and DOHH_RH revealed a higher number of only expressed genes in WT_IC. However, the number of up-regulated genes was lower by 67 genes in comparison to the down-regulated genes in WT_IC. Nevertheless, the categories with more up-regulated or only expressed genes in WT_IC were again those involved in penetration and host manipulation (Table 23). In addition, many genes essential for fungal cell morphology were up-regulated too. The numbers and categories suggest that the overexpression of DOHH is inhibiting or stopping the expression of several genes necessary for the formation of infection structures, penetration and plant host immune response modification. The results in table 24 and appendix table 2 show genes (mostly unknown) which are good candidate genes for further study.

4.2.2.2. General comparison of differentially expressed genes between DHSoex and wild type

The next comparison was between the wild type and the hypervirulent DHSoex mutant. In the analysis of the differentially expressed genes between WT_RH and DHS_RH we did not expect many differences. Nevertheless, the analysis revealed a high number of down regulated genes as well as missing genes (only expressed in WT_RH) in DHS_RH (Table 29). The majority of the down-regulated or missing genes in DHS_RH encode for GH, SM, PCWDE, ROS-related enzymes, putative effectors, categories involved during the initial infection process.

Analysis of differentially expressed genes between WT_IC and DHS_IC revealed higher number of up-regulated genes in DHS_IC than in WT_IC (Table 30). Again the categories with more up-regulated genes in DHS_IC were involved most of all in pathogenicity function. Although genes only expressed in DHS_IC are less than in WT_IC, significantly up-regulated genes in DHS_IC are more than in WT_IC (Table 30). These genes could be essential in the hyper virulence process and be good candidate genes for further study (Table 31). It could be the answer for why DHSoex was more virulent and DHS_IC were formed and expanded faster than WT. In addition, the differences in gene expression in those specific categories reflect the difference in infection stage of DHSoex compared to wild type. While the wild type is getting ready for infection, the DHSoex mutant is already infecting. Therefore, many genes necessary for infection are down regulated in RH but up regulated in IC of DHSoex. This result is in agreement with the microscopy observation where DHSoex produces more and earlier infection structures than wild type on wheat glumes.

4.2.3. Comparison of differential gene expression of *F. graminearum* grown in culture and during wheat glume infection

In order to better define fungal genes which are directly associated with pathogenicity, we compared the transcriptomes from fungal infection structures (including RH and IC) of an avirulent and hypervirulent mutants involved in eIF5A pathway and the wild type strain to mycelium grown in culture (mycelium in complete media).

In culture grown *F. graminearum* transcriptome data has been described in several previous studies. Seong *et al.* (2008) found that 5000 to 6000 genes were expressed at the 0-, 2-, 8-, and 24-h time points, which represent the in culture growth stages, including spore, spore swelling, early hyphal growth, and hyphal growth with branching, respectively. Zhang *et al.* (2012) performed microarray analysis of *F. graminearum* grown in culture at the 72-h time point and detected 5746 (43%) genes that were expressed. In another study, Boedi *et al.* (2016) found 8987 significantly expressed genes in culture growth stages. There were a different number of expressed genes in each study due to the distribution of expression values over the genome. The majority of genes are expressed between $1 \leq \log_2(\text{FPKM}) \leq 5$. We performed transcriptome analysis of *F. graminearum* grown in culture at 3 dpi (days post inoculation) and detected 5834 genes ($\log_2(\text{FPKM})>4$) or 8832 genes ($\log_2(\text{FPKM})>2$). These results also demonstrate that, although we used different methods from others, the total number of genes expressed in culture were similar to hyphae grown in culture in previous studies.

A general analysis in the transcriptome data shows that the transcriptomes of *F. graminearum* grown in wheat glumes (including all RH and IC of mutants and WT) have 10619 genes (log_2(FPKM)>2). However, out of that number there are 539 genes which are only expressed during infection. These genes are designated "during infection preferential genes". Among these genes we determined 139 highly expressed genes. Zhang *et al.* (2012) also identified 344 genes that were more strongly expressed during the infective growth stages than in culture growth stages. We compared our list (539 genes) to Zhang's list (139 genes) and identified only 12 common genes (11 genes with Log_2>2). Boedi *et al.* (2016) indentified 368 genes which were expressed during infection and required the living plant. Twenty-seven genes were recognized as common genes in comparison between our data to Boedi's data. These results were expected, given the difference in growth environments during infection and the differences in morphology between RH and IC from two types of mutants. The transcriptomes with two different mutants have provided genes which are only expressed in specific modification of each mutant. By overexpressing DOHH gene, many genes related to pathogenic process have been deactivated or reduced in expression (374 genes were missed in 539 genes only expressed during infection). On the contrary, overexpressing DHS gene has activated unique genes which are highly expressed in IC (40 genes only expressed in DHS_IC and 8 genes with Log_2>2). These 8 genes have no description in other studies and are suggested as hyper virulent factors. In case of genes only expressed in DHS_IC we assumed that they represent function not only required for pathogenicity but also increased the virulence of fungi. The genes which are expressed in all tissues (both in culture and during infection) are the genes truly required for the growth and development of fungi (basic cellular processes). Data analysis has indicated that many genes existing in both in mycelium and in infection structures are strongly expressed during infection. However, in a recent publication it is described that only a limited number of during infection- expressed genes require the living plant for induction but the majority uses the plant tissue simply as a signal (Boedi *et al.*, 2016).
Our main interest was to explore the gene set specific to pathogenicity and the role of eIF5A process in that virulent condition. The results indicated that the two enzymes DHS and DOHH in eIF5A process play and important role in pathogenicity of *F. graminearum*. By overexpression of DOHH or DHS genes we were able to restrict or allow the large number of genes expressed during infection condition to revealed novel virulence factors (Section 3.7.6.3, Table 38).

4.2.4. Detailed comparison of differentially expressed genes encoding for PCWDE, ROS, SM, FCWRE of *F. graminearum* grown in culture and during wheat infection

The global transcriptome has been surveyed during infection of *F. graminearum* on barley spikes, wheat spikes, stalks, crown, and coleoptiles using Affymetrix gene chips (Güldener *et al.,* 2006; Stephens *et al.,* 2008; Guenther *et al.,* 2009; Lysøe *et al.,* 2011; Zhang *et al.,* 2012). These data revealed a global viewpoint of *F. graminearum* gene expression in conjunction with its host plant. Based on these results, we selected the following functional categories for detailed analysis: genes encoding plant cell wall–degrading enzymes (PCWDE), ROS producing and scavenging proteins, secondary metabolite (SM) and fungal cell wall remodeling enzymes (FCWRE).

Plant cell wall–degrading enzymes (PCWDE)

During infection initiation, *F. graminearum* produces cell wall degrading enzymes (PCWDE) including cellulases, xylanases and pectinases to attack and enter host plant tissue (Kang and Buchenauer, 2000; Wanjiru *et al.*, 2002; Jenczmionka and Schäfer, 2005). More than 70 PCWDE genes were found during *F. graminearum* infection of plants or incubation with plant extracts (Walter *et al.*, 2010). Using laser microdissection to isolate a homogenous population of *F. graminearum* hyphae inside the coleoptiles, 134 putative plant PCWDE genes were identified. In addition, two phases of PCWDE accumulation were described; (1) targeting preferentially the main chains of cell wall components and (2) a more extensive round encompassing the digestion of side chains (Zhang *et al.*, 2012). Comparison between DOHHoex or DHSoex to WT (Table 60 and Table 54) determined many up and down-regulated PCWDE encoding genes during penetration. The majority of PCWDE that target major cell wall components such as pectin, cellulose, hemicellulose and cutin are highly up-regulated in DHS_IC but down-regulated in DOHH_RH in comparison to WT mycelia, in accordance to their hypervirulent and avirulent phenotypes (Figure 57).

Firstly, the PCWDE that target pectin, the major component of intercellular middle lamella, were surveyed. The expression of PCWDE that cleave the primary chains of pectin, including endo- and exopolygalacturonases, petin/pectate lyases, and rhamnogalacturonate lyases, was up-regulated in WT_IC and DHS_IC and showed highest results in DHS_IC. This expression pattern suggests that DHS_IC strongly secretes enzymes to cleave and digest the primary chain of pectin, the pectin side chains and the remaining main chains of the cell wall. In case of cellulose, an important structural component of the primary cell wall, the expression of genes encoding cellulose-targeting enzymes displayed a similar increase at DHS_IC. Interestingly, in our comparison we recognized the high expression from a group of GH61-

type proteins which were reported to be enhancers of cellulose breakdown (Harris *et al.*, 2010; Quinlan *et al.*, 2011). These group were also observed in Zhang *et al.* (2012) in which the highest expression level was indicated in wheat coleoptile after 16 hours of infection. These enzymes are involved in the initial stage of digesting cellulose surrounded by a hemicellulose sheath (Zhang *et al.*, 2012). Xylanase enzymes which degrade the linear polysaccharide beta-1-4-xylan into xylose, thus breaking down hemicellulose, were also highly up-regulated (~12 times fold) in DHS_IC. Putative feruloyl esterases and cutinases, which can release cell wall–bound ferulic acids and cutin layer, respectively, also displayed increased expression during glumes infection, similarly as in coleoptiles (Zhang *et al.*, 2012). In the coleoptiles transcriptome study they individually knocked out three during infection preferentially expressed PCWDE genes: FGSG_00989, which encodes a probable rhamnogalacturonase B (RGaseB); *FGSG_00571*, which encodes a probable cellulose 1-4-β-cellobiosidase (*CbhC1*); and *FGSG_00184*, which encodes a putative endo-1-3(4)-β-glucanase (*Eng1*) of the GH16 family. Knockout mutants for *CbhC1* or *Eng1* showed reduced virulence and mutants lacking RGaseB showed similar virulence level to the wild type on coleoptiles (Zhang *et al.*, 2012). In this study, those three genes are up-regulated in DHS_IC and down-regulated in DOHH_RH compared to WT_IC.

The overexpression of DOHH in *F. graminearum* affected the pathway and regulation of PCWDE enzymes expression. The reduction of fungal virulence on the respective host plants has been recorded when disrupted genes encoding pectinolytic enzymes from *Aspergillus flavus*, *B. cinerea* and *Claviceps purpurea* (Kikot *et al.*, 2009). PCWDE are crucial during the initial infection process of *F. graminearum*, the host cell wall underneath infection cushions is perforated by activation of PCWDE and without the formation of compound appressoria the virulence of fungi can decrease (Kikot *et al.*, 2009). Changes in the expression levels of two enzymes DHS and DOHH leads to alteration of posttranslational hypusination of the eukaryotic translation initiation factor-5A which may regulate *F. graminearum* virulence pathways required for PCWDE production.

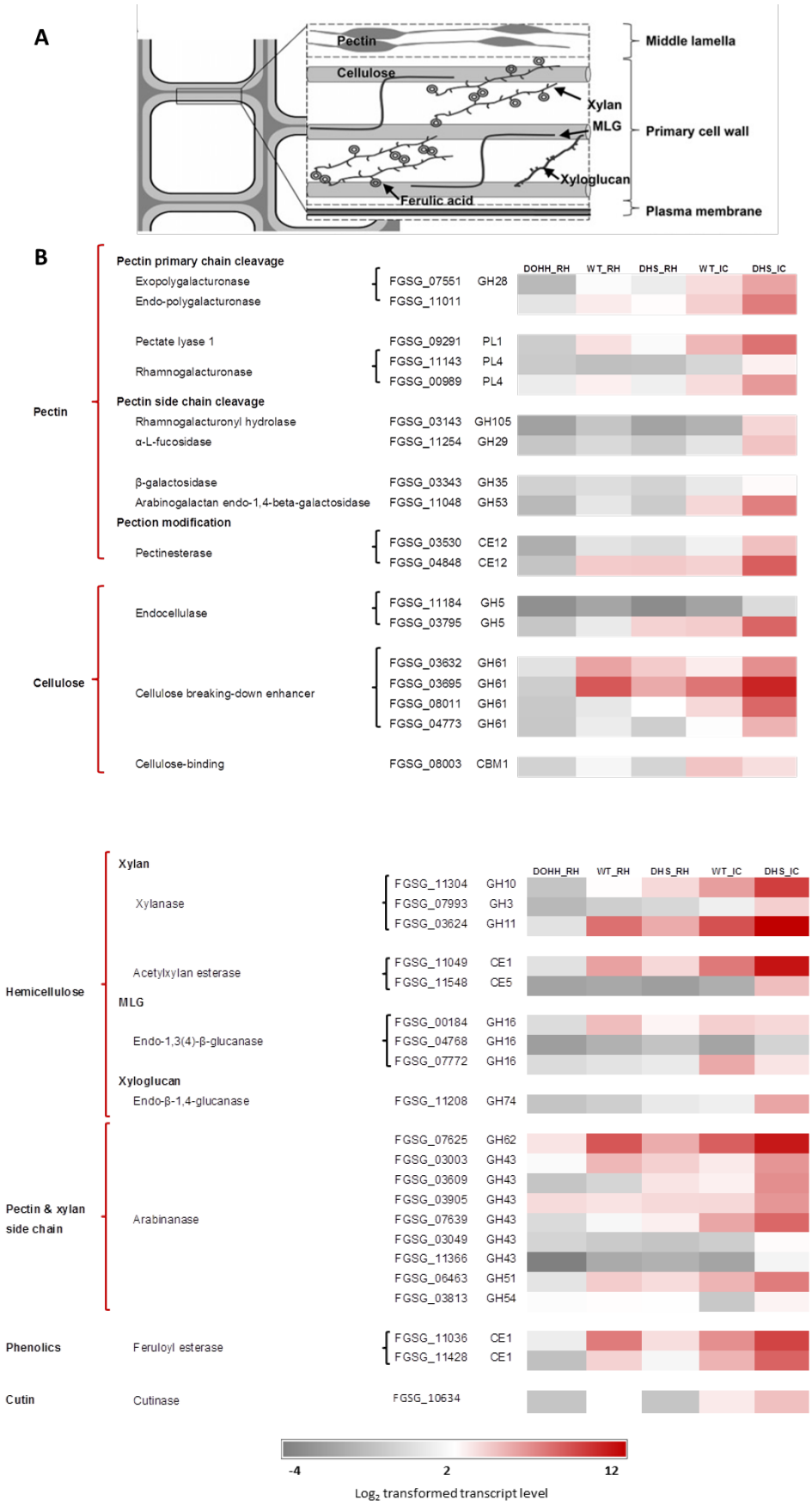

Figure 57. PCWDE genes are induced during infection. (A) Targeted plant cell wall components of the encoded PCWDE (Taken from Zhang *et al.*, 2012). **(B)** PCWDE gene expression in RH and IC of WT, DHS and DOHH in comparison to WT_Myc.

Reactive oxygen species (ROS)

Reactive oxygen species (ROS) play an essential role in pathogen–plant interactions. According to Zhang's report (2012) *F. graminearum* encodes 28 putative enzymes involved in intracellular ROS production or clearance and 19 putative enzymes involved in extracellular ROS production or clearance (i.e., enzymes that might contribute to changes in ROS levels). The alteration of posttranslational hypusination of the eukaryotic translation initiation factor-5A had not much effect on genes encoding extracellular ROS producing proteins. Key regulator genes in extracellular ROS producing proteins are activated in DHS_IC however this expression is not too strong (Figure 53). Among extracellular ROS producing genes, the Nox family has been involved in fungal virulence (Lara-Ortiz *et al.*, 2003). Deletion of both *Nox1* and *Nox2* in *M. oryzae* caused apathogenicity (Egan *et al.*, 2007). In this study the orthologues *NoxA* and *NoxB* are slightly up-regulated in DHS_IC in comparison to WT_IC. These genes are slightly up-regulated in WT_IC compared to DOHH_RH (Figure 47). It is possible that a high activation of the Nox complex is not necessary to have an important role in virulence, and the slight differences in gene expression are enough to make an impact on the virulence of DHSoex and DOHHoex.

Recent publication showed that overexpression of DOHH in *F. graminearum* leads to overproduction of ROS and increased sexual reproduction (Martinez-Rocha *et al.*, 2016). Results in diferentially expressed genes revealed that two ROS scavenging genes, a peroxidase (*FGSG_04434*) and a catalase (*FGSG_06733*), are up-regulated (~3-fold and 1 fold) in DOHH_RH compared to WT_IC (Figure 47). These results suggest a ROS detoxification in DOHHoex mutant is ongoing. However, none of the extracellular ROS producing genes are up-regulated in DOHHoex, suggesting that ROS production comes from different genes than the extracellular ROS producing genes (e.g. mitochondrial and peroxisomal intracellular ROS producing genes).

Secondary metabolite (SM)

Secondary metabolites are an essential factor for virulence and mycotoxin production in *F. graminearum*. Using the pathway genes of well characterized mycotoxins, including trichothecene (Alexander *et al.*, 2009, Figure 58), aurofusarin (Malz *et al.*, 2005) and secondary metabolite biosynthetic (SMB) gene cluster (Zhang *et al.*, 2012) analysis of the expression has been indicated in different infection structures of each mutant.

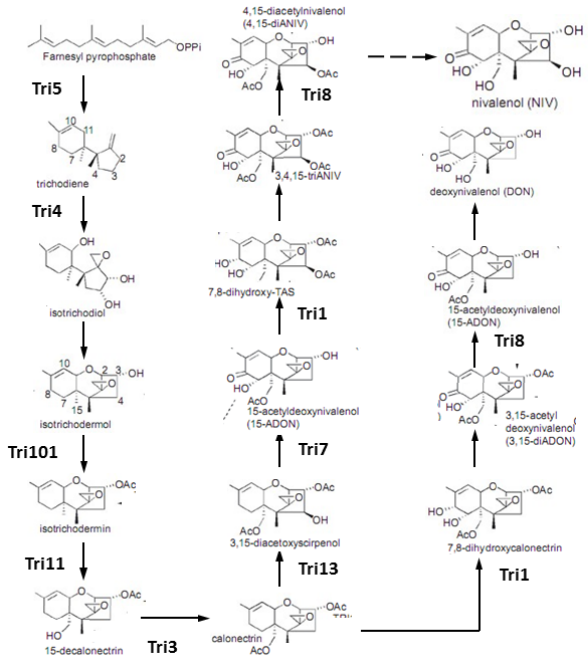

Figure 58. Trichothecene biosynthetic pathway. A proposed pathway for trichothecene biosynthesis from farnesyl pyrophosphate to DON showing the genes known to encode enzymatically mediated steps. The pathway was drawn based on Alexander *et al.*, 2009.

In trichothecene biosynthetic pathway genes, a high up-regulation was recorded in both RH and IC of WT and DHSoex. In contrast, a dramatic down-regulation was observed in DOHH_RH compared to WT or DHSoex (Table 49). These results are in accordance to previous studies, where WT and DHSoex showed elevated production of DON, but DOHHoex showed low levels of DON production during plant infection (Martinez-Rocha *et al.*, 2016). The regulation of DON at the transcriptional level partly explained the hyper and hypo-virulence phenotypes of DHSoex and DOHHoex mutants in wheat glumes. During coleoptile infection, no DON biosynthesis genes are induced and it is suggested that *F. graminearum* might not employ DON releasing as a coleoptile infection strategy (Zhang *et al.*, 2012).

Fungal secondary metabolite biosynthetic (SMB) pathway genes are often clustered and their coordinated transcription is controlled in a complex way which includes genes encoding nonribosomal peptide synthetase (NPS) or polyketide synthase. Ma *et al.*, (2010) have annotated 15 SMB gene clusters. Among these, FG3_40 and FG3_54 cluster genes (C37 and C40 in this study, Table 24) show significant upregulated coexpression of the entire gene cluster during coleoptile infection (Zhang *et al.*, 2012). In this study analysis of the expression of those predicted NPS and polyketide synthase genes are in agreement with the hypothesis that these gene clusters are involved in secondary metabolite biosynthesis and virulence of *F. graminearum*. The C40 gene cluster contains eight genes, all of which are induced in IC and

especially dramatically up-regulated in DHS_IC (Figure 59). This gene cluster locus has two putative NPS genes. NPS5 includes five full adenylation (A)–pantothenylation (P) – condensation (C) modules and NPS9 contains only A and P domains. Also in this cluster, *FGSG_10991* encodes a putative benzoate 4-monooxygenase cytochrome P450 and *FGSG_10992* protein is similar to a peptidoglycan deacetylase (PD). *FGSG_10995* encodes a putative multidrug resistance protein that might function as an efflux transporter and *FGSG_10993* encodes a putative selenocysteine lyase (SCL) (Zhang *et al.*, 2012). Reduction of virulence during coleoptile infection is recorded in mutants with individual deletion of *NPS9*, *FGSG_10992*, or FGSG_10995 (Zhang *et al.*, 2012). *NPS9* also increased expression at 96 HAI during floret infection (Lysøe *et al.*, 2011). In my study, this gene is dramatically up-regulated in DHS_IC and down regulated in DOHH_RH compared to mycelium.

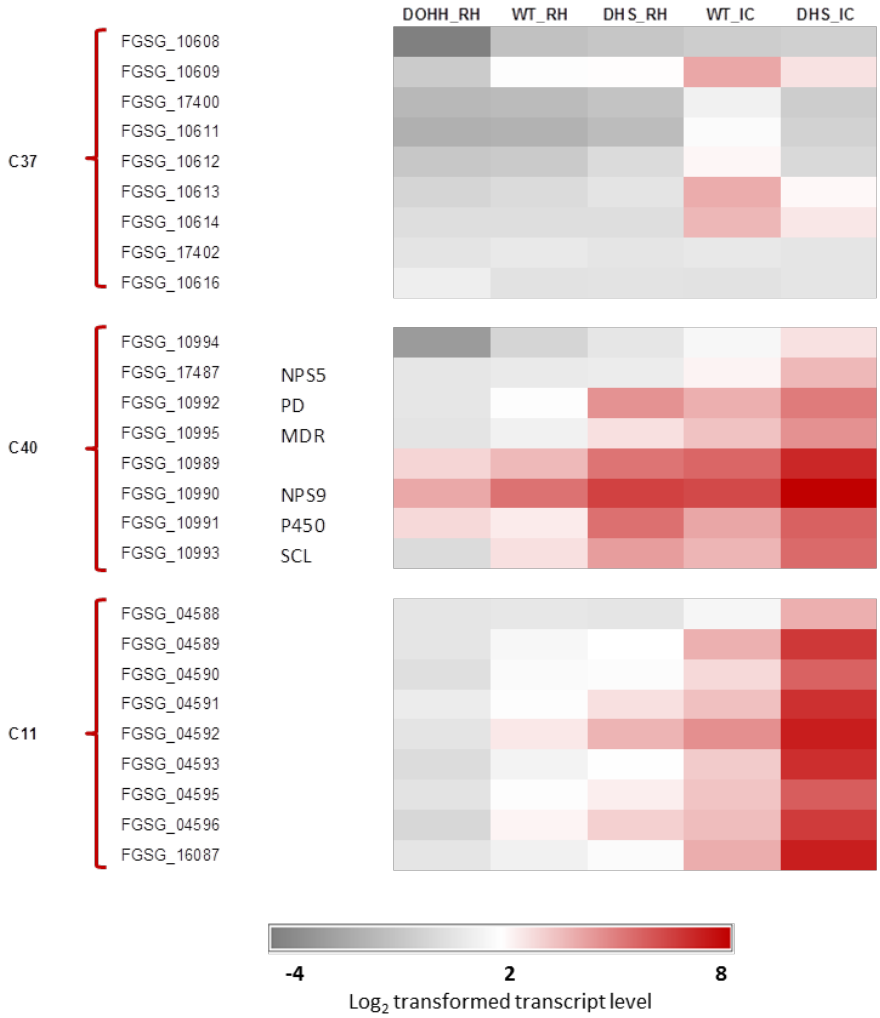

Figure 59. Several SM cluster genes are induced during infection. The C37 (FG3_40), C40 (FG3_54) cluster are required for virulence (Zhang *et al.*, 2012). C11 showed extremely high expression in DHS_IC and WT_IC in comparison to WT mycelium.

Interestingly, another gene cluster called C11 has shown extremely high expression in DHS_IC in comparison to mycelium and WT_IC. In Zhang's report, this cluster gene is called

FG3_26 and showed high expression after 64 hpi but not as high as FG3_40 and FG3_54. The overexpression of DHS gene in *F. graminearum* has directly affected the expression of this cluster and boosted it up many times. This cluster gene could be an important factor in hypervirulence of DHSoex.

The expression of these gene clusters, suggest that DHS overexpression in *F. graminearum* increases the transcript level of SMB gene clusters and leads to hypervirulence during the initial stage of infection. On the contrary this could be the explanation in the avirulence of DOHHoex. By overexpressing DOHH gene in *F. graminearum* this process reduces or inactivates the transcript level of SMB gene clusters.

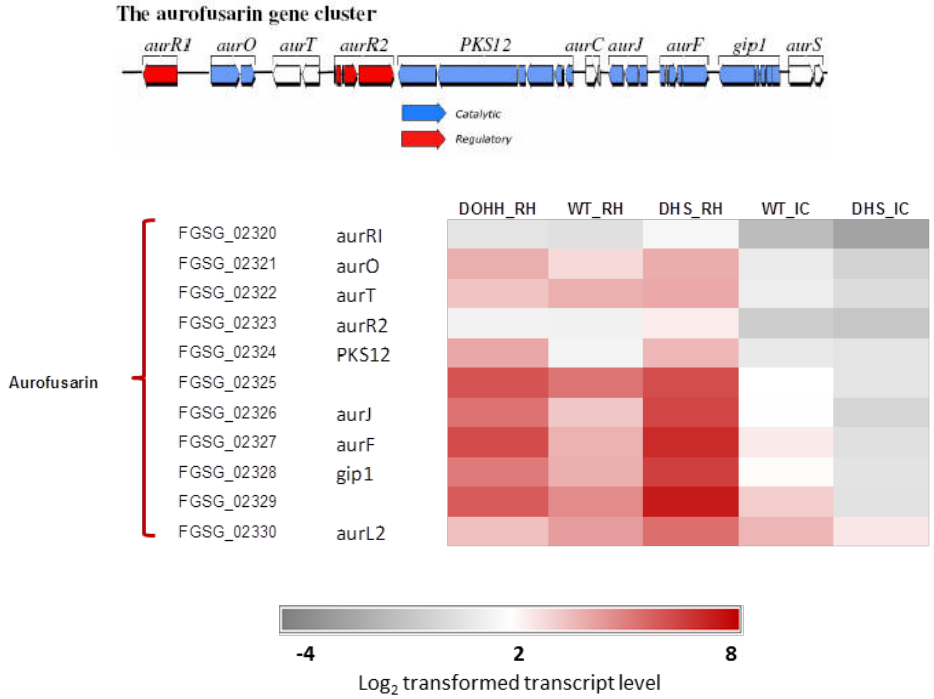

Figure 60. Aurofusarin **cluster genes are induced in RH growing on wheat glumes.** The aurofusarin gene cluster in *F. graminearum*, located on contig 1.116 as defined by Malz *et al.* (2005), is highly up regulated in RH but not in IC.

Another gene cluster containing *PKS12* and responsible for the synthesis of the pigment aurofusarin (Frandsen *et al.*, 2006) was also examined (Figure 60). According to Malz *et al.* (2005) and Kim *et al.* (2005), deletion of *gip1* (*FGSG_02328*) and PKS12, respectively, resulted in a loss of both aurofusarin and an uncharacterized yellow pigment. Another gene, AurR1, has significant similarity to the aflatoxin/sterigmatocystin-specific transcription factor AflR from *Aspergillus* sp. The affected genes in aurofusarin pathway include two putative transcription factors (*aurR2* and *aurJ*), one pump (*aurT*), five catalytic enzymes (*PKS12*, *aurO*, *aurF*, *gip1* and *aurL2*) and two open reading frames (ORFs) that show no similarity to any characterized proteins. A recent experiment to determine the function of AUR cluster in Prof. Schäfer´s lab showed that a wild type extract with AUR is able to inhibit bacterial and fungal

growth while the Aur-deficient mutant (deleted *PKS12*) is not. The result suggests that AUR may suppress competitors prior to colonization of the host plant (personal communication-unpublished data). In agreement to this result, the AUR gene cluster is up-regulated mainly in RH but not in IC in all analysed strains suggesting that aurofusarin is necessary during *F. graminearum* expansion on plant surfaces where competitors grow but not during host plant penetration. Again, those results are a confirmation of the hypothesis of eIF5A being involved in diverse signaling pathways including secondary metabolism.

Fungal cell wall remodeling genes (FCWRE)

A main difference between the hypervirulent DHSoex and WT is the ability to produce more and bigger infection structures. On the contrary, the avirulent DOHHoex is unable to produce infection structures and penetrate the plant cell wall. In order to produce infection structures, filamentous fungi undergo a morphological differentiation where the fungal cell wall suffers multiple reorganizations (Xu *et al.*, 2008). It is known that the fungal cell wall is essential for integrity, strength and shape of the fungi, as well as for protection against harmful agents from the environment (Rolli *et al.*, 2009). Besides that, the fungal cell wall is also the initial point of contact with the host and based on it, plant immune defence can interact and respond to signals from fungal cell wall components (Netea *et al.*, 2006; Gow and Hube, 2012; Wagener *et al.*, 2014). The principal fungal cell wall components are glucan (β-1-3- and β-1-6-glucans) and chitin (β-1-4-linked GlcNAc) polymers (Cid *et al.*, 1995). The changes in fungal cell wall structure during growth or infection have been reported in several fungi such as *Coprinopsis cinerea* and *Galerina marginata* (Nagendran *et al.*, 2009). A focus of this study was the fungal cell wall remodeling enzymes (FCWRE) which play an important role in cell wall morphogenesis.

The results from this analysis indicated that many genes encoding glucanases, including endo-1-4-beta-glucanase, endo-1-3-beta-glucanase, endoglucanase I precursor and beta-1-3-glucan binding are deactivated or expression is reduced in the DOHHoex mutant leading to failed in infection structure formation (Table 26). On the contrary, in DHSoex these genes are highly expressed in comparison to WT_IC and possibly speeded up the formation of infection structures. Chitin deacetylase (*FGSG_06549*) is up-regulated in WT_IC compared to DOHH_RH and this gene is also described in Yang's report (2011). In other fungi such as *Saccharomyces cerevisiae, Ustilago maydis, Trichoderma reesei* and *Ectomycorrhizal* similar proteins have also been determined and have been involved in modification of the fungal cell walls (Mueller *et al.*, 2008; Nagendran *et al.*, 2009). The identification of these proteins suggests that cell wall

remodeling is likely to be important not only during vegetative growth but also during the penetration of the fungus.

Through this analysis we determine that the alteration of eIF5A pathway is involved in diverse signaling pathways including the fungal cell wall remodeling affecting the morphological differentiation and pathogenicity of *F. graminearum*.

In conclusion, the analysis and comparison of differentially expressed genes in each infection structures of the wild type strain and DHSoex and DOHHoex mutants provided more understanding of pathogenesis-related events in the plant pathogen *F. graminearum.* Alteration of posttranslational hypusination of the eukaryotic translation initiation factor-5A had affected many pathways involved in production of plant cell wall–degrading enzymes (PCWDE), ROS and scavenging proteins, secondary metabolite (SM) and fungal cell wall remodeling enzymes (FCWRE).

The overexpression of DHS in *F. graminearum* increased the transcript level in secreted enzymes and SM cluster genes (especially butenolide, C11, C40 and C41 cluster) which are required for virulence. Furthermore, the FCWREs were highly expressed suggesting the speed up in cell wall morphogenesis and formation of infection structures. All these differences in gene expression could be the explanation for the hypervirulent phenotype of DHSoex mutant. On the contrary, overexpression of DOHH gene in *F. graminearum* reduced or inactivated the transcript level of PCWDE genes and SM gene clusters. This study also revealed that aurofusarin gene cluster is mainly expressed in epiphytically growing and expanding hyphae (RH) but not in penetrating structures (IC). Additionally some FCWREs were inactivated and led to a fall in the formation of infection structures. Many pathogenicity pathways were affected conducting to the avirulence phenotype of DOHHoex.

Summary

The posttranslational modification of the eukaryotic translation initiation factor 5A (eIF5A) is indispensable for its function. This modification requeries two enzymes, deoxyhypusine synthase (DHS) and deoxyhypusine hydroxylase (DOHH) to produce the unique amino acid hypusine. The genes encoding for the biosynthetic enzymes DHS, DOHH and the substrate eIF5A are indispensable in plants and fungi. Therefore, a way to study the eIF5A-hypusine synthesis and its implications is by altering the expression levels of the modifying genes DHS or DOHH.

In the first part of this study, the importance of DHS expression levels was investigated in *Zea mays*. In previous studies, silencing or overexpressing *ZmDHS1* maize lines were generated. Here, these transgenic maize lines were cultivated until T3 generation and verified. The *ZmDHS*1 gene expression results provided a strong evidence of activation of the silencing and overexpressing DHS constructs in the transgenic maize plants. In addition, in silico analysis revealed the presence of two DHS genes in *Z. mays*. Expression analysis of the DHS genes indicated a transcriptional co-expression of *ZmDHS1* and *ZmDHS2* genes, but no effect on the expression of *ZmDOHH* or the three *ZmeIF5A* genes in the silencing and overexpressing lines.

Aditionally, differences in expression of *ZmDHS1* produced diverse effects in germination, growth and development in the silencing and overexpressing maize lines. Nevertheless, no evident physiological phenotype could be attributed to silencing or overexpression of *ZmDHS1*.

Exceptionally, the DHS-overexpressing lines exhibit resistance towards the fungal pathogens *Bipolaris sorokiniana*, *Cochliobolus heterostrophus*, and *Colletotrichum graminicola*, while the DHS-silencing lines showed similar susceptibility as the control plants. Expression analysis of key genes involved in plant defence response revealed that more than a hormonal defence response, the resistance of overexpressing lines could be attributed to the thickening of a physical barrier.

In the second part of this study, a comparative analysis of differentially expressed genes was produced using two mutants and the wild type strain of *Fusarium graminearum*. The two mutants were generated in previous studies, a DHS overexpressing mutant (DHSoex) with a hypervirulent phenotype and a DOHH overexpressing mutant (DOHHoex) with an avirulent phenotype.

By using different microscopic techniques, infection structures of the WT and overexpressing mutants growing on wheat glumes were analyzed. While DHSoex produced similar infection structures (IC) to the wild type, the DOHHoex did not produce infection structures, only epiphytically growing runner hyphae (RH).

A combination of laser microdissection and LD_PCR was used to create cDNA libraries from low amount of mRNA extracted from RH or IC of the wild type strain and the two overexpressing mutants. Using Ilumina Next Generation Sequencing we determined the differentially transcribed genes of all samples.

The results revealed a global viewpoint of *F. graminearum* gene expression during early infection of wheat. Here, we analysed not only the total expression but also a number of regulated genes involved in several functions such as transcription factors (TF), transporters (TP), glycoside hydrolases (GH), secondary metabolite (SM), ROS-related proteins, effectors, fungal cell wall remodeling enzymes (FCWRE), protein kinases (PK) and plant cell wall degrading enzymes (PCWDE).

During the analyses, several specific genes emerged as being responsible for expansion on the plant surface but not for penetration or pathogenicity. Among the SM gene clusters, while the aurofusarin gene cluster is necessary during *F. graminearum* expansion on plant surfaces where competitors grow, it is not needed during penetration. On the contrary, the gene clusters such as C31, C37, C40 and C11 were involved during penetration more than during expansion of the fungus.

The comparison of *F. graminearum* gene expression *in vitro* and *in planta* of wild type and the overexpressing DHSoex and DOHHoex mutants allowed to restrict the large number of genes expressed during infection and revealed novel virulence factors involved specifically during penetration of the host plant.

Finally, the transcriptome analysis confirmed the influence of diverse genes affecting the morphological differentiation and pathogenicity in *F. graminearum* due to the alteration of hypusine-eIF5A biosynthesis.

Appendix

Appendix Table 1. Seventy seven genes which are up-regulated (Log2>2) and only expressed in WT_RH compared to DOHH_RH.

FGSG_Number	WT_RH vs DOHH_RH Log2	Description	Enzyme substrat	Gene_cluster
FGSG_11202	3.402	probable guanylate kinase (ident 100.0%)		
FGSG_03177	5.698	related to amidase (ident 100.0%)	Cellobiose	
FGSG_12402	5.815	related to flavoprotein (ident 34.4%)		
FGSG_04665	3.066	related to fumarate reductase flavoprotein subunit precursor (ident 100.0%)		
FGSG_07716	2.141	related to G protein coupled receptor like protein (ident 100.0%)	HG,RGII primary chain	
FGSG_04709	2.224	related to multidrug resistant protein (ident 100.0%)	xyloglucan	
FGSG_16114	3.99	related to multidrug transporter (yeast bile transporter) (ident 52.1%)		C37
FGSG_03706	2.312	related to non-ribosomal peptide synthetase (ident 66.5%)		
FGSG_07557	2.037	related to transcription co-repressor GAL80 (ident 100.0%)		
FGSG_01831	3.316	related to trihydrophobin precursor (ident 100.0%)	hemicellulose	
FGSG_15635	6.825	uncharacterized protein		
FGSG_16406	6.344	uncharacterized protein		
FGSG_10597	4.7	uncharacterized protein		
FGSG_15152	4.603	uncharacterized protein		
FGSG_09133	4.56	uncharacterized protein		
FGSG_12294	4.549	uncharacterized protein		C37
FGSG_15274	4.447	uncharacterized protein		
FGSG_04952	4.335	uncharacterized protein	cellulose	
FGSG_15242	4.296	uncharacterized protein		
FGSG_15339	3.81	uncharacterized protein		C37
FGSG_03025	3.791	uncharacterized protein	cutin	
FGSG_15502	3.778	uncharacterized protein		
FGSG_15298	3.68	uncharacterized protein		
FGSG_15074	3.589	uncharacterized protein		C11
FGSG_15088	3.539	uncharacterized protein	Pectin/Xylan side chain	
FGSG_12803	3.304	uncharacterized protein	HG,RGII primary chain	
FGSG_13421	3.204	uncharacterized protein		C37
FGSG_15564	3.202	uncharacterized protein		
FGSG_11753	3.17	uncharacterized protein		
FGSG_15523	3.147	uncharacterized protein		
FGSG_15621	3.143	uncharacterized protein		
FGSG_02447	3.115	uncharacterized protein		
FGSG_15569	3.108	uncharacterized protein		

FGSG_13193	3.106	uncharacterized protein		
FGSG_16222	3.081	uncharacterized protein		
FGSG_15236	3.049	uncharacterized protein		
FGSG_04441	3.044	uncharacterized protein		C37
FGSG_15208	3.007	uncharacterized protein		
FGSG_08054	2.89	uncharacterized protein		
FGSG_05672	2.847	uncharacterized protein	cellulose	
FGSG_15081	2.846	uncharacterized protein	Xylan	
FGSG_08100	2.825	uncharacterized protein		
FGSG_15440	2.798	uncharacterized protein		
FGSG_15425	2.785	uncharacterized protein		
FGSG_08080	2.748	uncharacterized protein		
FGSG_15476	2.739	uncharacterized protein		
FGSG_08145	2.683	uncharacterized protein		
FGSG_01763	2.659	uncharacterized protein		
FGSG_03334	2.603	uncharacterized protein		
FGSG_04663	2.597	uncharacterized protein		
FGSG_15781	2.549	uncharacterized protein		
FGSG_15384	2.534	uncharacterized protein		
FGSG_04682	2.531	uncharacterized protein		
FGSG_15646	2.524	uncharacterized protein		
FGSG_05936	2.472	uncharacterized protein		
FGSG_13539	2.47	uncharacterized protein		
FGSG_15456	2.455	uncharacterized protein		
FGSG_15383	2.442	uncharacterized protein		
FGSG_07713	2.412	uncharacterized protein		
FGSG_00322	2.37	uncharacterized protein		C15
FGSG_15238	2.367	uncharacterized protein		
FGSG_15543	2.342	uncharacterized protein		
FGSG_15286	2.331	uncharacterized protein		
FGSG_02856	2.324	uncharacterized protein		
FGSG_13948	2.255	uncharacterized protein		
FGSG_16437	2.242	uncharacterized protein		
FGSG_15173	2.235	uncharacterized protein		
FGSG_15289	2.214	uncharacterized protein		
FGSG_13104	2.208	uncharacterized protein		
FGSG_15362	2.207	uncharacterized protein		
FGSG_15175	2.183	uncharacterized protein		
FGSG_15392	2.167	uncharacterized protein		
FGSG_15239	2.151	uncharacterized protein		
FGSG_16254	2.147	uncharacterized protein		
FGSG_15302	2.112	uncharacterized protein		
FGSG_15508	2.062	uncharacterized protein		

FGSG_15337	2.028	uncharacterized protein		

Appendix Table 2. Eighty two genes specifically expressed and up-regulated in WT_IC compared to DOHH_RH - Log2>2.

FGSG_Number	Log2 FPKM WT_IC	Description	Enzyme substrat	SM_Cluster
FGSG_06098	3.402	probable arginosuccinate synthetase (ident 100.0%)		
FGSG_09085	5.698	probable cellobiose dehydrogenase (ident 100.0%)	Cellobiose	
FGSG_12440	5.815	probable lysine permease (ident 100.0%)		
FGSG_15973	3.066	probable neutral amino acid permease (ident 100.0%)		
FGSG_04864	2.141	probable pectate lyase (ident 100.0%)	HG,RGII primary chain	
FGSG_11208	2.224	probable Xyloglucanase (ident 65.0%)	xyloglucan	
FGSG_10611	3.99	related to 6-hydroxy-d-nicotine oxidase (ident 100.0%)		C37
FGSG_16895	2.312	related to acetylxylan esterase (ident 50.0%)		
FGSG_10986	2.037	related to alcohol oxidase (ident 100.0%)		
FGSG_04678	3.316	related to beta-mannanase (ident 100.0%)	hemicellulose	
FGSG_03605	2.37	related to bifunctional 4-hydroxyphenylacetate degradation enzyme (ident 100.0%)		C15
FGSG_17091	2.659	related to capsule-associated protein (ident 100.0%)		
FGSG_07668	3.115	related to Carboxypeptidase 2 (ident 42.9%)		
FGSG_00773	2.324	related to copper transport protein (ident 100.0%)		
FGSG_10634	3.791	related to cutinase 1 precursor (ident 100.0%)	cutin	
FGSG_16565	2.603	related to CYB2 - Lactate dehydrogenase cytochrome b2 (ident 100.0%)		
FGSG_17400	3.044	related to cytochrome P450 monooxygenase (ident 100.0%)		C37
FGSG_07887	2.597	related to dehydrogenase/reductase (ident 36.7%)		
FGSG_08042	2.531	related to dihydroxyacetone kinase (ident 100.0%)		
FGSG_03918	4.335	related to endoglucanase (ident 100.0%)	cellulose	
FGSG_04773	2.847	related to endoglucanase IV precursor (ident 100.0%)	cellulose	
FGSG_09137	2.472	related to hydrolases or acyltransferases (alpha/beta hydrolase superfamily) (ident 35.9%)		
FGSG_11215	2.412	related to hydroxylase (ident 100.0%)		
FGSG_05793	2.89	related to integral membrane protein pth11 (ident 100.0%)		
FGSG_03790	2.748	related to metalloprotease MEP1 (ident 100.0%)		
FGSG_11528	2.825	related to monophenol monooxygenase (tyrosinase) (ident 100.0%)		
FGSG_10474	2.683	related to myo-inositol transport protein ITR1 (ident 100.0%)		
FGSG_00118	4.56	related to neutral amino acid permease (ident 100.0%)		
FGSG_03568	4.7	related to O-methyltransferase B (ident 100.0%)		
FGSG_03888	3.17	related to ornithine aminotransferase (ident 100.0%)		
FGSG_10613	4.549	related to para-hydroxybenzoate polyprenyltransferase precursor (ident 100.0%)		C37
FGSG_03131	3.304	related to pectate lyase L precursor (ident 100.0%)	HG,RGII primary chain	
FGSG_16173	2.208	related to phosphoenolpyruvate phosphomutase (ident 53.9%)		
FGSG_10561	3.106	related to RF2 protein (ident 100.0%)		
FGSG_10612	3.204	related to salicylate hydroxylase (ident 100.0%)		C37

FGSG_07662	2.47	related to TAM domain methyltransferase (ident 33.6%)		
FGSG_12522	2.255	related to TAM domain methyltransferase (ident 40.1%)		
FGSG_04589	3.589	related to tetracenomycin polyketide synthesis O-methyltransferase tcmP (ident 100.0%)		C11
FGSG_07993	2.846	related to xylan 1,4-beta-xylosidase (ident 100.0%)	Xylan	
FGSG_03609	3.539	related to xylosidase/glycosyl hydrolase (ident 50.7%)	Pectin/Xylan side chain	
FGSG_15254	6.825	uncharacterized protein		
FGSG_16366	6.344	uncharacterized protein		
FGSG_01771	4.603	uncharacterized protein		
FGSG_04615	4.447	uncharacterized protein		
FGSG_04089	4.296	uncharacterized protein		
FGSG_10614	3.81	uncharacterized protein		C37
FGSG_12312	3.778	uncharacterized protein		
FGSG_07899	3.68	uncharacterized protein		
FGSG_17073	3.358	uncharacterized protein		
FGSG_14010	3.202	uncharacterized protein		
FGSG_13227	3.147	uncharacterized protein		
FGSG_15168	3.143	uncharacterized protein		
FGSG_15067	3.108	uncharacterized protein		
FGSG_15587	3.081	uncharacterized protein		
FGSG_03455	3.049	uncharacterized protein		
FGSG_03287	3.007	uncharacterized protein		
FGSG_11648	2.798	uncharacterized protein		
FGSG_11501	2.785	uncharacterized protein		
FGSG_12185	2.739	uncharacterized protein		
FGSG_17621	2.618	uncharacterized protein		
FGSG_15488	2.549	uncharacterized protein		
FGSG_11145	2.534	uncharacterized protein		
FGSG_15387	2.524	uncharacterized protein		
FGSG_16960	2.503	uncharacterized protein		
FGSG_11830	2.455	uncharacterized protein		
FGSG_11078	2.442	uncharacterized protein		
FGSG_03463	2.367	uncharacterized protein		
FGSG_13654	2.342	uncharacterized protein		
FGSG_04649	2.331	uncharacterized protein		
FGSG_16880	2.242	uncharacterized protein		
FGSG_01822	2.235	uncharacterized protein		
FGSG_04867	2.214	uncharacterized protein		
FGSG_11009	2.207	uncharacterized protein		
FGSG_02183	2.183	uncharacterized protein		
FGSG_11461	2.167	uncharacterized protein		
FGSG_03896	2.151	uncharacterized protein		
FGSG_15652	2.147	uncharacterized protein		

FGSG_09094	2.112	uncharacterized protein		
FGSG_12491	2.062	uncharacterized protein		
FGSG_10401	2.028	uncharacterized protein		
FGSG_17401	2.011	uncharacterized protein		C37
FGSG_15938	2.012	uncharacterized protein - related to integral membrane protein (ident 26.7%)		

Appendix Table 3. Thirty-nine genes which are up-regulated (Log2>2) and only expressed in DHS_IC compared to WT_IC.

Locus	log2 DHS_IC	Description
FGSG_03048	5.535	related to dTDP-glucose 4,6-dehydratase (ident 100.0%)
FGSG_17495	2.528	related to GNT1 – N-acetylglucosaminyltransferase transferase capable of modification of N-linked (ident 100.0%)
FGSG_03840	3.057	related to spore coat protein SP96 precursor (ident 100.0%)
FGSG_01749	2.161	uncharacterized protein
FGSG_04850	5.829	uncharacterized protein
FGSG_07755	5.309	uncharacterized protein
FGSG_08625	2.182	uncharacterized protein
FGSG_11342	2.151	uncharacterized protein
FGSG_11477	2.058	uncharacterized protein
FGSG_12104	3.123	uncharacterized protein
FGSG_12581	5.118	uncharacterized protein
FGSG_13701	7.450	uncharacterized protein
FGSG_15060	2.782	uncharacterized protein
FGSG_15137	3.892	uncharacterized protein
FGSG_15176	3.420	uncharacterized protein
FGSG_15194	3.260	uncharacterized protein
FGSG_15197	2.126	uncharacterized protein
FGSG_15274	2.986	uncharacterized protein
FGSG_15286	3.829	uncharacterized protein
FGSG_15287	2.300	uncharacterized protein
FGSG_15305	2.649	uncharacterized protein
FGSG_15344	4.013	uncharacterized protein
FGSG_15386	2.869	uncharacterized protein
FGSG_15415	4.357	uncharacterized protein
FGSG_15425	3.530	uncharacterized protein
FGSG_15427	2.566	uncharacterized protein
FGSG_15453	4.315	uncharacterized protein
FGSG_15478	2.167	uncharacterized protein
FGSG_15501	3.743	uncharacterized protein
FGSG_15517	4.490	uncharacterized protein
FGSG_15549	3.435	uncharacterized protein
FGSG_15591	4.317	uncharacterized protein
FGSG_15645	2.099	uncharacterized protein
FGSG_15781	2.611	uncharacterized protein

FGSG_16158	2.452	uncharacterized protein
FGSG_16375	2.266	uncharacterized protein
FGSG_16382	2.481	uncharacterized protein
FGSG_16670	2.040	uncharacterized protein
FGSG_11320	2.153	uncharacterized protein – related to Protein moaF (ident 32.1%)

Appendix Table 4. 139 up regulated genes only expressed *in planta* vs Myc - Log2>2.

	DOHH_RH	WT_RH	DHS_RH	WT_IC	DHS_IC	Description	Cluster
TF							
FGSG_03794	0.000	0.046	0.938	0.169	3.894	uncharacterized protein	
FGSG_08080	0.000	2.103	0.876	1.865	3.847	uncharacterized protein	
FGSG_00154	0.000	3.789	1.008	2.768	5.666	uncharacterized protein	
TP							
FGSG_07584	3.438	0.750	1.167	0.489	1.893	related to DAL5 - Allantoate and ureidosuccinate permease	
FGSG_04709	0.000	2.475	0.215	0.000	0.000	related to multidrug resistant protein	
FGSG_16391	0.321	0.980	2.453	2.590	1.362	hypothetical protein	
FGSG_00118	0.000	0.025	0.091	4.560	0.134	related to neutral amino acid permease	
FGSG_08055	0.710	1.018	2.322	3.677	4.196	related to neutral amino acid permease	
GH							
FGSG_03384	0.000	0.025	0.091	0.770	2.206	probable exopolygalacturonase	
FGSG_03908	0.000	0.000	0.647	0.600	6.406	probable pectate lyase 1	
FGSG_04681	0.000	0.153	0.000	0.571	3.027	probable endoglucanase IV precursor	
FGSG_07533	0.162	1.327	0.423	1.810	5.014	conserved hypothetical protein	
FGSG_04773	0.000	1.917	0.348	2.847	5.676	related to endoglucanase IV precursor	
FGSG_04864	0.000	0.064	0.000	2.141	6.424	probable pectate lyase	
SM							
FGSG_03969	8.367	9.400	10.315	7.720	10.402	uncharacterized protein	K4
FGSG_02325	6.207	5.274	6.393	1.354	0.000	uncharacterized protein	C7
FGSG_03728	1.195	0.529	0.000	1.452	5.110	uncharacterized protein	C14
FGSG_08080	0.000	2.103	0.876	1.865	3.847	uncharacterized protein	C31 Butenolide
FGSG_01784	1.303	4.078	1.352	2.678	0.000	related to phosphatidylinositol/phosphatidylcholine transfer protein (ident 100.0%)	K3
FGSG_03493	0.000	0.707	2.260	1.216	0.000	uncharacterized protein	K5
FGSG_04667	0.779	2.037	1.605	2.725	2.839	related to sulfonate dioxygenase (ident 100.0%)	C10
FGSG_06449	1.744	1.617	2.002	1.558	2.808	probable fumarylacetoacetate hydrolase (ident 100.0%)	C24
FGSG_15645	1.374	2.843	1.179	0.000	2.099	uncharacterized protein	C43
FGSG_03531	0.117	2.579	1.307	4.067	4.242	monooxygenase (ident 100.0%)	C16 Tri
FGSG_03542	0.215	6.968	4.460	5.353	9.862	probable cytochrome P450 (ident 100.0%)	C16 Tri
FGSG_04589	0.000	0.972	1.364	3.589	6.972	related to tetracenomycin polyketide synthesis O-methyltransferase tcmP (ident 100.0%)	C11
FGSG_08082	0.273	3.334	0.115	0.284	9.179	related to GNAT family N-acetyltransferase (ident 35.6%)	C31 Butenolide

ROS-related							
FGSG_00078	3.524	0.790	0.394	0.065	0.869	related to aldo/keto reductase (ident 100.0%)	
FGSG_13196	6.243	1.048	3.422	0.902	0.000	related to 3-oxoacyl-(acyl-carrier-protein) reductase (ident 100.0%)	
FGSG_03348	0.000	0.653	0.000	1.359	3.793	related to monophenol monooxygenase (tyrosinase) (ident 73.8%)	
FGSG_03728	1.195	0.529	0.000	1.452	5.110	uncharacterized protein	C14
FGSG_02917	1.737	2.764	2.535	1.599	1.123	related to cellobiose dehydrogenase (ident 100.0%)	
FGSG_03546	1.569	1.944	2.789	0.851	0.000	putative 3-hydroxyacyl-CoA-dehydrogenase (ident 100.0%)	
FGSG_04667	0.779	2.037	1.605	2.725	2.839	related to sulfonate dioxygenase (ident 100.0%)	C10
FGSG_11568	2.108	2.208	2.928	1.665	2.844	related to monooxigenase (ident 100.0%)	
FGSG_13514	1.274	2.188	2.963	1.557	3.013	related to pyridoxine 4-dehydrogenase (ident 100.0%)	
FGSG_03436	3.253	1.748	1.169	2.841	4.471	related to chloroperoxidase (ident 100.0%)	
FGSG_03531	0.117	2.579	1.307	4.067	4.242	monooxygenase (ident 100.0%)	C16 Tri
Effector							
FGSG_02378	4.293	3.623	4.422	2.343	3.890	uncharacterized protein	
FGSG_17159	2.380	3.581	5.326	3.405	4.144	related to mannosyltransferase	
FGSG_16366	0.000	0.770	0.000	6.344	3.439	uncharacterized protein	
FGSG_15136	0.000	4.204	0.867	4.953	8.026	uncharacterized protein	
FGSG_03334	0.000	2.007	3.858	1.877	4.902	uncharacterized protein	
FGSG_03209	0.025	1.824	1.961	4.223	4.168	triacylglycerol lipase II precursor	
FGSG_08002	1.192	2.091	0.155	5.239	4.057	glucan 1,4-alpha-glucosidase	
FGSG_04818	0.065	3.205	0.285	1.288	0.000	triacylglycerol lipase precursor	
FGSG_09133	0.000	3.059	0.000	0.562	0.000	uncharacterized protein	
FGSG_03130	0.000	0.398	0.000	0.961	2.132	uncharacterized protein	
FGSG_07699	0.000	0.925	0.327	1.087	2.684	uncharacterized protein	
FGSG_08085	0.000	0.677	0.000	1.344	2.305	uncharacterized protein	
FGSG_12104	0.000	0.000	0.757	0.000	3.123	uncharacterized protein	
FGSG_14010	0.000	0.468	0.000	3.202	2.261	uncharacterized protein	
FGSG_16880	0.000	0.442	0.000	2.242	3.993	uncharacterized protein	
FGSG_01723	0.764	1.495	1.505	1.587	3.438	uncharacterized protein	
FGSG_17388	0.000	0.000	0.000	1.400	3.959	uncharacterized protein	
PCWDE							
FGSG_02917	1.737	2.764	2.535	1.599	1.123	related to cellobiose dehydrogenase (ident 100.0%)	
FGSG_03384	0.000	0.025	0.091	0.770	2.206	probable exopolygalacturonase (ident 100.0%)	
FGSG_03908	0.000	0.000	0.647	0.600	6.406	probable pectate lyase 1 (ident 100.0%)	
FGSG_04681	0.000	0.153	0.000	0.571	3.027	probable endoglucanase IV precursor (ident 100.0%)	
FGSG_07533	0.162	1.327	0.423	1.810	5.014	uncharacterized protein - related to pectin methylesterase family protein (ident 43.6%)	
FGSG_04773	0.000	1.917	0.348	2.847	5.676	related to endoglucanase IV precursor (ident 100.0%)	
FGSG_03436	3.253	1.748	1.169	2.841	4.471	related to chloroperoxidase (ident 100.0%)	
FGSG_04864	0.000	0.064	0.000	2.141	6.424	probable pectate lyase (ident 100.0%)	

Other						
FGSG_06692	11.046	14.132	11.906	8.631	9.548	probable DDR48 - heat shock protein (ident 100.0%)
FGSG_13046	6.314	10.880	4.292	4.988	5.530	putative protein (EST hit) (ident 100.0%)
FGSG_11405	2.643	2.532	2.242	1.364	0.053	related to alkaline protease (oryzin) (ident 100.0%)
FGSG_16233	0.284	1.488	1.460	2.439	4.924	related to ATO2 - Integral membrane protein, involved in ammonia production (ident 100.0%)
FGSG_16565	0.000	0.466	1.135	2.603	3.149	related to CYB2 - Lactate dehydrogenase cytochrome b2 (ident 100.0%)
FGSG_03504	0.472	4.144	3.580	3.976	6.468	related to integral membrane protein (ident 100.0%)
FGSG_07839	3.602	0.878	3.680	0.290	0.243	related to integral membrane protein PTH11 (ident 100.0%)
FGSG_10678	0.041	2.244	1.232	2.858	0.033	related to IQ calmodulin-binding motif protein (ident 46.8%)
FGSG_00061	0.670	3.485	0.000	0.272	3.478	related to KP4 killer toxin (ident 100.0%)
FGSG_16282	2.737	3.375	3.425	2.489	2.363	related to L-fucose permease (ident 100.0%)
FGSG_11566	2.900	1.142	3.330	0.718	1.191	related to oxidoreductase (ident 40.2%)
FGSG_03886	0.838	1.130	0.878	1.995	5.078	related to phospholipase C (ident 100.0%)
FGSG_16658	1.446	2.791	1.700	1.646	2.176	related to RTM1 protein (ident 100.0%)
FGSG_12920	4.515	4.313	0.769	2.501	4.121	related to stress responsive A/B barrel domain protein (ident 45.1%)
FGSG_17467	1.491	2.142	3.463	0.808	1.590	related to zinc finger transcription factor (ident 71.6%)
FGSG_07822	8.922	10.672	8.328	10.642	12.639	uncharacterized protein
FGSG_00134	2.534	0.341	1.727	0.120	0.000	uncharacterized protein
FGSG_01714	2.186	0.820	1.527	0.000	0.000	uncharacterized protein
FGSG_01756	3.360	1.810	2.071	0.267	0.000	uncharacterized protein
FGSG_11296	6.078	2.083	3.804	2.928	0.177	uncharacterized protein
FGSG_11682	2.778	1.066	0.923	0.000	0.000	uncharacterized protein
FGSG_11711	2.338	0.160	0.158	0.131	0.000	uncharacterized protein
FGSG_15196	4.207	1.264	0.000	0.000	0.000	uncharacterized protein
FGSG_15234	2.687	0.000	0.000	0.000	0.000	uncharacterized protein
FGSG_15394	4.289	2.645	0.000	1.046	0.000	uncharacterized protein
FGSG_15457	4.298	3.597	0.000	0.000	0.000	uncharacterized protein
FGSG_15492	5.053	0.000	0.000	0.000	0.000	uncharacterized protein
FGSG_17062	2.978	0.000	0.790	0.679	0.000	uncharacterized protein
FGSG_02182	0.317	0.476	0.719	0.488	3.600	uncharacterized protein
FGSG_02183	0.000	0.072	0.237	2.183	4.564	uncharacterized protein
FGSG_04850	0.000	0.000	0.000	0.000	5.829	uncharacterized protein
FGSG_07755	0.949	0.680	0.000	0.000	5.309	uncharacterized protein
FGSG_09126	0.000	0.000	0.127	0.513	3.305	uncharacterized protein
FGSG_09127	0.000	0.000	0.000	0.906	4.053	uncharacterized protein
FGSG_12453	0.221	0.280	0.000	0.522	2.752	uncharacterized protein
FGSG_12581	0.000	0.000	0.000	0.000	5.118	uncharacterized protein
FGSG_12818	0.000	0.000	1.401	0.451	2.035	uncharacterized protein
FGSG_13081	0.564	0.180	0.332	0.894	2.082	uncharacterized protein
FGSG_13447	0.000	0.000	0.280	0.359	3.104	uncharacterized protein
FGSG_13654	0.000	0.752	0.618	2.342	3.955	uncharacterized protein
FGSG_13940	0.000	1.242	0.000	1.013	2.198	uncharacterized protein
FGSG_15137	2.340	0.000	0.000	0.000	3.892	uncharacterized protein
FGSG_15188	0.000	1.012	0.000	0.497	2.891	uncharacterized protein

FGSG_15197	0.000	0.000	0.000	0.000	2.126	uncharacterized protein
FGSG_15258	1.027	0.861	0.739	1.073	2.947	uncharacterized protein
FGSG_15344	3.516	0.000	0.000	0.000	4.013	uncharacterized protein
FGSG_15386	0.000	0.000	0.000	0.000	2.869	uncharacterized protein
FGSG_15405	0.000	1.530	0.000	1.153	3.210	uncharacterized protein
FGSG_15417	0.000	0.000	0.000	0.843	2.116	uncharacterized protein
FGSG_15427	0.000	0.000	0.375	0.000	2.566	uncharacterized protein
FGSG_15453	0.000	0.000	0.000	0.000	4.315	uncharacterized protein
FGSG_15517	0.000	0.000	0.000	0.000	4.490	uncharacterized protein
FGSG_15549	0.000	0.792	1.277	0.000	3.435	uncharacterized protein
FGSG_15556	0.000	0.000	0.000	0.771	2.337	uncharacterized protein
FGSG_15804	0.000	1.613	0.000	0.881	2.181	uncharacterized protein
FGSG_16158	0.000	0.000	0.000	0.000	2.452	uncharacterized protein
FGSG_16382	0.000	0.000	0.000	0.000	2.481	uncharacterized protein
FGSG_17079	0.000	0.000	0.956	0.073	2.736	uncharacterized protein
FGSG_01763	0.000	3.921	3.918	0.163	0.000	uncharacterized protein
FGSG_02337	2.917	2.508	0.595	2.863	1.717	uncharacterized protein
FGSG_04649	0.000	0.109	0.000	2.331	0.000	uncharacterized protein
FGSG_04663	0.000	3.913	2.001	1.398	2.145	uncharacterized protein
FGSG_04896	0.000	1.672	2.167	1.818	2.063	uncharacterized protein
FGSG_08100	0.000	2.309	0.000	1.397	0.000	uncharacterized protein
FGSG_12185	0.000	0.000	0.000	2.739	0.000	uncharacterized protein
FGSG_12491	0.000	0.833	1.545	2.062	0.000	uncharacterized protein
FGSG_12532	0.000	0.000	2.141	0.540	0.000	uncharacterized protein
FGSG_12824	1.335	2.469	0.548	0.690	0.000	uncharacterized protein
FGSG_13227	0.000	1.299	2.134	3.147	2.803	uncharacterized protein
FGSG_13537	0.622	2.207	0.393	1.665	2.615	uncharacterized protein
FGSG_13781	0.000	1.796	1.504	1.298	2.827	uncharacterized protein
FGSG_15123	0.000	0.000	2.391	0.497	0.000	uncharacterized protein
FGSG_15183	0.713	2.673	0.000	0.000	0.000	uncharacterized protein
FGSG_15208	0.000	2.758	0.000	0.000	0.000	uncharacterized protein
FGSG_15243	1.558	4.183	0.000	3.235	2.695	uncharacterized protein
FGSG_15254	0.000	0.000	0.000	6.825	0.000	uncharacterized protein
FGSG_15289	0.000	2.164	0.000	0.000	1.511	uncharacterized protein
FGSG_15308	2.062	2.181	0.000	1.094	0.000	uncharacterized protein
FGSG_15378	2.290	2.621	2.383	1.257	3.629	uncharacterized protein
FGSG_15530	1.729	3.319	0.000	0.000	0.000	uncharacterized protein
FGSG_15646	0.000	2.140	1.482	1.577	2.712	uncharacterized protein
FGSG_04792	0.000	3.496	3.524	3.241	4.244	uncharacterized protein
FGSG_09827	0.000	3.069	2.840	5.953	6.935	uncharacterized protein
FGSG_12432	1.636	3.654	1.135	2.522	4.551	uncharacterized protein
FGSG_15302	0.000	3.189	0.000	1.936	4.901	uncharacterized protein
FGSG_15521	0.000	2.027	1.815	2.857	7.166	uncharacterized protein
FGSG_07829	2.114	1.212	0.470	0.328	2.253	uncharacterized protein - related to extracellular serine-rich protein (ident 41.9%)
FGSG_04866	0.029	1.724	1.970	0.980	5.271	uncharacterized protein - related to LysR family regulatory protein (ident 31.0%)

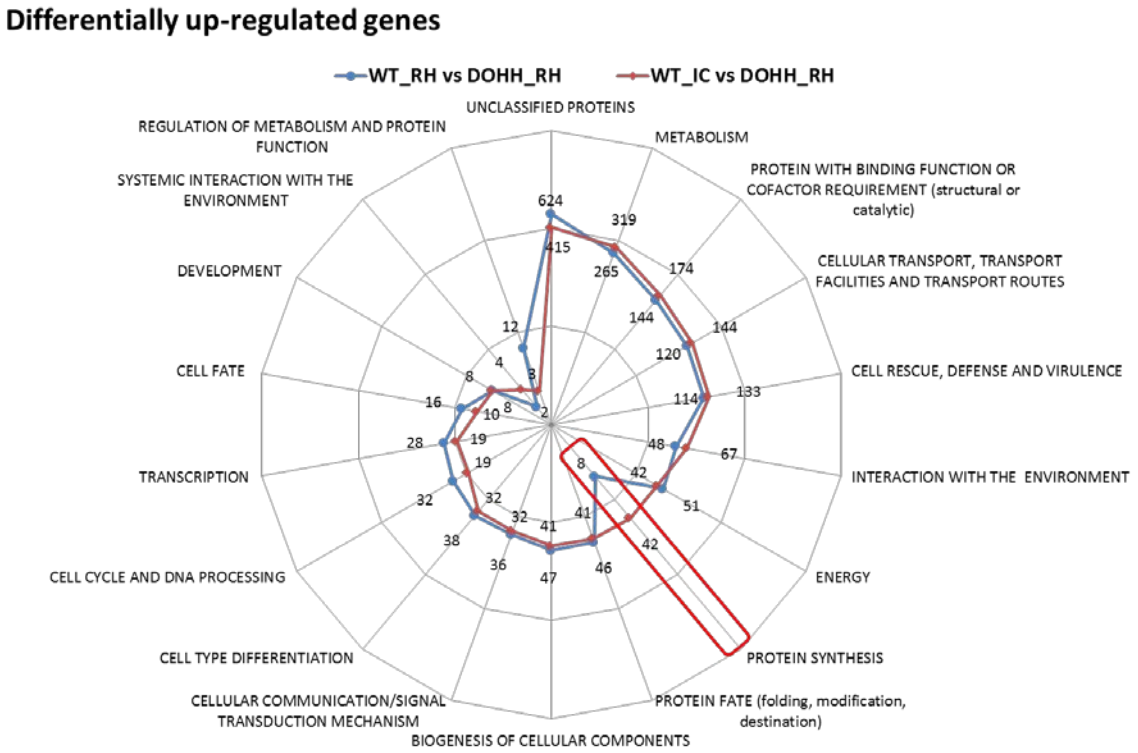

Appendix Figure 1. Radar graph representation for differentially up-regulated genes in transcriptome analyses according to the biological process of fungi. WT_RH vs DOHH_RH in blue line and WT_IC vs DOHH_RH in red line. The axes of the radar correspond to the number of up-regulated genes, resulting in the center is zero and the edge line is 8000 genes.

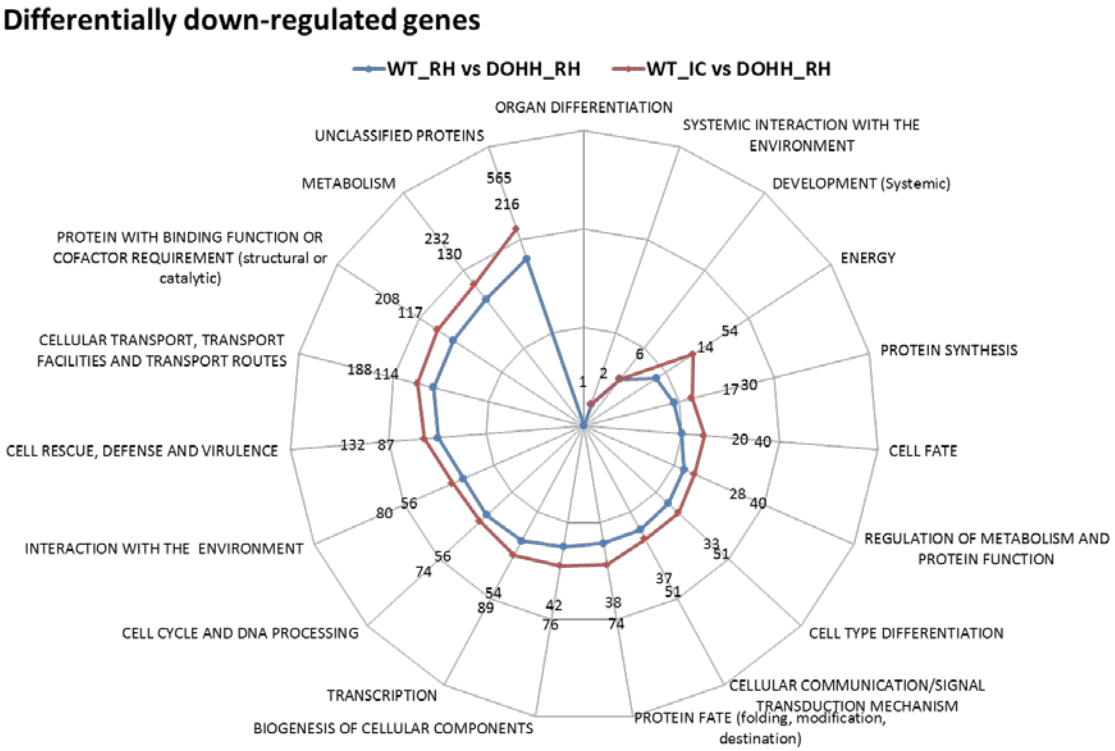

Appendix Figure 2. Radar graph representation for differentially down-regulated genes in transcriptome analyses according to the biological process of fungi. WT_RH vs DOHH_RH in blue line and WT_IC vs DOHH_RH in red line. The axes of the radar correspond to the number of down-regulated genes, resulting in the center is zero and the edge line is 8000 genes.

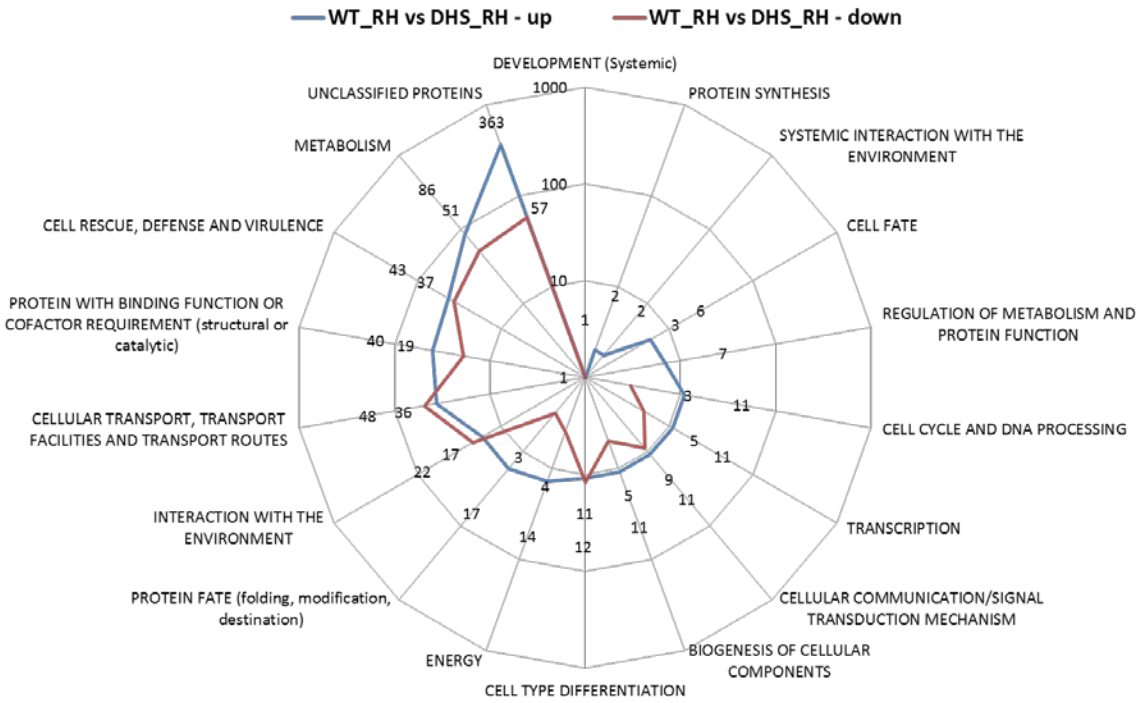

Appendix Figure 3. Radar graph representation for differentially up-regulated and down-regulated genes in transcriptome analyses according to the biological process of fungi. WT_RH vs DHS_RH in blue line and WT_RH vs DHS_RH in red line. The axes of the radar correspond to the number of up-regulated and down-regulated genes, resulting in the center is zero and the edge line is 1000 genes.

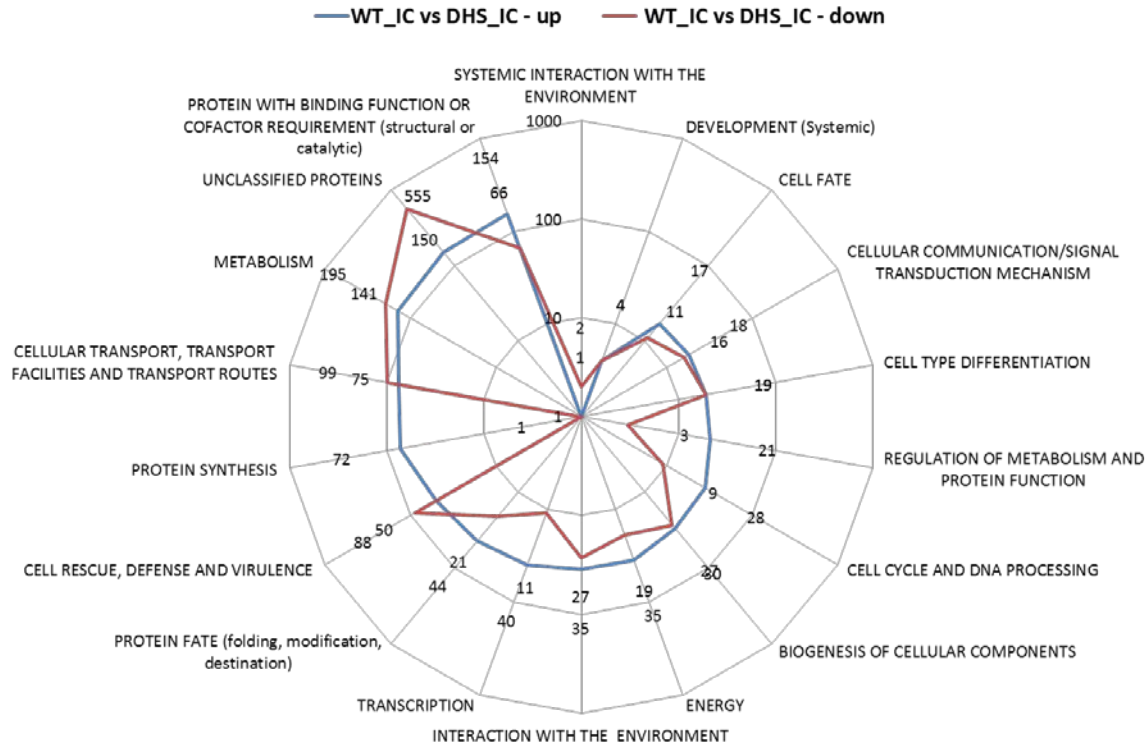

Appendix Figure 4. Radar graph representation for differentially up-regulated and down-regulated genes in transcriptome analyses according to the biological process of fungi. WT_IC vs DHS_IC in blue line and WT_IC vs DHS_IC in red line. The axes of the radar correspond to the number of up-regulated regulated and down-regulated genes, resulting in the center is zero and the edge line is 1000 genes.

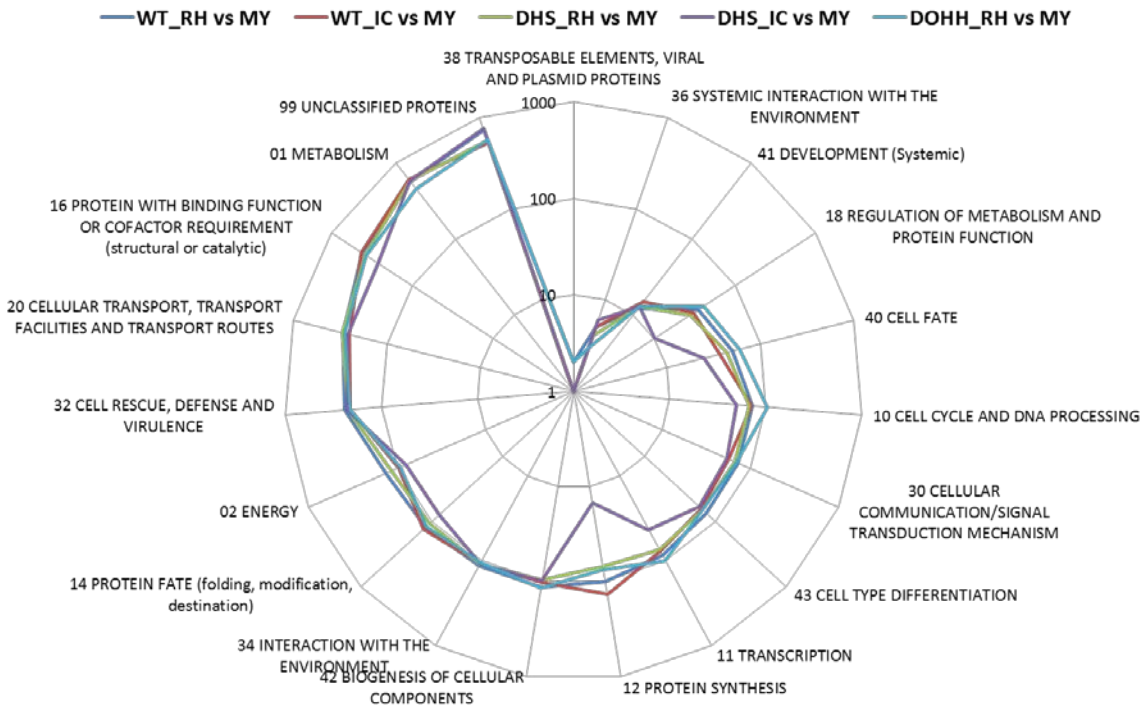

Appendix Figure 5. Radar graph representation for differentially up-regulated genes in transcriptome analyses according to the biological process of fungi. WT_RH, WT_IC, DHS_RH, DHS_IC, DOHH_RH compared to Myc. The axes of the radar correspond to the number of up-regulated genes, resulting in the center is zero and the edge line is 1000 genes.

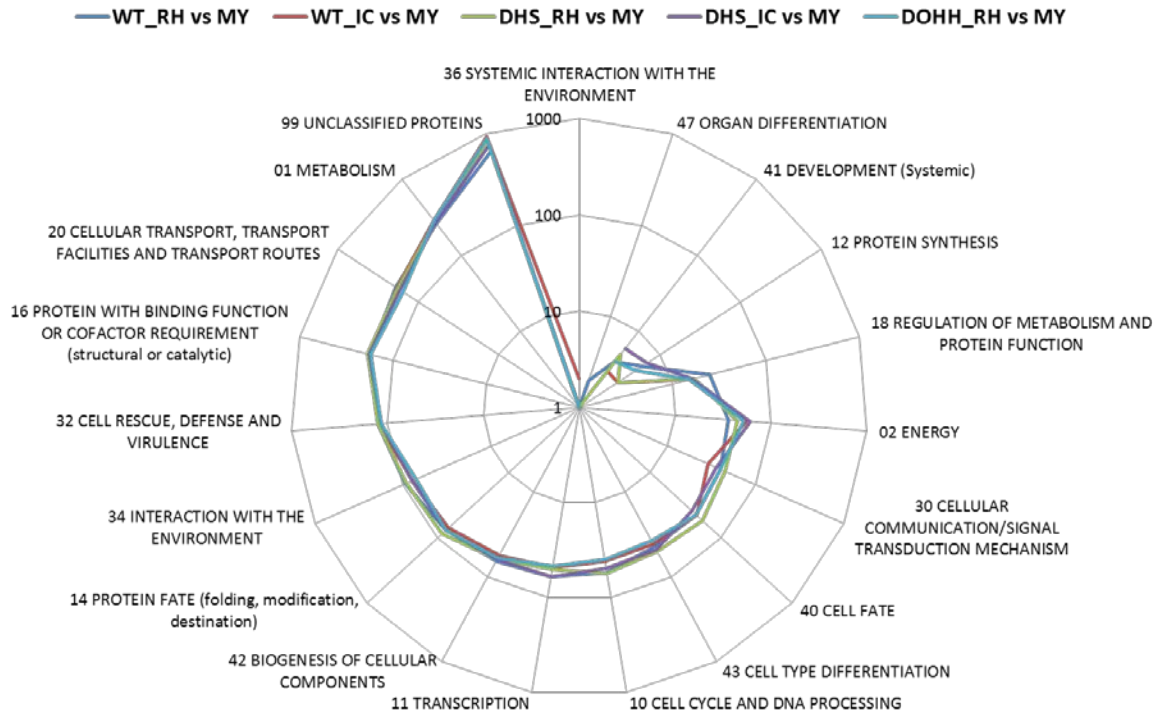

Appendix Figure 6. Radar graph representation for differentially down-regulated genes in transcriptome analyses according to the biological process of fungi. WT_RH, WT_IC, DHS_RH, DHS_IC, DOHH_RH compared to Myc. The axes of the radar correspond to the number of down-regulated genes, resulting in the center is zero and the edge line is 1000 genes

References

1. Aist, J. R. 1976. Papillae and related wound plugs of plant cells. *Ann Rev Phytopathol,* 14.
2. Alexander, N. J., Proctor, R. H. & Mccormick, S. P. 2009. Genes, gene clusters, and biosynthesis of trichothecenes and fumonisins in *Fusarium*. *Toxin Reviews,* 28**,** 198-215.
3. Ali, F. & Yan, J. 2012. Disease resistance in maize and the role of molecular breeding in defending against global threat. *J Integr Plant Biol,* 54**,** 134-51.
4. Altschul, S. F., Madden, T. L., Schaffer, A. A., Zhang, J., Zhang, Z., Miller, W. & Lipman, D. J. 1997. Gapped BLAST and PSI-BLAST: a new generation of protein database search programs. *Nucleic Acids Res,* 25**,** 3389-402.
5. Armentrout, V. N. & Downer, A. J. 1987. Infection cushion development by Rhizoctonia solanion cotton. *Phytopathology,* 77.
6. Balestrini, R., Gomez-Ariza, J., Lanfranco, L. & Bonfante, P. 2007. Laser microdissection reveals that transcripts for five plant and one fungal phosphate transporter genes are contemporaneously present in arbusculated cells. *Mol Plant Microbe Interact,* 20**,** 1055-62.
7. Balestrini, R., Nerva, L., Sillo, F., Girlanda, M. & Perotto, S. 2014. Plant and fungal gene expression in mycorrhizal protocorms of the orchid Serapias vomeracea colonized by Tulasnella calospora. *Plant Signal Behav,* 9**,** e977707.
8. Balint-Kurti, P. J. & Johal, G. S. 2009. Maize Disease Resistance. *In:* Bennetzen, J. L. & Hake, S. C. (eds.) *Handbook of Maize: Its Biology*. New York, NY: Springer New York.
9. Balint-Kurti, P. J., Yang, J., Van Esbroeck, G., Jung, J. & Smith, M. E. 2010. Use of a maize advanced intercross line for mapping of QTL for northern leaf blight resistance and multiple disease resistance. *Crop Science,* 50**,** 458-466.
10. Bauer, S., Gagneur, J. & Robinson, P. N. 2010. GOing Bayesian: model-based gene set analysis of genome-scale data. *Nucleic Acids Research,* 38**,** 3523-3532.
11. Beaudoin, N., Serizet, C., Gosti, F. & Giraudat, J. 2000. Interactions between abscisic acid and ethylene signaling cascades. *Plant Cell,* 12**,** 1103-15.
12. Belda-Palazón, B., Almendáriz, C., Martí, E., Carbonell, J. & Ferrando, A. 2016. Relevance of the axis spermidine/eIF5A for plant growth and development. *Frontiers in Plant Science,* 7**,** 245.

13. Benjamini, Y. & Hochberg, Y. 1995. Controlling the false discovery rate: a practical and powerful approach to multiple testing. *J R Stat Soc Ser B Stat Methodol,* 57.

14. Benne, R. & Hershey, J. W. 1978. The mechanism of action of protein synthesis initiation factors from rabbit reticulocytes. *J Biol Chem,* 253**,** 3078-87.

15. Berruti, A., Borriello, R., Lumini, E., Scariot, V., Bianciotto, V. & Balestrini, R. 2013. Application of laser microdissection to identify the mycorrhizal fungi that establish arbuscules inside root cells. *Frontiers in Plant Science,* 4**,** 135.

16. Bewley, J. D. 1997. Seed germination and dormancy. *The Plant Cell,* 9**,** 1055-1066.

17. Bluhm, B. H., Zhao, X., Flaherty, J. E., Xu, J. R. & Dunkle, L. D. 2007. RAS2 regulates growth and pathogenesis in *Fusarium graminearum*. *MPMI,* 20.

18. Boddu, J., Cho, S., Kruger, W. M. & Muehlbauer, G. J. 2006. Transcriptome analysis of the barley-*Fusarium graminearum* interaction. *Mol Plant Microbe Interact,* 19**,** 407-17.

19. Boedi, S., Berger, H., Sieber, C., Münsterkötter, M., Maloku, I., Warth, B., Sulyok, M., Lemmens, M., Schuhmacher, R., Güldener, U. & Strauss, J. 2016. Comparison of *Fusarium graminearum* transcriptomes on living or dead wheat differentiates substrate-responsive and defense-responsive genes. *Frontiers in Microbiology,* 7.

20. Boenisch, M. J. 2013. *Structural and molecular characterisation of the penetration process of Fusarium graminearum during fusarium head blight infection.* PhD, University of Hamburg.

21. Boenisch, M. J. & Schäfer, W. 2011. *Fusarium graminearum* forms mycotoxin producing infection structures on wheat. *BMC Plant Biology,* 11**,** 1-14.

22. Boller, T. & Felix, G. 2009. A renaissance of elicitors: perception of microbe-associated molecular patterns and danger signals by pattern-recognition receptors. *Annu Rev Plant Biol,* 60**,** 379-406.

23. Bradford, K. J., Chen, F., Cooley, M. B., Dahal, P., Downie, B., Fukunaga, K. K., Gee, O. H., Gurusinghe, S., Mella, R. A., Nonogaki, H., Wu, C. T., Yang, H. & Yim, K. O. 2000. Gene expression prior to radicle emergence in imbibed tomato seeds. Wallingford: *CABI Publishing.*

24. Brown, I., Trethowan, J., Kerry, M., Mansfield, J. & Bolwell, G. P. 1998. Localization of components of the oxidative cross-linking of glycoproteins and of callose synthesis in papillae formed during the interaction between non-pathogenic strains of *Xanthomonas campestris* and French bean mesophyll cells. *The Plant Journal,* 15**,** 333-343.

25. Brown, N. A., Urban, M., Van De Meene, A. M. & Hammond-Kosack, K. E. 2010. The infection biology of *Fusarium graminearum*: defining the pathways of spikelet to spikelet colonisation in wheat ears. *Fungal Biol,* 114**,** 555-71.

26. Buckler, E. S. T., Thornsberry, J. M. & Kresovich, S. 2001. Molecular diversity, structure and domestication of grasses. *Genet Res,* 77**,** 213-8.

27. Bushnell, W. R., Hazen, B. E. & Pritsch, C. 2003a. Histology and physiology of Fusarium head blight. St. Paul: *American Phytopathological Society (APS Press).*

28. Bushnell, W. R., Hazen, B. E. & Pritsch, C. 2003b. Histology and physiology of Fusarium head blight. *In:* Leonard, K. J. & Bushnell, W. R. (eds.) *Fusarium Head Blight of Wheat & Barley.* Minnesota: St. Paul, *USA APS Press.*

29. Byers, T. L., Lakanen, J. R., Coward, J. K. & Pegg, A. E. 1994. The role of hypusine depletion in cytostasis induced by S-adenosyl-L-methionine decarboxylase inhibition: new evidence provided by 1-methylspermidine and 1,12-dimethylspermine. *Biochem J,* 303 (Pt 2)**,** 363-8.

30. Chamot, D. & Kuhlemeier, C. 1992. Differential expression of genes encoding the hypusine-containing translation initiation factor, eIF-5A, in tobacco. *Nucleic Acids Res,* 20**,** 665-9.

31. Chattopadhyay, M. K., Park, M. H. & Tabor, H. 2008. Hypusine modification for growth is the major function of spermidine in *Saccharomyces cerevisiae* polyamine auxotrophs grown in limiting spermidine. *Proc Natl Acad Sci U S A,* 105**,** 6554-9.

32. Chattopadhyay, M. K., Tabor, C. W. & Tabor, H. 2003. Spermidine but not spermine is essential for hypusine biosynthesis and growth in *Saccharomyces cerevisiae*: spermine is converted to spermidine in vivo by the FMS1-amine oxidase. *Proc Natl Acad Sci U S A,* 100**,** 13869-74.

33. Chen, K. Y. & Liu, A. Y. 1997. Biochemistry and function of hypusine formation on eukaryotic initiation factor 5A. *Biol Signals,* 6**,** 105-9.

34. Chen, X.-Y. & Kim, J.-Y. 2009. Callose synthesis in higher plants. *Plant Signaling and Behavior*, 4, 489-492.

35. Chern, M., Fitzgerald, H. A., Canlas, P. E., Navarre, D. A. & Ronald, P. C. 2005. Overexpression of a rice NPR1 homolog leads to constitutive activation of defense response and hypersensitivity to light. *Mol Plant Microbe Interact,* 18**,** 511-20.

36. Chern, M. S., Fitzgerald, H. A., Yadav, R. C., Canlas, P. E., Dong, X. & Ronald, P. C. 2001. Evidence for a disease-resistance pathway in rice similar to the NPR1-mediated signaling pathway in *Arabidopsis*. *Plant J,* 27**,** 101-13.

37. Chou, W. C., Huang, Y. W., Tsay, W. S., Chiang, T. Y., Huang, D. D. & Huang, H. J. 2004. Expression of genes encoding the rice translation initiation factor, eIF5A, is involved in developmental and environmental responses. *Physiol Plant,* 121.

38. Cid, V. J., Duran, A., Del Rey, F., Snyder, M. P., Nombela, C. & Sanchez, M. 1995. Molecular basis of cell integrity and morphogenesis in *Saccharomyces cerevisiae*. *Microbiol Rev,* 59**,** 345-86.

39. Clement, P. M., Henderson, C. A., Jenkins, Z. A., Smit-Mcbride, Z., Wolff, E. C., Hershey, J. W., Park, M. H. & Johansson, H. E. 2003. Identification and characterization of eukaryotic initiation factor 5A-2. *Eur J Biochem,* 270**,** 4254-63.

40. Constantino, N., Mastouri, F., Damarwinasis, R., Borrego, E., Moran-Diez, M. E., Kenerley, C. M., Gao, X. & Kolomiets, M. V. 2013. Root-expressed maize lipoxygenase 3 negatively regulates induced systemic resistance to *Colletotrichum graminicola* in shoots. *Frontiers in Plant Science,* 4.

41. Cubero, O. F., Crespo, A., Fatehi, J. & Bridge, P. D. 1999. DNA extraction and PCR amplification method suitable for fresh, herbarium-stored, lichenized, and other fungi. *Plant Systematics and Evolution,* 216**,** 243-249.

42. Cui, L., Fan, Q., Hu, Y., Karamycheva, S. A., Quackenbush, J., Khuntirat, B., Sattabongkot, J. & Carlton, J. M. 2005. Gene discovery in *Plasmodium vivax* through sequencing of ESTs from mixed blood stages. *Mol Biochem Parasitol,* 144.

43. Cui, X., Ge, C., Wang, R., Wang, H., Chen, W., Fu, Z., Jiang, X., Li, J. & Wang, Y. 2010. The BUD2 mutation affects plant architecture through altering cytokinin and auxin responses in *Arabidopsis*. *Cell Res,* 20**,** 576-86.

44. Cuomo, C. A., Gueldener, U., Xu, J. R., Trail, F., Turgeon, B. G., Di Pietro, A., Walton, J. D., Ma, L. J., Baker, S. E., Rep, M., Adam, G., Antoniw, J., Baldwin, T., Calvo, S., Chang, Y. L., Decaprio, D., Gale, L. R., Gnerre, S., Goswami, R. S., Hammond-Kosack, K., Harris, L. J., Hilburn, K., Kennell, J. C., Kroken, S., Magnuson, J. K., Mannhaupt, G., Mauceli, E., Mewes, H. W., Mitterbauer, R. & Muehlbauer, G. 2007a. The *Fusarium graminearum* genome reveals a link between localized polymorphism and pathogen specialization. *Science,* 317.

45. Damiani, I., Baldacci-Cresp, F., Hopkins, J., Andrio, E., Balzergue, S., Lecomte, P., Puppo, A., Abad, P., Favery, B. & Herouart, D. 2012. Plant genes involved in harbouring symbiotic rhizobia or pathogenic nematodes. *New Phytol,* 194**,** 511-22.

46. Day, C. D., Lee, E., Kobayashi, J., Holappa, L. D., Albert, H. & Ow, D. W. 2000. Transgene integration into the same chromosome location can produce alleles that express at a predictable level, or alleles that are differentially silenced. *Genes Dev*, 14, 2869-80.

47. De Bekker, C., Bruning, O., Jonker, M. J., Breit, T. M. & Wösten, H. A. 2011. Single cell transcriptomics of neighboring hyphae of *Aspergillus niger*. *Genome Biology,* 12**,** 1-12.

48. Dean, R. A., Talbot, N. J., Ebbole, D. J., Farman, M. L., Mitchell, T. K., Orbach, M. J., Thon, M., Kulkarni, R., Xu, J. R., Pan, H., Read, N. D., Lee, Y. H., Carbone, I., Brown, D., Oh, Y. Y., Donofrio, N., Jeong, J. S., Soanes, D. M., Djonovic, S., Kolomiets, E., Rehmeyer, C., Li, W., Harding, M., Kim, S., Lebrun, M. H., Bohnert, H., Coughlan, S., Butler, J., Calvo, S., Ma, L. J., Nicol, R., Purcell, S., Nusbaum, C., Galagan, J. E. & Birren, B. W. 2005. The genome sequence of the rice blast fungus *Magnaporthe grisea*. *Nature,* 434**,** 980-6.

49. Demirci, E. & Döken, M. T. 1998. Host penetration and infection by the anastomosis groups of *Rhizoctonia solani* Kühn isolated from potatoes. *Turk J Agric For,* 22.

50. Dias, C. A., Cano, V. S., Rangel, S. M., Apponi, L. H., Frigieri, M. C., Muniz, J. R., Garcia, W., Park, M. H., Garratt, R. C. & Zanelli, C. F. 2008. Structural modeling and mutational analysis of yeast eukaryotic translation initiation factor 5A reveal new critical residues and reinforce its involvement in protein synthesis. *FEBS J,* 275.

51. Djonovic, S., Vargas, W. A., Kolomiets, M. V., Horndeski, M., Wiest, A. & Kenerley, C. M. 2007. A proteinaceous elicitor Sm1 from the beneficial fungus *Trichoderma virens* is required for induced systemic resistance in maize. *Plant Physiol,* 145**,** 875-89.

52. Doerfel, L. K., Wohlgemuth, I., Kothe, C., Peske, F., Urlaub, H. & Rodnina, M. V. 2013. EF-P is essential for rapid synthesis of proteins containing consecutive proline residues. *Science,* 339**,** 85-8.

53. Dong, X. 2004. NPR1, all things considered. *Curr Opin Plant Biol,* 7**,** 547-52.

54. Dresselhaus, T., Cordts, S. & Lorz, H. 1999. A transcript encoding translation initiation factor eIF-5A is stored in unfertilized egg cells of maize. *Plant Mol Biol,* 39**,** 1063-71.

55. Duguay, J., Jamal, S., Liu, Z., Wang, T. W. & Thompson, J. E. 2007. Leaf-specific suppression of deoxyhypusine synthase in *Arabidopsis* thaliana enhances growth without negative pleiotropic effects. *J Plant Physiol,* 164**,** 408-20.

56. Egan, M. J., Wang, Z. Y., Jones, M. A., Smirnoff, N. & Talbot, N. J. 2007. Generation of reactive oxygen species by fungal NADPH oxidases is required for rice blast disease. *Proc Natl Acad Sci U S A,* 104**,** 11772-7.

57. Emmert-Buck, M. R., Bonner, R. F., Smith, P. D., Chuaqui, R. F., Zhuang, Z., Goldstein, S. R., Weiss, R. A. & Liotta, L. A. 1996. Laser capture microdissection. *Science,* 274**,** 998-1001.

58. Emmett, R. W. & Parbery, D. G. 1975. Appressoria. *Annu Rev Phytopathol,* 13.

59. Erayman, M., Turktas, M., Akdogan, G., Gurkok, T., Inal, B., Ishakoglu, E., Ilhan, E. & Unver, T. 2015. Transcriptome analysis of wheat inoculated with *Fusarium graminearum*. *Front Plant Sci,* 6**,** 867.

60. Espina, V., Wulfkuhle, J. D., Calvert, V. S., Vanmeter, A., Zhou, W., Coukos, G., Geho, D. H., Petricoin, E. F., 3rd & Liotta, L. A. 2006. Laser-capture microdissection. *Nat Protoc,* 1**,** 586-603.

61. Farag, M. A., Fokar, M., Abd, H., Zhang, H., Allen, R. D. & Pare, P. W. 2005. (Z)-3-Hexenol induces defense genes and downstream metabolites in maize. *Planta,* 220**,** 900-9.

62. Farr, D. F., Bills, G.F., Chamuris, G.P. And Rossman, A.Y. 1989. *Fungi on Plants and Plant Products in the United States*, MN: APS Press.

63. Feng, H., Chen, Q., Feng, J., Zhang, J., Yang, X. & Zuo, J. 2007. Functional characterization of the *Arabidopsis* eukaryotic translation initiation factor 5A-2 that plays a crucial role in plant growth and development by regulating cell division, cell growth, and cell death. *Plant Physiol,* 144**,** 1531-45.

64. Feussner, I. & Wasternack, C. 2002. The lipoxygenase pathway. *Annu Rev Plant Biol,* 53**,** 275-97.

65. Fisher, R. A. 1922. On the Interpretation of $\chi 2$ from Contingency Tables, and the Calculation of P. *Journal of the Royal Statistical Society,* 85**,** 87-94.

66. Foroud, N. A., Ouellet, T., Laroche, A., Oosterveen, B., Jordan, M. C., Ellis, B. E. & Eudes, F. 2012. Differential transcriptome analyses of three wheat genotypes reveal different host response pathways associated with fusarium head blight and trichothecene resistance. *Plant Pathol,* 61.

67. Fosu-Nyarko, J., Jones, M. G. & Wang, Z. 2010. Application of laser microdissection to study plant-fungal pathogen interactions. *Methods Mol Biol,* 638**,** 153-63.

68. Frigieri, M. C., Joao Luiz, M. V., Apponi, L. H., Zanelli, C. F. & Valentini, S. R. 2008. Synthetic lethality between eIF5A and Ypt1 reveals a connection between translation and the secretory pathway in yeast. *Mol Genet Genomics,* 280**,** 211-21.

69. Frigieri, M. C., Thompson, G. M., Pandolfi, J. R., Zanelli, C. F. & Valentini, S. R. 2007. Use of a synthetic lethal screen to identify genes related to TIF51A in *Saccharomyces cerevisiae*. *Genet Mol Res,* 6**,** 152-65.

70. Gao, X., Shim, W. B., Gobel, C., Kunze, S., Feussner, I., Meeley, R., Balint-Kurti, P. & Kolomiets, M. 2007. Disruption of a maize 9-lipoxygenase results in increased resistance to fungal pathogens and reduced levels of contamination with mycotoxin fumonisin. *Mol Plant Microbe Interact,* 20**,** 922-33.

71. Gardiner, D. M., Kazan, K. & Manners, J. M. 2009. Novel genes of *Fusarium graminearum* that negatively regulate deoxynivalenol production and virulence. *Mol Plant Microbe Interact,* 22**,** 1588-600.

72. Gatsukovich, Y. 2004. *Characterization of eukaryotic translation initiation factor 5A-2 (eIF5A-2) in Arabidopsis thaliana: Effects of wounding and pathogen attack*. Master thesis University of Waterloo.

73. Gaude, N., Bortfeld, S., Duensing, N., Lohse, M. & Krajinski, F. 2012. Arbuscule-containing and non-colonized cortical cells of mycorrhizal roots undergo extensive and specific reprogramming during arbuscular mycorrhizal development. *Plant J,* 69**,** 510-28.

74. Glick, B. R. & Ganoza, M. C. 1975. Identification of a soluble protein that stimulates peptide bond synthesis. *Proc Natl Acad Sci U S A,* 72**,** 4257-60.

75. Gorlach, J., Volrath, S., Knauf-Beiter, G., Hengy, G., Beckhove, U., Kogel, K. H., Oostendorp, M., Staub, T., Ward, E., Kessmann, H. & Ryals, J. 1996. Benzothiadiazole, a novel class of inducers of systemic acquired resistance, activates gene expression and disease resistance in wheat. *Plant Cell,* 8**,** 629-43.

76. Goswami, R. S. & Kistler, H. C. 2004. Heading for disaster: *Fusarium graminearum* on cereal crops. *Mol Plant Pathol,* 5**,** 515-25.

77. Gow, N. A. & Hube, B. 2012. Importance of the *Candida albicans* cell wall during commensalism and infection. *Curr Opin Microbiol,* 15**,** 406-12.

78. Grant, M. & Lamb, C. 2006. Systemic immunity. *Curr Opin Plant Biol,* 9**,** 414-20.

79. Guan, X. Y., Fung, J. M., Ma, N. F., Lau, S. H., Tai, L. S., Xie, D., Zhang, Y., Hu, L., Wu, Q. L., Fang, Y. & Sham, J. S. 2004. Oncogenic role of eIF-5A2 in the development of ovarian cancer. *Cancer Res,* 64**,** 4197-200.

80. Guan, X. Y., Sham, J. S., Tang, T. C., Fang, Y., Huo, K. K. & Yang, J. M. 2001. Isolation of a novel candidate oncogene within a frequently amplified region at 3q26 in ovarian cancer. *Cancer Res,* 61**,** 3806-9.

81. Guenther, J. C., Hallen-Adams, H. E., Bücking, H., Shachar-Hill, Y. & Trail, F. 2009. Triacylglyceride metabolism by *Fusarium graminearum* during colonization and sexual development on wheat. *Molecular Plant-Microbe Interactions,* 22**,** 1492-1503.

82. Güldener, U., Seong, K.-Y., Boddu, J., Cho, S., Trail, F., Xu, J.-R., Adam, G., Mewes, H.-W., Muehlbauer, G. J. & Kistler, H. C. 2006. Development of a *Fusarium graminearum* Affymetrix GeneChip for profiling fungal gene expression *in vitro* and *in planta*. *Fungal Genetics and Biology,* 43**,** 316-325.

83. Gutierrez, E., Shin, B. S., Woolstenhulme, C. J., Kim, J. R., Saini, P., Buskirk, A. R. & Dever, T. E. 2013. eIF5A promotes translation of polyproline motifs. *Mol Cell,* 51**,** 35-45.

84. Hacquard, S., Tisserant, E., Brun, A., Legue, V., Martin, F. & Kohler, A. 2013. Laser microdissection and microarray analysis of *Tuber melanosporum ectomycorrhizas* reveal functional heterogeneity between mantle and Hartig net compartments. *Environ Microbiol,* 15**,** 1853-69.

85. Hahlbrock K, S. D. 1989. Physiology and molecular biology of phenylpropanoid metabolism. *Annu Rev Plant Physiol Plant Mol Biol,* 40**,** 347–369.

86. Hanawa-Suetsugu, K., Sekine, S., Sakai, H., Hori-Takemoto, C., Terada, T., Unzai, S., Tame, J. R., Kuramitsu, S., Shirouzu, M. & Yokoyama, S. 2004. Crystal structure of elongation factor P from *Thermus thermophilus* HB8. *Proc Natl Acad Sci U S A,* 101**,** 9595-600.

87. Hanazawa, M., Kawasaki, I., Kunitomo, H., Gengyo-Ando, K., Bennett, K. L., Mitani, S. & Iino, Y. 2004. The *Caenorhabditis elegans* eukaryotic initiation factor 5A homologue, IFF-1, is required for germ cell proliferation, gametogenesis and localization of the P-granule component PGL-1. *Mech Dev,* 121**,** 213-24.

88. Harris, L. J., Balcerzak, M., Johnston, A., Schneiderman, D. & Ouellet, T. 2016. Host-preferential *Fusarium graminearum* gene expression during infection of wheat, barley, and maize. *Fungal Biology,* 120**,** 111-123.

89. Harris, P. V., Welner, D., Mcfarland, K. C., Re, E., Navarro Poulsen, J. C., Brown, K., Salbo, R., Ding, H., Vlasenko, E., Merino, S., Xu, F., Cherry, J., Larsen, S. & Lo Leggio, L. 2010. Stimulation of lignocellulosic biomass hydrolysis by proteins of glycoside hydrolase family 61: structure and function of a large, enigmatic family. *Biochemistry,* 49**,** 3305-16.

90. Hayes Pm, J. B. Malting Quality from a QTL Perspective. *In:* S, L., ed. the Eighth International Barley Genet., 2000 Adelaide, South Australia. 99–105.

91. Hobbs, S. L., Kpodar, P. & Delong, C. M. 1990. The effect of T-DNA copy number, position and methylation on reporter gene expression in tobacco transformants. *Plant Mol Biol*, 15, 851-64.

92. Holdsworth, M. J., Bentsink, L. & Soppe, W. J. 2008. Molecular networks regulating *Arabidopsis* seed maturation, after-ripening, dormancy and germination. *New Phytol,* 179**,** 33-54.

93. Hopkins, M. T., Lampi, Y., Wang, T.-W., Liu, Z. & Thompson, J. E. 2008. Eukaryotic Translation initiation factor 5A is involved in pathogen-induced cell death and development of disease symptoms in *Arabidopsis*. *Plant Physiology,* 148**,** 479-489.

94. Horwitz, B. A., Sharon, A., Lu, S. W., Ritter, V., Sandrock, T. M., Yoder, O. C. & Turgeon, B. G. 1999. A G protein alpha subunit from *Cochliobolus heterostrophus* involved in mating and appressorium formation. Fungal Genet Biol, 26, 19-32.

95. Huang, H. C., Kokko, E. G. & Erickson, R. S. 1999. Infection of alfalfa pollen by *Botrytis cinerea*. *Bot Bull Acad Sin,* 40.

96. Huang, L., Buchenauer, H., Han, Q., Zhang, X. & Kang, Z. 2008. Ultrastructural and cytochemical studies on the infection process of *Sclerotinia sclerotiorum* in oilseed rape. *J Plant Dis Protect,* 115.

97. Ilgen, P., Hadeler, B., Maier, F. J. & Schafer, W. 2009. Developing kernel and rachis node induce the trichothecene pathway of *Fusarium graminearum* during wheat head infection. *Mol Plant Microbe Interact,* 22**,** 899-908.

98. Jansen, C., Von Wettstein, D., Schafer, W., Kogel, K. H., Felk, A. & Maier, F. J. 2005. Infection patterns in barley and wheat spikes inoculated with wild-type and trichodiene synthase gene disrupted *Fusarium graminearum*. *Proc Natl Acad Sci U S A,* 102**,** 16892-7.

99. Jenczmionka, N. J. & Schafer, W. 2005. The Gpmk1 MAP kinase of *Fusarium graminearum* regulates the induction of specific secreted enzymes. *Curr Genet,* 47**,** 29-36.

100. Jenkins, Z. A., Haag, P. G. & Johansson, H. E. 2001. Human eIF5A2 on chromosome 3q25-q27 is a phylogenetically conserved vertebrate variant of eukaryotic translation initiation factor 5A with tissue-specific expression. *Genomics,* 71**,** 101-9.

101. Jiménez-López, S., Mancera-Martínez, E., Donayre-Torres, A., Rangel, C., Uribe, L., March, S., Jiménez-Sánchez, G. & Sánchez De Jiménez, E. 2011. Expression profile of maize (*Zea mays* L.) embryonic axes during germination: translational regulation of ribosomal protein mRNAs. *Plant and Cell Physiology,* 52**,** 1719-1733.

102. Joe, Y. A., Wolff, E. C. & Park, M. H. 1995. Cloning and expression of human deoxyhypusine synthase cDNA. Structure-function studies with the recombinant enzyme and mutant proteins. *J Biol Chem,* 270**,** 22386-92.

103. Jones, J. D. G. & Dangl, J. L. 2006. The plant immune system. *Nature,* 444.

104. Jorgensen, R. A., Cluster, P. D., English, J., Que, Q. & Napoli, C. A. 1996. Chalcone synthase cosuppression phenotypes in petunia flowers: comparison of sense vs. antisense constructs and single-copy vs. complex T-DNA sequences. *Plant Mol Biol*, 31, 957-73.

105. Kang, H. A. & Hershey, J. W. 1994. Effect of initiation factor eIF-5A depletion on protein synthesis and proliferation of *Saccharomyces cerevisiae*. *J Biol Chem,* 269**,** 3934-40.

106. Kang, H. A., Schwelberger, H. G. & Hershey, J. W. 1993. Translation initiation factor eIF-5A, the hypusine-containing protein, is phosphorylated on serine in *Saccharomyces cerevisiae*. *J Biol Chem,* 268**,** 14750-6.

107. Kang, K. R., Wolff, E. C., Park, M. H., Folk, J. E. & Chung, S. I. 1995. Identification of YHR068w in *Saccharomyces cerevisiae* chromosome VIII as a gene for deoxyhypusine synthase. Expression and characterization of the enzyme. *J Biol Chem,* 270**,** 18408-12.

108. Kang, Z. & Buchenauer, H. 2000a. Ultrastructural and cytochemical studies on cellulose, xylan and pectin degradation in wheat spikes infected by *Fusarium culmorum*. *Journal of Phytopathology,* 148**,** 263-275.

109. Kang, Z. & Buchenauer, H. 2000b. Ultrastructural and immunocytochemical investigation of pathogen development and host responses in resistant and susceptible wheat spikes infected by *Fusarium culmorum*. *Physiological and Molecular Plant Pathology,* 57**,** 255-268.

110. Kang, Z. S. & Buchenauer, H. 2000c. Cytology and ultrastructure of the infection of wheat spikes by *Fusarium culmorum*. *Mycol Res,* 104.

111. Kang, Z. S., Zingen-Sell, I. & Buchenauer, H. 2005. Infection of wheat spikes by *Fusarium avenaceum* and alterations of cell wall components in the infected tissue. *Eur J Plant Pathol,* 111.

112. Kato, M., Hayakawa, Y., Hyodo, H., Ikoma, Y. & Yano, M. 2000. Wound-induced ethylene synthesis and expression and formation of 1-aminocyclopropane-1-carboxylate (ACC) synthase, ACC oxidase, phenylalanine ammonia-lyase, and peroxidase in wounded mesocarp tissue of Cucurbita maxima. *Plant Cell Physiol,* 41**,** 440-7.

113. Kikot, G. E., Hours, R. A. & Alconada, T. M. 2009. Contribution of cell wall degrading enzymes to pathogenesis of *Fusarium graminearum*: a review. *J Basic Microbiol,* 49**,** 231-41.

114. Kim, D., Pertea, G., Trapnell, C., Pimentel, H., Kelley, R. & Salzberg, S. L. 2013. TopHat2: accurate alignment of transcriptomes in the presence of insertions, deletions and gene fusions. *Genome Biol,* 14**,** R36.

115. Kim, J.-E., Han, K.-H., Jin, J., Kim, H., Kim, J.-C., Yun, S.-H. & Lee, Y.-W. 2005. Putative polyketide synthase and laccase genes for biosynthesis of aurofusarin in *Gibberella zeae*. *Applied and Environmental Microbiology,* 71**,** 1701-1708.

116. Klier, H., Wohl, T., Eckerskorn, C., Magdolen, V. & Lottspeich, F. 1993. Determination and mutational analysis of the phosphorylation site in the hypusine-containing protein Hyp2p. *FEBS Lett,* 334**,** 360-4.

117. Klug, K., Hogekamp, C., Specht, A., Myint, S. S., Bloink, D., Kuster, H. & Horst, W. J. 2015. Spatial gene expression analysis in tomato hypocotyls suggests cysteine as key precursor of vascular sulfur accumulation implicated in *Verticillium dahliae* defense. *Physiol Plant,* 153**,** 253-68.

118. Kogel, K. H. & Hückelhoven, R. 1999. Superoxide generation in chemically activated resistance of barley in response to inoculation with the Powdery Mildew Fungus. *J Plant Pathol,* 147**,** 1-4.

119. Kogel, K. H. & Langen, G. 2005. Induced disease resistance and gene expression in cereals. *Cell Microbiol,* 7**,** 1555-64.

120. Koike, N., Hyakumachi, M., Kageyama, K., Tsuyumu, S. & Doke, N. 2001. Induction of systemic resistance in cucumber against several diseases by plant growth-promoting Fungi: lignification and superoxide generation. *European Journal of Plant Pathology,* 107**,** 523-533.

121. Ku, M. S., Agarie, S., Nomura, M., Fukayama, H., Tsuchida, H., Ono, K., Hirose, S., Toki, S., Miyao, M. & Matsuoka, M. 1999. High-level expression of maize phosphoenolpyruvate carboxylase in transgenic rice plants. *Nat Biotechnol*, 17, 76-80.

122. Lamb, C. & Dixon, R. A. 1997. The oxidative burst in plant disease resistance. *Annu Rev Plant Physiol Plant Mol Biol,* 48**,** 251-275.

123. Lara-Ortiz, T., Riveros-Rosas, H. & Aguirre, J. 2003. Reactive oxygen species generated by microbial NADPH oxidase NoxA regulate sexual development in *Aspergillus nidulans*. *Mol Microbiol,* 50**,** 1241-55.

124. Leach, J., Lang, B. R. & Yoder, O. C. 1982. Methods for selection of mutants and *in vitr*o culture of *Cochliobolus hetrostrophus*. *J. Gen. Microbial,* 128**,** 1719-1729.

125. Lebska, M., Ciesielski, A., Szymona, L., Godecka, L., Lewandowska-Gnatowska, E., Szczegielniak, J. & Muszynska, G. 2010. Phosphorylation of maize eukaryotic translation initiation factor 5A (eIF5A) by casein kinase 2: identification of phosphorylated residue and influence on intracellular localization of eIF5A. *J Biol Chem,* 285**,** 6217-26.

126. Lenzi, L., Caruso, C., Bianchedi, P. L., Pertot, I. & Perazzolli, M. 2016. Laser microdissection of grapevine leaves reveals site-specific regulation of transcriptional response to *Plasmopara viticola*. *Plant Cell Physiol,* 57**,** 69-81.

127. Li, C. H., Ohn, T., Ivanov, P., Tisdale, S. & Anderson, P. 2010. eIF5A promotes translation elongation, polysome disassembly and stress granule assembly. *PLoS ONE,* 5**,** e9942.

128. Li, T., Belda-Palazon, B., Ferrando, A. & Alepuz, P. 2014. Fertility and polarized cell growth depends on eIF5A for translation of polyproline-rich formins in *Saccharomyces cerevisiae*. *Genetics,* 197**,** 1191-200.

129. Linkies, A., Muller, K., Morris, K., Tureckova, V., Wenk, M., Cadman, C. S., Corbineau, F., Strnad, M., Lynn, J. R., Finch-Savage, W. E. & Leubner-Metzger, G. 2009. Ethylene interacts with abscisic acid to regulate endosperm rupture during germination: a comparative approach using *Lepidium sativum* and *Arabidopsis thaliana*. *Plant Cell,* 21**,** 3803-22.

130. Liu, Z., Duguay, J., Ma, F., Wang, T. W., Tshin, R., Hopkins, M. T., Mcnamara, L. & Thompson, J. E. 2008. Modulation of eIF5A1 expression alters xylem abundance in *Arabidopsis thaliana*. *J Exp Bot,* 59**,** 939-50.

131. Lysøe, E., Seong, K.-Y. & Kistler, H. C. 2011. The Transcriptome of *Fusarium graminearum* During the Infection of Wheat. *Molecular Plant-Microbe Interactions,* 24**,** 995-1000.

132. Ma, F., Liu, Z., Wang, T. W., Hopkins, M. T., Peterson, C. A. & Thompson, J. E. 2010a. *Arabidopsis* eIF5A3 influences growth and the response to osmotic and nutrient stress. *Plant Cell Environ,* 33**,** 1682-96.

133. Ma, L.-J., Van Der Does, H. C., Borkovich, K. A., Coleman, J. J., Daboussi, M.-J., Di Pietro, A., Dufresne, M., Freitag, M., Grabherr, M., Henrissat, B., Houterman, P. M., Kang, S., Shim, W.-B., Woloshuk, C., Xie, X., Xu, J.-R., Antoniw, J., Baker, S. E., Bluhm, B. H., Breakspear, A., Brown, D. W., Butchko, R. a. E., Chapman, S., Coulson, R., Coutinho, P. M., Danchin, E. G. J., Diener, A., Gale, L. R., Gardiner, D. M., Goff, S., Hammond-Kosack, K. E., Hilburn, K., Hua-Van, A., Jonkers, W., Kazan, K., Kodira, C. D., Koehrsen, M., Kumar, L., Lee, Y.-H., Li, L., Manners, J. M., Miranda-Saavedra, D., Mukherjee, M., Park, G., Park, J., Park, S.-Y., Proctor, R. H., Regev, A., Ruiz-Roldan, M. C., Sain, D., Sakthikumar, S., Sykes, S., Schwartz, D. C., Turgeon, B. G., Wapinski, I., Yoder, O., Young, S., Zeng, Q., Zhou, S., Galagan, J., Cuomo, C. A., Kistler, H. C. & Rep, M. 2010b. Comparative genomics reveals mobile pathogenicity chromosomes in *Fusarium. Nature,* 464**,** 367-373.

134. Ma, Y., Miura, E., Ham, B. K., Cheng, H. W., Lee, Y. J. & Lucas, W. J. 2010c. Pumpkin eIF5A isoforms interact with components of the translational machinery in the cucurbit sieve tube system. *Plant J,* 64**,** 536-50.

135. Magdolen, V., Klier, H., Wohl, T., Klink, F., Hirt, H., Hauber, J. & Lottspeich, F. 1994. The function of the hypusine-containing proteins of yeast and other eukaryotes is well conserved. *Mol Gen Genet,* 244**,** 646-52.

136. Maher, C. A., Kumar-Sinha, C., Cao, X., Kalyana-Sundaram, S., Han, B., Jing, X., Sam, L., Barrette, T., Palanisamy, N. & Chinnaiyan, A. M. 2009. Transcriptome sequencing to detect gene fusions in cancer. *Nature,* 458**,** 97-101.

137. Maier, F. J., Miedaner, T., Hadeler, B., Felk, A., Salomon, S., Lemmens, M., Kassner, H. & Schäfer, W. 2006. Involvement of trichothecenes in fusarioses of wheat, barley and maize evaluated by gene disruption of the trichodiene synthase (Tri5) gene in three field isolates of different chemotype and virulence. *Mol Plant Path,* 7.

138. Malz, S., Grell, M. N., Thrane, C., Maier, F. J., Rosager, P., Felk, A., Albertsen, K. S., Salomon, S., Bohn, L., Schafer, W. & Giese, H. 2005. Identification of a gene cluster responsible for the biosynthesis of aurofusarin in the *Fusarium graminearum* species complex. *Fungal Genet Biol,* 42**,** 420-33.

139. Mandal, A., Mandal, S. & Park, M. H. 2014. Genome-wide analyses and functional classification of proline repeat-rich proteins: potential role of eIF5A in eukaryotic evolution. *PLoS One,* 9**,** e111800.

140. Martinez-Rocha, A. L., Woriedh, M., Chemnitz, J., Willingmann, P., Kröger, C., Hadeler, B., Hauber, J. & Schäfer, W. 2016. Posttranslational hypusination of the eukaryotic translation initiation factor-5A regulates *Fusarium graminearum* virulence. *Scientific Reports,* 6**,** 24698.

141. Matsui, K. 2006. Green leaf volatiles: hydroperoxide lyase pathway of oxylipin metabolism. *Curr Opin Plant Biol,* 9**,** 274-80.

142. Mendgen, K., Hahn, M. & Deising, H. 1996. Morphogenesis and mechanisms of penetration by plant pathogenic fungi. *Annu Rev Phytopathol,* 34.

143. Miedaner, T., Reinbrecht, C. & Schilling, A. G. 2000. Association among aggressiveness, fungal colonization, and mycotoxin production of 26 isolates of *Fusarium graminearum* in winter rye head blight. *J Plant Dis Protect,* 107.

144. Moll, S., Anke, S., Kahmann, U., Hansch, R., Hartmann, T. & Ober, D. 2002. Cell-specific expression of homospermidine synthase, the entry enzyme of the pyrrolizidine alkaloid pathway in *Senecio vernalis*, in comparison with its ancestor, deoxyhypusine synthase. *Plant Physiol,* 130**,** 47-57.

145. Morris, S. W., Vernooij, B., Titatarn, S., Starrett, M., Thomas, S., Wiltse, C. C., Frederiksen, R. A., Bhandhufalck, A., Hulbert, S. & Uknes, S. 1998. Induced resistance responses in maize. *Mol Plant Microbe Interact,* 11**,** 643-58.

146. Mueller, O., Kahmann, R., Aguilar, G., Trejo-Aguilar, B., Wu, A. & De Vries, R. P. 2008. The secretome of the maize pathogen *Ustilago maydis*. *Fungal Genet Biol,* 45 Suppl 1**,** S63-70.

147. Nagendran, S., Hallen-Adams, H. E., Paper, J. M., Aslam, N. & Walton, J. D. 2009. Reduced genomic potential for secreted plant cell-wall-degrading enzymes in the ectomycorrhizal fungus Amanita bisporigera, based on the secretome of *Trichoderma reesei*. *Fungal Genet Biol,* 46**,** 427-35.

148. Nakamura, S. & Hatanaka, A. 2002. Green-leaf-derived C6-aroma compounds with potent antibacterial action that act on both Gram-negative and Gram-positive bacteria. *J Agric Food Chem,* 50**,** 7639-44.

149. Nemchenko, A., Kunze, S., Feussner, I. & Kolomiets, M. 2006. Duplicate maize 13-lipoxygenase genes are differentially regulated by circadian rhythm, cold stress, wounding, pathogen infection, and hormonal treatments. *J Exp Bot,* 57**,** 3767-79.

150. Netea, M. G., Gow, N. A., Munro, C. A., Bates, S., Collins, C., Ferwerda, G., Hobson, R. P., Bertram, G., Hughes, H. B., Jansen, T., Jacobs, L., Buurman, E. T., Gijzen, K., Williams, D. L., Torensma, R., Mckinnon, A., Maccallum, D. M., Odds, F. C., Van Der Meer, J. W., Brown, A. J. & Kullberg, B. J. 2006. Immune sensing of *Candida albicans* requires cooperative recognition of mannans and glucans by lectin and Toll-like receptors. *J Clin Invest,* 116**,** 1642-50.

151. Nirenberg, H. I. 1981. A simplified method for identifying *Fusarium spp.* occurring on wheat. *Canadian Journal of Botany,* 59**,** 1599-1609.

152. Nishimura, K., Murozumi, K., Shirahata, A., Park, M. H., Kashiwagi, K. & Igarashi, K. 2005. Independent roles of eIF5A and polyamines in cell proliferation. *Biochem J,* 385**,** 779-85.

153. Njuguna, J. T., Nassar, M., Hoerauf, A. & Kaiser, A. E. 2006. Cloning, expression and functional activity of deoxyhypusine synthase from *Plasmodium vivax*. *BMC Microbiology,* 6**,** 91.

154. Nurmberg, P. L., Knox, K. A., Yun, B. W., Morris, P. C., Shafiei, R., Hudson, A. & Loake, G. J. 2007. The developmental selector AS1 is an evolutionarily conserved regulator of the plant immune response. *Proc Natl Acad Sci U S A,* 104**,** 18795-800.

155. Ober, D. & Hartmann, T. 1999a. Deoxyhypusine synthase from tobacco. cDNA isolation, characterization, and bacterial expression of an enzyme with extended substrate specificity. *J Biol Chem,* 274**,** 32040-7.

156. Ober, D. & Hartmann, T. 1999b. Homospermidine synthase, the first pathway-specific enzyme of pyrrolizidine alkaloid biosynthesis, evolved from deoxyhypusine synthase. *Proceedings of the National Academy of Sciences of the United States of America,* 96**,** 14777-14782.

157. Pallotta, M. A., Graham, R. D., Langridge, P., Sparrow, D. H. B. & Barker, S. J. 2000. RFLP mapping of manganese efficiency in barley. *Theoretical and Applied Genetics,* 101**,** 1100-1108.

158. Pannecoucque, J. & Höfte, M. 2009. Interactions between cauliflower and *Rhizoctonia anastomosis* groups with different levels of aggressiveness. *BMC Plant Biology,* 9**,** 1-12.

159. Park, M. H. 2006. The post-translational synthesis of a polyamine-derived amino acid, hypusine, in the eukaryotic translation initiation factor 5A (eIF5A). *J Biochem,* 139**,** 161-9.

160. Park, M. H., Lee, Y. B. & Joe, Y. A. 1997. Hypusine is essential for eukaryotic cell proliferation. *Biol Signals,* 6**,** 115-23.

161. Park, M. H., Nishimura, K., Zanelli, C. F. & Valentini, S. R. 2010. Functional significance of eIF5A and its hypusine modification in eukaryotes. *Amino Acids,* 38**,** 491-500.

162. Parlevliet, J. E. 2002. Durability of resistance against fungal, bacterial and viral pathogens; present situation. *Euphytica,* 124**,** 147-156.

163. Planchamp, C., Glauser, G. & Mauch-Mani, B. 2014. Root inoculation with *Pseudomonas putida* KT2440 induces transcriptional and metabolic changes and systemic resistance in maize plants. *Frontiers in Plant Science,* 5**,** 719.

164. Pritsch, C., Muehlbauer, G. J., Bushnell, W. R., Somers, D. A. & Vance, C. P. 2000. Fungal development and induction of defense response genes during early infection of wheat spikes by *Fusarium graminearum*. *Mol Plant-Microbe Interact,* 13.

165. Proctor, R. H., Hohn, T. M. & Mccormick, S. P. 1995. Reduced virulence of *Gibberella zeae* caused by disruption of a trichothecene toxin biosynthetic gene. *Mol Plant Microbe Interact,* 8**,** 593-601.

166. Jorgensen, R. A., Cluster, P. D., English, J., Que, Q. & Napoli, C. A. 1996. Chalcone synthase cosuppression phenotypes in petunia flowers: comparison of sense vs. antisense constructs and single-copy vs. complex T-DNA sequences. *Plant Mol Biol*, 31, 957-73.

167. Quinlan, R. J., Sweeney, M. D., Lo Leggio, L., Otten, H., Poulsen, J. C., Johansen, K. S., Krogh, K. B., Jorgensen, C. I., Tovborg, M., Anthonsen, A., Tryfona, T., Walter, C. P., Dupree, P., Xu, F., Davies, G. J. & Walton, P. H. 2011. Insights into the oxidative degradation of cellulose by a copper metalloenzyme that exploits biomass components. *Proc Natl Acad Sci U S A,* 108**,** 15079-84.

168. Ramakrishna, W., Emberton, J., Ogden, M., Sanmiguel, P. & Bennetzen, J. L. 2002. Structural analysis of the maize RP1 complex reveals numerous sites and unexpected mechanisms of local rearrangement. *The Plant Cell,* 14**,** 3213-3223.

169. Ren, B., Chen, Q., Hong, S., Zhao, W., Feng, J., Feng, H. & Zuo, J. 2013. The *Arabidopsis* eukaryotic translation initiation factor eif5a-2 regulates root protoxylem development by modulating cytokinin signaling. *The Plant Cell,* 25**,** 3841-3857.

170. Ribnicky, D. M., Shulaev, V. V. & Raskin, I. I. 1998. Intermediates of salicylic acid biosynthesis in tobacco. *Plant Physiol,* 118**,** 565-72.

171. Ritchie, S. W., J.J. Hanway, G.O. Benson. 1993. *How a corn plant develops,* Iowa State University of Science and Technology Cooperative Extension Service, Ames.

172. Rittenour, W. R. & Harris, S. D. 2010. An *in vitro* method for the analysis of infection-related morphogenesis in *Fusarium graminearum*. *Mol Plant Pathol,* 11**,** 361-9.

173. Rolli, E., Ragni, E., Calderon, J., Porello, S., Fascio, U. & Popolo, L. 2009. Immobilization of the glycosylphosphatidylinositol-anchored Gas1 protein into the chitin ring and septum is required for proper morphogenesis in yeast. *Mol Biol Cell,* 20**,** 4856-70.

174. Rosorius, O., Reichart, B., Kratzer, F., Heger, P., Dabauvalle, M. C. & Hauber, J. 1999. Nuclear pore localization and nucleocytoplasmic transport of eIF-5A: evidence for direct interaction with the export receptor CRM1. *J Cell Sci,* 112 (Pt 14)**,** 2369-80.

175. Roux, B., Rodde, N., Jardinaud, M. F., Timmers, T., Sauviac, L., Cottret, L., Carrere, S., Sallet, E., Courcelle, E., Moreau, S., Debelle, F., Capela, D., De Carvalho-Niebel, F., Gouzy, J., Bruand, C. & Gamas, P. 2014. An integrated analysis of plant and bacterial gene expression in symbiotic root nodules using laser-capture microdissection coupled to RNA sequencing. *Plant J,* 77**,** 817-37.

176. Ruepp, A., Zollner, A., Maier, D., Albermann, K., Hani, J., Mokrejs, M., Tetko, I., Güldener, U., Mannhaupt, G., Münsterkötter, M. & Mewes, H. W. 2004. The FunCat, a functional annotation scheme for systematic classification of proteins from whole genomes. *Nucleic Acids Res,* 32.

177. Saini, P., Eyler, D. E., Green, R. & Dever, T. E. 2009. Hypusine-containing protein eIF5A promotes translation elongation. *Nature,* 459**,** 118-121.

178. Saldajeno, M. G. B., Chandanie, W. A., Kubota, M. & Hyakumachi, M. 2008. Effects of interactions of arbuscular mycorrhizal fungi and beneficial saprophytic mycoflora on plant growth and disease protection. *In:* Siddiqui, Z. A., Akhtar, M. S. & Futai, K. (eds.) *Mycorrhizae: Sustainable Agriculture and Forestry*. Dordrecht: Springer Netherlands.

179. Santi, S., Grisan, S., Pierasco, A., F, D. E. M. & Musetti, R. 2013. Laser microdissection of grapevine leaf phloem infected by stolbur reveals site-specific gene responses associated to sucrose transport and metabolism. *Plant Cell Environ,* 36**,** 343-55.

180. Schnier, J., Schwelberger, H. G., Smit-Mcbride, Z., Kang, H. A. & Hershey, J. W. 1991. Translation initiation factor 5A and its hypusine modification are essential for cell viability in the yeast *Saccharomyces cerevisiae*. *Mol Cell Biol,* 11**,** 3105-14.

181. Schubert, D., Lechtenberg, B., Forsbach, A., Gils, M., Bahadur, S. & Schmidt, R. 2004. Silencing in *Arabidopsis* T-DNA transformants: the predominant role of a gene-specific RNA sensing mechanism versus position effects. *The Plant Cell,* 16, 2561-2572.

182. Schwessinger, B. & Ronald, P. C. 2012. Plant innate immunity: perception of conserved microbial signatures. *Annu Rev Plant Biol,* 63**,** 451-82.

183. Seong, K. Y., Zhao, X., Xu, J. R., Guldener, U. & Kistler, H. C. 2008. Conidial germination in the filamentous fungus *Fusarium graminearum*. *Fungal Genet Biol,* 45**,** 389-99.

184. Sepulveda, G. & Sanchez De Jimenez, E. 1988. Polyamine distribution among maize embryonic tissues and its relation to seed germination. *Biochem Biophys Res Commun,* 153**,** 881-7.

185. Shah, J. 2009. Plants under attack: systemic signals in defence. *Curr Opin Plant Biol,* 12**,** 459-64.

186. Shaner, G. 2003. Epidemiology of *Fusarium* head blight of small grain cereals in North America. St. Paul: American Phytopathological Society (APS Press).

187. Shiba, T., Mizote, H., Kaneko, T., Nakajima, T. & Kakimoto, Y. 1971. Hypusine, a new amino acid occurring in bovine brain. Isolation and structural determination. *Biochim Biophys Acta,* 244**,** 523-31.

188. Shimono, M., Sugano, S., Nakayama, A., Jiang, C. J., Ono, K., Toki, S. & Takatsuji, H. 2007. Rice WRKY45 plays a crucial role in benzothiadiazole-inducible blast resistance. *Plant Cell,* 19**,** 2064-76.

189. Shoresh, M., Yedidia, I. & Chet, I. 2005. Involvement of jasmonic acid/ethylene signaling pathway in the systemic resistance induced in cucumber by *Trichoderma asperellum* T203. *Phytopathology,* 95**,** 76-84.

190. Sieber, C. M. K., Lee, W., Wong, P., Münsterkötter, M., Mewes, H.-W., Schmeitzl, C., Varga, E., Berthiller, F., Adam, G. & Güldener, U. 2014. The *Fusarium graminearum* genome reveals more secondary metabolite gene clusters and hints of horizontal gene transfer. *PLoS ONE,* 9**,** e110311.

191. Snijders, C. H. A. 1990. Fusarium head blight and mycotoxin contamination of wheat, a review. *Netherlands Journal of Plant Pathology,* 96**,** 187-198.

192. Stärkel, C. 2011. *Host Induced Gene Silencing - strategies for the improvement of resistance against Cercospora beticola in sugar beet (B. vulgaris L.) and against Fusarium graminearum in wheat (T. aestivum L.) and maize (Z. mays L.).* PhD, University of Hamburg.

193. Steffenson, B. J. 1992. Analysis of durable resistance to stem rust in barley. *In:* Johnson, R. & Jellis, G. J. (eds.) *Breeding for Disease Resistance.* Dordrecht: Springer Netherlands.

194. Stephens, A. E., Gardiner, D. M., White, R. G., Munn, A. L. & Manners, J. M. 2008a. Phases of infection and gene expression of *Fusarium graminearum* during crown rot disease of wheat. *Mol Plant Microbe Interact,* 21**,** 1571-81.

195. Stephens, A. E., Gardiner, D. M., White, R. G., Munn, A. L. & Manners, J. M. 2008b. Phases of infection and gene expression of *Fusarium graminearum* during crown rot disease of wheat. *Molecular Plant-Microbe Interactions,* 21**,** 1571-1581.

196. Stone, B. a. a. C., A.E. 1992. Chemistry and physiology of higher plant (1-3)-β-D-Glucans (callose). *In:* Stone, B. A. (ed.) *Chemistry and Biology of (1-3)-β-D-Glucans.* Victoria, Australia: La Trobe University Press.

197. Sutton, J. C. 1982. Epidemiology of wheat head blight and maize ear rot caused by *Fusarium graminearum. Canadian Journal of Plant Pathology,* 4**,** 195-209.

198. Tang, W., Coughlan, S., Crane, E., Beatty, M. & Duvick, J. 2006. The application of laser microdissection to *in planta* gene expression profiling of the maize anthracnose stalk rot fungus *Colletotrichum graminicola. Mol Plant Microbe Interact,* 19**,** 1240-50.

199. Teichert, I., Wolff, G., Kück, U. & Nowrousian, M. 2012. Combining laser microdissection and RNA-seq to chart the transcriptional landscape of fungal development. *BMC Genomics,* 13**,** 1-18.

200. Tenberge, K. B. 2004. Infection sites and infection structures. *In:* Elad, Y., Williamson, B., Tudzynski, P. & Delen, N. (eds.) *Botrytis: Biology, Pathology and Control.* Dordrecht, The Netherlands: Kluwer Academic Publishers.

201. Thompson, J. E., Hopkins, M. T., Taylor, C. & Wang, T.-W. 2004. Regulation of senescence by eukaryotic translation initiation factor 5A: implications for plant growth and development. *Trends in Plant Science,* 9**,** 174-179.

202. Trail, F. 2009a. For blighted waves of grain: *Fusarium graminearum* in the postgenomics era. *Plant Physiol,* 149.

203. Trail, F. 2009b. For Blighted Waves of Grain: *Fusarium graminearum* in the Postgenomics Era. *Plant Physiology,* 149**,** 103-110.

204. Trapnell, C., Pachter, L. & Salzberg, S. L. 2009. TopHat: discovering splice junctions with RNA-Seq. *Bioinformatics,* 25**,** 1105-11.

205. Trapnell, C., Roberts, A., Goff, L., Pertea, G., Kim, D., Kelley, D. R., Pimentel, H., Salzberg, S. L., Rinn, J. L. & Pachter, L. 2012. Differential gene and transcript expression analysis of RNA-seq experiments with TopHat and cufflinks. *Nat Protoc,* 7.

206. Trapnell, C., Williams, B. A., Pertea, G., Mortazavi, A., Kwan, G., Baren, M. J., Salzberg, S. L., Wold, B. J. & Pachter, L. 2010. Transcript assembly and quantification by RNA-Seq reveals unannotated transcripts and isoform switching during cell differentiation. *Nat Biotechnol,* 28.

207. Tremblay, A., Li, S., Scheffler, B. E. & Matthews, B. F. 2008. Laser capture microdissection and expressed sequence tag analysis of uredinia formed by *Phakopsora pachyrhizi*, the causal agent of Asian soybean rust. *Physiological and Molecular Plant Pathology,* 73**,** 163-174.

208. Ude, S., Lassak, J., Starosta, A. L., Kraxenberger, T., Wilson, D. N. & Jung, K. 2013. Translation elongation factor EF-P alleviates ribosome stalling at polyproline stretches. *Science,* 339**,** 82-5.

209. Umland, T. C., Wolff, E. C., Park, M. H. & Davies, D. R. 2004. A new crystal structure of deoxyhypusine synthase reveals the configuration of the active enzyme and of an enzyme NAD inhibitor ternary complex. *J Biol Chem,* 279**,** 28697-705.

210. Vallad, G. E. & Goodman, R. M. 2004. Systemic acquired resistance and induced systemic resistance in conventional agriculture. *Crop Science,* 44.

211. Van Der Ent, S., Koornneef, A., Ton, J. & Pieterse, C. M. J. 2009. Induced resistance – orchestrating defence mechanisms through crosstalk and priming. *Annual Plant Reviews Volume 34: Molecular Aspects of Plant Disease Resistance.* Wiley-Blackwell.

212. Van Egmond, H. P., Schothorst, R. C. & Jonker, M. A. 2007. Regulations relating to mycotoxins in food: perspectives in a global and European context. *Anal Bioanal Chem,* 389**,** 147-57.

213. Verma, D. P. & Hong, Z. 2001. Plant callose synthase complexes. *Plant Mol Biol*, 47, 693-701.

214. Wagener, J., Malireddi, R. K., Lenardon, M. D., Koberle, M., Vautier, S., Maccallum, D. M., Biedermann, T., Schaller, M., Netea, M. G., Kanneganti, T. D., Brown, G. D., Brown, A. J. & Gow, N. A. 2014. Fungal chitin dampens inflammation through IL-10 induction mediated by NOD2 and TLR9 activation. *PLoS Pathog,* 10**,** e1004050.

215. Walter, S., Nicholson, P. & Doohan, F. M. 2010. Action and reaction of host and pathogen during *Fusarium* head blight disease. *New Phytol,* 185.

216. Wang, T.-W., Lu, L., Zhang, C.-G., Taylor, C. & Thompson, J. 2003. Pleiotropic effects of suppressing deoxyhypusine synthase expression in *Arabidopsis thaliana*. *Plant Molecular Biology,* 52**,** 1223-1235.

217. Wang, T. W., Lu, L., Wang, D. & Thompson, J. E. 2001. Isolation and characterization of senescence-induced cDNAs encoding deoxyhypusine synthase and eucaryotic translation initiation factor 5A from tomato. *J Biol Chem,* 276**,** 17541-9.

218. Wang, T. W., Lu, L., Zhang, C. G., Taylor, C. & Thompson, J. E. 2003. Pleiotropic effects of suppressing deoxyhypusine synthase expression in *Arabidopsis thaliana*. *Plant Mol Biol,* 52.

219. Wang, T. W., Zhang, C. G., Wu, W., Nowack, L. M., Madey, E. & Thompson, J. E. 2005. Antisense suppression of deoxyhypusine synthase in tomato delays fruit softening and alters growth and development. *Plant Physiol,* 138**,** 1372-82.

220. Wang, Z., Gerstein, M. & Snyder, M. 2009. RNA-Seq: a revolutionary tool for transcriptomics. *Nat Rev Genet,* 10**,** 57-63.

221. Wanjiru, W. M., Kang, Z. S. & Buchenauer, H. 2002. Importance of cell wall degrading enzymes produced by *Fusarium graminearum* during infection of wheat heads. *Eur J Plant Pathol,* 108.

222. Weirauch, M. T. 2011. Gene coexpression networks for the analysis of DNA microarray data. *Applied Statistics for Network Biology*. Wiley-VCH Verlag GmbH & Co. KGaA.

223. Welz, H. 2000. Genes for resistance to northern corn leaf blight in diverse maize populations. *Plant Breeding,* 119.

224. Wisser, R. J., Balint-Kurti, P. J. & Nelson, R. J. 2006. The genetic architecture of disease resistance in maize: a synthesis of published studies. *Phytopathology,* 96**,** 120-9.

225. Wisser, R. J., Sun, Q., Hulbert, S. H., Kresovich, S. & Nelson, R. J. 2005. Identification and characterization of regions of the rice genome associated with broad-spectrum, quantitative disease resistance. *Genetics,* 169**,** 2277-2293.

226. Wolff, E. C., Folk, J. E. & Park, M. H. 1997. Enzyme-substrate intermediate formation at lysine 329 of human deoxyhypusine synthase. *Journal of Biological Chemistry,* 272**,** 15865-15871.

227. Wolff, E. C., Kang, K. R., Kim, Y. S. & Park, M. H. 2007. Posttranslational synthesis of hypusine: evolutionary progression and specificity of the hypusine modification. *Amino Acids,* 33**,** 341-50.

228. Wolff, E. C., Lee, Y. B., Chung, S. I., Folk, J. E. & Park, M. H. 1995. Deoxyhypusine synthase from rat testis: purification and characterization. *Journal of Biological Chemistry,* 270**,** 8660-8666.

229. Wolff, E. C. & Park, M. H. 1999. Identification of lysine350 of yeast deoxyhypusine synthase as the site of enzyme intermediate formation. *Yeast,* 15**,** 43-50.

230. Wolff, E. C., Wolff, J. & Park, M. H. 2000. Deoxyhypusine synthase generates and uses bound NADH in a transient hydride transfer mechanism. *Journal of Biological Chemistry,* 275**,** 9170-9177.

231. Wong, P., Walter, M., Lee, W., Mannhaupt, G., Munsterkotter, M., Mewes, H. W., Adam, G. & Guldener, U. 2011. FGDB: revisiting the genome annotation of the plant pathogen *Fusarium graminearum*. *Nuc Acids Res,* 39.

232. Woriedh, M. 2010. *Cloning, expression and functional characterization of deoxyhypusine synthase from the pathogenic fungus Fusarium graminearum Schwabe (teleomorph Gibberella zeae), wheat (Triticum aestivum L.) and maize (Zea mays L.)*. PhD, University of Hamburg.

233. Woriedh, M., Hauber, I., Martinez-Rocha, A. L., Voigt, C., Maier, F. J., Schroder, M., Meier, C., Hauber, J. & Schafer, W. 2011. Preventing Fusarium head blight of wheat and cob rot of maize by inhibition of fungal deoxyhypusine synthase. *Mol Plant Microbe Interact,* 24**,** 619-27.

234. Xu, A., Jao, D. L. & Chen, K. Y. 2004. Identification of mRNA that binds to eukaryotic initiation factor 5A by affinity co-purification and differential display. *Biochem J,* 384**,** 585-90.

235. Xu, H., Chater, K. F., Deng, Z. & Tao, M. 2008. A cellulose synthase-like protein involved in hyphal tip growth and morphological differentiation in *Streptomyces*. *Journal of Bacteriology,* 190**,** 4971-4978.

236. Xu, J., Zhang, B., Jiang, C. & Ming, F. 2011. RceIF5A, encoding an eukaryotic translation initiation factor 5A in *Rosa chinensis*, can enhance thermotolerance, oxidative and osmotic stress resistance of *Arabidopsis thaliana*. *Plant Mol Biol,* 75.

237. Yalpani, N., Leon, J., Lawton, M. A. & Raskin, I. 1993. Pathway of salicylic acid biosynthesis in healthy and virus-inoculated tobacco. *Plant Physiol,* 103**,** 315-321.

238. Yan, Y. P., Tao, Y. & Chen, K. Y. 1996. Molecular cloning and functional expression of human deoxyhypusine synthase cDNA based on expressed sequence tag information. *Biochem J,* 315 (Pt 2)**,** 429-34.

239. Yang, F., Jensen, J. D., Svensson, B., Jorgensen, H. J., Collinge, D. B. & Finnie, C. 2012. Secretomics identifies *Fusarium graminearum* proteins involved in the interaction with barley and wheat. *Mol Plant Pathol,* 13**,** 445-53.

240. Yedidia, I., Shoresh, M., Kerem, Z., Benhamou, N., Kapulnik, Y. & Chet, I. 2003. Concomitant induction of systemic resistance to *Pseudomonas syringae* pv. lachrymans in cucumber by *Trichoderma asperellum* (T-203) and accumulation of phytoalexins. *Appl Environ Microbiol,* 69**,** 7343-53.

241. Yuan, Y., Zhong, S., Li, Q., Zhu, Z., Lou, Y., Wang, L., Wang, J., Wang, M., Li, Q., Yang, D. & He, Z. 2007. Functional analysis of rice NPR1-like genes reveals that OsNPR1/NH1 is the rice orthologue conferring disease resistance with enhanced herbivore susceptibility. *Plant Biotechnol J,* 5**,** 313-24.

242. Zhang, X. W., Jia, L. J., Zhang, Y., Jiang, G., Li, X., Zhang, D. & Tang, W. H. 2012. *In planta* stage-specific fungal gene profiling elucidates the molecular strategies of *Fusarium graminearum* growing inside wheat coleoptiles. *Plant Cell,* 24**,** 5159-76.

243. Zwonitzer, J. C., Coles, N. D., Krakowsky, M. D., Arellano, C., Holland, J. B., Mcmullen, M. D., Pratt, R. C. & Balint-Kurti, P. J. 2010. Mapping resistance quantitative trait Loci for three foliar diseases in a maize recombinant inbred line population-evidence for multiple disease resistance? *Phytopathology,* 100**,** 72-9.

Acknowledgments

I would like to gratefully acknowledge those of people, especially everyone in the PPA Lab, who has supported and helped me, in anyway, so much throughout this period.

Most of all, I would like to express my sincere gratitude to my supervisor **Prof. Dr. Wilhem Schäfer** for giving me a chance to be member of his laboratory, the continuous support of my Ph.D study and related research, for his patience, motivation, and immense knowledge. His guidance helped me in all the time of research and writing of this thesis. It's been a pleasure working with him over the past few years.

I am thankful to **Prof. Dr. Joachim Hauber** for being the second reviewer of this study.

I would like to thank my committee members **Prof. Dr. Stefan Hoth** and **Prof. Dr. Julia Kehr** for their patience and for reading my thesis.

I am very grateful to **Dr**. **Ana Lilia Martinez-Rocha.** Thanks for her valuable guidance and advice during my PhD time. She is not only my exellent supervisor but also one of my best friends. She supported me greatly and was always willing to help me. Without her precious support it would not be possible to conduct this thesis.

I wish to thank **Dr. Thuat Nguyen Van** whose help has been inestimable. I am sorry that he can not see me graduate. His memory will be with me always.

I will forever be grateful to **Associate Prof. Dr. Quyen Dinh Thi** for giving me a chance to know and work in this wonderful lab.

My sincere thanks also goes to to **Dr. Jörg Bormann** for many useful advices, encouragement and support during my PhD time.

I am very thankful to **Prof. Dr. Christian Voigt** for his valuable discussion and advice.

Many thanks are due to **Ellis Monaghan** who did the language evaluation for this thesis.

I thank all my fellow labmates, former and present colleagues, **Marike Boenisch, Anika Glasenapp, Christine Blum, Annemarie Glöckner, Michael Mentges, Tobias Hanak, Björn Sode, Christian Falter**, **Sophie Brandt, Martin Gand** for the sleepless nights we were working and drinking together, and for all the fun we had in the last four years. Special thanks to **Jakob Bönnighausen, Gunnar Baermann** and **Lewin Günther** for their supports in many ways from official papers to lab works.

I would also like to thank **Cathrin Kröger** and **Birgit Hadeler** for their technical assistance, as well as **Brigitte Doormann** for helping in all official work. I am grateful to all of the people I have had the pleasure of working with from **Molecular Phytopathology and Genetics** lab as well as from the **Biocenter Klein Flottbek.**

I would like to thank Vietnam Government for the PhD fellowship.

Thanks to my friends **Trang Pham, Duc Nm, Hieu Sun** and **Linh Nhat Nguyen** for their friendship and support.

And last but not least, I would like to thank **my family**: **my parents** and **my sister** for always being there with their immortal love and emotional support. My parent and my sister are always in my heart.

Thank you very much, everyone!